

Springer Theses

Recognizing Outstanding Ph.D. Research

Daniel Yuan Qiang Wong

Rethinking Platinum
Anticancer Drug
Design: Towards
Targeted and Immuno-
chemotherapeutic
Approaches

 Springer

Springer Theses

Recognizing Outstanding Ph.D. Research

Aims and Scope

The series “Springer Theses” brings together a selection of the very best Ph.D. theses from around the world and across the physical sciences. Nominated and endorsed by two recognized specialists, each published volume has been selected for its scientific excellence and the high impact of its contents for the pertinent field of research. For greater accessibility to non-specialists, the published versions include an extended introduction, as well as a foreword by the student’s supervisor explaining the special relevance of the work for the field. As a whole, the series will provide a valuable resource both for newcomers to the research fields described, and for other scientists seeking detailed background information on special questions. Finally, it provides an accredited documentation of the valuable contributions made by today’s younger generation of scientists.

Theses are accepted into the series by invited nomination only and must fulfill all of the following criteria

- They must be written in good English.
- The topic should fall within the confines of Chemistry, Physics, Earth Sciences, Engineering and related interdisciplinary fields such as Materials, Nanoscience, Chemical Engineering, Complex Systems and Biophysics.
- The work reported in the thesis must represent a significant scientific advance.
- If the thesis includes previously published material, permission to reproduce this must be gained from the respective copyright holder.
- They must have been examined and passed during the 12 months prior to nomination.
- Each thesis should include a foreword by the supervisor outlining the significance of its content.
- The theses should have a clearly defined structure including an introduction accessible to scientists not expert in that particular field.

More information about this series at <http://www.springer.com/series/8790>

Daniel Yuan Qiang Wong

Rethinking Platinum Anticancer Drug Design: Towards Targeted and Immuno-chemotherapeutic Approaches

Doctoral Thesis accepted by
the National University of Singapore, Singapore

 Springer

Author

Dr. Daniel Yuan Qiang Wong
Department of Chemistry
National University of Singapore
Singapore
Singapore

Supervisor

Prof. Ang Wee Han
Department of Chemistry
National University of Singapore
Singapore
Singapore

ISSN 2190-5053

Springer Theses

ISBN 978-981-10-8593-2

<https://doi.org/10.1007/978-981-10-8594-9>

ISSN 2190-5061 (electronic)

ISBN 978-981-10-8594-9 (eBook)

Library of Congress Control Number: 2018934379

© Springer Nature Singapore Pte Ltd. 2018

This work is subject to copyright. All rights are reserved by the Publisher, whether the whole or part of the material is concerned, specifically the rights of translation, reprinting, reuse of illustrations, recitation, broadcasting, reproduction on microfilms or in any other physical way, and transmission or information storage and retrieval, electronic adaptation, computer software, or by similar or dissimilar methodology now known or hereafter developed.

The use of general descriptive names, registered names, trademarks, service marks, etc. in this publication does not imply, even in the absence of a specific statement, that such names are exempt from the relevant protective laws and regulations and therefore free for general use.

The publisher, the authors and the editors are safe to assume that the advice and information in this book are believed to be true and accurate at the date of publication. Neither the publisher nor the authors or the editors give a warranty, express or implied, with respect to the material contained herein or for any errors or omissions that may have been made. The publisher remains neutral with regard to jurisdictional claims in published maps and institutional affiliations.

Printed on acid-free paper

This Springer imprint is published by Springer Nature

The registered company is Springer Nature Singapore Pte Ltd.

The registered company address is: 152 Beach Road, #21-01/04 Gateway East, Singapore 189721, Singapore

Supervisor's Foreword

As Daniel Wong's graduate advisor during his Ph.D., I am pleased to write this foreword for this publication in Springer Theses. Daniel joined my laboratory as my first batch of final year project undergraduate students in 2010. He was working on the synthesis of targeted platinum(IV) anticancer complexes. He subsequently received a departmental scholarship and continued on to do his Ph.D. with me. In his 5 years with me, Daniel has been a self-motivated, independent and creative scientist. He has been highly curious and always discussing new potential project ideas with me. As a scientist, Daniel is willing to dive into the 'unknown' and take calculated risks in his research direction instead of sticking with the 'tried and proven'. I have watched him grown from a trainee student under my tutelage into a proficient scientist, himself mentoring another younger generation of scientists. In recognition of his research excellence, Daniel has won the prestigious Wang Gungwu Medal (2016) for the best Ph.D. thesis in the Natural Sciences in the National University of Singapore.

Broadly, this thesis is outstanding in its effort to propose new avenues for future platinum-based drug development. Platinum-based chemotherapeutics such as cisplatin has been a workhorse of chemotherapy regimens for decades. Nonetheless, clinical interest in new platinum-based chemical entities (NCEs) has been waning in recent years. In this era of cancer genomics and immunotherapy, traditional cytotoxic chemotherapeutics have seemingly been left behind. It is in this context that this thesis attempts to offer a rethink of platinum-based agents and to suggest new directions for the future research.

The first contribution of this thesis is a proof-of-concept, deploying a targeted drug while retaining a broad spectrum of action in the form of a targeted cisplatin-based derivative (Chap. 4). Daniel demonstrated that such a strategy could be therapeutically favourable because it could circumvent multi-factorial apoptosis resistance inherent in heterogeneous tumours, a problem which plagues conventional molecularly targeted drugs.

Daniel's second contribution is the conceptualisation of combined platinum-based immuno-chemotherapeutics which combines chemotherapy with immunotherapy. Back when this idea was first floated, it seemed like a longshot that platinum agents,

long held to be immunosuppressive, could modulate the immune microenvironment in a way that could be therapeutically favourable. There was some evidence supporting this hypothesis in literature but they were scarce and not widely recognized within the community. Daniel has made pioneering efforts in exploring this idea with some early promising results, and as two orthogonal approaches. The first approach is a 'macrophage-centric' approach which looks at activating macrophages directly with platinum agents (Chap. 5), while the second approach is a 'tumour-centric' approach of triggering immunogenic cell death of cancer cells (Chap. 6).

The discoveries of this work have been published in outstanding top-tiered journals, including two papers in *Angewandte Chemie*, one of which as a VIP paper, and another paper in *Chemical Science*. This Springer Theses award has been well-deserved.

Singapore, Singapore
February 2018

Prof. Ang Wee Han

Parts of this thesis have been published in the following articles:

1. D. Y. Q. Wong*, W. W. F. Ong*, W. H. Ang, Induction of immunogenic cell death by chemotherapeutic platinum complexes, *Angew. Chem. Int. Ed.* 2015
2. D. Y. Q. Wong*, J. H. Lim*, W. H. Ang, Induction of targeted necrosis with HER2-targeted platinum(IV) anticancer prodrugs, *Chem. Sci.* 2015, 6, 3051–3056–
Published by The Royal Society of Chemistry
3. D. Y. Q. Wong*, C. H. F. Yeo*, and W. H. Ang, Immuno-chemotherapeutic platinum(IV) prodrugs of cisplatin as multimodal anticancer agents, *Angew. Chem. Int. Ed.*, 2014, 26, 6752–6756
4. D. Y. Q. Wong, J. Y. Lau, W. H. Ang, Harnessing chemoselective imine ligation for tethering bioactive molecules to platinum(IV) prodrugs, *Dalton Trans.*, 2012, 41, 6104–6111

*** Equal contribution**

Acknowledgements

There are many who have contributed significantly towards the progress of my research in one way or another. Here, I will just like to acknowledge and thank them. First, I would like to express my unreserved appreciation towards my supervisor, Prof. Ang Wee Han. Without him, this research work would simply not have existed. Having been with the lab from its inception till now, I feel a sense of pride to be part of this competent, resource-rich and well-equipped lab. I'm grateful too, for Prof. Ang's confidence in me which has moulded me into a more self-assured researcher.

I'm also thankful for the presence of my fellow labmates. Thanks to Cheefei, for having shouldered the heavy burden of being the safety lead and also for being a great pal and the life of the lab. Thanks to Jianyu, the new safety lead, and Siewqi, the biological lead, for their sense of responsibility and their proactive efforts which have made the lab's working environment so much better for everyone. Thanks to Junxiang for constantly waiting for me to have lunch and whose work effort is commendable. Not forgetting—Mun Juinn, my lab 'BFF'. Thanks for being a great friend, whom I can confide in, and whose friendship I will always treasure. Finally, to the newcomers, Keefe, Sebastian and Marsha—I wish you all well.

It has been said that *the true credit belongs to the man in the arena, whose face is marred by dust and sweat and blood*. Thus, I cannot adequately thank and acknowledge the contributions of all my final year students enough. It is them, who have driven and achieved much of the work described here. Thanks to Lau Jiayi (Chap. 2, 2012), Charmian Yeo (Chaps. 3 and 5, 2013), Lim Jun Han (Chap. 4, 2014) and Wendy Ong (Chap. 6, 2014). Although not included in this thesis, Stephanie Loh and Valerie Chu (2015) made substantial progress on understanding macrophage activation and on immune checkpoint inhibitors respectively.

My family has been a constant unwavering pillar of support during these 4 years. Thanks to my dad for nudging me up every morning and for driving me to school. You are truly the most selfless and loving dad ever. Thanks to my mum for taking care of the household and for keeping me well-fed. No words are sufficient to express my gratitude. I thank my brother, Alex, and my sister, Jenny, for holding

the family together and supporting the family financially all these while throughout all the ups and downs. I also thank my sister-in-law, Meilin. It's amazing how she could juggle her research, become 'woman of the year' and still cook dinner for us! Thanks Sabbie, for your unconditional love and for everything, even though you are no longer with us. I will always miss you.

Finally, I thank my wife, Candice, for her unwavering belief and support. Without her, this Ph.D. journey would have been so much lonelier and the world would seem so much darker. Thanks for all the little words of encouragements to keep me going and for sticking with me through the tough times. I'm sorry you had to wait so long. I promise to cherish you for all the days of my life, together, forever.

feci quod potui, faciant meliora potentes

I have done what I could, let whoever can do more, do so.

Declaration

I hereby declare that this thesis is my original work and it has been written by me in its entirety, under the supervision of Dr. Ang Wee Han, Chemistry Department, National University of Singapore, between 8th Aug 2011 and 30th June 2015.

I have duly acknowledged all the sources of information which have been used in the thesis.

This thesis has also not been submitted for any degree in any university previously.

Contents

1 Introduction	1
1.1 Overview	1
1.2 Cellular Uptake and Molecular Mechanism of Action	3
1.3 Limitations	5
1.4 The Platinum(IV) Prodrug Strategy	8
1.5 Immuno-modulation by Platinum-Based Agents	18
1.6 Outline of Thesis	22
References	23
2 Harnessing Chemoselective Imine Ligation for Tethering Bioactive Molecules to Platinum(IV) Prodrugs	33
2.1 Introduction	33
2.2 Results and Discussion	35
2.3 Conclusion	41
2.4 Methods	42
Supplementary Information	45
References	51
3 Probing the Platinum(IV) Prodrug Hypothesis. Are Platinum(IV) Complexes Really Prodrugs of Cisplatin?	55
3.1 Introduction	55
3.2 Results and Discussion	58
3.3 Conclusion	63
3.4 Experimental	63
Supplementary Information	66
References	69

4 Induction of Targeted Necrosis with HER2-Targeted Platinum(IV) Anticancer Prodrugs	73
4.1 Introduction	74
4.2 Results and Discussion	75
4.3 Conclusion	82
4.4 Materials and Methods	83
Supplementary Information	87
References	100
5 Immuno-Chemotherapeutic Platinum(IV) Prodrugs of Cisplatin as Multimodal Anticancer Agents	103
5.1 Introduction	103
5.2 Results and Discussion	105
5.3 Conclusion	111
5.4 Methods	112
Supplementary Information	115
References	127
6 Induction of Immunogenic Cell Death by Chemotherapeutic Platinum Complexes	131
6.1 Introduction	131
6.2 Results and Discussion	133
6.3 Conclusion	138
6.4 Methods	139
Supplementary Information	142
References	144
7 Concluding Remarks	147
7.1 Concluding Remarks	147

List of Figures

Fig. 1.1	Platinum-based anticancer drugs which have recieved international clinical approval.	2
Fig. 1.2	The uptake and cytotoxic pathway of cisplatin. Upon entering the cell, cisplatin is hydrolyzed forming a reactive aquated species which then binds to cellular DNA leading to eventual cell death	3
Fig. 1.3	Illustration of the kink formed by the major 1,2-d(GpG) intrastrand crosslink in double stranded DNA. Reproduced from Ref. 20 with permission from The Royal Society of Chemistry [20]	4
Fig. 1.4	The platinum(IV) prodrug hypothesis: reductive elimination of platinum(IV) prodrugs occurs with the release the active platinum(II) core as well as both axial carboxylate ligands . . .	9
Fig. 1.5	JM335—an active platinum(IV) complex bearing <i>trans</i> equatorial geometry	10
Fig. 1.6	Ethacraplatin and mitaplatin are two examples of platinum(IV) complexes with active axial ligands	13
Fig. 1.7	Series of estrogen tethered platinum(IV) complexes.	14
Fig. 1.8	<i>cis</i> and <i>trans</i> isomers of light activated platinum(IV) diazido complexes.	15
Fig. 1.9	Formation of Pt-DNA adduct upon irradiation	15
Fig. 1.10	Combined immuno-chemotherapy. Cisplatin can exert both direct cytotoxicity against cancer cells as well as activating macrophages against cancer cells by upregulating TLR4 receptors on macrophages.	19
Fig. 1.11	Postulate: We hypothesize that platinum-based therapy is able to repolarize tumor-supporting M2 macrophages into cancer-killing M1 macrophages	20
Fig. 1.12	Some platinum-based agents can trigger immunogenic cell death of tumour cells by triggering ER-stress which induces the translocation of calreticulin, a potent “eat me” signal.	

	Recognition and phagocytosis of these tumour cells by dendritic cells eventually leads to the development of an acquired immune response against the tumour cells via a tumour-specific cytotoxic T cells response	20
Fig. 2.1	a Cisplatin, b satraplatin, c ethacrynic acid-conjugated platinum(IV) complex, synthesized by direct axial carboxylation with acid chloride and, d estrogen-tethered platinum(IV) complexes formed by amide coupling of an uncoordinated pendant carboxyl functional group with an amine-linker functionalized estrogen.	34
Fig. 2.2	Structures of hydrazide or aminoxy functionalized substrates, a benzhydrazide, b 4-methoxybenzhydrazide, c l-tyrosine hydrazide, d Girard's reagent D, e Girard's reagent T, f benzylhydroxylamine and g hydrazide-functionalised AMVSEF peptide.	37
Fig. 2.3	HPLC monitoring of formation Pt-benzhydrazide (top) and Pt-benzylhydroxylamine (bottom) over time in 50% DMF/aq. NaOAc (2 M, pH 4.8).	38
Fig. 2.4	Comparison between rate of imine ligation between the catalysed and uncatalysed reaction mixture; the solid and dotted line represents the fitted curves for the catalysed and uncatalysed reaction respectively to the differential rate equations for a two-step consecutive reversible reaction; Uncatalysed reaction: 0.263 mM Pt-benzaldehyde 1 , 8.71 mM benzhydrazide; Catalysed reaction: 0.263 mM Pt-benzaldehyde 1 , 8.71 mM benzhydrazide, 100 mM <i>p</i> -anisidine. Legend: Δ unreacted complex 1 , \circ mono-Pt-benzhydrazide, \square bis-Pt-benzhydrazide. Filled black symbols and hollow gray symbols represent the catalysed and uncatalysed reactions, respectively	39
Fig. 2.5	RP-HPLC (254 nm) reaction monitoring of formation of Pt-AMVSEF peptide 3 over time in 20% DMF. The free hydrazide-functionalised peptide ($R_t = 13.80$ min) is not visible at 254 nm. Legend: * bis-conjugated Pt-AMVSEF 3 , \blacklozenge mono-conjugated Pt-AMVSEF and \circ unreacted complex 1	41
Fig. S2.1	^1H NMR spectra of platinum(IV)-benzaldehyde complex 1 in DMSO- d_6	46
Fig. S2.2	^1H NMR spectra of complex 1 in acetone- d_6 and ESI-MS characterization.	47
Fig. S2.3	RP-HPLC assessment of purity of Pt-benzaldehyde 1 dissolved in DMF/H $_2$ O. Elution conditions for both spectra (a) and (b): 20–80% gradient elution system with aq. NH $_4$ OAc buffer (10 mM, pH 5.5) (solvent A) and MeCN (solvent B) over 15 min at 1.0 mL/min. Columns used are:	

	a Phenomenex Luna C18(2) (250 × 4.60 mm i.d), b Shimpack VP-ODS column (150 × 4.60 mm i.d)	48
Fig. S2.4	Similarities between ¹ H NMR spectrum of: a Pt-tyrosine hydrazide (2c) and b the purely organic hydrazone ligation between 4-carboxylbenzaldehyde and tyrosine hydrazide. The 3D visual illustration is generated by CORINA [46].	49
Fig. S2.5	Only slight hydrolysis of Pt-Girard's reagent T 2e was observed at pH 7.4 and 37 °C over 24 h; the λ _{max} of the spectra was at 303 nm, attributable to the hydrazone bond.	49
Fig. S2.6	Illustration of imine ligation between Pt-benzaldehyde 1 (a) and benzhydrazide to yield the mono-ligated product (b) and the bis-ligated product 2a (c)	50
Fig. 3.1	Top: <i>cisplatin</i> and <i>oxaliplatin</i> are two platinum(II) agents in clinical use today. Bottom: Satraplatin is a promising platinum(IV) anticancer prodrug under clinical trials. Complexes 1 and 2 are newly synthesized asymmetrical platinum(IV) complexes bearing a benzaldehyde moiety for facile imine ligation to any therapeutically-relevant substrate	56
Fig. 3.2	The platinum(IV) prodrug hypothesis: reductive elimination of platinum(IV) prodrugs occurs with the release the active platinum(II) core as well as both axial carboxylate ligands	56
Fig. 3.3	Top left and top right: HILIC (230 nm) and RPLC (214 nm) chromatograms respectively of the reduction of 1 by ascorbic acid. Legend: a 4-carboxylbenzaldehyde, b 1 , c dehydroascorbic acid, d ascorbic acid, e cisplatin. Bottom: Release profile of cisplatin over time. Legend: • 1 , Δ cisplatin. Note that figures show representative experiments conducted at different times using different initial concentrations of 1	59
Fig. 3.4	Top left and top right: HILIC (214 nm) and RPLC (214 nm) chromatograms respectively of the reduction of satraplatin by ascorbic acid. Legend: a satraplatin, b JM118, c ascorbic acid. Bottom: Release profile of JM118 over time. Legend: • satraplatin, Δ JM118. Note that figures show representative experiments conducted at different times using different initial concentrations of satraplatin	61
Fig. 3.5	Rate of reduction of 180 μM of 1 , 2 and satraplatin dissolved in 200 mM phosphate buffer + 137 mM NaCl in the presence of 2 mM ascorbic acid (left) or 4 mM ascorbic acid (right). Curve was fitted using graphpad prism 5	62
Fig. S3.1	Semi-preparative trace of the crude Pt(II)(NH ₃) ₂ (Cl) (carboxylbenzaldehyde). The desired product is at 16.9 min	66
Fig. S3.2	ESI-MS of the isolated Pt(II)(NH ₃) ₂ (Cl) (carboxylbenzaldehyde). m/z 411.8 [M-H] ⁻	67

- Fig. S3.3 Aquation of cisplatin to form an unidentified product. HILIC chromatograms of **a** cisplatin in PBS (containing 139 mM Cl^-) after leaving to stand and **b** cisplatin in 50 mM phosphate buffer pH 7 (without Cl^-) after 1 h, **c** the DAD-UV-vis spectrum of the peak at 15.6 min showed an absence of any chromophores, excluding the possibility that it was a reduction product containing a carboxylbenzaldehyde moiety since the latter has a characteristic absorbance at 258 nm 67
- Fig. S3.4 Left and right: HILIC (230 nm) and RPLC (214 nm) chromatograms respectively of the reduction of **2** by 2–4 mM ascorbic acid. Legend: **a** 4-carboxylbenzaldehyde, **b** **2**, **c** dehydroascorbic acid, **d** ascorbic acid, **e** cisplatin 68
- Fig. S3.5 Representative calibration curves. A fresh calibration curve was plotted per experiment. Top row: Calibration curves for cisplatin and **1** respectively at 230 and 305 nm. Bottom row: Calibration curve for JM118 and satraplatin respectively at 214 nm. 68
- Fig. 4.1 Synthesis of HER2-targeted platinum(IV)-AHNP conjugate consisting of an AHNP motif tethered to a cytotoxic platinum pharmacophore. The AHNP motif was separated with a small tripeptide spacer (GGK) and functionalized with an aminoxy(acetate) linker at the terminal lysine residue. Peptide sequence: $\text{H}_2\text{N}-\text{YC}^*\text{DGFYAC}^*\text{YMDVGGKK}$ (aminoxy)- CONH_2 (*—Linked disulfide bridge) 75
- Fig. 4.2 **a** Platinum(IV)-AHNP conjugates are much more efficiently taken up into cells. Whole cell (left) and nuclear (right) uptake after drug treatment (20 μM) for 4 h in NCI-N87 as measured by ICP-MS. Statistical analysis by unpaired Student's *t* test. **b** Platinum(IV)-AHNP conjugates selectively kill HER2 over-expressing NCI-N87 over the normal HER2 expressing A2780. A co-culture of NCI-N87 and A2780 (pre-stained with CellTracker™ Green) was drug-treated for 24 h before viability staining with PI. Statistical analysis by two-way ANOVA and Bonferroni post-tests. Means \pm s.e.m. (**p* < 0.05, ***p* < 0.01, ****p* < 0.001). 77
- Fig. 4.3 Apoptosis was evaluated by AnnexinV/PI staining of drug-treated cells after 24 h. **a** Scatter plot of treated NCI-N87 cells (15 μM drug). **b** Barchart of apoptosis-sensitive NCI-N87 (left) and apoptosis-resistant BT-474 (right) after 24 h exposure. Each bar depicts % of cells at either early-stage apoptosis, late-stage apoptosis or necrosis. Tabulated data in Table S4.1 . . . 78
- Fig. 4.4 **a** Representative overlaid microscopy images of control and treated NCI-N87 (15 μM drug for 24 h and allowed to recover

	in fresh media for a week). Differences in nuclear morphology were visualized by Hoechst 3342 staining. Untreated cells were shown at day 1 while drug-treated cells were shown at day 6. b 4a-treated NCI-N87 undergoes short-term proliferation 24 h after drug treatment but display increasing severe nuclear fragmentation over 7 d (left to right). c Clonogenic assay of NCI-N87 (left) and BT-474 (right) to assess the long-term proliferation ability of single cells drug-treated for 24 h and allowed to recover in fresh complete media. Representative image of AHNP-treated NCI-N87 colonies shown in the inset. Statistical analysis by unpaired Student's <i>t</i> test against non-treated control. Means \pm s.e.m. (***) <i>p</i> < 0.001)	79
Fig. S4.1	Measurements of cellular ROS on NCI-N87 after drug-treatment using 2',7'-dichlorofluorescein diacetate (DCFDA) which measures general oxidative stress. In some cases, cells were co-treated with butylated hydroxyanisole (BHA), an antioxidant. t-butyl hydroperoxide-treated cells was included as a positive control	87
Fig. S4.2	Intermediate-term potency of the drug conjugates as determined by MTT measurements of cellular metabolic activity after 72 h drug treatment against the NCI-N87 gastric cancer cell line. a Representative dosage-response curves. b Table of absolute IC ₅₀ (μ M). Platinum concentrations were calibrated by ICP-OES.	88
Fig. S4.3	Visual fluorescence microscopy monitoring of drug-treated NCI-N87 over time. NCI-N87 was drug-treated (15 μ M for 24 h and then allowed to recover in fresh media). Nuclear morphology were visualized by Hoechst 3342 staining. There were substantial floating dead cells in drug-treated cells in the initial 24 h drug-treatment period (not shown here). When allowed to recover after 24 h drug-treatment, 4a -treated cells undergoes a transient phase of cell-proliferation, as evidenced by a decrease in empty space at 144 h. The cells exhibited increasingly abnormal nuclear morphology over time, implying that continued long-term proliferation was unviable	89
Fig. S4.4	Cell-cycle distribution of drug-treated NCI-N87 cells over time. Drug-treated cells were permeabilized with 70% v/v ethanol and stained with propidium iodide to determine DNA content	90
Fig. S4.5	Representative photos of clonogenic assay on NCI-N87 to assess the long-term proliferation ability of drug-treated cells.	

	Single cells were seeded in a 6-well plate, drug-treated for 24 h and allowed to recover in fresh complete media for a further 15 d before counting the number of colonies formed. The number of single cells seeded per well is written on the plates	91
Fig. S4.6	a ^1H NMR of oxaliplatin(IV)-benzaldehyde scaffold 2 in DMSO- d_6 . b ESI-MS (-) characterisation of 2 : Fullscan, zoom scan (isotopic pattern) and MS/MS (top to bottom). m/z : Calculated 604.5 $[\text{M}-\text{H}]^-$, found 604.0. c RP-HPLC purity assessment of 2 dissolved in MeCN-H $_2$ O using Shimpack VP-ODS column (150 \times 5.60 mm i.d). Elution condition: 8–30% solvent B for 10 min, 30% solvent B for 8 min and finally 30–80% solvent B for 7 min	93
Fig. S4.7	a ESI-MS (-) characterisation of cisplatin(IV)-AHNP conjugate 3a : Fullscan and zoom scan (isotopic pattern) m/z : calculated 1189.1 $[\text{M}-2\text{H}]^{2-}$, found 1188.6. b HPLC chromatogram of cisplatin(IV)-AHNP conjugate 3a . The purity of the compound was assessed using Shimpack VP-ODS column (150 \times 5.60 mm i.d). Elution Condition: 8–30% solvent B for 10 min, 30% solvent B for 8 min and finally 30–80% solvent B for 7 min	96
Fig. S4.8	a ESI-MS (-) characterisation of cisplatin(IV)-dAHNP conjugate 3b : Fullscan and zoom scan (isotopic pattern) m/z : calculated 1181.1 $[\text{M}-2\text{H}]^{2-}$, found 1180.9. b HPLC chromatogram of cisplatin(IV)-dAHNP conjugate 3b . The purity of the compound was assessed using Shimpack VP-ODS column (150 \times 5.60 mm i.d). Elution Condition: 8–30% solvent B for 10 min, 30% solvent B for 8 min and finally 30–80% solvent B for 7 min	97
Fig. S4.9	a ESI-MS (-) characterisation of oxaliplatin(IV)-AHNP conjugate 4a : Fullscan and zoom scan (isotopic pattern) m/z : calculated 1237.8 $[\text{M}-2\text{H}]^{2-}$, found 1237.1. b HPLC chromatogram of oxaliplatin(IV)-AHNP conjugate 4a . The purity of the compound was assessed using Shimpack VP-ODS column (150 \times 5.60 mm i.d). Elution Condition: 8–30% solvent B for 10 min, 30% solvent B for 8 min and finally 30–80% solvent B for 7 min	98
Fig. S4.10	a ESI-MS (-) characterisation of oxaliplatin(IV)-dAHNP conjugate 4b : Fullscan and zoom scan (isotopic pattern) m/z : calculated 1229.8 $[\text{M}-2\text{H}]^{2-}$, found 1229.6. b HPLC chromatogram of oxaliplatin(IV)-dAHNP conjugate 4b . The purity of the compound was assessed using Shimpack VP-ODS column (150 \times 5.60 mm i.d). Elution Condition:	

	8–30% solvent B for 10 min, 30% solvent B for 8 min and finally 30–80% solvent B for 7 min	99
Fig. 5.1	Putative multimodal immuno-chemotherapeutic action	105
Fig. 5.2	Synthesis of <i>cis,cis,trans</i> -diamminedichlorohydroxy (4-formylbenzoate) platinum(IV) (1), <i>cis,cis,trans</i> - diamminedichloro(acetato)(4-formylbenzoate) platinum(IV) (2) and subsequent oxime ligation with various peptides	106
Fig. 5.3	Cytotoxicity IC ₅₀ of FPR1/2-targeted platinum(IV)-peptide prodrugs against FPR1/2 overexpressing cell-lines. The cell-viability of drug-treated cells was measured after 72 h incubation to plot a dose-response curve and determine the absolute IC50. Drug concentrations were calibrated to platinum measurements via ICP-OES. Means ± s.e.m. (* <i>p</i> < 0.05, *** <i>p</i> < 0.0001; Student's <i>t</i> test).	107
Fig. 5.4	Summary of drug induced cell-mediated cytotoxicity. Average cell viability (%) of U-87MG, MCF-7 and MDA-MB-231 when co-incubated with drug-treated PBMCS after 72 h. Means ± s.e.m. (*** <i>p</i> < 0.0001; Student's <i>t</i> test compared against non-activated PBMCS).	109
Fig. 5.5	Secretion of the extracellular cytokines, IFN-γ and TNF-α, after treatment of the complex 4 , free WKYMVm peptide and cisplatin for 24 h, as determined by sandwich ELISA of the cellular supernatant. Means ± s.e.m. (** <i>p</i> < 0.01, *** <i>p</i> < 0.0001; Student's <i>t</i> test)	110
Fig. S5.1	Platinum uptake studies of platinum(IV)-WKYMVm conjugate 4 in FPR1/2-expressing U-87MG cells after 4 h of incubation following pre-incubation with increasing concentrations of free competitive WKYMVm. ICP-MS readings were adjusted to pmol Pt per 10 ⁶ cells	115
Fig. S5.2	¹ H NMR spectra of complex 1 in DMSO-d ₆ with water suppression.	116
Fig. S5.3	ESI-MS (Methanol, -ve mode) characterization of complex 1 : Fullscan, MS/MS and zoomscan (top to bottom): m/z: found: 464.9 [M-H] ⁻ , calculated: 466.1.	116
Fig. S5.4	¹ H NMR spectra of complex 2 in DMSO-d ₆	117
Fig. S5.5	ESI-MS (Methanol, -ve mode) characterization of complex 2 : Fullscan, zoomscan and MS/MS (top to bottom): m/z: found: 506.82 [M-H] ⁻ , calculated: 508.2.	118
Fig. S5.6	RP-HPLC assessment of purity of Pt-Ac-benzaldehyde 2 dissolved in MeCN-H ₂ O. Elution conditions for both spectra (A) and (B): 20–80% gradient elution system with aq. NH ₄ OAc buffer (10 mM, pH 7) (solvent A) and MeCN (solvent B) over 20 min at 1.0 mL/min. Column used is: Shimpack VP-ODS column (150 × 4.60 mm i.d)	119

Fig. S5.7	HPLC spectra of crude reaction mixture of Pt(IV)-OH-aminooxy-2-12 (3a) at 295 nm. Elution conditions: 8–45% B for 30 min followed by 90% B for the next 10 min. NH ₄ OAc buffer (10 mM, pH 7) (solvent A) and MeCN (solvent B) at 2.0 mL/min	119
Fig. S5.8	RP-HPLC assessment of purity of Pt(IV)-OH-aminooxy-2-12 (3a) dissolved in MeCN–H ₂ O. Elution conditions: 20–80% gradient elution system with aq. NH ₄ OAc buffer (10 mM, pH 7) (solvent A) and MeCN (solvent B) over 20 min at 1.0 mL/min. Column used is: Shimpack VP-ODS column (150 × 4.60 mm i.d)	120
Fig. S5.9	ESI-MS (Methanol, +ve) characterization of conjugate 3a : fullscan, zoomscan and MS/MS (top to bottom): m/z: found: 915.6 [M+2H] ²⁺ and 1831.3 [M+H] ⁺ ; calculated: 1830.7.	120
Fig. S5.10	HPLC spectra of crude reaction mixture of Pt(IV)-OH-aminooxy-2-26 (3b) at 295 nm. Elution conditions: 8–45% B for 38 min, 45–80% B for 2 min followed by 90% B for the next 10 min. NH ₄ OAc buffer (20 mM, pH 7) (solvent A) and MeCN (solvent B) at 2.0 mL/min	121
Fig. S5.11	RP-HPLC assessment of purity of Pt(IV)-OH-aminooxy-2-26 (3b) dissolved in MeCN–H ₂ O. Elution conditions: 20–80% gradient elution system with aq. NH ₄ OAc buffer (10 mM, pH 7) (solvent A) and MeCN (solvent B) over 20 min at 1.0 mL/min. Column used is: Shimpack VP-ODS column (150 × 4.60 mm i.d)	121
Fig. S5.12	ESI-MS (Methanol, +ve) characterization of conjugate 3b : fullscan, zoomscan and MS/MS (top to bottom): m/z: found: 1784.2 [M+2H] ²⁺ ; calculated: 3568.6	122
Fig. S5.13	HPLC spectra of crude reaction mixture of Pt(IV)-OH-aminooxy-WKYMVm (3c) at 295 nm. Elution conditions: 8–50% B for 45 min followed by 90% B for the next 15 min. NH ₄ OAc buffer (10 mM, pH 7) (solvent A) and MeCN (solvent B) at 2.0 mL/min	122
Fig. S5.14	RP-HPLC assessment of purity of Pt(IV)-OH-aminooxy-WKYMVm (3c) dissolved in MeCN–H ₂ O. Elution conditions: 20–80% gradient elution system with aq. NH ₄ OAc buffer (10 mM, pH 7) (solvent A) and MeCN (solvent B) over 20 min at 1.0 mL/min. Column used is: Shimpack VP-ODS column (150 × 4.60 mm i.d)	123
Fig. S5.15	ESI-MS (Methanol, +ve) characterization of conjugate 3c : fullscan, zoomscan and MS/MS (top to bottom): m/z: found: 1376.9 [M+H] ⁺ ; calculated: 1375.4.	123
Fig. S5.16	HPLC spectra of crude reaction mixture of Pt(IV)-OH-aminooxy-fMLFK (3d) at 295 nm. Elution conditions:	

	8–45% B for 30 min followed by 90% B for the next 10 min. NH ₄ OAc buffer (10 mM, pH 7) (solvent A) and MeCN (solvent B) at 2.0 mL/min	124
Fig. S5.17	RP-HPLC assessment of purity of Pt(IV)-OH-aminooxy-fMLFK (3d) dissolved in MeCN–H ₂ O. Elution conditions: 20–80% gradient elution system with aq. NH ₄ OAc buffer (10 mM, pH 7) (solvent A) and MeCN (solvent B) over 20 min at 1.0 mL/min. Column used is: Shimpack VP-ODS column (150 × 4.60 mm i.d)	124
Fig. S5.18	ESI-MS (Methanol, –ve) characterization of conjugate 3d : zoomscan, MS/MS and fullscan (top to bottom): m/z: found: 1084.1 [M–H] [–] ; calculated: 1085.3.	125
Fig. S5.19	HPLC spectra of crude reaction mixture of Pt(IV)-Ac-aminooxy-WKYMVm (4) at 295 nm. Elution conditions: 8–50% B for 45 min followed by 90% B for the next 15 min. NH ₄ OAc buffer (10 mM, pH 7) (solvent A) and MeCN (solvent B) at 2.0 mL/min	125
Fig. S5.20	RP-HPLC assessment of purity of Pt(IV)-Ac-aminooxy-WKYMVm (4) dissolved in MeCN–H ₂ O. Elution conditions: 20–80% gradient elution system with aq. NH ₄ OAc buffer (10 mM, pH 7) (solvent A) and MeCN (solvent B) over 20 min at 1.0 mL/min. Column used is: Shimpack VP-ODS column (150 × 4.60 mm i.d)	126
Fig. S5.21	ESI-MS (Methanol, +ve) characterization of conjugate 4 : zoomscan, MS/MS and fullscan (top to bottom): m/z: found: 1419.1 [M–H] [–] ; calculated: 1419.4.	126
Fig. 6.1	Schematic of drug-induced immunogenic cell death (ICD)	132
Fig. 6.2	Structures of platinum agents used in this study.	133
Fig. 6.3	Phagocytosis screening: a orange-stained CT-26 cells were drug-treated (4 h) before co-incubating (2 h) with green-stained J774 macrophages and analysed by flow cytometry. The phagocytosis % was calculated from the no. of double-stained macrophages over total no. of macrophages. Inset: Fluorescence microscopy of J774 macrophages (green) engulfing CT-26 (red) as evident by mixing of the dyes. b Representative flow cytometry scatter plots showing increased phagocytosis (top right quadrant) with Pt-NHC over control. c Coating CT-26 with rCRT enabled phagocytosis while co-incubation with a CRT blocking peptide abolished phagocytosis. Means ± s.e.m. (* <i>p</i> < 0.05, ** <i>p</i> < 0.01, *** <i>p</i> < 0.0001; Student's <i>t</i> test)	135
Fig. 6.4	a Left: rapid patch-like surface exposure of CRT observed by confocal microscopy after drug-treatment (1 h) of CT-26 followed by surface immuno-fluorescence staining with	

	anti-CRT mAb. Right: HMGB1 release from the nuclei of CT-26 after 24 h drug-exposure (permeabilised and stained with both anti-HMGB1-Dy488 mAb and PI). b Pt-NHC enhanced ecto-CRT exposure in live cells (red shaded) compared to non-treated control (dotted line). CT26 cells were treated for 1 h (gated against PI-cells) and 4 h (gated against AnnexinV-cells) and surface-stained with an anti-CRT-PE mAb. c Left: extracellular release of ATP (left) and HMGB1 (right) of CT-26 after 24 h exposure. Means \pm s.e.m. ($*p < 0.05$, $**p < 0.01$; Student's <i>t</i> test).	136
Fig. 6.5	The anti-oxidant, trolox, quenches cellular ROS and this in turn inhibits phagocytosis. CT-26 was first pre-treated with trolox (30 min) prior to drug exposure and later co-treated with trolox and Pt-NHC (4 h). a Trolox quenched Pt-NHC induced ROS as analysed by flow cytometry. b Co-incubation of Pt-NHC with trolox significantly inhibited tumour cell phagocytosis. Means \pm s.e.m. ($*p < 0.05$, $**p < 0.01$; Student's <i>t</i> test).	137
Fig. 6.6	Cytotoxicity of Pt agents via Annexin V apoptosis assay. CT-26 cells were treated for 24 h and stained with AnnexinV-eGFP and propidium iodide. Means \pm s.e.m.	138
Fig. S6.1	Cells observed under confocal microscopy after drug treatment (4 h) and incubation with H ₂ DCFDA (ROS indicator, green) and ER-Tracker Red (red). a CT-26. b MDA-MB-231. c Colocalisation analysis after Pt-NHC treatment (1 μ M) on MDA-MB-231. White pixels indicate areas of colocalisation as determined by Costes method.	142

List of Tables

Table 1.1	Standard reduction potentials of various platinum(IV) complexes adjusted against standard hydrogen electrode reference [108]	17
Table S2.1	Representative summary of experimental data for curve fitting	50
Table 3.1	Conversion yields of 1 and 2 to cisplatin as well as satraplatin to JM118. Values are reported as mean with standard error	63
Table S3.1	Maximum solubility of 1 and 2 and satraplatin in PBS (pH 7.4). Values are reported as mean with standard error	69
Table S4.1	Tabulated data of apoptosis as evaluated by AnnexinV/PI staining of drug-treated NCI-N87 or BT-474 cells after 24 h. Each cell depicts mean % of cells at either early apoptosis, late apoptosis or necrosis	92

List of Schemes

Scheme 1.1	Oxidation of platinum(II) to platinum(IV) complexes.	11
Scheme 1.2	Schematic diagram for symmetrical dicarboxylation of platinum(IV) complexes	12
Scheme 1.3	Schematic diagram for asymmetrical carboxylation of platinum(IV) complexes	13
Scheme 2.1	Synthesis of <i>trans,cis,cis</i> -bis(4-formylbenzoate) dichlorodiammine platinum(IV) (1) and subsequent imine ligation with various substrates.	36
Scheme S4.1	Synthesis of platinum(IV)-AHNP conjugates. Reaction conditions: (I) succinimidyl 4-formylbenzoate, in DMSO, r.t. (II) acetic anhydride in DMF, r.t. (III) H ₂ O ₂ in acetic acid, r.t. (IV) 4-formyl-benzoyl chloride in acetone, pyridine, reflux. AHNP: H ₂ N-YC*DGFYAC*YMDVGGKK(aminooxy)-CONH ₂ ; dAHNP: fC*DGFYAC*yMDVGGKK(aminooxy)-CONH ₂ (*—Linked disulfide bridge).	87

Summary

Platinum-based chemotherapeutics such as cisplatin, carboplatin and oxaliplatin have been the mainstay of chemotherapy regimens for the treatment of many cancers for the last few decades. Nonetheless, clinical interest in new platinum agents appears to be waning with only a handful entering clinical trials recently. Till date, thousands of novel cytotoxic platinum complexes have been synthesized but only a few attain clinical relevance. This thesis highlights existing limitations of platinum drug design and proposes avenues for further exploration with focuses on molecularly targeted platinum chemotherapeutics with novel mechanisms of action and on combined immuno-chemotherapeutic platinum agents.

The work described in Chaps. 2 and 3 are the foundation underpinning the subsequent chapters. In Chap. 2, we developed a facile conjugation strategy via chemoselective imine ligation to tether relevant biomolecules to a platinum(IV) prodrug scaffold. This strategy was used repeatedly to synthesize the targeted platinum(IV)-peptide conjugates described in Chaps. 4 and 5. In Chap. 3, we sought to answer whether our class of asymmetrical platinum(IV) aryl scaffolds were really prodrugs of cisplatin. Validation of the platinum(IV) prodrug hypothesis is important because it is the underlying working assumption behind the targeted platinum(IV)-peptide strategies described in Chaps. 4 and 5.

The recognition that certain molecular pathways are critical to carcinogenesis and continued tumour progression and may therefore represent an Achilles' heel has triggered a revolution in cancer drug development. These molecularly targeted chemotherapeutics have made considerable progress in the clinical outcomes for many malignancies. In Chap. 4, we have developed highly potent and selective HER2-targeted platinum(IV)-AHNP prodrugs which demonstrate the feasibility of an idea of 'targeted necrosis' as a novel strategy to circumvent apoptosis resistance.

Finally, in Chaps. 5 and 6, we describe our conceptualization and realization of combined platinum-based immuno-chemotherapeutic agents which represents a significant paradigm shift from the conventional approach of directly targeting cancer. Historically, the role of the immune system towards chemotherapy outcomes has been neglected as anticancer drugs were believed to be immuno- and myelo-suppressive. Nonetheless, this has been challenged by contemporary evidence which

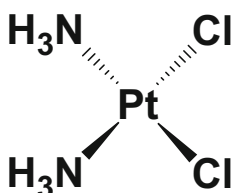
now suggests that many chemotherapeutics, including platinum-based agents, do stimulate the innate and/or adaptive immune system and that these ‘secret allies’ contribute tangibly towards clinical outcomes. While it has been generally accepted that platinum agents principally exert direct cytotoxic action against cancer cells via the formation of covalent platinum-DNA adducts, the recognition of platinum-induced antitumour immunomodulation is only beginning to gain traction. There have been compelling empirical evidences corroborating the immunomodulating capacity of platinum-based therapy with favourable chemotherapy outcomes. The work described here may ultimately pave the way towards superior immuno-chemotherapeutic agents and a better clinical outcome in patients.

Chapter 1

Introduction



Cisplatin—Now and Future



1.1 Overview

Cancer has been a leading cause of mortality both globally and locally, with increasing incidence rates as a consequence of an aging population, environmental factors and lifestyle choices [1]. The life-time risk of cancer has been estimated to be over 1 in 3 persons [2]. Worldwide, there are appx. 6 million cancer-related deaths annually, a figure which is expected to nearly treble to appx. 17 million deaths annually by 2030 according to recent estimates by the International Agency of Cancer Research [1]. The undisputable human cost and economic burden of cancer has been a driving force spurring substantial investments into cancer research which has since yielded tangible payoffs within the last few decades [3]. The five-year survival rate for all cancers in the United States is expected to rise from 38% in the 1960s to 80% by 2015 [4]. The ten-year survival rates of many previously “untreatable” cancers such as testicular cancer, malignant melanoma, prostate cancer and many forms of leukemia already exceeds >80%. Even so, the prognosis for many common types of cancer such as lung, pancreatic, colon and stomach cancers remains dismal.

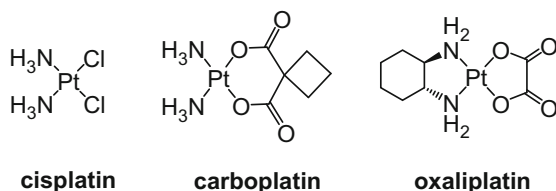
Contemporary cancer treatment can be viewed as a four-legged stool perched on the legs of surgery, radiation therapy, chemotherapy and immunotherapy [4]. At present, advancements in surgery and radiation techniques have tremendously

improved treatment outcomes in patients diagnosed with early-stage cancers. For instance, the surgical resection of stage I/II breast cancer (where the tumor is localized and has not spread) has achieved an impressive cure rate of appx. 90% [5]. However, it was already known since the 1950s that surgical excision and radiation therapy could ever only achieve curative potential in about one-third of incidences when the cancer has not yet metastasized [4]. Metastasis, which is the cause of 90% of cancer-related deaths [6], has been the biggest, as yet insurmountable challenge in cancer treatment which can only be addressed by systemic whole-body modalities like chemotherapy. Neither surgery nor radiation therapy can replace this niche. Immunotherapy, which harnesses the body's own immune response against cancer, is another form of systematic therapy. It has only very recently cemented its position as the fourth leg in the anticancer repertoire [7].

Today, platinum-based agents such as cisplatin, carboplatin and oxaliplatin (Fig. 1.1) are amongst the most widely used and effective cytotoxic agents in clinical use as part of a chemotherapy regime [8–10] in combination with a broad range of other drugs such as doxorubicin, gemcitabine, vinblastine and paclitaxel [11]. It has been estimated that between 50 and 70% of chemotherapy cocktails include a platinum-based agent [12]. With the exception of breast and prostate cancer, platinum-based therapy has been indicated for almost all solid malignancies including testicular, ovarian, bladder and non-small cell lung cancer [13, 14]. Indeed, the dramatic improvement in testicular cancer mortality from 90 to <5% could be attributed to the serendipitous discovery of the anti-cancer properties of cisplatin in 1965 by Rosenberg and colleagues [15, 16].

The key focus of this thesis is on creating a new generation of platinum-based agents. Despite its therapeutic value, cisplatin has severe adverse side effects such as renal nephrotoxicity, neurotoxicity and nausea [17]. Another major limitation is that many common tumours such as colorectal, ovarian and breast cancers are either inherently resistant to cisplatin or develop acquired resistance after initial treatment [18]. Spurred by the clinical success of cisplatin, other platinum(II) analogues such as carboplatin (approved in 1989) and oxaliplatin (approved in 2002) were developed to address some of the aforementioned shortcomings. Nonetheless, despite extensive research and evaluation of thousands of platinum(II) complexes, only a handful have shown distinguishing pharmacological properties to be singled out for clinical use [19]. Thus in this context, this thesis attempts to offer a rethink of platinum-based anticancer drug design via two distinct approaches, molecularly-targeted chemotherapeutics and by amalgamated immuno-chemotherapeutic agents which combines both chemotherapy and immunotherapy into a synergistic two-pronged agent.

Fig. 1.1 Platinum-based anticancer drugs which have recieved international clinical approval



1.2 Cellular Uptake and Molecular Mechanism of Action

The cellular uptake and molecular mechanism of action of cisplatin has been extensively studied (Fig. 1.2). Following intravenous administration, the majority of cisplatin is inactivated due to irreversible binding to plasma proteins (e.g. human serum albumin) and is renally excreted [20]. Only a fraction of administered cisplatin (about 30%) remains active and is circulated in the bloodstream. The uptake of cisplatin across the cell membrane has been linked to both passive diffusion across the lipophilic barrier as well as active transport via copper transporter (Ctr1) [21]. Cisplatin binds to the methionine-rich motifs of the extracellular domains of Ctr1, a transmembrane-bound transporter for monovalent copper which is ubiquitously expressed. Downregulation of Ctr1 in yeast and fibroblast cells is tied to decreased cisplatin uptake. Accordingly, high Ctr1 expression has been correlated to cisplatin efficacy in cancer cells where else mutations in Ctr1 has been associated with cisplatin resistance [22]. Another set of transporters, ATP7A and ATP7B (which are also involved in cisplatin efflux), have been implicated in mediating the sub-cellular compartmentalization of cisplatin [22]. The organic cation transporter (OCT1/2) has been implicated in oxaliplatin uptake, perhaps reflecting its more organic nature due to its cyclohexane moiety [23].

Within cells, cisplatin is rapidly hydrolyzed due to sharply lowered chloride concentrations of between 2 and 30 mM in intracellular regions as compared to extracellular concentrations of around 100 mM. This forms a very reactive

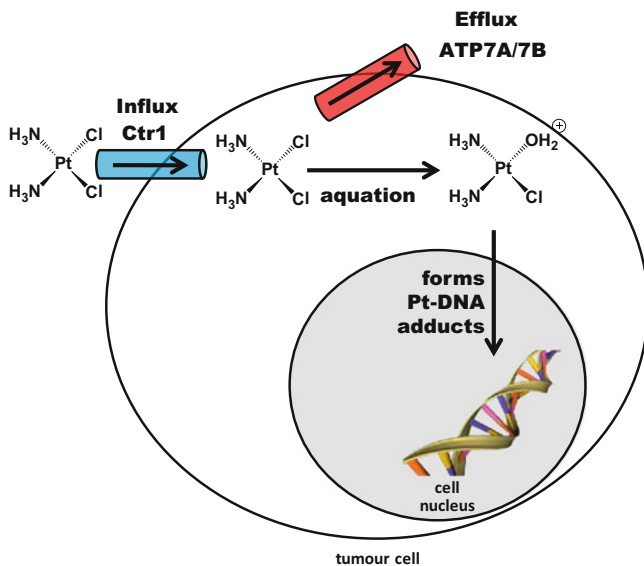
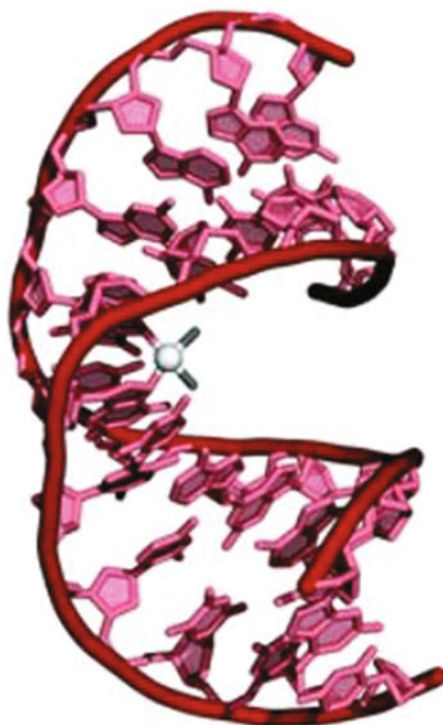


Fig. 1.2 The uptake and cytotoxic pathway of cisplatin. Upon entering the cell, cisplatin is hydrolyzed forming a reactive aquated species which then binds to cellular DNA leading to eventual cell death

positively charged $[\text{Pt}(\text{H}_2\text{O})(\text{Cl})(\text{NH}_3)_2]^+$ complex which is highly reactive because H_2O is a very good leaving group [24, 25].

These positively charged aquated species binds preferentially to the electron rich N7 site of guanine residues, and adenosine to a lesser extent, on negatively charged DNA to form a mono-adduct. The other chloride can then undergo hydrolysis leading to the formation of a bifunctional adduct. Cisplatin-DNA binding can form many types of adducts including 1,2-d(GpG) or 1,2-d(ApG) intrastrand cross links, 1,3-intrastrand cross links as well as interstrand cross links between DNA molecules or with cellular proteins [9, 11–13]. It is generally accepted that the primary cause of cisplatin cytotoxicity is the formation of 1,2-intrastrand cross links which cause DNA to distort significantly towards the major groove in double stranded DNA [26–28] although this is still debatable [20]. These 1,2-d(GpG) intrastrand cross links accounts for 60–65% of bound platinum [29] and bend the DNA double helix by 30° – 60° towards the major groove with consequent unwinding of the helix by up to 23° [30], thus hindering normal DNA replication and transcription processes [13]. These distortions are then recognized by various DNA-damage recognition proteins and histones, ultimately leading to cell death through apoptosis, necrosis or a combination of both [31–33]. These proteins include high-mobility group box protein 1 (HMGB1), TATA box-binding protein and 3-methyladenine DNA glycosylase (AAG) mammalian repair proteins among others. These proteins recognize and process DNA lesion formed by cisplatin and oxaliplatin differently as

Fig. 1.3 Illustration of the kink formed by the major 1,2-d(GpG) intrastrand crosslink in double stranded DNA. Reproduced from Ref. 20 with permission from The Royal Society of Chemistry [20]



they are structurally different, which may account for their differences in cytotoxicity [33]. DNA interstrand crosslinks and DNA-protein cross-links do play a role in cytotoxicity as well [32].

Besides DNA binding, cisplatin cytotoxicity has also been linked to non-DNA cellular targets. For instance, cisplatin binds to ubiquitin [34], an enzyme responsible for the selective degradation of cellular proteins, and to heat shock protein (Hsp90) [35], a protein responsible for the correct folding of cellular proteins including those pivotal in cell cycle regulation. There have also been some inquiry into the role of mitochondria as the fundamental target of cisplatin cytotoxicity [36]. Cisplatin also interferes with cellular RNA processing through platinum-RNA adducts but the biological significance of this remains to be elucidated [37].

As mentioned above, the formation of 1,2-intrastrand cross links as the primary cause of cisplatin cytotoxicity is debatable as only approximately 1% of intracellular cisplatin interacts with DNA. A simple molecule like cisplatin without intricate 3-dimensional pharmacophore features is likely to bind promiscuously to a myriad of cellular nucleophiles. It has been shown that the cisplatin binds preferentially to macromolecules with molecular masses greater than 30 kDa as compared to more abundant smaller molecular weight nucleophiles which runs counterintuitive to conventional logic [38]. It was suggested that the tendency of cisplatin to bind irreversibly to sulfhydryl groups, inhibits numerous sulfhydryl-containing enzymes, contributing to cisplatin-induced cytotoxicity [39]. Furthermore, Price and colleagues elegantly demonstrated that cisplatin could initiate apoptosis from the cytoplasm independent of the nucleus in kidney cells [40]. The participation of CDK2 in cisplatin-triggered apoptosis was shown *in vivo* and *in vitro* while inhibition of CDK2 by p21 conferred protection against cisplatin cytotoxicity. Surprisingly, the deletion of the nuclear localization signal of p21 did not affect its cytoprotective action against cisplatin toxicity, bringing into question the role of the nuclear DNA.

While a short introduction of the biochemical mechanisms of cisplatin activity has been given herein, an in-depth review is beyond the scope of this introduction as the subject matter is very extensive and studies are still on-going. In particular, platinum cellular influx mechanisms as well as the precise mechanisms by which DNA platination triggers various cellular signaling pathways remain to be elucidated [41, 42]. Nonetheless, detailed and comprehensive reviews on this subject matter have been written by Lippard, Perez and Natiles among others [6, 18, 25, 26].

1.3 Limitations

Side effects. Historically, cisplatin is notorious for having harsh dose-limiting side effects which can be grueling to tolerate and which compromises its efficacy in a hospitalization setting where many patients are already frail. This is not unexpected, given the indiscriminate killing nature of a non-targeted compound like cisplatin. These side effects, which include nephrotoxicity, neurotoxicity, ototoxicity and nausea, have been somewhat attenuated but not completely resolved by later generations of platinum agents such as carboplatin and oxaliplatin [43]. For

instance, over 85–95% of patients treated with oxaliplatin suffered adversely from neurotoxicity, with up to 26% of patients requiring hospitalization as a result and which is often the basis for treatment discontinuation [22, 44]. The symptoms of oxaliplatin-induced neurotoxicity includes numbness in the extremities as well as a loss of fine sensory-motor coordination [22].

The general toxicity profile differs among different platinum agents. Cisplatin triggers acute and/or chronic kidney injury in about 1/3 of patients, even with pre-hydration and prophylactic administration of diuretics [45], and is an independent risk factor which dramatically increases mortality by 10 to 15-fold [46]. In contrast, carboplatin is only rarely nephrotoxic while nephrotoxicity with oxaliplatin is unheard of [22]. Likewise, ototoxicity is clinically significant with cisplatin, which occurs in up to 50% of adults and over 50% of pediatric patients, but not with oxaliplatin [22]. In contrast, neurotoxicity occurs at a higher frequency in association with oxaliplatin compared to cisplatin [47].

Drug resistance phenomena. Drug resistance phenomena against platinum agents remains an enduring problem. Many tumours are either inherently resistant (e.g. colon cancer) to platinum-based antitumour agents or develop acquired resistance (e.g. ovarian cancer) after several treatment cycles. In many cases, the initial favorable response rates of cisplatin treatment are not durable due to the onset of resistance which results in high relapse rates and consequently low 5-year survival [48]. Cellular resistance to cisplatin is multi-factorial and has been linked to (1) up-regulation of DNA repair and damage tolerance pathways [20, 42], (2) decreased intracellular accumulation associated to copper efflux transporters ATP7A and ATP7B [49, 50] and (3) inactivation by thiol containing small molecules such as glutathione [51]. Platinum-based drugs are also particularly vulnerable to irreversible sequestration by macromolecular plasma proteins such as albumin which deactivates the drug and has also been associated with some severe side effects of treatment [52].

In addition, it is well recognized that the failure of many chemotherapeutics (including platinum agents) arises due to an inability, at a cellular level, to induce apoptosis [48, 53]. Most cancers acquire a bewildering array of pro-survival adaptations such as a mutated p53 tumor suppressor gene and upregulation of the anti-apoptotic Bcl-2 signal which renders the cancer refractory to cisplatin along with many other chemotherapeutics. Although a number of experimental strategies to restore apoptosis sensitivity has been explored, these are severely challenged by the vast heterogeneity and accumulation of multiple unrelated pro-survival mutations simultaneously even within the same tumor mass which hinders such molecular-targeted strategies [54].

Continued relevance in an age of molecularly-targeted therapy? Traditionally, the design of novel platinum(II) complexes entails the permutations of both the non-labile non-leaving groups and the labile leaving groups [55]. As the thermodynamically stable non-leaving groups (NH_3 in cisplatin and DACH in oxaliplatin) affect the structure of the consequent platinum-DNA adducts, they determine the cytotoxicity and spectrum of activity against various cancers. It has been hypothesized that oxaliplatin overcomes cisplatin resistance by virtue of its bulky hydrophobic DACH ligand which thwarts the binding of DNA repair proteins [11].

On the other hand, the lability of the leaving groups (chloride in cisplatin, 1,1-cyclobutanedicarboxylate in carboplatin and oxalate in oxaliplatin), has been associated with toxicity. Thus carboplatin has fewer side effects than cisplatin due to the replacement of the chloride ligands (aquation rate constant of 10^{-5} s^{-1}) with 1,1-cyclobutanedicarboxylate (aquation rate constant of 10^{-8} s^{-1}) [11].

Today, molecularly-targeted therapies have dramatically altered the landscape of cancer treatment and have supplanted traditional cytotoxic chemotherapies for many malignancies [56, 57]. This is paralleled by waning interest in the discovery of new cytotoxics with the majority of newly approved anticancer agents being now targeted therapies [56, 57]. The key idea of molecularly-targeted chemotherapy stems from the recognition that certain biomolecular pathways are critical to carcinogenesis and continued tumor growth and therefore represent an Achilles' heel which can be exploited. These pathways can be inhibited by either small molecule inhibitors or by specific antibodies. Molecularly targeted drugs are very different from traditional chemotherapy because it actually reverses the aberrant pathway driving the cancer in the first place. Gleevec (Imatinib), which inhibits BCR-Abl responsible for chronic myeloid leukemia (CML), is often referred to as a miracle drug which has transformed the field of chemotherapeutics. Before Gleevec in 2001, the 5 year survival rate for patients with CML was only 30% compared to a remarkable >89% after Gleevec [58].

Critically, the development of molecularly-targeted therapies is directed by a hypothesis-driven, rationale drug discovery approach involving biomolecular target identification, lead compound generation and subsequent optimization with clear well-delineated molecular mechanisms of action [56]. In contrast, current design strategies of platinum(II) anticancer agents may be described as somewhat "trial and error" with only some room for rationale design. In many cases, the molecular targets and mechanism of action of novel platinum agents are not well-defined, which may discourage commercial pharmaceutical interest in the compounds.

In this context, it is important to ask oneself: What is the relevance of traditional platinum agents given the rapid scientific advances made in today's treatment strategies? The author feels that current platinum agents, which continue to adhere to the age-old strategy of targeting DNA, are unlikely to have clinical relevance in today's drug regulatory climate, simply because they can only offer incremental improvements over their older counterparts. To date, over 3000 platinum compounds have been synthesized and evaluated, driven by the need to circumvent the deficiencies of existing platinum(II)-based drugs [59]. Disappointingly, only fewer than 30 potential candidates have entered clinical trials and only oxaliplatin has been approved by the FDA in 2002 since the approval of carboplatin back in 1989! [42]. While most of these platinum-based compounds have shown much promise in vitro, clinically they were more or less like their predecessors and fell short of conferring distinct clinical advantages over cisplatin [11]. This is unsurprising, since most of these complexes tend to be structural congeners of cisplatin and thus inheriting its shortcomings [41]. In addition, the predominant priority when synthesizing and evaluating platinum complexes has primarily been cytotoxicity (e.g. screening for cytotoxicity against a panel of cancer cell-lines) which may end up

overlooking other important criteria such as anti-metastatic activity and immune-modulation; properties which may differentiate novel platinum complexes from their predecessors. It has been suggested that it would be difficult to find a promising candidate having clinical properties distinct from cisplatin and oxaliplatin, from within this pool of classical platinum(II) complexes [43, 60]. In summary, the author believes that it is unlikely, short of a major paradigm shift that incremental improvements will lead to a viable clinical candidate.

In order to stay relevant, post-modern platinum drug design should adopt hypothesis-driven design from molecularly-targeted therapy while at the same time, occupying niches where targeted therapies fail. For instance, the majority of lung cancers, one of the most common cancer subtypes, do not have any validated “druggable” targets yet and would still require systemic chemotherapy [61]. In addition, the vast tumor heterogeneity within the same mass with accumulation of multiple unrelated pro-survival mutations simultaneously [62] has been a frustrating factor which limits the response rate of well-defined molecularly-targeted therapies [57, 61]. On the other hand, non-specific alkylating agents like cisplatin and oxaliplatin may have multiple modes of action arising from different biological targets including DNA [63, 64]. This broader spectrum of action could be therapeutically favorable because it potentially circumvents multi-factorial apoptosis-resistance signaling pathways. As a case in point, in Chap. 4, we describe the development of HER2/neu-targeted platinum(IV) complexes which induces targeted necrosis as a novel means of circumventing and outwitting apoptosis-resistant cancers.

1.4 The Platinum(IV) Prodrug Strategy

In recent years, there has been increasing interest in exploiting inert platinum(IV) as a prodrug strategy to mitigate the aforementioned limitations of platinum(II) anti-cancer complexes (Fig. 1.4). In principle, the kinetic inertness of platinum(IV) complexes (low spin d_6 third row transitional-metal complexes) would minimize unwanted side reactions in the bloodstream, thus reducing toxicity [9]. Also, the introduction of two axial ligands in an octahedral geometry facilitates fine-tuning of pharmacological properties of the prodrug such its specificity, activity and lipophilicity. More excitingly, these axial ligands are released concomitantly with the two electron-reduction of the platinum(IV) prodrug into its active platinum(II) congener [65], offering the possibility of conjugating targeting groups or bioactive co-drugs which may synergistically enhance cytotoxicity on cancer cells [9].

In general, platinum(IV) anti-cancer prodrugs are based on the octahedral [Pt(IV)(A₂)(X₂)(L₂)] motif, where L and X represents the equatorial ammine ligands and leaving groups respectively while A represents the axial ligands. The metal-ligand bonds of platinum(IV) complexes are kinetically inert, a property which have been exploited to chemically modify and design the axial ligands [66]. While platinum(IV) dihydroxo complexes are substitutionally inert, the oxygen atom of dihydroxo groups are strongly nucleophilic and readily attacks suitable

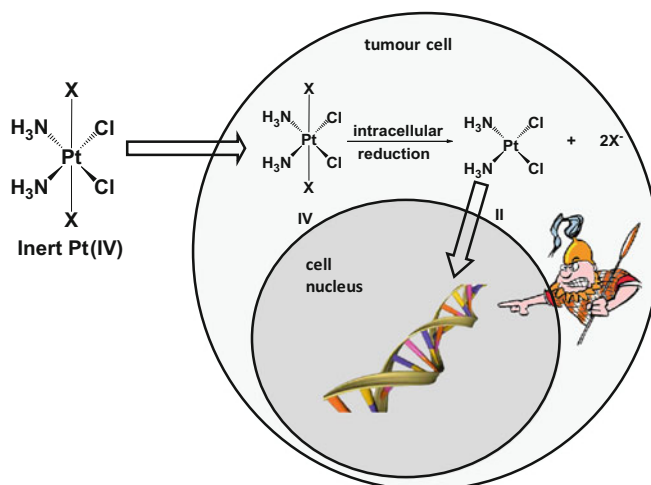
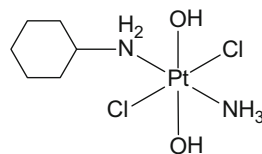


Fig. 1.4 The platinum(IV) prodrug hypothesis: reductive elimination of platinum(IV) prodrugs occurs with the release the active platinum(II) core as well as both axial carboxylate ligands

electrophiles, facilitating the preparation of platinum(IV) complexes bearing diverse axial carboxylate ligands [66]. The kinetic inertness of platinum(IV) complexes was experimentally shown by [^1H , ^{15}N] NMR spectroscopy of the aquation reactions of a series of platinum(IV) complexes bearing the general *cis,trans,cis* $[\text{Pt}(\text{II})(\text{X}_2)(^{15}\text{NH}_3)_2(\text{Cl}_2)]$ ($\text{X} = \text{Cl}$, OH and acetate) [67]. Compared to cisplatin which undergoes rapid aquation in water, aquation of the $[\text{Pt}(\text{IV})(\text{OAc})_2(^{15}\text{NH}_3)_2(\text{Cl}_2)]$ and $[\text{Pt}(\text{IV})(\text{OH})_2(^{15}\text{NH}_3)_2(\text{Cl}_2)]$ complexes was not observed on a timescale of several weeks although significant aquation of *cis*- $[\text{Pt}(\text{IV})\text{Cl}_4(^{15}\text{NH}_3)_2]$ did occur.

While there are evidences indicating that platinum(IV) complexes can bind slowly to DNA *in vitro* [38, 39, 68, 69], the general consensus is that platinum(IV) complexes are prodrugs which must be activated by reduction to its platinum(II) congener since platinum(IV) complexes are very unreactive [8]. In an early study, the antitumoral activity of several platinum(II) derivatives and their corresponding platinum(IV) complexes were tested *in vivo* and only platinum(IV) complexes which gives active platinum(II) reduction products were found to be active [70]. Therefore, platinum(IV) complexes such as *mer*- $[\text{PtCl}_3(\text{diethylenediamine})]$ which is reduced to the inactive platinum(II) $[\text{PtCl}(\text{diethylenediamine})]^+$ complex are likewise inactive too. More recently, an algorithmic analysis was conducted of 107 platinum(II) and platinum(IV) complexes from the National Cancer Institute's anticancer drug screen against its diverse panel of 60 human cancer cell lines (NCI-60). The results revealed that the spectrum of activity of these drugs could be correlated to the nature of their non-leaving groups and are independent of both the leaving groups and oxidation state [71]. This is in agreement with the prodrug hypothesis. Nonetheless, there are exceptions to this rule as certain inactive *trans*-platinum(II) complexes do have

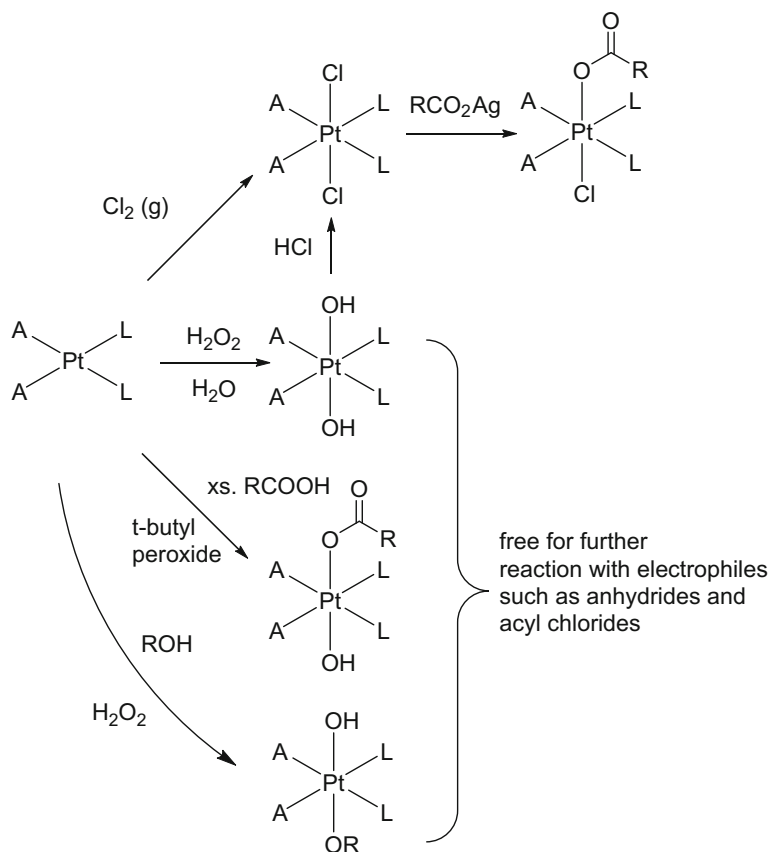
Fig. 1.5 JM335—an active platinum(IV) complex bearing *trans* equatorial geometry



corresponding active platinum(IV) counterparts. One such example is JM335, *trans*-amine(cyclohexylamine)dichlorodihydroxo-platinum(IV) (Fig. 1.5) [72]. In this case, it may be rationalized that oxidation to platinum(IV) can stabilize otherwise overly-reactive *trans* complexes.

Schemes 1.1, 1.2 and 1.3 comprehensively summarizes the most common synthetic routes for preparing axial platinum(IV) carboxylates reported thus far. By far the most common and diverse class of platinum(IV) complexes is by coordination to axial carboxylate ligands. Oxidation of platinum(II) complexes by excess hydrogen peroxide in water yields the corresponding symmetrical *trans*-dihydroxo platinum(IV) species (Scheme 1.1). The nucleophilic dihydroxo axial ligands can then be reacted in a general reaction scheme with various electrophiles such as anhydrides [73], acid chlorides [74, 75], pyrocarbonates and isocyanates [73] under mild conditions to afford dicarboxylate, dicarbonate and dicarbamate platinum(IV) complexes respectively. This enormously versatile synthetic route has been used to good effect to prepare a wide range of dicarboxylate complexes [76–78]. Besides oxidation to symmetrical dihydroxo platinum(IV) complexes, synthesis of asymmetrical mixed hydroxo-carboxylato complexes can be achieved via oxidation in a large excess of carboxylic acid with stoichiometric amount of either hydrogen peroxide or tert-butyl hydrogen peroxide [79]. This works because oxidation of platinum(II) by peroxide occurs via a mechanism whereby the axial hydroxido ligand arises from H_2O_2 while the other axial ligand originates from the bulk “solvent”. These complexes can then be further derivatised to yield a mixed dicarboxylate complex. Similarly, the facile synthesis of *cis,cis,trans*-[Pt(A)₂(L)₂(OH)(OR)] alkoxy platinum(IV) complexes could be achieved via oxidation with hydrogen peroxide in alcohol [80, 81] which can then be carboxylated to give *cis,cis,trans*-[Pt(A)₂(L)₂(OCOR¹)(OR)] [82] (Scheme 1.1). The precursor *trans*-dichloro platinum(IV) species can be made by oxidizing platinum(II) with chlorine gas [83] or by hydrolysis of dihydroxo ligands with hydrochloric acid (Scheme 1.1) [84]. The mono-carboxylated *cis,cis,trans*-[Pt(A)₂(L)₂(OCOR)(Cl)] may be then be prepared by reacting *trans*-dichloro platinum(IV) with silver carboxylates [85].

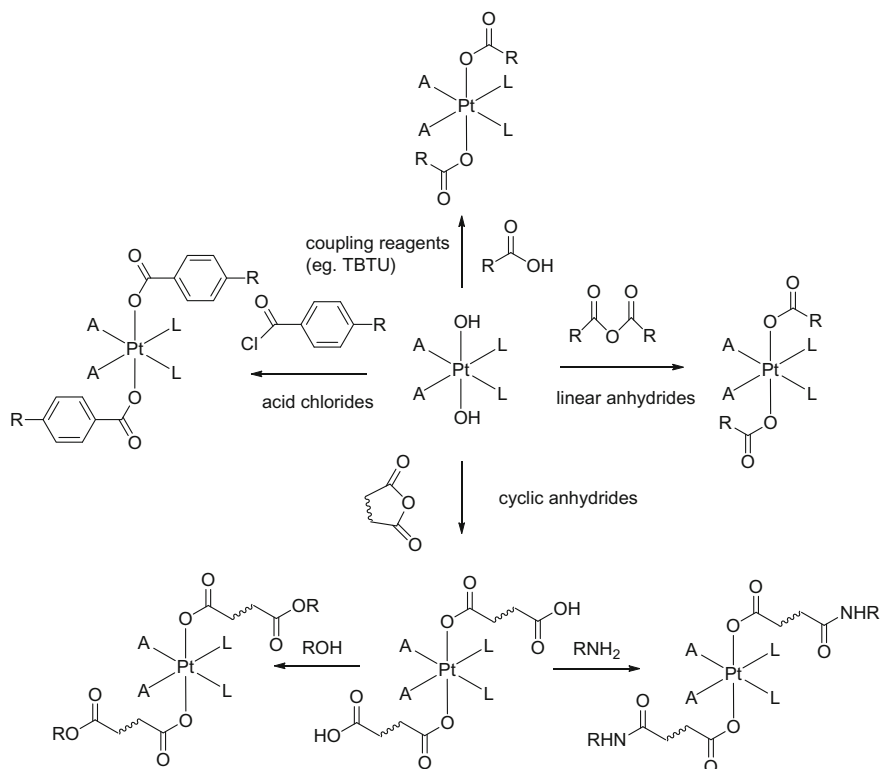
So far, symmetrical axial dicarboxylates have been the most common and most synthetically accessible type of platinum(IV) complexes reported in literature. Apart from simple anhydrides and acid chlorides, carboxylation with cyclic anhydrides (succinic, glutaric, phthalic and maleic anhydrides) [86–90] yield platinum(IV) carboxylates carrying an uncoordinated pendant carboxyl functional group which can be further conjugated via typical amide or ester coupling chemistry (Scheme 1.2) [89, 90]. Activated carboxylic acids formed by typical coupling



Scheme 1.1 Oxidation of platinum(II) to platinum(IV) complexes

reagents such as TBTU can also be used as convenient alternatives to avoid the need for reactive anhydride or acyl chloride intermediates (Scheme 1.2) [79]. These generic reaction schemes have been widely exploited to tether a considerable array of bioactive or targeting groups to platinum(IV) complexes with the aim of potentiating cytotoxicity [9].

Recently, there has been an emergent movement towards the preparation of asymmetrical platinum(IV) complexes which allows for more customization and fine-tuning of the axial ligands [91]. One synthetic route is to react *trans*-dihydroxo platinum(IV) with limiting acid anhydride under mild and dilute conditions to favor the formation of the monocarboxylate instead of the dicarboxylate product (Scheme 1.3a) [55, 91]. The use of limiting pre-activated carboxylic acids with *N,N'*-dicyclohexylcarbodiimide (DCC) also preferentially yielded the monocarboxylate species [79]. Alternatively, we have found that the comparatively less reactive *N*-hydroxysuccinimide (NHS)-ester activated carboxylic acid could be

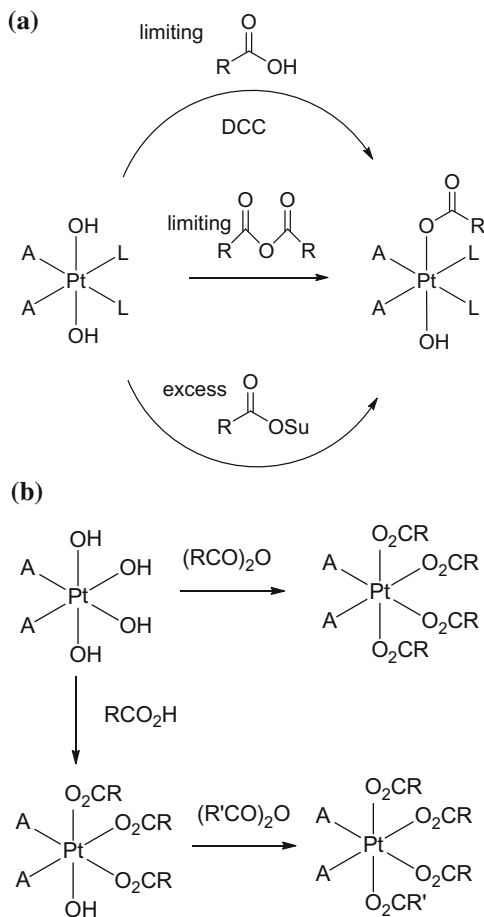


Scheme 1.2 Schematic diagram for symmetrical dicarboxylation of platinum(IV) complexes

used in great excess and still favor the formation of the monocarboxylate product under mild and dilute reaction conditions [92, 93]. Finally, it was observed that reaction of *cis*-[Pt(A)₂(OH)₄] with acid anhydrides yielded the tetracarboxylated product but reaction with less electrophilic carboxylic acids yielded the *cis, fac*-[Pt(OCOR)₃(OH)] tricarboxylated product instead (Scheme 1.3b) [94].

Bioactive molecules with a free carboxylic acid functional group can be conjugated directly to dihydroxo platinum(IV) (Fig. 1.6). In an oft-cited example, ethacrynic acid was conjugated to cisplatin by acylation of *cis, cis, trans*-[Pt(NH₃)₂(Cl)₂(OH)₂] with ethacrynic acyl chloride to form ethacraplatin [95]. It was postulated that ethacrynic acid, a broad-spectrum inhibitor of glutathione-S-transferase (GST), may reverse drug resistance as GST has been implicated in cellular defense against xenobiotics. Somewhat unexpectedly, ethacraplatin was a potent inhibitor of GST, even more so than ethacrynic acid alone. Incubation of a panel of cancer cell lines with ethacraplatin also revealed higher cytotoxicity than cisplatin alone within 24 h exposure but with similar cytotoxicity after 72 h.

Another research group attached dichloroacetate (DCA), a pyruvate dehydrogenase kinase (PDK) inhibitor, to cisplatin to form mitaplatin [96]. There is



Scheme 1.3 Schematic diagram for asymmetrical carboxylation of platinum(IV) complexes

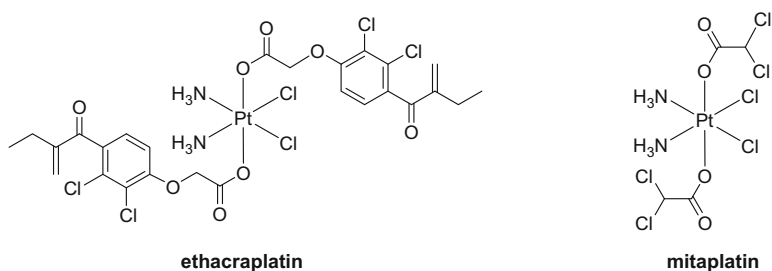


Fig. 1.6 Ethacraplatin and mitaplatin are two examples of platinum(IV) complexes with active axial ligands

substantial evidence from preclinical trials that DCA induces apoptosis selectively in cancer cells by reversing the Warburg effect. The Warburg effect is an observation that cancer cells predominately produce energy by glycolysis (anaerobic respiration) rather than oxidative phosphorylation (aerobic respiration) in mitochondria. This disrupts apoptosis because the mitochondria triggers apoptosis by releasing proapoptotic factors such as cytochrome c and apoptosis inducing factor. Therefore DCA induces apoptosis selectively in cancer cells by inhibiting PDK, shifting cellular metabolism from glycolysis to oxidative phosphorylation and reactivating the mitochondria. It was postulated that DCA released upon intracellular reduction of mitaplatin would sensitize cancer cells towards the cisplatin congener. Remarkably, not only did mitaplatin exhibited high cytotoxicity, it was also more selective towards cancer cells. In a co-culture of cancer cells with normal fibroblasts, cisplatin and the mixture of cisplatin and DCA killed both healthy fibroblasts and cancer cells, but mitaplatin only targeted the latter. However, these results should be treated with cautious optimism as the reduction potential of mitaplatin was measured to be -173 mV, higher than satraplatin, indicating that it might be prematurely reduced in blood [97].

Besides tethering bioactive ligands directly to the platinum(IV) center, it's also possible to conjugate the bioactive moiety via a linker. For instance, an linker-modified estrogen derivative was conjugated via the pendant carboxyl group of succinate in the hope of selectively sensitizing estrogen receptor positive ER(+) cancer cells compared to ER(-) cancer cells (Fig. 1.7) [86]. It was hypothesized that the estrogen-tethered platinum(IV) complex would accumulate selectively in estrogen receptor positive ER(+) breast cancer cells and the estradiol 3-benzoate ligands released upon reduction and ester hydrolysis would induce apoptosis by upregulating HMGB1, a protein which shields platinated DNA from nucleotide excision repair. In vitro, it was shown that varying the linker length had a tangible effect on cytotoxicity, hinting that the kinetics of ester hydrolysis of the linker may affect the drug's pharmacological profile. This same strategy has also been employed to bind targeting peptide motifs designed to selectively target extracellular matrix proteins which are highly expressed in tumor-induced angiogenesis as a "tumour homing device" [98]. Against a panel of endothelial and non-endothelial cells, platinum(IV) complexes containing either the targeting RGD or NGR motif were found to be strong inhibitors of cell growth, at levels that approach cisplatin. In contrast, platinum(IV) complexes containing the non-targeting AGR and Gly

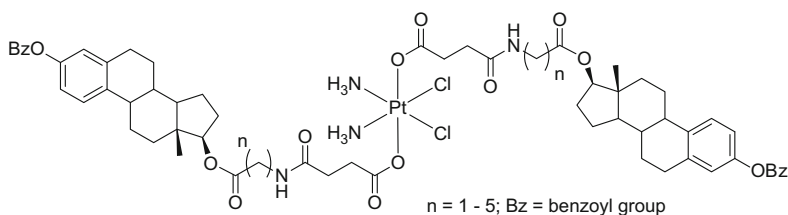
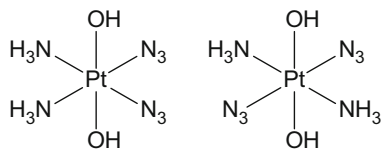


Fig. 1.7 Series of estrogen tethered platinum(IV) complexes

Fig. 1.8 *cis* and *trans* isomers of light activated platinum(IV) diazido complexes



peptides were poorly efficacious, supporting the view that the strategy could be exploited to develop “tumour homing” drugs.

Besides conjugating bioactive molecules, another interesting class of platinum (IV) complexes are the photoactivatable diazido platinum(IV) complexes, *cis,cis,-trans*-[Pt(NH₃)₂(N₃)₂(OH)₂] and its geometrical isomer *trans,trans,trans*-[Pt(NH₃)₂(N₃)₂(OH)₂] (Fig. 1.8) [99–101]. The diazido complexes were both stable towards blood plasma and glutathione over a several weeks. UV irradiation initiates photoconversion of the platinum(IV) prodrug to its active cytotoxic platinum(II) form (possibly a reactive diaqua species) [8]. Photoactivatable platinum(IV) prodrugs represent a promising strategy which circumvents the dose-limiting side effects of cisplatin by locally targeting tumour cells with light, leaving healthy tissue unharmed. Moreover, photoactivation of diazido platinum(IV) has an advantage over conventional photodynamic therapy in hypoxic tumours because it does not rely on the presence of oxygen to generate transient reactive oxygen species. It was observed that the diazido complexes only formed platinum–DNA adducts and bound to guanosine monophosphate and d(GpG) upon light irradiation and that the rate of DNA platination is correlated to light exposure (Fig. 1.9). Encouragingly, tests against a panel of cell lines have shown the diazido complexes to be relatively nontoxic in the dark but significantly more cytotoxic upon irradiation. In particular, the *trans*-azido complex exhibited higher cytotoxicity than cisplatin and was not cross resistant with the cisplatin-resistant 5637-CDDP cell line.

Issue of premature reduction in blood. One of the key concerns of employing platinum(IV) as a prodrug strategy hinges on whether platinum(IV) complexes are reduced with the concomitant release of axial ligands intracellularly or if the reduction of platinum(IV) occurs prematurely along with undesirable extracellular release of the axial ligands. Some evidence endorsing former comes from a series of *in vitro* studies by Hambley and coworkers [102–105]. X-ray absorption near edge spectroscopy (XANES), which can monitor the oxidation state of platinum complexes, was employed to show the uptake of platinum(IV) complexes and subsequent reduction to platinum(II) within 24 h of incubation in ovarian (A2780) cancer

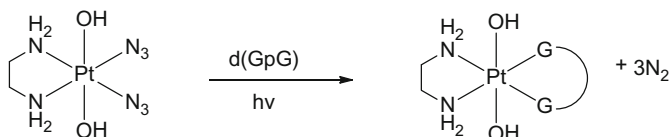


Fig. 1.9 Formation of Pt–DNA adduct upon irradiation

cells [102]. In a similar experiment, synchrotron resonance induced X-ray emission (SRIXE) imaging was used to monitor cellular uptake and distribution in ovarian (A2780) cancer cells treated with *cis,trans,cis*-[PtCl₂(OC(O)CH₂Br)₂(NH₃)₂], creatively using bromine as an elemental tag of the axial ligands [104]. The results showed diffuse distribution of Br throughout the cell, seemingly confirming the loss of axial ligands on reduction intracellularly. These results should be interpreted with caution however, due to the presence of significant amounts of endogenous bromine in the ovarian cells [104].

Nonetheless despite numerous *in vitro* substantiation of the intracellular reduction of platinum(IV) prodrugs, there are still insufficient evidence to substantiate this within actual clinical settings *in vivo*. The benefits of platinum(IV) prodrug will be muted if reduction with concurrent loss of the axial ligands occur prematurely in blood. While it has been shown that platinum(IV) complexes are inert to most proteins in an *in vitro* setting [52], in reality, the half-life of satraplatin [PtCl₂(OAc)₂(NH₃)(cyclohexylamine)] in human blood is only 6.3 min compared to 22 h in a cell culture medium [97] while tetraplatin (PtCl₄(D,L-cyclohexane-1,2-diamine)) has a half-life of only 3 s in blood [106]. This may imply that the platinum(IV) complexes may not persist long enough in blood to reach its intended destination. The rapid reduction has been attributed to the presence of heme proteins in hemoglobin. Satraplatin was found to be stable in hemoglobin, cytochrome c and glutathione but was rapidly reduced in the presence of NADH with either hemoglobin or cytochrome c [107]. Conventional viewpoint holds that the reductive biotransformation of platinum(IV) prodrugs are mediated primarily by highly reducing glutathione and other thiol-containing proteins. However, this is challenged by findings that satraplatin remained fairly stable at physiological levels (2 mM) of glutathione [107]. In an experiment, cell extracts were separated into low and high molecular weight fractions in order to assess the role of low molecular mass fractions (such as glutathione) in the reduction of platinum(IV) complexes [38]. Surprisingly, the rate of reduction by the high molecular weight fraction was very much faster than the low molecular weight fraction and similar to that of the whole cell extract. These findings suggest that metalloproteins such as hemoglobin and cytochrome c are the primary reducing agents *in vivo* and not glutathione.

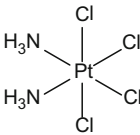
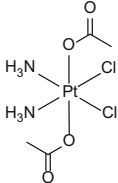
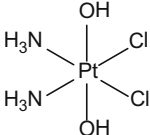
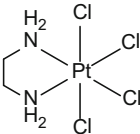
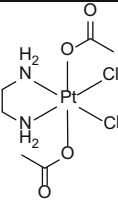
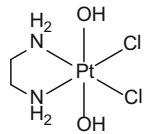
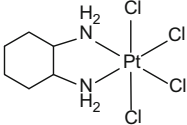
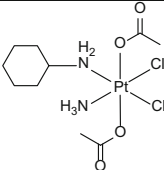
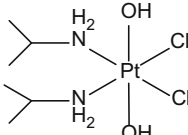
These results may have somber implications on the efficacy of the platinum(IV) prodrug strategy and should be investigated further. It was observed that analogues of satraplatin exhibited lower activity than cisplatin *in vivo* despite being three orders of magnitude more active on *in vitro* assays. This supports the view that platinum(IV) prodrugs may deceptively exhibit more pronounced activity *in vitro* than in reality [8].

Although there are exceptions, it is generally believed that the rate of reduction of platinum(IV) complexes coincides with its reduction potential and that the nature of axial ligands exert significant influence on the reduction potentials (Table 1.1) [109]. In a class of platinum(IV) complexes bearing the general form, *cis,cis,trans*-[Pt(A)Cl₂(X)₂], where A can be ethylenediamine, cyclohexylamine, diaminocyclohexane or 1,4-butanediamine, the reduction potentials increase in the following order of axial substitution: OH < OAc < Cl < OCOCF₃ and the ease of reduction

correlated to cytotoxicity at least in vitro [84, 109, 110]. This is consistent with clinical observations that tetraplatin, containing axial chloride ligands, was too readily reduced in the bloodstream and sequestered by plasma proteins, leading to low clinical anti-cancer activity and severe neurotoxicity [9]. In contrast, iproplatin (*cis,trans,cis*-[PtCl₂(OH)₂(isopropylamine)₂]) was far too inactive due to its unfavorable reduction potential and was relatively inert in vivo [43, 108].

In essence, the reduction potentials of existing platinum(IV) complexes poses a real dilemma. On one hand, complexes like satraplatin with high reduction potential are too susceptible to premature reduction in the bloodstream but on the other hand, complexes like iproplatin with low reduction potentials are far too inactive. One approach of circumventing premature reductions is by using delivery vehicles such as tethering to single-walled carbon nanotubes [82] and by encapsulation with targeted controlled release polymeric nanoparticles [111].

Table 1.1 Standard reduction potentials of various platinum(IV) complexes adjusted against standard hydrogen electrode reference [108]

		
+64 mV	-347 mV	-592 mV
		
+64 mV	-258 mV	-596 mV
		
Tetraplatin +198 mV	Satraplatin +38 mV	Iproplatin -442 mV

1.5 Immuno-modulation by Platinum-Based Agents

Background. The contribution of the immune system in chemotherapy has long been disregarded as cytotoxic drugs were generally believed to be immunosuppressive [112–114]. Consequently, new chemotherapeutic agents are evaluated on immunodeficient mice which neglects any possible immune contribution. However, a substantial body of recent work has challenged this assumption. There is now a growing consensus that a number of chemotherapeutics do stimulate the innate and/or the adaptive immune system and that at least part of the observed clinical therapeutic efficacy of these agents actually hinges on these off-target immunostimulating mechanisms [112, 113, 115–117]. Thus, certain chemotherapeutics (such as anthracyclines, taxanes and gemcitabine) actually relies on off-target immune mechanisms which cooperates with direct cytotoxicity for successful tumour eradication in a two pronged approach [113, 118]. A multi-pronged immuno-chemotherapeutic approach would not only shrink tumours but more importantly, reactivate dormant immune response against malignancies, eliminating residual cancer cells. Accordingly, higher densities of tumour-infiltrating lymphocytes following chemotherapy has been correlated with significantly better survival outcomes in colorectal and breast cancers [119, 120].

Despite being effective anti-cancer agents which form the mainstay of many chemotherapy combination regimes [13], the recognition of platinum-induced anti-tumor immunomodulation has been barely recognized and is only recently beginning to gain gradual traction due to the work described here and by others [121]. It is conceivable that the contribution of the immune system in the clinical efficacy of cisplatin has been underestimated. In this dissertation, we are interested in the concept of combined immuno-chemotherapy with platinum agents and we have explored two orthogonal approaches. The first approach is a “macrophage-centric” approach which looks at activating macrophages directly with platinum agents (Fig. 1.10) while the second approach is a “tumour-centric” approach of triggering immunogenic cell death of cancer cells (Fig. 1.12).

Although formation of covalent platinum-DNA adducts is generally accepted as the principal mode of action [122], classical platinum agents like cisplatin have also been known to exert off-target effects on the immune system and are potent immunomodulators of both the innate and adaptive immune system [123]. Platinum agents can indirectly promote immune-mediated killing of cancer cells through its action on cancer cells by (1) triggering an immunogenic mode of tumor cell death via exposure of specific “eat-me” signals [124], (2) increasing tumour-cell susceptibility for T-cell killing [125, 126], and (3) by down-regulating immunosuppressive PD-L2 in a STAT6-dependent manner on tumour cells leading to enhanced recognition by T-cells [127]. In addition, platinum agents can also directly engage immune effector functions by (1) stimulating both monocyte and natural killer (NK) cell mediated cytotoxicity [128–132], (2) promoting antigen-presenting capacity of dendritic cells [133, 134], and (3) by reversing immunosuppressive tumour microenvironments by downregulating PD-L2 on dendritic cells [127] and

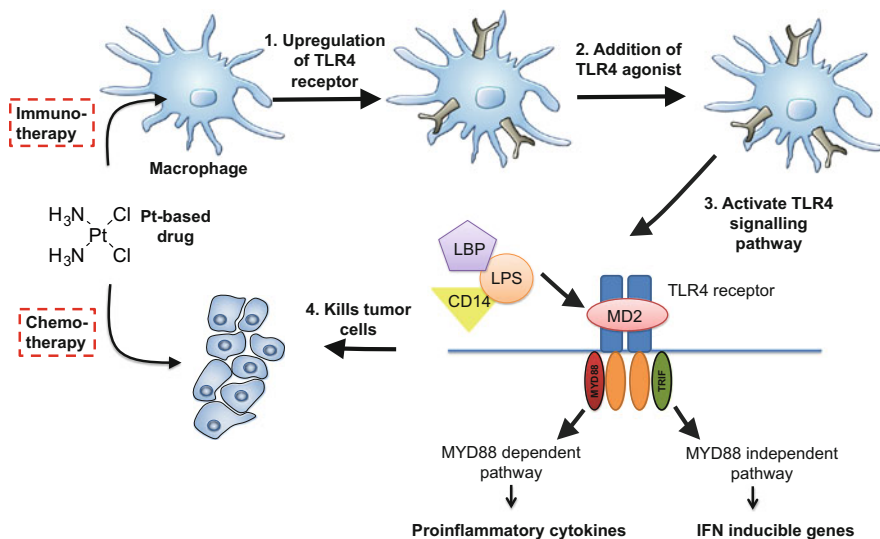


Fig. 1.10 Combined immuno-chemotherapy. Cisplatin can exert both direct cytotoxicity against cancer cells as well as activating macrophages against cancer cells by upregulating TLR4 receptors on macrophages

by selective depletion of inhibitory myeloid-derived suppressor cells (MDSC) and T_{reg} cells [135]. Interestingly, there has been compelling empirical evidence corroborating the immunomodulating capacity of platinum-based therapy with favorable chemotherapy outcomes [124, 135, 136]. Nonetheless, the immune-mediating activity of platinum-based agents has been neglected in the development of new therapeutics which has focused primarily on the principle of targeting DNA within tumor cells.

Macrophage activation and repolarization. The first approach we have explored is the phenomena of macrophage activation with platinum complexes. Although macrophages are one of the primary line of defense against cancer by eliminating nascent tumours in many cases, the sustained proliferation of cancer despite the afore-mentioned immune-surveillance actually represents immune-evasion of cancer [137]. It has been established that tumour-associated macrophages (TAMs) infiltrating most tumour masses have been perversely co-opted into a tumor-supporting M2 phenotype which stimulate the proliferation and metastasis through the secretion of growth factors and by suppressing the adaptive immune response [138]. The presence of these tumor associated macrophages (TAMs) has been correlated with poor clinical outcomes. Thus, there has been some research interest in “re-educating” the M2-tumor supporting macrophages back into M1-tumoural macrophages as macrophages display a flexible polarization state (Fig. 1.11) [138]. Recently, an anti-CD40 mAb agonist displayed promising activity against human pancreatic cancer via macrophage activation [139]. Nonetheless, there are not many reported agent till date that can polarize protumour M2-like TAMs to

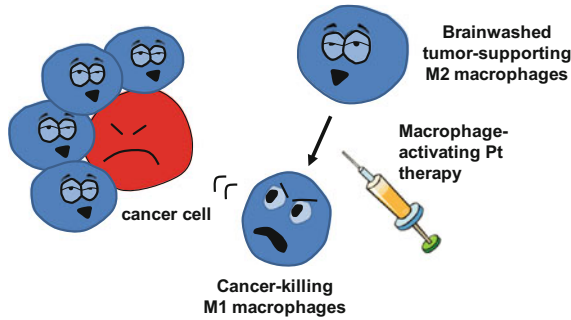


Fig. 1.11 Postulate: We hypothesize that platinum-based therapy is able to repolarize tumor-supporting M2 macrophages into cancer-killing M1 macrophages

tumor-inhibitory M1-like TAMs. While poorly studied [140], there has been circumstantial evidence which suggest that platinum-based agents can polarize macrophages into a M1-phenotype. Thus, cisplatin-treatment has been associated with increased M1 polarization in vivo in several cases [135, 138, 141]. The author hypothesize that cisplatin may activate macrophages via upregulation of TLR4 receptors rendering it more sensitive to endogenous macrophage-activating TLR4 agonists (Fig. 1.10).

Immuno-modulation: Immunogenic cell death. The second approach focuses on the capacity of platinum agents to induce immunogenic cell death in tumor cells (Fig. 1.12). One of several ways in which chemotherapeutics engage a tumor-specific immune response is by triggering immunogenic cell death (ICD) whereby the dying cancer cells initiate a robust immune response, acting as a de facto anticancer vaccine [117, 142]. Thus, immunocompetent (but not immunodeficient)

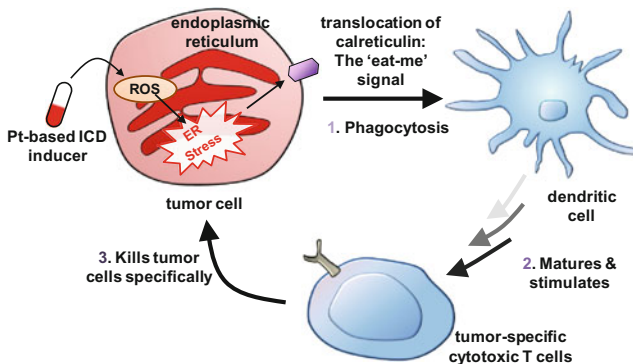


Fig. 1.12 Some platinum-based agents can trigger immunogenic cell death of tumour cells by triggering ER-stress which induces the translocation of calreticulin, a potent “eat me” signal. Recognition and phagocytosis of these tumour cells by dendritic cells eventually leads to the development of an acquired immune response against the tumour cells via a tumour-specific cytotoxic T cells response

mice vaccinated with dying cancer cells pre-treated with ICD inducers (e.g. anthracyclines, shikonin and hypericin-PDT) are protected against subsequent challenges with live cancer cells [143]. Retrospective analysis of multiple cancers suggest that human patients treated with chemotherapy together with digoxin, an ICD-promoting agent, had improved overall survival, especially when the chemotherapy cocktail does not already contain an ICD inducer [144]. It was demonstrated that the therapeutic efficacy of anthracyclines (ICD-inducer) was negated in mice models when the host immune system was compromised [118, 145]. This observation suggested that, at least in some models of cancer, it was the immune-modulating capacity of chemotherapeutics, and not cytotoxicity, which was important.

The ICD-inducing capacity of anticancer drugs has been tied with their capacity to elicit endoplasmic reticulum (ER) stress and associated reactive oxygen species (ROS) (Fig. 1.12) [117, 142, 146]. It is believed that cancer cells dying in response to ROS-mediated ER stress emit a combination of three distinct spatiotemporally-defined “danger” signals, which are recognized by the immune system and required for ICD [144]. These signals, which are now established as the biochemical hallmarks of ICD, are: (i) translocation of ER-resident calreticulin (CRT) to the cell surface during early apoptosis (ii) active secretion of ATP and (iii) extracellular secretion of nuclear high-mobility group box 1 protein (HMGB1) at late-stage apoptosis. Cell-surface CRT, the dominant pro-phagocytotic “eat me” signal [147], promotes the engulfment of cancer cells by professional macrophages such as dendritic cells (DCs) for tumour antigen presentation [143]. Secreted ATP acts as a “find me” signal as well as stimulating purinergic P2RX7 receptors on DCs, triggering production of IL-1 β , a pro-inflammatory cytokine which is required for IFN- γ production by tumour-specific cytotoxic T cells [117, 142, 146]. Finally, HMGB1 binds to toll-like receptor 4 (TLR4) on DCs, triggering a myeloid differentiation primary response gene 88 (MYD88)-dependent signalling cascade, which promotes antigen processing and presentation to T cells [117, 142, 146]. Thus, a dysfunctional P2RX7 or TLR4 has been correlated with negative therapeutic outcomes in both mice and human studies with ICD-inducing chemotherapeutics such as doxorubicin, highlighting the immune component as an essential contribution to the efficacy of these agents [117, 142, 146]. Dendritic cells which are professional antigen-presenting cells (APCs), recognize the DAMPs emitted by the dying cancer cells and phagocytize them. After phagocytizing tumour cells, DCs degrade the tumour-associated antigens (TAAs) into smaller peptide fragments which are used to assemble antigen-major histocompatibility complex (MHC)-class II complexes. The MHC-class II complexes then prime naïve T cells so as to generate CD8+ T lymphocytes (CTLs) which specifically recognize and bind to TAAs on cancer cells before destroying them, giving rise to T-cell-mediated adaptive immunity.

So far, there has only been limited work done to study the ICD inducing ability of platinum-based drugs even though platinum-based drugs, in particular cisplatin, form the cornerstone of chemotherapeutic treatment for many cancers.

1.6 Outline of Thesis

Chapter 2. Harnessing chemoselective imine ligation for tethering bioactive molecules to platinum(IV) prodrugs

In recent years, there has been increasing interest in exploiting platinum(IV) as a prodrug strategy to mitigate limitations of conventional platinum(II) anticancer complexes. Although this strategy embodies a burgeoning new direction to drive the development of platinum(IV) anticancer drugs, existing synthetic methodologies of tethering bioactive molecules to the axial sites are inadequate to fully exploit its latent potential. These methods suffer from limited scope, poor yields and low reliability. This work explores the applications of current chemoselective ligation chemistries to platinum(IV) anticancer complexes with the aim of addressing the aforementioned limitations. Here, we describe the synthesis of a platinum(IV) complex bearing an aromatic aldehyde functionality and explored the scope of imine ligation with various hydrazide and aminoxy functionalized substrates.

Chapter 3. Probing the platinum(IV) prodrug hypothesis. Are platinum(IV) complexes really prodrugs of cisplatin?

The general consensus is that platinum(IV) scaffolds bearing axial carboxylate ligands undergo reductive elimination to generate the active square-planar *cis* platinum(II) core together with concomitant elimination and release of the axial ligands. However, recent works has thrown doubts to the prodrug hypothesis. It was postulated that reduction does not solely progress via reductive elimination of the axial acetate ligands but instead occurs via dissociation of any combination of the axial acetate and equatorial chloride ligands. Validation of the platinum(IV) prodrug hypothesis is important because it is the underlying working assumption behind the development of platinum(IV)-conjugates. Here, we used a combination of normal and reversed phase chromatography to study the reduction of the model platinum(IV) complexes by ascorbic acid. Our results clearly demonstrate that our class of *mono*- and *bis*-functionalised asymmetrical aryl platinum(IV) complexes do indeed yield cisplatin upon reduction.

Chapter 4. HER2-targeted platinum(IV) agents induce selectively targeted necrosis of HER2/+ tumors following massive cellular influx

It is well recognized that the failure of many chemotherapeutics arises due to an inability to induce apoptosis. Most cancers acquire a myriad of pro-survival adaptations. The vast heterogeneity and accumulation of multiple often unrelated anti-apoptotic signaling pathways have been a major stumbling block towards the development of conventional molecular-targeted therapy which can overcome drug resistance phenomena. We have developed highly potent and selective HER2-targeted platinum(IV)-AHNP prodrugs which employ an idea of “targeted necrosis” as a novel strategy to circumvent apoptosis-resistance and demonstrate the feasibility of this approach. The platinum(IV)-AHNP conjugates exhibited a

unique biphasic mode of killing. The first phase comprise of a rapid killing via necrosis followed by an extended and gradual phase of delayed cell death. Our results indicate that the platinum(IV)-AHNP conjugates were more potent compared to the free drugs in direct cell-killing along with comparable long-term inhibition of proliferative capacity and with greater selectivity against HER2-positive cancers.

Chapter 5. Immuno-chemotherapeutic platinum(IV) prodrugs of cisplatin as multimodal anticancer agents

There is growing consensus that the clinical therapeutic efficacy of some chemotherapeutic agents depends on its off-target immune-modulating effects. Pt anticancer drugs have earlier been identified to be potent immunomodulators of both the innate immune system as well as the adaptive immune system. Nevertheless, there has been little development in the rational design of Pt-based chemotherapeutic agents to exploit their immune-activating capabilities. FPR1/2 receptors are highly expressed in immune cells as well as many metastatic cancers. Herein, we report a rationally-designed multimodal Pt(IV) prodrug containing a FPR1/2-targeting peptide that combines chemotherapy with immunotherapy to achieve therapeutic synergy and demonstrate the feasibility of this approach.

Chapter 6. Discovery of a potent inducer of immunogenic cell death from a screening of platinum complexes

One way which chemotherapeutics can engage a tumor-specific immune response is by triggering an immunogenic mode of tumor cell death (ICD) which then acts as a de facto anticancer vaccine. Although a mainstay of chemotherapy, there has not been a systematic attempt to screen both existing and upcoming Pt agents for their ICD ability. In this work, we have evaluated a small library of Pt agents via an in vitro phagocytosis assay and found no correlation between cytotoxicity and phagocytosis. We subsequently identified a Pt(II) N-heterocyclic carbene complex which displayed the characteristic hallmarks of a type II ICD inducer (focused oxidative ER stress, calreticulin exposure and both HMGB1 and ATP release). To the best of our knowledge, this complex is the first reported instance of a small-molecule type II ICD inducer and may represent a new paradigm of Pt-based immuno-chemotherapy.

References

1. Teo, M.C.C., Soo, K.C.: Cancer trends and incidences in Singapore. *Jpn. J. Clin. Oncol.* **43**, 219–224 (2013)
2. Sasieni, P.D., Shelton, J., Ormiston-Smith, N., Thomson, C.S., Silcocks, P.B.: What is the lifetime risk of developing cancer?: the effect of adjusting for multiple primaries. *Br. J. Cancer* **105**, 460–465 (2011)
3. Ramsey, S.D.: How should we value lives lost to cancer? *J. Natl Cancer Inst.* **100**, 1742–1743 (2008)

4. DeVita, V.T., Rosenberg, S.A.: Two hundred years of cancer research. *N. Engl. J. Med.* **366**, 2207–2214 (2012)
5. Agarwal, S., Pappas, L., Neumayer, L., Kokeny, K., Agarwal, J.: Effect of breast conservation therapy vs mastectomy on disease-specific survival for early-stage breast cancer. *JAMA Surg.* **149**, 267–274 (2014)
6. Mehlen, P., Puisieux, A.: Metastasis: a question of life or death. *Nat. Rev. Cancer* **6**, 449–458 (2006)
7. Couzin-Frankel, J.: Cancer Immunotherapy. *Science* **342**, 1432–1433 (2013)
8. Hall, M.D., Mellor, H.R., Callaghan, R., Hambley, T.W.: Basis for design and development of platinum(IV) anticancer complexes. *J. Med. Chem.* **50**, 3403–3411 (2007)
9. Hall, M.D., Hambley, T.W.: Platinum(IV) antitumour compounds: their bioinorganic chemistry. *Coord. Chem. Rev.* **232**, 49–67 (2002)
10. Chin, C.F., Wong, D.Y.Q., Jothibasu, R., Ang, W.H.: Anticancer platinum(IV) prodrugs with novel modes of activity. *Curr. Top. Med. Chem.* **11**, 2602–2612 (2011)
11. Wheate, N.J., Walker, S., Craig, G.E., Oun, R.: The status of platinum anticancer drugs in the clinic and in clinical trials. *Dalton Trans.* **39**, 8113–8127 (2010)
12. Galanski, M., Jakupec, M.A., Keppler, B.K.: Update of the preclinical situation of anticancer platinum complexes: novel design strategies and innovative analytical approaches. *Curr. Med. Chem.* **12**, 2075–2094 (2005)
13. Kelland, L.: The resurgence of platinum-based cancer chemotherapy. *Nat. Rev. Cancer* **7**, 573–584 (2007)
14. Abu-Surrah, A.S., Kettunen, M.: Platinum group antitumor chemistry: design and development of new anticancer drugs complementary to cisplatin. *Curr. Med. Chem.* **13**, 1337–1357 (2006)
15. Alderden, R.A., Hall, M.D., Hambley, T.W.: The discovery and development of cisplatin. *J. Chem. Educ.* **83**, 728 (2006)
16. Rosenberg, B.: Platinum complexes for the treatment of cancer. *Interdiscip. Sci. Rev.* **3**, 134–147 (1978)
17. Abu-Surrah, A.S., Kettunen, M.: Platinum group antitumor chemistry: design and development of new anticancer drugs complementary to cisplatin. *Curr. Med. Chem.* **13**, 1337–1357 (2006)
18. Weiss, R.B., Christian, M.C.: New cisplatin analogues in development: a review. *Drugs* **46**, 360–377 (1993)
19. Montana, A.M., Batalla, C.: The rational design of anticancer platinum complexes: the importance of the structure-activity relationship. *Curr. Med. Chem.* **16**, 2235–2260 (2009)
20. Todd, R.C., Lippard, S.J.: Inhibition of transcription by platinum antitumor compounds. *Metallomics* **1**, 280–291 (2009)
21. Nitiss, J.L.: A copper connection to the uptake of platinum anticancer drugs. *Proc. Natl. Acad. Sci. U. S. A.* **99**, 13963–13965 (2002)
22. Harrach, S., Ciarimboli, G.: Role of transporters in the distribution of platinum-based drugs. *Front. Pharmacol.* **6** (2015)
23. Zhang, S., Lovejoy, K.S., Shima, J.E., Lagpacan, L.L., Shu, Y., Lapuk, A., Chen, Y., Komori, T., Gray, J.W., Chen, X., Lippard, S.J., Giacomini, K.M.: Organic cation transporters are determinants of oxaliplatin cytotoxicity. *Cancer Res.* **66**, 8847–8857 (2006)
24. Eastman, A.: The mechanism of action of cisplatin: from adducts to apoptosis. In: Bernhard, L. (ed.) *Cisplatin*, pp. 111–134 (2006)
25. Jamieson, E.R., Lippard, S.J.: Structure, recognition, and processing of cisplatin-DNA adducts. *Chem. Rev.* **99**, 2467–2498 (1999)
26. Legendre, F., Chottard, J.-C.: Kinetics and selectivity of DNA-platination. In: Bernhard, L. (ed.) *Cisplatin*, pp. 223–245 (2006)
27. Pil, P., Lippard, S.: Specific binding of chromosomal protein HMG1 to DNA damaged by the anticancer drug cisplatin. *Science* **256**, 234–237 (1992)
28. Zamble, D.B., Mu, D., Reardon, J.T., Sancar, A., Lippard, S.J.: Repair of cisplatin-DNA adducts by the mammalian excision nucleases. *Biochemistry* **35**, 10004–10013 (1996)

29. Fichtinger-Schepman, A.M.J., Van der Veer, J.L., Den Hartog, J.H.J., Lohman, P.H.M., Reedijk, J.: Adducts of the antitumor drug cis-diamminedichloroplatinum(II) with DNA: formation, identification, and quantitation. *Biochemistry* **24**, 707–713 (1985)
30. Jamieson, E.R., Lippard, S.J.: Structure, recognition, and processing of cisplatin–DNA adducts. *Chem. Rev.* **99**, 2467–2498 (1999)
31. Eguchi, Y., Shimizu, S., Tsujimoto, Y.: Intracellular ATP levels determine cell death fate by apoptosis or necrosis. *Cancer Res.* **57**, 1835–1840 (1997)
32. Gonzalez, V.M., Fuertes, M.A., Alonso, C., Perez, J.M.: Is cisplatin-induced cell death always produced by apoptosis? *Mol. Pharmacol.* **59**, 657–663 (2001)
33. Wang, D., Lippard, S.J.: Cellular processing of platinum anticancer drugs. *Nat. Rev. Drug Discov.* **4**, 307–320 (2005)
34. Peleg-Shulman, T., Gibson, D.: Cisplatin–protein adducts are efficiently removed by glutathione but not by 5-guanosine monophosphate. *J. Am. Chem. Soc.* **123**, 3171–3172 (2001)
35. Soti, C., Racz, A., Csermely, P.: A nucleotide-dependent molecular switch controls ATP binding at the C-terminal domain of Hsp90. *J. Biol. Chem.* **277**, 7066–7075 (2002)
36. Cullen, K., Yang, Z., Schumaker, L., Guo, Z.: Mitochondria as a critical target of the chemotherapeutic agent cisplatin in head and neck cancer. *J. Bioenerg. Biomembr.* **39**, 43–50 (2007)
37. Chapman, E.G., DeRose, V.J.: Enzymatic processing of platinated RNAs. *J. Am. Chem. Soc.* **132**, 1946–1952 (2010)
38. Gibson, D.: The mechanism of action of platinum anticancer agents—what do we really know about it? *Dalton Trans.* 10681–10689 (2009)
39. Sheikh-Hamad, D.: Cisplatin-induced cytotoxicity: is the nucleus relevant? *Am. J. Physiol. Renal Physiol.* **295**, F42–F43 (2008)
40. Yu, F., Megyesi, J., Price, P.M.: Cytoplasmic initiation of cisplatin cytotoxicity. *Am. J. Physiol. Renal Physiol.* **295**, F44–F52 (2008)
41. Wang, X., Guo, Z.: Towards the rational design of platinum(ii) and gold(iii) complexes as antitumour agents. *Dalton Trans.* 1521–1532 (2008)
42. Jung, Y., Lippard, S.J.: Direct cellular responses to platinum-induced DNA damage. *Chem. Rev.* **107**, 1387–1407 (2007)
43. Galanski, M., Keppler, B.K.: Searching for the magic bullet: anticancer platinum drugs which can be accumulated or activated in the tumor tissue. *Anticancer Agents Med. Chem.* **7**, 55–73 (2007)
44. McWhinney, S.R., Goldberg, R.M., McLeod, H.L.: Platinum neurotoxicity pharmacogenetics. *Mol. Cancer Ther.* **8**, 10–16 (2009)
45. Pabla, N., Dong, Z.: Cisplatin nephrotoxicity: mechanisms and renoprotective strategies. *Kidney Int.* **73**, 994–1007 (2008)
46. Ozkok, A., Edelman, C.L.: Pathophysiology of cisplatin-induced acute kidney injury. *Biomed. Res. Int.* **2014**, 17 (2014)
47. Screnci, D., McKeage, M.J.: Platinum neurotoxicity: clinical profiles, experimental models and neuroprotective approaches. *J. Inorg. Biochem.* **77**, 105–110 (1999)
48. Siddik, Z.H.: Cisplatin: mode of cytotoxic action and molecular basis of resistance. *Oncogene* **22**, 7265–7279 (2003)
49. Samimi, G., Varki, N.M., Wilczynski, S., Safaei, R., Alberts, D.S., Howell, S.B.: Increase in expression of the copper transporter ATP7A during platinum drug-based treatment is associated with poor survival in ovarian cancer patients. *Clin. Cancer Res.* **9**, 5853–5859 (2003)
50. Samimi, G., Safaei, R., Katano, K., Holzer, A.K., Rochdi, M., Tomioka, M., Goodman, M., Howell, S.B.: Increased expression of the copper efflux transporter ATP7A mediates resistance to cisplatin, carboplatin, and oxaliplatin in ovarian cancer cells. *Clin. Cancer Res.* **10**, 4661–4669 (2004)
51. Wang, X., Guo, Z.: The role of sulfur in platinum anticancer chemotherapy. *Anti-Cancer Agents Med. Chem.* **7**, 19–34 (2007)

52. Dolman, R.C., Deacon, G.B., Hambley, T.W.: Studies of the binding of a series of platinum (IV) complexes to plasma proteins. *J. Inorg. Biochem.* **88**, 260–267 (2002)
53. Shah, M.A., Schwartz, G.K.: Cell cycle-mediated drug resistance: an emerging concept in cancer therapy. *Clin. Cancer Res.* **7**, 2168–2181 (2001)
54. Gerlinger, M., Rowan, A.J., Horswell, S., Larkin, J., Endesfelder, D., Gronroos, E., Martinez, P., Matthews, N., Stewart, A., Tarpey, P., Varela, I., Phillimore, B., Begum, S., McDonald, N.Q., Butler, A., Jones, D., Raine, K., Latimer, C., Santos, C.R., Nohadani, M., Eklund, A.C., Spencer-Dene, B., Clark, G., Pickering, L., Stamp, G., Gore, M., Szallasi, Z., Downward, J., Futreal, P.A., Swanton, C.: Intratumor heterogeneity and branched evolution revealed by multiregion sequencing. *N. Engl. J. Med.* **366**, 883–892 (2012)
55. Wilson, J.J., Lippard, S.J.: Synthetic methods for the preparation of platinum anticancer complexes. *Chem. Rev.* **114**, 4470–4495 (2014)
56. Collins, I., Workman, P.: New approaches to molecular cancer therapeutics. *Nat. Chem. Biol.* **2**, 689–700 (2006)
57. Izar, B., Rotow, J., Gainor, J., Clark, J., Chabner, B.: Pharmacokinetics, clinical indications, and resistance mechanisms in molecular targeted therapies in cancer. *Pharmacol. Rev.* **65**, 1351–1395 (2013)
58. Iqbal, N., Iqbal, N.: Imatinib: a breakthrough of targeted therapy in cancer. *Chemother. Res. Pract.* **2014**, 9 (2014)
59. Lebwohl, D., Canetta, R.: Clinical development of platinum complexes in cancer therapy: an historical perspective and an update. *Eur. J. Cancer* **34**, 1522–1534 (1998)
60. O'Dwyer, P.J., Stevenson, J.P., Johnson, S.W.: Clinical status of cisplatin, carboplatin, and other platinum-based antitumor drugs. In: Bernhard L (ed.) *Cisplatin*, pp. 29–69 (2006)
61. Chen, Z., Fillmore, C.M., Hammerman, P.S., Kim, C.F., Wong, K.-K.: Non-small-cell lung cancers: a heterogeneous set of diseases. *Nat. Rev. Cancer* **14**, 535–546 (2014)
62. Gerlinger, M., Rowan, A.J., Horswell, S., Larkin, J., Endesfelder, D., Gronroos, E., Martinez, P., Matthews, N., Stewart, A., Tarpey, P., Varela, I., Phillimore, B., Begum, S., McDonald, N.Q., Butler, A., Jones, D., Raine, K., Latimer, C., Santos, C.R., Nohadani, M., Eklund, A.C., Spencer-Dene, B., Clark, G., Pickering, L., Stamp, G., Gore, M., Szallasi, Z., Downward, J., Futreal, P.A., Swanton, C.: Intratumor heterogeneity and branched evolution revealed by multiregion sequencing. *New Engl. J. Med.* **366**, 883–892 (2012)
63. Fuertes, M.A., Alonso, C., Perez, J.M.: Biochemical modulation of Cisplatin mechanisms of action: enhancement of antitumor activity and circumvention of drug resistance. *Chem. Rev.* **103**, 645–662 (2003)
64. Wang, D., Lippard, S.J.: Cellular processing of platinum anticancer drugs. *Nat. Rev. Drug Discov.* **4**, 307–320 (2005)
65. Lemma, K., Sargeson, A.M., Elding, L.I.: Kinetics and mechanism for reduction of oral anticancer platinum(IV) dicarboxylate compounds by L-ascorbate ions. *J. Chem. Soc., Dalton Trans.* 1167–1172 (2000)
66. Clarke, M.J., Sadler, P.J., Alessio, E.: *Metallopharmaceuticals: DNA interactions*. Springer, Berlin (1999)
67. Berners-Price, S.J., Ronconi, L., Sadler, P.J.: Insights into the mechanism of action of platinum anticancer drugs from multinuclear NMR spectroscopy. *Prog. Nucl. Magn. Reson. Spectrosc.* **49**, 65–98 (2006)
68. Nováková, O., Vrána, O., Kiseleva, V.I., Brabec, V.: DNA interactions of antitumor platinum(IV) complexes. *Eur. J. Biochem.* **228**, 616–624 (1995)
69. Roat, R.M., Reedijk, J.: Reaction of mer-trichloro (diethylenetriamine)platinum(IV) chloride, (mer-[Pt(dien)Cl₃]Cl), with purine nucleosides and nucleotides results in formation of platinum(II) as well as platinum(IV) complexes. *J. Inorg. Biochem.* **52**, 263–274 (1993)
70. Rotondo, E., Fimiani, V., Cavallaro, A., Ainis, T.: Does the antitumoral activity of platinum (IV) derivatives result from their in vivo reduction? *Tumori* **69**, 31–36 (1983)

71. Tito, F., Nick, F., Waldo, O., Hideyuki, T., John, W., Timothy, G.M.: Identification of non-cross-resistant platinum compounds with novel cytotoxicity profiles using the NCI anticancer drug screen and clustered image map visualizations. *Crit. Rev. Oncol. Hematol.* **53**, 25–34 (2005)
72. Aris, S.M., Farrell, N.P.: Towards antitumor active trans-platinum compounds. *Eur. J. Inorg. Chem.* **2009**, 1293–1302 (2009)
73. Giandomenico, C.M., Abrams, M.J., Murrer, B.A., Vollano, J.F., Rheinheimer, M.I., Wyer, S.B., Bossard, G.E., Higgins, J.D.: Carboxylation of kinetically inert platinum(IV) hydroxy complexes. An entree into orally active platinum(IV) antitumor agents. *Inorg. Chem.* **34**, 1015–1021 (1995)
74. Galanski, M., Keppler, B.K.: Carboxylation of dihydroxoplatinum(IV) complexes via a new synthetic pathway. *Inorg. Chem.* **35**, 1709–1711 (1996)
75. Galanski, M., Keppler, B.K.: Carboxylation of dihydroxoplatinum(IV) complexes with acyl chlorides. Crystal structures of the trans-R, R- and trans-S, S-isomer of (OC-6-33)-bis(1-adamantanecarboxylato)-(cyclohexane-1,2-diamine)dichloroplatinum(IV). *Inorg. Chim. Acta* **265**, 271–274 (1997)
76. Lee, E.J., Jun, M.-J., Lee, S.S., Sohn, Y.S.: Synthesis, structure, and properties of isopropylidenemalonatoplatinum(IV) complexes. *Polyhedron* **16**, 2421–2428 (1997)
77. Ali, M.S., Ali Khan, S.R., Ojima, H., Guzman, I.Y., Whitmire, K.H., Siddik, Z.H., Khokhar, A.R.: Model platinum nucleobase and nucleoside complexes and antitumor activity: X-ray crystal structure of [PtIV(trans-1R,2R-diaminocyclohexane)trans-(acetate)2(9-ethylguanine)Cl]NO₃·H₂O. *J. Inorg. Biochem.* **99**, 795–804 (2005)
78. Hambley, T.W., Battle, A.R., Deacon, G.B., Lawrenz, E.T., Fallon, G.D., Gatehouse, B.M., Webster, L.K., Rainone, S.: Modifying the properties of platinum(IV) complexes in order to increase biological effectiveness. *J. Inorg. Biochem.* **77**, 3–12 (1999)
79. Zhang, J.Z., Bonnitcha, P., Wesselblatt, E., Klein, A.V., Najajreh, Y., Gibson, D., Hambley, T.W.: Facile preparation of mono-, di- and mixed-carboxylato platinum(IV) complexes for versatile anticancer prodrug design. *Chem. Eur. J.* **19**, 1672–1676 (2013)
80. Lee, Y.-A., Jung, O.-S.: Synthesis and characterization of stable bis(methoxy)platinum(IV) complexes. A facile synthesis via fluorenylidene-philic interactions. *Bull. Chem. Soc. Jpn* **75**, 1533–1537 (2002)
81. Lee, Y.-A., Ho Yoo, K., Jung, O.-S.: Oxidation of Pt(II) to Pt(IV) complex with hydrogen peroxide in glycols. *Inorg. Chem. Commun.* **6**, 249–251 (2003)
82. Feazell, R.P., Nakayama-Ratchford, N., Dai, H., Lippard, S.J.: Soluble single-walled carbon nanotubes as longboat delivery systems for platinum(IV) anticancer drug design. *J. Am. Chem. Soc.* **129**, 8438–8439 (2007)
83. Kauffman, G.B., Slusarczuk, G., Kirschner, S.: cis and trans-Tetrachlorodiammineplatinum (IV). In: Jacob, K. (ed.) *Inorganic synthesis*, pp. 236–238 (2007)
84. Ellis, L., Er, H., Hambley, T.: The influence of the axial ligands of a series of platinum(IV) anti-cancer complexes on their reduction to platinum(II) and reaction with DNA. *Aust. J. Chem.* **48**, 793–806 (1995)
85. Kizu, R., Nakanishi, T., Hayakawa, K., Matsuzawa, A., Eriguchi, M., Takeda, Y., Akiyama, N., Tashiro, T., Kidani, Y.: A new orally active antitumor 1R,2R-cyclohexanediamine-platinum(IV) complex: trans-(n-valerato)chloro(1R,2R-cyclohexanediamine) (oxalato)platinum(IV). *Cancer Chemother. Pharmacol.* **43**, 97–105 (1999)
86. Barnes, K.R., Kutikov, A., Lippard, S.J.: Synthesis, characterization, and cytotoxicity of a series of estrogen-tethered platinum(IV) complexes. *Chem. Biol.* **11**, 557–564 (2004)
87. Ang, W.H., Pilet, S., Scopelliti, R., Bussy, F., Juillerat-Jeanneret, L., Dyson, P.J.: Synthesis and characterization of platinum(IV) anticancer drugs with functionalized aromatic carboxylate ligands: influence of the ligands on drug efficacies and uptake. *J. Med. Chem.* **48**, 8060–8069 (2005)

88. Perez, J.M., Camazón, M., Alvarez-Valdes, A., Quiroga, A.G., Kelland, L.R., Alonso, C., Navarro-Ranninger, M.C.: Synthesis, characterization and DNA modification induced by a novel Pt(IV)-bis(monoglutarate) complex which induces apoptosis in glioma cells. *Chem-Biol. Interact.* **117**, 99–115 (1999)
89. Reithofer, M., Galanski, M., Roller, A., Keppler, B.K.: An entry to novel platinum complexes: carboxylation of dihydroxoplatinum(IV) complexes with succinic anhydride and subsequent derivatization. *Eur. J. Inorg. Chem.* **2006**, 2612–2617 (2006)
90. Reithofer, M.R., Valiahdi, S.M., Jakupec, M.A., Arion, V.B., Egger, A., Galanski, M., Keppler, B.K.: Novel di- and tetracarboxylatoplatinum(IV) complexes. Synthesis, characterization, cytotoxic activity, and DNA platination. *J. Med. Chem.* **50**, 6692–6699 (2007)
91. Chin, C.F., Tian, Q., Setyawati, M.I., Fang, W., Tan, E.S.Q., Leong, D.T., Ang, W.H.: Tuning the activity of platinum(IV) anticancer complexes through asymmetric acylation. *J. Med. Chem.* **55**, 7571–7582 (2012)
92. Wong, D.Y.Q., Lim, J.H., Ang, W.H.: Induction of targeted necrosis with HER2-targeted platinum(IV) anticancer prodrugs. *Chem. Sci.* **6**, 3051–3056 (2015)
93. Wong, D.Y.Q., Yeo, C.H.F., Ang, W.H.: Immuno-chemotherapeutic platinum(IV) prodrugs of cisplatin as multimodal anticancer agents. *Angew. Chem. Int. Ed.* **53**, 6752–6756 (2014)
94. Song, R., Kim, K.M., Sohn, Y.S.: Synthesis and characterization of novel tricarboxylatoplatinum(IV) complexes. Nucleophilic substitution of (diamine)-tetrahydroxoplatinum(IV) with carboxylic acid. *Inorg. Chim. Acta* **338**, 89–93 (2002)
95. Ang, W.H., Khalaila, I., Allardyce, C.S., Juillerat-Jeanneret, L., Dyson, P.J.: Rational design of platinum(IV) compounds to overcome glutathione-S-transferase mediated drug resistance. *J. Am. Chem. Soc.* **127**, 1382–1383 (2005)
96. Dhar, S., Lippard, S.J.: Mitaplatin, a potent fusion of cisplatin and the orphan drug dichloroacetate. *Proc. Natl. Acad. Sci. U. S. A.* **106**, 22199–22204 (2009)
97. Carr, J., Tingle, M., McKeage, M.: Rapid biotransformation of satraplatin by human red blood cells in vitro. *Cancer Chemother. Pharmacol.* **50**, 9–15 (2002)
98. Mukhopadhyay, S., Barnes, C.M., Haskel, A., Short, S.M., Barnes, K.R., Lippard, S.J.: Conjugated platinum(IV) peptide complexes for targeting angiogenic tumor vasculature. *Bioconjugate Chem.* **19**, 39–49 (2007)
99. Bednarski, P.J., Grünert, R., Zielzki, M., Wellner, A., Mackay, F.S., Sadler, P.J.: Light-activated destruction of cancer cell nuclei by platinum diazide complexes. *Chem. Biol.* **13**, 61–67 (2006)
100. Mackay, F.S., Woods, J.A., Moseley, H., Ferguson, J., Dawson, A., Parsons, S., Sadler, P.J.: A photoactivated trans-diammine platinum complex as cytotoxic as cisplatin. *Chem. Eur. J.* **12**, 3155–3161 (2006)
101. Mackay, F.S., Moggach, S.A., Collins, A., Parsons, S., Sadler, P.J.: Photoactive trans ammine/amine diazido platinum(IV) complexes. *Inorg. Chim. Acta* **362**, 811–819 (2009)
102. Hall, M.D., Foran, G.J., Zhang, M., Beale, P.J., Hambley, T.W.: XANES determination of the platinum oxidation state distribution in cancer cells treated with platinum(IV) anticancer agents. *J. Am. Chem. Soc.* **125**, 7524–7525 (2003)
103. Hall, M., Dillon, C., Zhang, M., Beale, P., Cai, Z., Lai, B., Stampfl, A.J., Hambley, T.: The cellular distribution and oxidation state of platinum(II) and platinum(IV) antitumour complexes in cancer cells. *J. Biol. Inorg. Chem.* **8**, 726–732 (2003)
104. Hall, M.D., Alderden, R.A., Zhang, M., Beale, P.J., Cai, Z., Lai, B., Stampfl, A.P.J., Hambley, T.W.: The fate of platinum(II) and platinum(IV) anti-cancer agents in cancer cells and tumours. *J. Struct. Biol.* **155**, 38–44 (2006)
105. New, E.J., Duan, R., Zhang, J.Z., Hambley, T.W.: Investigations using fluorescent ligands to monitor platinum(IV) reduction and platinum(II) reactions in cancer cells. *Dalton Trans.* 3092–3101 (2009)
106. Chaney, S.G., Wyrick, S., Till, G.K.: In vitro biotransformations of tetrachloro(d, l-trans)-1,2-diaminocyclohexaneplatinum(IV) (tetraplatin) in rat plasma. *Cancer Res.* **50**, 4539–4545 (1990)

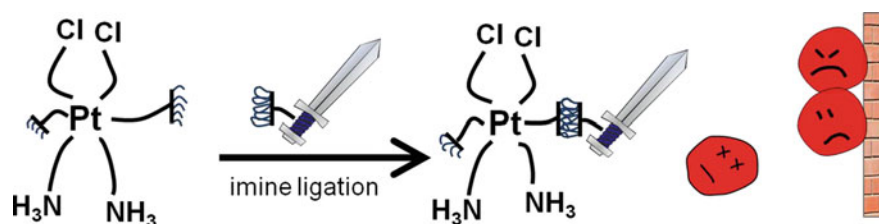
107. Carr, J., Tingle, M., McKeage, M.: Satraplatin activation by haemoglobin, cytochrome C and liver microsomes in vitro. *Cancer Chemother. Pharmacol.* **57**, 483–490 (2006)
108. Galanski, M., Jakupec, M.A., Keppler, B.K.: Update of the preclinical situation of anticancer platinum complexes: novel design strategies and innovative analytical approaches. *Curr. Med. Chem.* **12**, 2075–2094 (2005)
109. Choi, S., Filotto, C., Bisanzo, M., Delaney, S., Lagasee, D., Whitworth, J.L., Jusko, A., Li, C., Wood, N.A., Willingham, J., Schwenker, A., Spaulding, K.: Reduction and anticancer activity of platinum(IV) complexes. *Inorg. Chem.* **37**, 2500–2504 (1998)
110. Kwon, Y.-E., Whang, K.-J., Park, Y.-J., Kim, K.H.: Synthesis, characterization and antitumor activity of novel octahedral Pt(IV) complexes. *Bioorg. Med. Chem.* **11**, 1669–1676 (2003)
111. Dhar, S., Gu, F.X., Langer, R., Farokhzad, O.C., Lippard, S.J.: Targeted delivery of cisplatin to prostate cancer cells by aptamer functionalized Pt(IV) prodrug-PLGA-PEG nanoparticles. *Proc. Natl. Acad. Sci. U. S. A.* **105**, 17356–17361 (2008)
112. Lake, R.A., Robinson, B.W.S.: Immunotherapy and chemotherapy—a practical partnership. *Nat. Rev. Cancer* **5**, 397–405 (2005)
113. Galluzzi, L., Senovilla, L., Zitvogel, L., Kroemer, G.: The secret ally: immunostimulation by anticancer drugs. *Nat. Rev. Drug Discov.* **11**, 215–233 (2012)
114. Zitvogel, L., Galluzzi, L., Smyth, M.J., Kroemer, G.: Mechanism of action of conventional and targeted anticancer therapies: reinstating immunosurveillance. *Immunity* **39**, 74–88 (2013).
115. Zitvogel, L., Apetoh, L., Ghiringhelli, F., Kroemer, G.: Immunological aspects of cancer chemotherapy. *Nat. Rev. Immunol.* **8**, 59–73 (2008)
116. Lesterhuis, W.J., Haanen, J.B.A.G., Punt, C.J.A.: Cancer immunotherapy—revisited. *Nat. Rev. Drug Discov.* **10**, 591–600 (2011)
117. Krysko, D.V., Garg, A.D., Kaczmarek, A., Krysko, O., Agostinis, P., Vandenabeele, P.: Immunogenic cell death and DAMPs in cancer therapy. *Nat. Rev. Cancer* **12**, 860–875 (2012)
118. Mattarollo, S.R., Loi, S., Duret, H., Ma, Y., Zitvogel, L., Smyth, M.J.: Pivotal role of innate and adaptive immunity in anthracycline chemotherapy of established tumors. *Cancer Res.* **71**, 4809–4820 (2011)
119. Halama, N., Michel, S., Kloor, M., Zoernig, I., Benner, A., Spille, A., Pommerencke, T., von Knebel, D.M., Folprecht, G., Lubner, B., Feyen, N., Martens, U.M., Beckhove, P., Gnjatic, S., Schirmacher, P., Herpel, E., Weitz, J., Grabe, N., Jaeger, D.: Localization and density of immune cells in the invasive margin of human colorectal cancer liver metastases are prognostic for response to chemotherapy. *Cancer Res.* **71**, 5670–5677 (2011)
120. Dieci, M.V., Criscitiello, C., Goubar, A., Viale, G., Conte, P., Guarneri, V., Ficarra, G., Mathieu, M.C., Delaloge, S., Curigliano, G., Andre, F.: Prognostic value of tumor-infiltrating lymphocytes on residual disease after primary chemotherapy for triple-negative breast cancer: a retrospective multicenter study. *Ann. Oncol.* **25**, 611–618 (2014)
121. de Biasi, A.R., Villena-Vargas, J., Adusumilli, P.S.: Cisplatin-Induced antitumor immunomodulation: a review of preclinical and clinical evidence. *Clin. Cancer Res.* **20**, 5384–5391 (2014)
122. Wang, D., Lippard, S.J.: Cellular processing of platinum anticancer drugs. *Nat. Rev. Drug Discov.* **4**, 307–320 (2005)
123. Reed, E.: Cisplatin, carboplatin, and oxaliplatin. In: Chabner, B.A., Longo, D.L. (eds.) *Cancer chemotherapy and biotherapy: principles and practice*, 5th edn, pp. 333–341. Lippincott Williams & Wilkins, Philadelphia (2011)
124. Tesniere, A., Schlemmer, F., Boige, V., Kepp, O., Martins, I., Ghiringhelli, F., Aymeric, L., Michaud, M., Apetoh, L., Barault, L., Mendiboure, J., Pignon, J.P., Jooste, V., van Endert, P., Ducreux, M., Zitvogel, L., Piard, F., Kroemer, G.: Immunogenic death of colon cancer cells treated with oxaliplatin. *Oncogene* **29**, 482–491 (2009)

125. Merritt, R.E., Mahtabifard, A., Yamada, R.E., Crystal, R.G., Korst, R.J.: Cisplatin augments cytotoxic T-lymphocyte-mediated antitumor immunity in poorly immunogenic murine lung cancer. *J. Thorac. Cardiovasc. Surg.* **126**, 1609–1617 (2003)
126. Ramakrishnan, R., Assudani, D., Nagaraj, S., Hunter, T., Cho, H.-I., Antonia, S., Altiock, S., Celis, E., Gabrilovich, D.I.: Chemotherapy enhances tumor cell susceptibility to CTL-mediated killing during cancer immunotherapy in mice. *J. Clin. Invest.* **120**, 1111–1124 (2010)
127. Lesterhuis, W.J., Punt, C.J.A., Hato, S.V., Eleveld-Trancikova, D., Jansen, B.J.H., Nierkens, S., Schreibelt, G., de Boer, A., Van Herpen, C.M.L., Kaanders, J.H., van Krieken, J.H.J.M., Adema, G.J., Figdor, C.G., de Vries, I.J.M.: Platinum-based drugs disrupt STAT6-mediated suppression of immune responses against cancer in humans and mice. *J. Clin. Invest.* **121**, 3100–3108 (2011)
128. Kleinerman, E.S., Zwelling, L.A., Muchmore, A.V.: Enhancement of naturally occurring human spontaneous monocyte-mediated cytotoxicity by cis-diamminedichloroplatinum(II). *Cancer Res.* **40**, 3099–3102 (1980)
129. Kleinerman, E., Howser, D., Young, R., Bull, J., Zwelling, L., Barlock, A., Decker, J., Muchmore, A.: Defective monocyte killing in patients with malignancies and restoration of function during chemotherapy. *Lancet* **316**, 1102–1105 (1980)
130. Lichtenstein, A.K., Pende, D.: Enhancement of natural killer cytotoxicity by cis-diamminedichloroplatinum(II) in vivo and in vitro. *Cancer Res.* **46**, 639–644 (1986)
131. Son, K., Kim, Y.-M.: In vivo cisplatin-exposed macrophages increase immunostimulant-induced nitric oxide synthesis for tumor cell killing. *Cancer Res.* **55**, 5524–5527 (1995)
132. Okamoto, M., Kasetani, H., Kaji, R., Goda, H., Ohe, G., Yoshida, H., Sato, M. and Kasatani, H.: cis-Diamminedichloroplatinum and 5-fluorouracil are potent inducers of the cytokines and natural killer cell activity in vivo and in vitro. *Cancer Immunol. Immunother.* **47**, 233–241 (1998).
133. Singh, R.A.K., Sodhi, A.: Antigen presentation by cisplatin-activated macrophages: role of soluble factor(s) and second messengers. *Immunol. Cell Biol.* **76**, 513–519 (1998)
134. Hu, J., Kinn, J., Zirakzadeh, A.A., Sherif, A., Norstedt, G., Wikström, A.C., Winqvist, O.: The effects of chemotherapeutic drugs on human monocyte-derived dendritic cell differentiation and antigen presentation. *Clin. Exp. Immunol.* **172**, 490–499 (2013)
135. Chang, C.-L., Hsu, Y.-T., Wu, C.-C., Lai, Y.-Z., Wang, C., Yang, Y.-C., Wu, T.-C., Hung, C.-F.: Dose-dense chemotherapy improves mechanisms of antitumor immune response. *Cancer Res.* **73**, 119–127 (2013)
136. Taniguchi, K., Nishiura, H., Yamamoto, T.: Requirement of the acquired immune system in successful cancer chemotherapy with cis-diamminedichloroplatinum (II) in a syngeneic mouse tumor transplantation model. *J. Immunother.* **34**, 480–489 (2011)
137. Dunn, G.P., Old, L.J., Schreiber, R.D.: The immunobiology of cancer immunosurveillance and immunoediting. *Immunity* **21**, 137–148
138. Allavena, P., Mantovani, A.: Immunology in the clinic review series; focus on cancer: tumour-associated macrophages: undisputed stars of the inflammatory tumour microenvironment. *Clin. Exp. Immunol.* **167**, 195–205 (2012)
139. Beatty, G.L., Chiorean, E.G., Fishman, M.P., Saboury, B., Teitelbaum, U.R., Sun, W., Huhn, R.D., Song, W., Li, D., Sharp, L.L., Torigian, D.A., O'Dwyer, P.J., Vonderheide, R. H.: CD40 agonists alter tumor stroma and show efficacy against pancreatic carcinoma in mice and humans. *Science* **331**, 1612–1616 (2011)
140. Sodhi, A., Chauhan, P.: Interaction between cisplatin treated murine peritoneal macrophages and L929 cells: involvement of adhesion molecules, cytoskeletons, upregulation of Ca²⁺ and nitric oxide dependent cytotoxicity. *Mol. Immunol.* **44**, 2265–2276 (2007)
141. Li, Y., Wang, Z., Ma, X., Shao, B., Gao, X., Zhang, B., Xu, G., Wei, Y.: Low-dose cisplatin administration to septic mice improves bacterial clearance and programs peritoneal macrophage polarization to M1 phenotype. *Pathog. Dis.* **72**, 111–123 (2014)
142. Kroemer, G., Galluzzi, L., Kepp, O., Zitvogel, L.: Immunogenic cell death in cancer therapy. *Annu. Rev. Immunol.* **31**, 51–72 (2013)

143. Obeid, M., Tesniere, A., Ghiringhelli, F., Fimia, G.M., Apetoh, L., Perfettini, J.L., Castedo, M., Mignot, G., Panaretakis, T., Casares, N., Metivier, D., Larochette, N., van Endert, P., Ciccosanti, F., Piacentini, M., Zitvogel, L., Kroemer, G.: Calreticulin exposure dictates the immunogenicity of cancer cell death. *Nat. Med.* **13**, 54–61 (2007)
144. Menger, L., Vacchelli, E., Adjemian, S., Martins, I., Ma, Y., Shen, S., Yamazaki, T., Sukkurwala, A.Q., Michaud, M., Mignot, G., Schlemmer, F., Sulpice, E., Locher, C., Gidrol, X., Ghiringhelli, F., Modjtahedi, N., Galluzzi, L., André, F., Zitvogel, L., Kepp, O., Kroemer, G.: Cardiac glycosides exert anticancer effects by inducing immunogenic cell death. *Sci. Transl. Med.* **4**, 143ra99 (2012)
145. Sukkurwala, A.Q., Adjemian, S., Senovilla, L., Michaud, M., Spaggiari, S., Vacchelli, E., Baracco, E.E., Galluzzi, L., Zitvogel, L., Kepp, O., Kroemer, G.: Screening of novel immunogenic cell death inducers within the NCI mechanistic diversity set. *OncoImmunology* **3**, e28473 (2014)
146. Kepp, O., Menger, L., Vacchelli, E., Locher, C., Adjemian, S., Yamazaki, T., Martins, I., Sukkurwala, A.Q., Michaud, M., Senovilla, L., Galluzzi, L., Kroemer, G., Zitvogel, L.: Crosstalk between ER stress and immunogenic cell death. *Cytokine Growth Factor Rev.* **24**, 311–318 (2013)
147. Chao, M.P., Jaiswal, S., Weissman-Tsukamoto, R., Alizadeh, A.A., Gentles, A.J., Volkmer, J., Weiskopf, K., Willingham, S.B., Raveh, T., Park, C.Y., Majeti, R., Weissman, I.L.: Calreticulin is the dominant pro-phagocytic signal on multiple human cancers and is counterbalanced by CD47. *Sci. Transl. Med.* **2**, 63ra94 (2010)

Chapter 2

Harnessing Chemoselective Imine Ligation for Tethering Bioactive Molecules to Platinum(IV) Prodrugs



2.1 Introduction

Platinum(II)-based drugs, namely *cisplatin*, *carboplatin* and *oxaliplatin*, are the first line of treatment for many types of malignancies, including testicular, ovarian and lung cancer [1, 2]. However, their efficacy is severely limited by adverse side-effects due to high toxicities and incidences of drug resistance, either inherent or acquired [3]. Though initially responsive to chemotherapy, some patients develop recurrent cancer characterized by acquired drug resistance and eventually succumb to the disease [4]. In recent years, there has been increasing interest in exploiting platinum(IV) as a prodrug strategy to mitigate the aforementioned limitations of conventional platinum(II) anticancer complexes with *satraplatin* currently undergoing Phase III clinical trials [5]. While themselves inactive, platinum(IV) complexes are readily reduced intracellularly to its active platinum(II) congener along with concomitant release of the axial ligands [6]. Platinum(IV) complexes are also coordinatively inert and

Reproduced with permission from the Royal Society of Chemistry.

amenable to further conjugation reactions [7]. They may therefore represent ideal scaffolds upon which to attach bioactive molecules which can act as targeting groups to enhance selectivity or as synergistic agents to overcome drug resistance [8]. Although this strategy embodies a burgeoning new direction to drive the development of platinum(IV) anticancer drugs, existing synthetic methodologies of tethering bioactive molecules to the axial sites are inadequate to fully exploit its latent potential.

When this work was first done, there were only two main techniques of functionalizing platinum(IV) complexes. The first is direct axial carboxylation with anhydrides [9] and acid chlorides (Fig. 2.1) [10, 11]. While this enormously versatile route has been used to prepare a wide range of simple aliphatic and aromatic dicarboxylate complexes [12–14] there have only several instances reported where it has been applied to conjugate bioactive ligands since the anhydrides or acid chlorides of these ligands may not be synthetically accessible [15–17]. The second approach is via carboxylation with cyclic anhydrides [18–20] to give platinum(IV) carboxylates bearing an uncoordinated pendant carboxyl functional group which can be further derivatized via classical amide or ester coupling chemistry (Fig. 2.1) [20–23]. Similarly, there have only been a handful of examples of conjugation to a genuine potentiating ligand e.g. estrogen, targeting peptides and carbon nanotubes [8, 24, 25]. The dearth of platinum(IV)-conjugates is possibly symptomatic of the limited synthetic scope of the aforementioned methods. This is due to poor reaction yields of classical amide/ester coupling protocols with platinum complexes as substrates. For example, low yields were observed with simple primary amines and alcohols [20], and conjugation with stoichiometric excess of several targeting tripeptides led to muted yields of the di-functionalized conjugate [24].

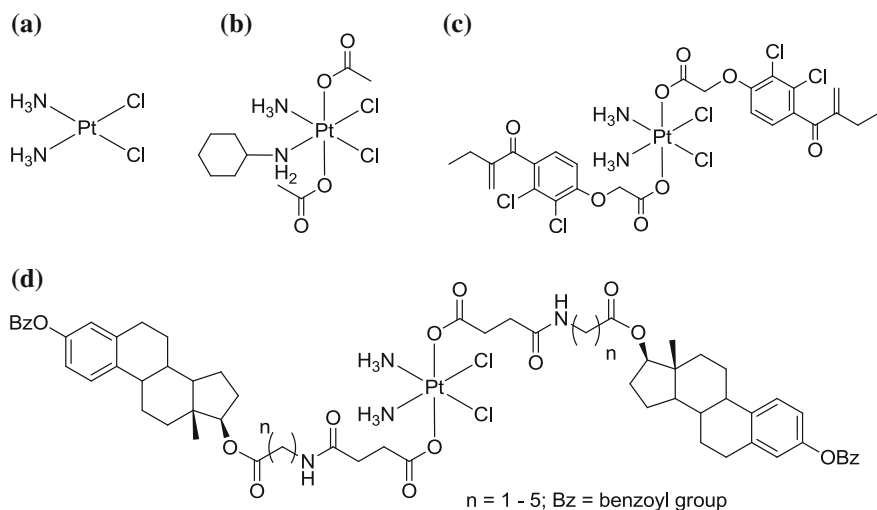


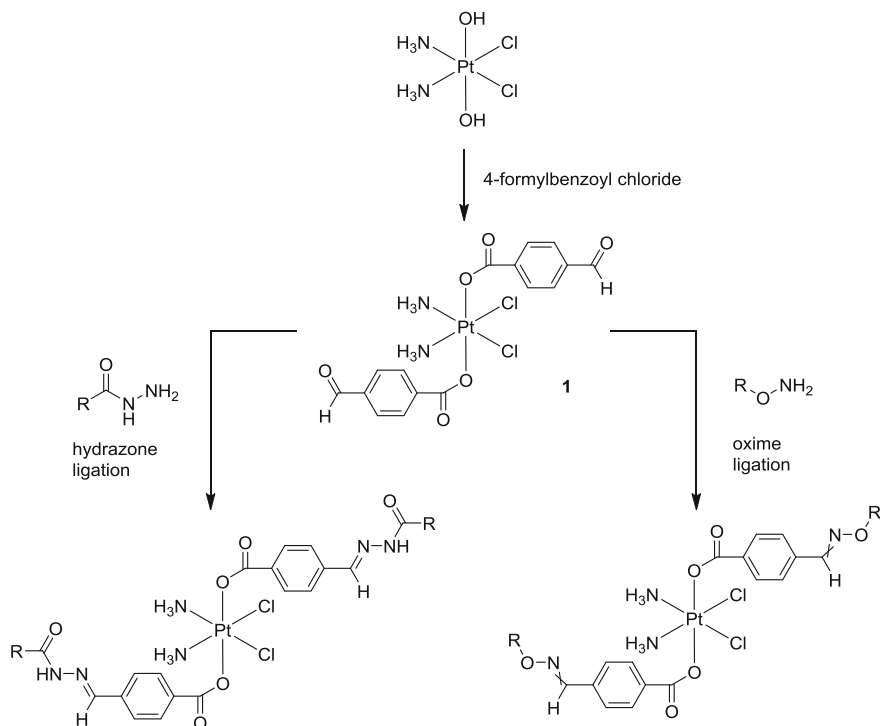
Fig. 2.1 **a** Cisplatin, **b** satraplatin, **c** ethacrynic acid-conjugated platinum(IV) complex, synthesized by direct axial carboxylation with acid chloride and, **d** estrogen-tethered platinum(IV) complexes formed by amide coupling of an uncoordinated pendant carboxyl functional group with an amine-linker functionalized estrogen

In order to expand utility of platinum(IV) scaffolds as functionalized prodrugs, there is a need to explore and apply current chemoselective ligation chemistries to platinum(IV) anticancer prodrugs. This work investigates the application of imine ligations for conjugation through hydrazone or oxime bond formation. Hydrazone or oxime bond formation are ideal as the condensation reaction between an α -effect amine with a carbonyl group are highly chemoselective and bioorthogonal to most biological functional groups [26, 27]. When catalyzed by aniline, hydrazone/oxime formation are among the fastest and mildest bioconjugation reactions available in literature, going to completion rapidly in aqueous solution at physiological pH and at low stoichiometric concentrations of reactants [28]. Hydrazide and aminoxy tags are also convenient handles to introduce onto biological macromolecules via established chemistries [29]. Here, we describe the synthesis of a *cis,cis,trans*-diamminedichlorobis(4-formylbenzoate)platinum(IV) scaffold bearing an aromatic aldehyde functionality and explored the scope of imine ligation with various hydrazide/aminoxy functionalized substrates. As a proof of concept, we tethered a six sequence long peptide mimetic (AMVSEF) of the anti-inflammatory protein, ANXA1. Related *N*-terminal peptides of ANXA1 have demonstrated antiproliferative activity against various cancer cell lines [30, 31]. The synthetic ease, yields and rate of conjugation reported here clearly exceeds all previous instances using conventional amide/ester coupling strategies.

2.2 Results and Discussion

Perhaps a major obstacle in the synthetic development of functionalized platinum (IV) bis-carboxylate prodrugs has been the absence of a conjugation methodology sufficiently robust to reliably and efficiently combine platinum(IV) complexes with relevant bioactive molecules. Being kinetically inert and unreactive, platinum(IV) prodrugs are postulated to be chemically reduced by endogenous bioreductants such as glutathione to cytotoxic platinum(II) species capable of DNA-binding [7]. We previously observed platinum(IV) bis-carboxylate complex bearing benzoate ligands to be highly stable but bind deoxyguanosine monophosphate (dGMP) to form Pt-dGMP adducts upon treatment with bioreductants such as ascorbic acid and glutathione. We hypothesized that these kinetically inert platinum(IV) complex would be sufficiently stable under the mildly acidic conditions typically employed in imine ligation and in the presence of the nucleophilic hydrazide and hydroxylamine linkers. We explored the scope of a platinum(IV) scaffold bearing symmetric axial benzaldehyde functionality for imine conjugation reactions.

Synthesis and characterization. The platinum(IV)-benzaldehyde complex (1) was synthesized via a modification of a versatile synthetic method previously described by Galanski and Dyson et al. for the preparation of *trans*-platinum(IV) carboxylates [10, 18]. Acylation of the dihydroxylplatinum(IV) precursor with the corresponding acid chloride, 4-formylbenzoyl chloride, in the presence of pyridine



Scheme 2.1 Synthesis of *trans,cis,cis*-bis(4-formylbenzoate)dichlorodiammine platinum(IV) (**1**) and subsequent imine ligation with various substrates

as an organic base gave the expected product **1** in good yield of about 75% (Scheme 2.1).

Characterization by ¹H NMR and ESI-MS were consistent with the expected structure (Figs. S2.1 and S2.2). The aldehydic proton was the most downfield at 10.10 ppm, as expected, and the aromatic protons exhibited an AA¹BB¹ splitting pattern consistent with a *para*-disubstituted phenyl ring. A well-defined spin-spin coupling of the ammine protons to quadrupolar ¹⁴N ($I = 1$, ¹J_{HN} = 52.9 Hz) as well as to ¹⁹⁵Pt ($I = 1/2$, ²J_{HPt} = 52.3 Hz) could be observed in deuterated acetone. Such distinct N–H coupling has also been observed with other platinum(IV) diammine complexes with axial aromatic ligands [18]. The purity of **1** was ascertained by RP-HPLC (>98% purity, 254 and 280 nm) under two separation conditions (Fig. S2.3). Notably, compound **1** was also effectively stable as monitored by HPLC at 254 nm in a solution of 50% DMF/aq. NaOAc (pH 4.8, 2 M) for over 2 weeks and does not undergo ligand exchange even in the presence of acetate nucleophiles and under weakly acidic conditions required for imine ligation.

In order to evaluate the efficiency and ease of imine ligation, we conjugated **1** to various hydrazide/aminooxy-functionalized substrates (Scheme 2.1 and Fig. 2.2). In general, the ligation reaction was carried out by stirring **1** with stoichiometric

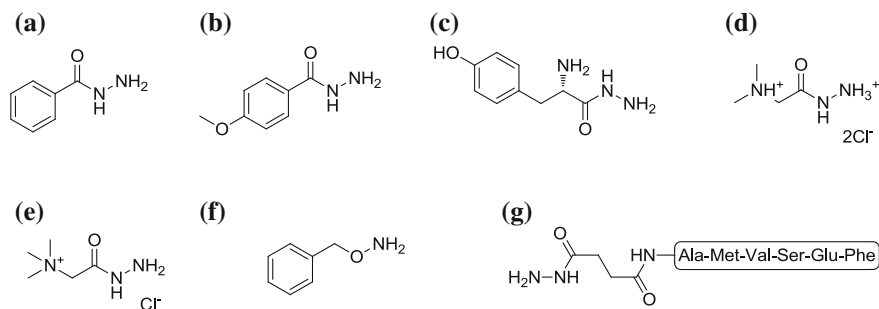


Fig. 2.2 Structures of hydrazide or aminoxy functionalized substrates, **a** benzhydrazide, **b** 4-methoxybenzhydrazide, **c** L-tyrosine hydrazide, **d** Girard's reagent D, **e** Girard's reagent T, **f** benzylhydroxylamine and **g** hydrazide-functionalised AMVSEF peptide

excess of the substrates in an aq. buffer solution containing 50% v/v DMF at r.t. and effectively gave the desired bis-conjugated products **2a-f** in high yields and purity. Often, only rudimentary washing in water or ethanol were necessary to remove the excess unreacted hydrazides/hydroxylamines. Conversion of **1** to **2a-f** was quantitative as monitored by HPLC although the recovered yields for the water-soluble conjugates **2c-e** were lowered due to aqueous washing during workup. These reactions conditions were found to versatile and robust. Though customarily catalysed by a slightly acidic medium, imine ligation could also be carried out at pH 7 or under catalytic condition in the presence of *p*-anisidine [32]. 50% v/v DMF/water was a favorable solvent composition to promote the solubility of **1** although the reaction can also be carried out as a heterogeneous reaction mixture in 10% v/v DMF/water, albeit at a slower rate.

Reaction monitoring of imine ligation. Reaction monitoring on the formation of **2a** with excess benzhydrazide using RP-HPLC showed a clean conversion of **1** to the bis-conjugated Pt-benzhydrazide **2a** via the mono-conjugated intermediate (Fig. 2.3). The mono-conjugated Pt-benzhydrazide product could be observed in an approximately 1:1 ratio with **2a** at equilibrium when only a stoichiometric equivalent amount of benzhydrazide was used, confirmed by ESI-MS analysis of isolated fractions. In general, the platinum(IV)-imine conjugates themselves were generally stable under the reaction conditions but we did observe noticeable side product formation in **2b** after 4 days in solution presumably due to the slow cleavage of the aryl methyl ether at pH 4.8. This was ameliorated when a less acidic 50% DMF/aq. pH 5.5 MES buffer was used as the reaction medium instead.

While hydrazone ligation of **1** to form **2a-e** gave a single bis-conjugated product at equilibrium, oxime ligation with *o*-benzylhydroxylamine yielded *EE* and *EZ* stereoisomeric mixture of **2f** with respect to the N=CH-Ph double bond. Unlike hydrazone formation, the (*E*) and (*Z*) stereoisomers of oximes may be chromatographically separated as the energy barrier towards (*E*)/(*Z*) isomerism is relatively higher. RP-HPLC of **2f** indicated the formation of two products with closely spaced retention times at 19.0 (87% by integration) and 18.6 min (10.2%) which were

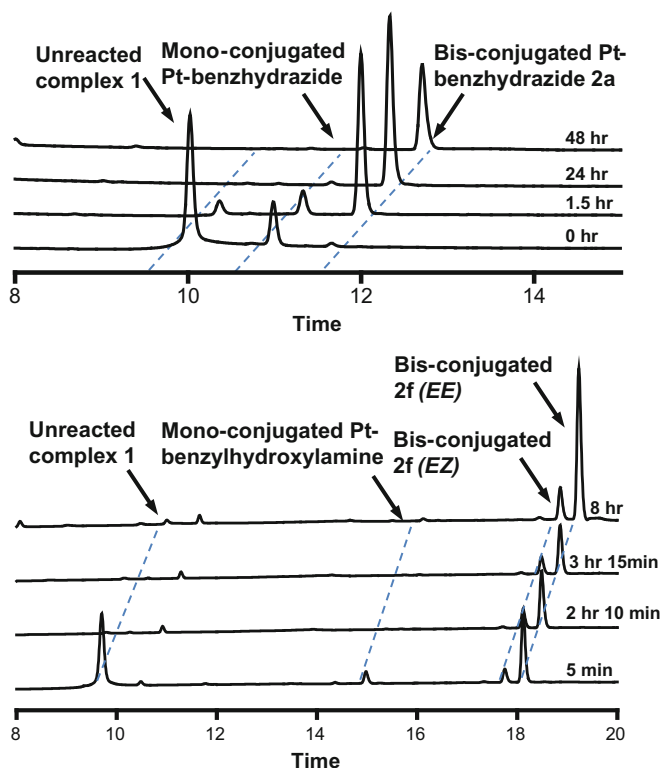


Fig. 2.3 HPLC monitoring of formation Pt-benzhydrazide (top) and Pt-benzylhydroxylamine (bottom) over time in 50% DMF/aq. NaOAc (2 M, pH 4.8)

assigned as belonging to the *EE* and *EZ* stereoisomers respectively. This was corroborated by the presence of two oxime protons ($N=CH-Ph$) at 8.38 and 8.32 ppm corresponding to the (*E*) and (*Z*) isomer, respectively. The assignment of both the HPLC and NMR peak was made on the basis that the (*E*) isomer should be the predominant product, as observed with other aromatic aldoximes, due to steric and thermodynamic reasons [33]. It has also been previously reported the resonance of the oxime proton in the (*E*)-isomer was shifted downfield relative to that of its (*Z*)-isomer [33, 34]. The ratio of *EE:EZ* stereoisomers varied only slightly when ligated under different conjugation conditions of pH 4.8, pH 7 and pH 4.8 at 50 °C. In general, imine formation in **2a-f** was supported by the disappearance of the aldehyde signal at 10.1 ppm and the appearance of a more upfield imine signal between 8.11 and 8.51 ppm in the 1H NMR. The 1H NMR and ESI-MS spectra of **2a-f** were consistent with their expected structures.

Catalysis by *p*-anisidine. In order to fully harness the utility of chemoselective imine ligation as part of our ongoing efforts to tether platinum(IV) prodrugs to therapeutically relevant biomolecules, we explored the use of *p*-anisidine as a

catalyst to afford milder conjugation conditions at physiological pH instead of under typical acidic conditions which may denature sensitive biomolecules. *p*-anisidine is a potent catalyst of imine ligation at pH 7 as the transient Schiff base it forms with aldehydes has a relatively high pK_a , leading to a high concentration of electrophiles for subsequent attack by α -effect amines like hydrazides and aminoxy groups [32]. Full conversion to the bis-conjugated **2a** was achieved within 8 h when catalysed by 100 mM *p*-anisidine at pH 7 (Fig. 2.4). In contrast, only about <2 and 50% conversion to the bis-conjugated **2a** and mono-conjugated product respectively was formed within the same period in the uncatalysed reaction. The use of *p*-anisidine as a catalyst was also useful in the synthesis of the water-soluble conjugates **2d** and **2e** with Girard's reagent D and T since they were difficult to separate from an acidic aq. buffer by washing with water. *p*-Anisidine could be easily removed from **2d** and **2e** by washing in ethanol. We observed that catalysis with *p*-anisidine led cleanly to the formation of the bis-product and that **1** and the conjugates formed were stable in 100 mM *p*-anisidine with little to no undesired side-product formation.

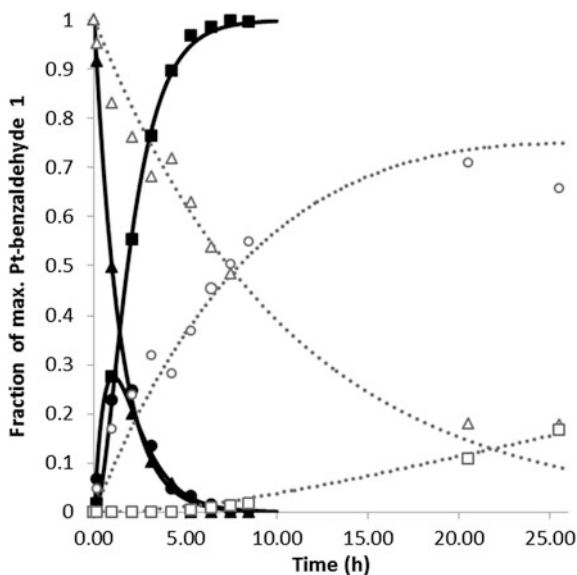


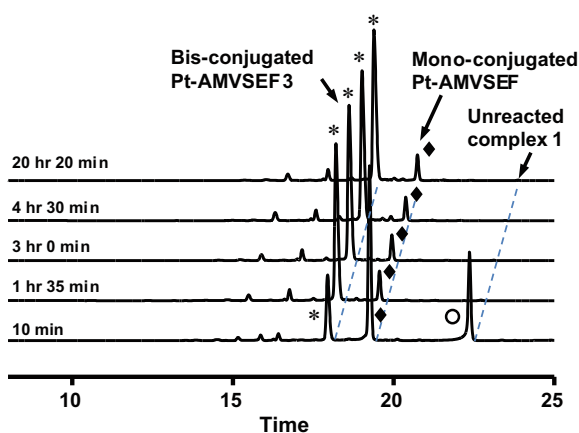
Fig. 2.4 Comparison between rate of imine ligation between the catalysed and uncatalysed reaction mixture; the solid and dotted line represents the fitted curves for the catalysed and uncatalysed reaction respectively to the differential rate equations for a two-step consecutive reversible reaction; Uncatalysed reaction: 0.263 mM Pt-benzaldehyde**1**, 8.71 mM benzhydrazide; Catalysed reaction: 0.263 mM Pt-benzaldehyde**1**, 8.71 mM benzhydrazide, 100 mM *p*-anisidine. Legend: Δ unreacted complex**1**, \circ mono-Pt-benzhydrazide, \square bis-Pt-benzhydrazide. Filled black symbols and hollow gray symbols represent the catalysed and uncatalysed reactions, respectively

Stability of imine-ligated platinum(IV)-conjugates. We also investigated the rate of hydrolysis of hydrazone bonds under physiological conditions as the relative lability of hydrazone bonds has often been flagged as a shortcoming of imine ligation as compared to other chemoselective ligation techniques such as the 1,3-Husigen click reaction [35]. Earlier on, the platinum(IV) scaffold **1** was intentionally designed with axial benzaldehyde handles since imines of benzaldehydes are known to exhibit significantly slower rate kinetics of hydrolysis compared to other aldehyde or ketone moieties [36]. To test this hypothesis, we monitored the hydrolysis of **2e** under physiological conditions by UV-vis spectroscopy in aq. pH 7.4 buffered solution at 37 °C over 24 h (Fig. S2.5). At low concentrations, the hydrolysis products should be predominant at equilibrium but the time it takes to reach equilibrium is a function of the rate of hydrolysis (k_{-1} and k_{-2}). There was little change in the UV spectra within 10 h, indicating negligible hydrolysis during this period. Hydrolysis occurred fairly slowly still nonetheless, with about 14% hydrolysis after 24 h as implied by the decreasing absorbance at 303 nm.

The rate constants for hydrazone hydrolysis reported in literature are typically in the magnitude of 10^{-5} to 10^{-7} s $^{-1}$ which will in principle, take days to hydrolyse appreciably [28, 36, 37]. Assuming pseudo 1st order irreversible hydrolysis in dilute solutions and a hypothetical k_{-1} of 1×10^{-6} s $^{-1}$, it will require approximately 29 and 194 h to reach 10 and 50% hydrolysis respectively. In contrast, the half-life for in vivo reduction of platinum(IV) to platinum(II) complexes with the concomitant release of axial ligands is estimated to range from a few minutes to a few hours depending on cell-line and conditions [38–40]. Therefore hydrazone ligation of targeting groups and other potentiating bioactive molecules to the platinum(IV)-benzaldehyde scaffold **1** would be sufficiently stable as its dissociation would be very slow relative to the rapid reduction of platinum(IV) carboxylates in vivo. Recently, another platinum(IV) scaffold bearing a ketone moiety for subsequent hydrazone ligation to hydrazide-functionalised polymeric nanoparticles was reported [41]. Although it fulfills the purpose of sustained cisplatin release, the half-life of ketone-based hydrazone hydrolysis at pH 7.4 will be much more rapid and in the order of minutes. In circumstances where hydrolysis is detrimental, oxime ligation such as in **2f** may be employed as oximes are inherently more resistant towards hydrolysis than hydrazones [42].

Till date, there have only been a few examples of platinum(IV)-peptide conjugates reported in literature. In one reported instance, several angiogenesis-targeting linear tripeptides and cyclic pentapeptides were conjugated to a platinum(IV) scaffold via EDC amide coupling with the aim of selectively targeting angiogenic tumor endothelial cells over normal tissues [24]. Encouragingly, the targeting peptide-tethered platinum(IV) complexes were more cytotoxic towards malignant endothelial cell lines compared to non-specific platinum(IV)-peptide controls as well as the free targeting peptides, demonstrating it is potentially possible to rationally alter the selectivity and activity of platinum(IV) prodrugs simply by judicious conjugation with therapeutically-relevant peptide moieties. However, the low yields obtained from EDC-mediated amide coupling reactions produced

Fig. 2.5 RP-HPLC (254 nm) reaction monitoring of formation of Pt-AMVSEF peptide $\mathbf{3}$ over time in 20% DMF. The free hydrazide-functionalised peptide ($R_t = 13.80$ min) is not visible at 254 nm. Legend: * bis-conjugated Pt-AMVSEF $\mathbf{3}$, \blacklozenge mono-conjugated Pt-AMVSEF and \circ unreacted complex $\mathbf{1}$



mixtures of mono-functionalised (11–16%) and di-functionalised (5–8%) platinum (IV) peptide, may be a potential stumbling block towards the development of more diverse platinum(IV)-peptide conjugates.

To demonstrate the improvement of imine ligation over amide coupling, we tethered **1** to a hydrazide-functionalized AMVSEF peptide, the *N*-terminus mimetic of anti-inflammatory protein ANXA1, as a proof of concept. When stirred at r.t., hydrazone ligation in a 20% DMF/H₂O solution rapidly attained equilibrium within 4.5 h with the complete consumption of **1** to give predominantly the bis-conjugate **3** as the major product along with the mono-conjugate peptide as the minor product (ca. 7%) as observed by RP-HPLC (Fig. 2.5). Excluding the unreacted free peptide, the crude reaction mixture was relatively clean as indicated by RP-HPLC at 214 and 254 nm which consisted of bis-conjugate **3** (82%) and mono-conjugate (7%) products. Their identities were confirmed by ESI-MS analysis on isolated RP-HPLC fractions of the individual peaks. These results highlighted that the advantage of imine ligation over amide conjugation in terms of reaction setup and yield.

2.3 Conclusion

In conclusion, imine ligation to the platinum(IV)-benzaldehyde scaffold **1** was found to be robust and high yielding, addressing the synthetic limitations of current amide/ester coupling methodologies. The reliability of imine ligation may open up the hereinbefore largely untapped potential of platinum(IV) conjugates as prodrugs by improving upon the synthetic ease by which these conjugates may be made.

2.4 Methods

Materials and methods. Unless otherwise stated, all reagents were purchased from commercial vendors and used without further purification. Potassium tetrachloroplatinate(II) was obtained from both Precious Metals Online and Strem Chemicals and was purified by filtering its aqueous solution through Celite to remove trace particulates. *cis*-diamminedichloroplatinum(II) and *cis,cis,trans*-diamminedichlorodihydroxoplatinum(IV) were synthesized and purified as per literature procedures [43, 44]. Resin-bound ANXA1 peptide (Ala-Met-Val-Ser-Glu-Phe) was obtained from GL Biochem (Shanghai). The hydrazide linker, 4-(*N*-tert-butoxycarbonyl-hydrazino)-4-oxo-butyric acid, was prepared as previously described [37]. 4-Formylbenzoic acid was further purified by recrystallization from boiling water with addition of decolorizing carbon. Dry tetrahydrofuran (THF) and diethyl ether were obtained directly from Glass Contour's Solvent Dispensing System. Acetone was dried by distillation over potassium carbonate.

¹H NMR was recorded on a Bruker Avance 300 or 500 MHz model. Chemical shifts are reported in parts per million relative to residual solvent peaks [45]. Electrospray ionization mass spectra (ESI-MS) were obtained on a Thermo Finnigan MAT ESI-MS system. UV-vis spectra were recorded on a Shimadzu UV-1800 UV-vis spectrophotometer. Analytical HPLC was conducted either on a Agilent 1200 series DAD using Phenomenex Luna C18(2) column (5 μm, 100 Å, 250 × 4.60 mm, 1.0 mL/min flow) or on Shimadzu Prominence using Shimpack VP-ODS column (5 μm, 120 Å, 150 × 4.60 mm, 1.0 mL/min flow). Purity of synthesized compounds was assessed on the Shimadzu Prominence using a gradient elution of 20–80% B over 15 min followed by 80% B for a further 5 min where solvent A is aq. NH₄OAc buffer (10 mM, pH 5.5) and solvent B is MeCN. Semi-preparative HPLC was performed on a Shimadzu Prominence using YMC-Pack Pro C18 column (5 μm, 120 Å, 250 × 10 mm, 2.0 mL/min flow).

Synthesis of 4-formylbenzoyl chloride. Catalytic amount of DMF (20 μL) was added to a vigorously stirred solution of 4-formylbenzoic acid (1000 mg, 6.67 mmol) dissolved in THF (15 mL) and cooled in an ice bath. Oxalyl chloride (687 μL, 7.99 mmol) was then added dropwise to the reaction mixture which was further stirred for 6 h before gradually allowing it to warm to room temperature. Unreacted oxalyl chloride was removed by evaporation in vacuo to yield a white residue. Trace amount of oxalyl chloride was removed by repeated washings in ether (3 × 10 mL) followed by evaporation in vacuo. The crude product, obtained in quantitative yield, was used directly in the next without further manipulation.

Synthesis of *cis,cis,trans*-diamminedichlorobis(4-formylbenzoate)platinum(IV) 1. 4-Formylbenzoyl chloride (1124 mg, 6.68 mmol) dissolved in acetone (40 mL) was added dropwise to a vigorously stirred suspension of *cis,cis,trans*-diamminedichloro-dihydroxoplatinum(IV) (100 mg, 0.30 mmol) and pyridine (723 μL, 8.98 mmol) in acetone (20 mL). The reaction mixture was refluxed for 5 h and left at r.t. for a further 8 h. The reaction mixture was treated with water (100 mL) and cooled at 4 °C for 12 h. The solvent volume was reduced by half,

centrifuged, and the solvent decanted. The residue was washed with water (3×50 mL) and ether (3×60 mL) to yield an off-white powder. The product was purified by dissolution in minimal DMF and precipitating with equivolume of ethyl acetate (EA). The desired product remained as a homogenous solution initially but gradually precipitates after 2–3 h as an off-white powder. To maximize the yield, the filtrate was evaporated to dryness, redissolved in minimal DMF, supersaturated with H₂O and recrystallized again by adding EA to slowly precipitate an additional crop of the desired product. Combined yield: 135 mg (75%). C₁₆H₁₆Cl₂N₂O₆Pt.1DMF (671.4): calc. C 33.99, H 3.45, N 6.26; found C 34.15, H 3.68, N 6.1 ¹H NMR (acetone-d₆, 300.13 Hz): 10.14 (s, 2H, CHO), 8.16 (d, 4H, Ar-H, ³J_{HH} = 8.2 Hz), 7.98 (d, 4H, Ar-H, ³J_{HH} = 8.2 Hz), 6.74 (m, 6H, NH₃, ¹J_{HN} = 53.9 Hz, ²J_{HPt} = 52.3 Hz); ESI-MS (–ve mode, m/z): 596.8 [M–H][–]; Purity (HPLC): 1 peak at 254 and 280 nm.

General procedure for synthesis of platinum(IV)-imine conjugates. In general, the platinum(IV)-imine conjugates were prepared by treating **1** with 5–10 times stoichiometric excess of the desired hydrazide/aminooxy-functionalised substrate in an aq. buffer solution containing 50% v/v DMF. Progress of the reactions was followed by RP-HPLC at periodic intervals. The reaction mixture was lyophilised, washed and dried to yield the final product.

Synthesis of platinum(IV)-benzhydrazide bis-conjugate (2a). Benzhydrazide (45.0 mg, 334 μmol) was stirred with **1** (20 mg, 33 μmol) in 50% v/v DMF/ H₂O for 24 h. The crude reaction mixture was lyophilized to yield an off-white precipitate and washed with H₂O (4×5 mL). Yield: 26.5 mg (95%). ¹H NMR (DMSO-d₆, 300.13 Hz): 8.51 (s, 2 × 1H, imine proton), 8.00–7.91 (m, 2 × 4H, ArH), 7.81–7.78 (m, 2 × 2H, ArH), 7.50–7.53 (m, 2 × 3H, ArH), 6.79 (br m, 2 × NH₃); ESI-MS (–ve mode, m/z): 833.0 [M–H][–]; Purity (HPLC): 96% at 254 nm.

Synthesis of platinum(IV)-methoxybenzhydrazide bis-conjugate (2b). 4-methoxybenzhydrazide (55.5 mg, 334 μmol) was stirred with **1** (20 mg, 33 μmol) in 50% v/v DMF/aq. MES (0.1 M, pH 5.5) for 20 h. The crude reaction mixture was then lyophilized to yield an off-white residue and washed with H₂O (4×5 mL). Depending on the quality of 4-methoxybenzhydrazide used, it was sometimes necessary to wash further with 30% DMF/H₂O (2 × 1 mL) and EA (1 × 1 mL). Yield: 28.9 mg (97%). ¹H NMR (DMSO-d₆, 300.13 Hz): 11.85 (s, 2 × 1H, NH), 8.50 (s, 2 × 1H, imine proton), 7.98 (d, 2 × 2H, ArH, ³J_{HH} = 8.4 Hz), 7.92 (d, 2 × 2H, ArH, ³J_{HH} = 8.73 Hz), 7.78 (d, 2 × 2H, ArH, ³J_{HH} = 7.7 Hz), 7.08 (d, 2 × 2H, ArH, ³J_{HH} = 8.85 Hz), 6.79 (br m, 2 × NH₃), 3.84 (s, 2 × 3H); ESI-MS (–ve mode, m/z): 893.0 [M–H][–]; Purity (HPLC): 95% at 254 nm.

Synthesis of platinum(IV)-tyrosine hydrazide bis-conjugate (2c). l-Tyrosine hydrazide (39.1 mg, 200 μmol) was stirred with **1** (24 mg, 40 μmol) in 50% DMF/ aq. NaOAc (2 M, pH 4.8). The crude reaction mixture was lyophilized after 4 h to yield a pale yellow solid which was then washed with cold H₂O (4×1 mL). Yield: ca. 32.4 mg (85%). ¹H NMR (DMSO-d₆, 500.13 Hz): 9.18 and 9.12 (s, 2 × 1H, NH amide), 8.27 (s, 2 × 1H, imine), 7.98–7.94 (m, 2 × 2H, ArH), 7.73–7.69

(m, 2 × 2H, ArH), 7.02–7.00 (m, 2 × 2H, ArH), 6.78 (br, 2 × NH₃), 6.67–6.61 (m, 2 × 2H, ArH), remaining protons were not observed or obscured by solvent; ESI-MS (–ve mode, m/z): 951.1 [M–H][–], Purity (HPLC): 94% at 254 nm.

Synthesis of platinum(IV)-Girard's reagent D. 2HCl (2d). Girard's reagent D dihydrochloride (31.8 mg, 167 μmol) was stirred with **1** (20 mg, 33 μmol) in 50% DMF/aq. *p*-anisidine (100 mM). The crude reaction mixture was lyophilized after 12 h to give a brownish residue and washed with chilled H₂O (2 × 1 mL), ethanol (2 × 1 mL) and ethyl acetate (1 × 0.5 mL) to yield a white precipitate. Yield: 24.5 mg (85%). ¹H NMR (DMSO-d₆, 300.13 Hz): 12.14 (s, 1H, NH), 8.11 (s, 2 × 1H, imine proton), 7.97–7.95 (d, 2 × 2H, ArH), 7.80–7.77 (d, 2 × 2H, ArH), 6.79 (br m, 2 × NH₃), 4.52 (s, 2 × 2H, CH₂), 2.87 (s, 2 × 3H, CH₃); ESI-MS (+ve mode, m/z): 797.0 [M–H]⁺; Purity (HPLC): 95% at 254 nm.

Synthesis of platinum(IV)-Girard's reagent T. 2Cl (2e). Girard's reagent T (28.1 mg, 167 μmol) was stirred with **1** (20 mg, 33 μmol) in 50% DMF/aq. *p*-anisidine (100 mM). The work-up was performed in the same manner as **2d**. Yield: 20.0 mg (67%). ¹H NMR (DMSO-d₆, 300.13 Hz): 8.11 (s, 2 × 1H, imine proton), 7.98–7.95 (m, 2 × 2H, ArH), 7.81–7.79 (m, 2 × 2H, ArH), 6.81 (br m, 2 × NH₃), 4.81 (s, 2 × 2H, CH₂), CH₃ obscured by solvent; ESI-MS (+ve mode, m/z): 413.4 [M]²⁺, 825.0 [M–H]⁺; Purity (HPLC): 95% at 254 nm.

Synthesis of platinum(IV)-benzylhydroxylamine (2f) bis-conjugate. *o*-Benzylhydroxylamine hydrochloride (53.3 mg, 334 μmol) was stirred with **1** (20 mg, 33 μmol) in 50% DMF/aq. NaOAc (2 M, pH 4.8). The crude reaction mixture was lyophilized after 24 h to yield an off-white precipitate which was then washed with H₂O (4 × 5 mL). Yield: 25.01 mg (93%). ¹H NMR (DMSO-d₆, 300.13 Hz): 8.34 (s, 2 × 1H, (E) imine proton), 8.32 (s, 2 × 1H, (Z) imine proton), 7.94–7.91 (d, 2 × 2H, ArH), 7.68–7.65 (d, 2 × 2H, ArH), 7.44–7.29 (d, 2 × 5H, ArH), 6.77 (br m, 2 × NH₃), 5.21 (s, 2 × 2H, CH₂); ESI-MS (–ve mode, m/z): 807.0 [M–H][–]; Purity (HPLC): 87.4% *EE* and 10.2% *EZ* stereoisomers at 254 nm.

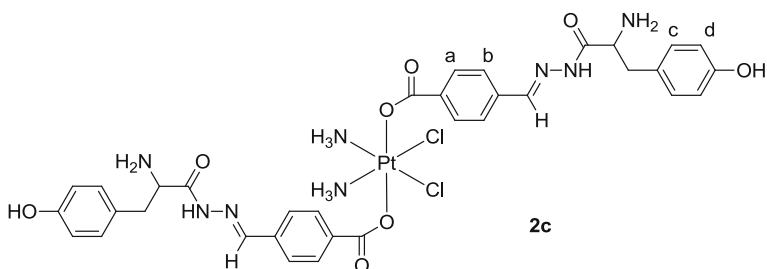
Synthesis of hydrazide linker-functionalised AMVSEF peptide. 4-(*N*-tert-butoxycarbonyl-hydrazino)-4-oxo-butyric acid (116.1 mg, 500 μmol) was treated with *N,N'*-diisopropylcarbodiimide (63.1 mg, 500 μmol) and *N*-hydroxysuccinimide (57.5 mg, 500 μmol) in DMF (0.5 mL) for 10 min. The emulsion was then added to the AMVSEF peptide resin (100 mg, ca. 100 μmol) and stirred at room temperature for 2 h. The resin was washed repeatedly with DMF, DCM and 1:1 v/v DCM/MeOH and dried thoroughly. Subsequently, the resin was incubated with a freshly prepared TFA cocktail (5% thioanisole, 3% EDT and 2% anisole v/v added as scavengers) for 1.5 h and filtered. The filtrate was added dropwise to cold ether (15 mL) to yield a white precipitate which was collected by centrifugation and washed with cold ether (3 × 5 mL). The residue was dissolved in glacial acetic acid and lyophilized to yield the crude hydrazide-functionalised peptide. The crude product (50 mg) was dissolved in 70% DMF/H₂O (100 μL) and purified by semi-preparative RP-HPLC (Shimadzu) using a 5–29% gradient elution system with aq. NH₄OAc buffer (10 mM, pH 7) (solvent A) and MeCN (solvent B) over 40 min at 2.0 mL/min; ESI-MS (–ve mode, m/z): 797.1 [M+H]⁺.

Synthesis of platinum(IV)-AMVSEF peptide bis-conjugate (3). Pt-benzaldehyde **1** (ca. 0.1 mg, 0.167 μmol) was stirred with hydrazide-functionalised AMVSEF peptide (ca. 1 mg, 1.17 μmol) in 20% DMF/H₂O (1.75 mL). The reaction mixture was monitored by RP-HPLC (Agilent) over 24 h using a gradient of 5–15% B in the first 10 min followed by 15–80% B for 20 min where solvent A is aq. NH₄OAc buffer (10 mM, pH 5.5) and solvent B is MeCN. The bis-conjugated product was subsequently purified by RP-HPLC (Shidmadzu) using a gradient elution system of 5–15% B for 10 min followed by 15–80% for the next 20 min where solvent A is aq. NH₄OAc buffer (10 mM, pH 7) and solvent B is MeCN; ESI-MS (–ve mode, m/z): 1076.8 [M–2H]^{2–}; Purity (HPLC): 1 peak at 254 nm.

Catalysis at physiological pH by *p*-anisidine. Benzhydrazide (4.15 mg) was added to 3.5 mL of a stock solution of **1** (0.263 mM) in 50% DMF/H₂O. The reaction mixture was divided equally into two portions and *p*-anisidine (21.5 mg) was added to one portion. The final reaction mixture comprises 0.263 mM **1** and 8.71 mM benzhydrazide, with the catalysed reaction containing an additional 100 mM *p*-anisidine. Both reactions were agitated and monitored at periodic intervals using RP-HPLC. The consumption of **1** and formation of the bis-conjugated product **2a** was quantified by integration at 254 and 280 nm. The experimental data was fitted to model a two-step pseudo 1st order consecutive reversible reaction using the chemical reactions module of Berkeley Madonna (Macey & Oster, UCLA). The experiment was repeated with 0.117 mM **1** and 27.7 mM benzhydrazide. Further details are described in SI.

Stability of Pt-Girard's reagent T (2e) under physiological conditions. 1 μM solution of **2e** was prepared by sequential dilution in aq. sodium phosphate buffer (0.1 M, pH 7.4). Its UV absorbance was measured from 250 to 800 nm at hourly intervals at 37 °C.

Supplementary Information



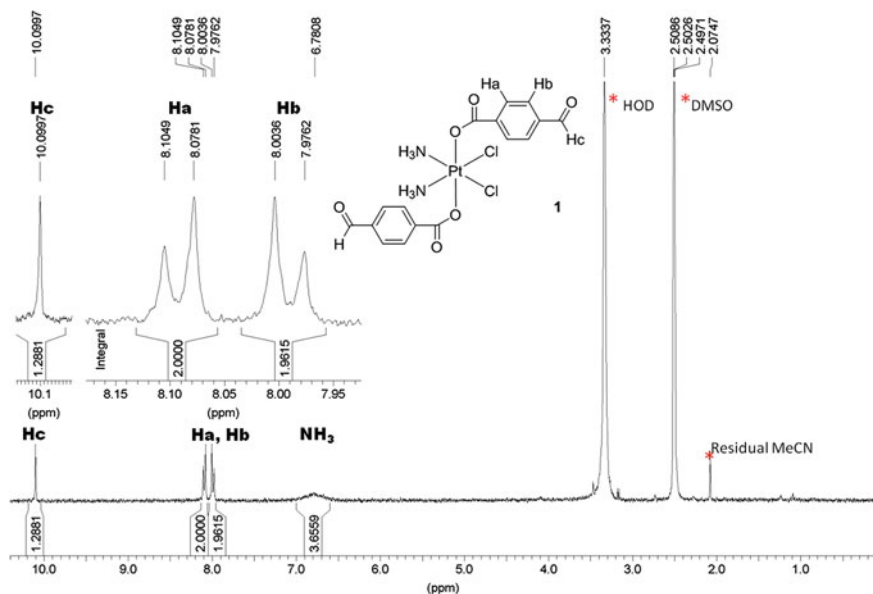


Fig. S2.1 ^1H NMR spectra of platinum(IV)-benzaldehyde complex **1** in DMSO-d_6

^1H NMR spectra of Pt-tyrosine hydrazone **2c.** The asymmetry of the aromatic protons observed in the ^1H NMR spectra of **2c** was initially puzzling as the protons H_a/H_a^1 , H_b/H_b^1 and H_d/H_d^1 exhibited greater magnetic inequivalence than was observed with the other Pt(IV)-imine conjugates where the same protons (though magnetically inequivalent) had closely overlapping chemical shifts. Consequently, in order to rule out the possibility of asymmetry of the axial ligands (eg. one side having *E* stereoisomerism with the other side being *Z*), we synthesized the purely organic hydrazone conjugate between 4-carboxylbenzaldehyde and tyrosine hydrazone for comparison. As shown in Fig. S2.6, the organic hydrazone displayed the same asymmetry of the aromatic protons. We postulated that this asymmetry arose due to slow rotation of the $\text{N}=\text{CH}-\text{Ph}$ double bond in the NMR timescale, resulting in more distinctive magnetic inequivalence of H_b versus H_b^1 .

Synthesis of hydrazone conjugate between 4-carboxylbenzaldehyde and l-tyrosine hydrazone as NMR reference. 4-carboxylbenzaldehyde (21.5 mg, 0.143 mmol) was added to a solution of l-tyrosine hydrazone (140 mg, 0.716 mmol) in 50% DMF/ H_2O (3 mL). The reaction mixture was lyophilized after

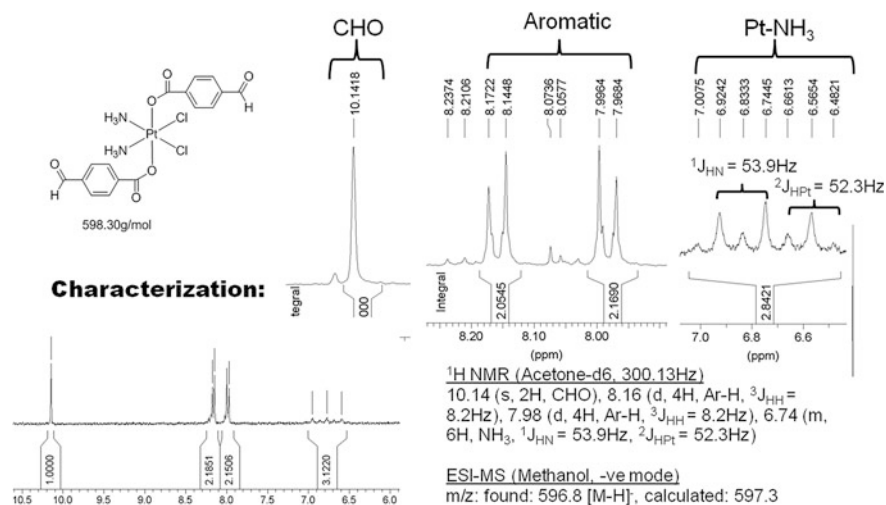


Fig. S2.2 $^1\text{H NMR}$ spectra of complex **1** in acetone- d_6 and ESI-MS characterization

24 h and washed with H_2O to yield a white precipitate. See Fig. S2.4 for $^1\text{H NMR}$ spectra; Purity (HPLC): 92% at 254 nm.

Catalysis at physiological pH by p-anisidine. The reaction between Pt-benzaldehyde **1** (A) and benzhydrazide to form the mono-ligated Pt-benzhydrazide (B) and bis-ligated Pt-benzhydrazide **2a** (C) product follows pseudo 1st order reaction kinetics in the presence of excess hydrazide and may be described by the following chemical equations.

The consumption of **1** and formation of the bis-conjugated product **2a** at hourly intervals was quantified by integration at 254 and 280 nm. In order to obtain a smooth plot of **[1]** and **[2a]** as a function of time, the experimental data was curve-fitted to model the chemical equilibriums as shown in Fig. S2.6 and Table S2.1 using the chemical reactions module of Berkeley Madonna, a commercial graphical differential equation solver.

In order to account for differences in molar absorptivity, the fraction of Pt-benzaldehyde (A) at any one point in time (t) was calculated as the current amount of A over the initial amount of A as quantified by HPLC integration. Similarly, the fraction of bis-ligated product (C) at any one point in time was calculated as the current amount of C over the maximum amount of C produced at the end of the reaction. Since it was difficult to extrapolate the maximum amount of

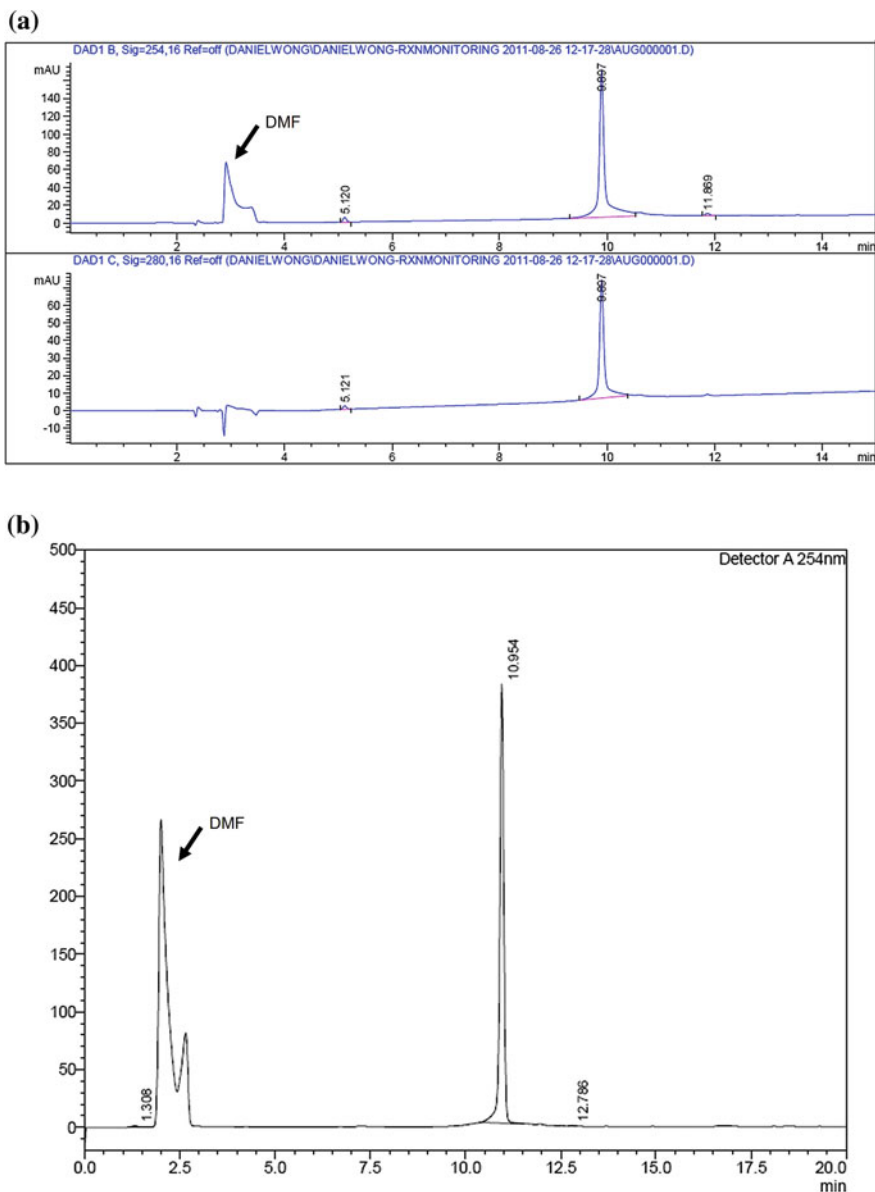


Fig. S2.3 RP-HPLC assessment of purity of Pt-benzaldehyde **1** dissolved in DMF/H₂O. Elution conditions for both spectra **(a)** and **(b)**: 20–80% gradient elution system with aq. NH₄OAc buffer (10 mM, pH 5.5) (solvent A) and MeCN (solvent B) over 15 min at 1.0 mL/min. Columns used are: **a** Phenomenex Luna C18(2) (250 × 4.60 mm i.d), **b** Shimpack VP-ODS column (150 × 4.60 mm i.d)

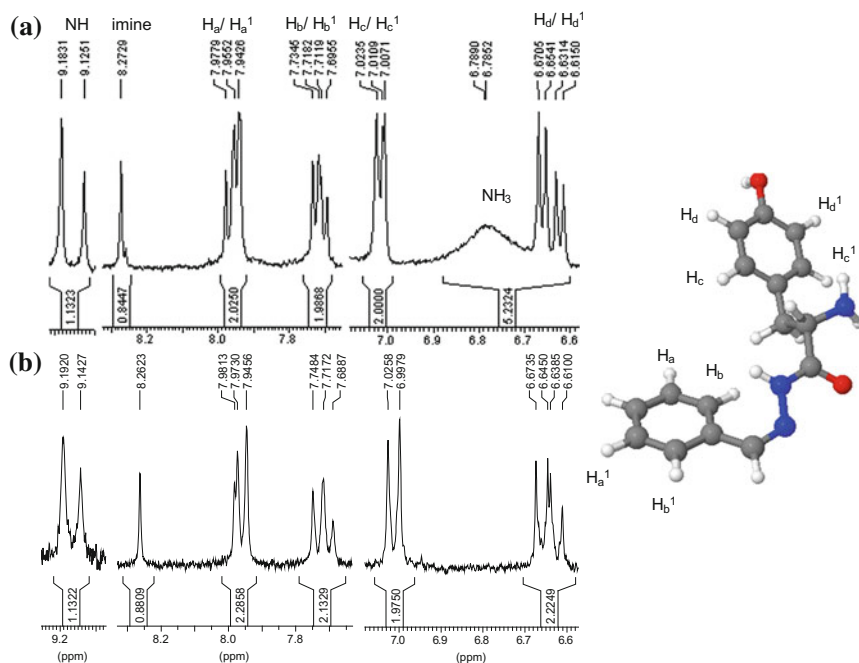


Fig. S2.4 Similarities between 1H NMR spectrum of: **a** Pt-tyrosine hydrazide (**2c**) and **b** the purely organic hydrazone ligation between 4-carboxylbenzaldehyde and tyrosine hydrazide. The 3D visual illustration is generated by CORINA [46]

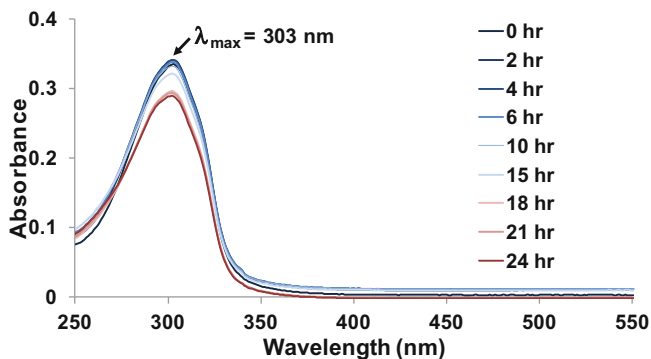


Fig. S2.5 Only slight hydrolysis of Pt-Girard's reagent **T 2e** was observed at pH 7.4 and 37 °C over 24 h; the λ_{max} of the spectra was at 303 nm, attributable to the hydrazone bond

mono-ligated product (**B**) from the experimental data, the fraction of **B** at any one point in time was calculated by subtracting from the fraction of **A** and **C**. This is summarized as the follows (Table S2.1):

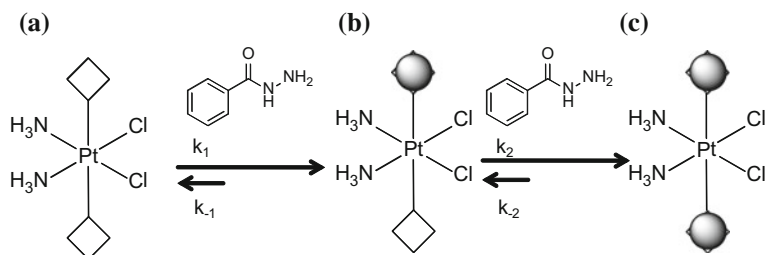


Fig. S2.6 Illustration of imine ligation between Pt-benzaldehyde **1** (a) and benzhydrazide to yield the mono-ligated product (b) and the bis-ligated product **2a** (c)

Table S2.1 Representative summary of experimental data for curve fitting

Hours	Fraction at 254 nm/ mAU			Fraction at 280 nm/ mAU			Average fraction of 254 and 280 nm		
	1	Mono	Bis	1	Mono	Bis	1	Mono	Bis
0.00	1.00	0.00	0.00	1.00	0.00	0.00	1.00	0.00	0.00
0.17	0.97	0.03	0.00	0.94	0.06	0.00	0.95	0.05	0.00
1.00	0.86	0.14	0.00	0.80	0.20	0.00	0.83	0.17	0.00
2.08	0.76	0.24	0.00	0.77	0.23	0.00	0.76	0.24	0.00
3.17	0.69	0.31	0.00	0.67	0.33	0.00	0.68	0.32	0.00
4.25	0.71	0.29	0.00	0.72	0.28	0.00	0.72	0.28	0.00
5.33	0.62	0.38	0.00	0.63	0.36	0.01	0.63	0.37	0.00
6.42	0.56	0.44	0.01	0.52	0.47	0.01	0.54	0.45	0.01
7.50	0.50	0.48	0.01	0.46	0.52	0.01	0.48	0.50	0.01
8.50	0.45	0.53	0.02	0.41	0.57	0.02	0.43	0.55	0.02
20.50	0.18	0.71	0.11	0.18	0.71	0.11	0.18	0.71	0.11
25.50	0.16	0.67	0.17	0.19	0.64	0.17	0.18	0.66	0.17

Data shown is for 100 mM p-anisidine catalysed reaction with 0.263 mM Pt-benzaldehyde and 8.71 mM benzhydrazide

$$\text{Fraction of A} = \text{Average of } \frac{\text{Absorbance of A at } t}{\text{Initial Absorbance of A at } t = 0} \text{ at 254 and 280 nm}$$

$$\text{Fraction of C} = \text{Average of } \frac{\text{Absorbance of C at } t}{\text{Absorbance of C at } t = \infty} \text{ at 254 and 280 nm}$$

$$\text{Fraction of B} = 1 - (\text{Fraction of A} + \text{Fraction of C})$$

References

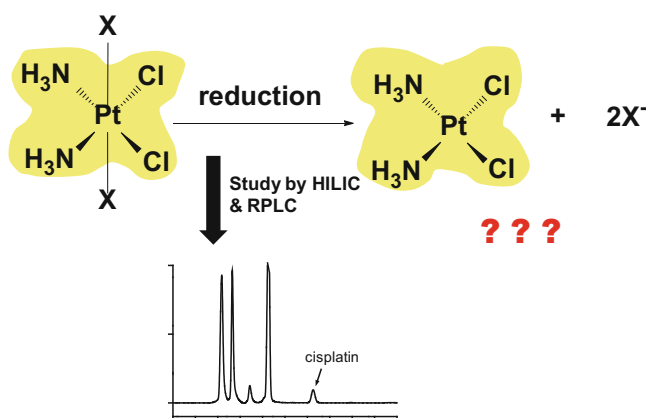
1. Kelland, L.: The resurgence of platinum-based cancer chemotherapy. *Nat. Rev. Cancer* **7**, 573–584 (2007)
2. Abu-Surrah, A.S., Kettunen, M.: Platinum group antitumor chemistry: design and development of new anticancer drugs complementary to cisplatin. *Curr. Med. Chem.* **13**, 1337–1357 (2006)
3. Fuertes, M.A., Alonso, C., Pérez, J.M.: Biochemical modulation of cisplatin mechanisms of action: enhancement of antitumor activity and circumvention of drug resistance. *Chem. Rev.* **103**, 645–662 (2003)
4. Galanski, M., Keppler, B.K.: Searching for the magic bullet: anticancer platinum drugs which can be accumulated or activated in the tumor tissue. *Anti-Cancer Agents Med. Chem.* **7**, 55–73 (2007)
5. Sternberg, C.N., Whelan, P., Hetherington, J., Paluchowska, B., Slee, P.H.T.J., Vekemans, K., Van Erps, P., Theodore, C., Koriakine, O., Oliver, T., Lebwohl, D., Debois, M., Zurlo, A., Collette, L.: Phase III trial of satraplatin, an oral platinum plus prednisone vs. prednisone alone in patients with hormone-refractory prostate cancer. *Oncology* **68**, 2–9 (2005)
6. Lemma, K., Sargeson, A.M., Elding, L.I.: Kinetics and mechanism for reduction of oral anticancer platinum(IV) dicarboxylate compounds by L-ascorbate ions. *J. Chem. Soc. Dalton Trans.* **7**, 1167–1172 (2000)
7. Hall, M.D., Hambley, T.W.: Platinum(IV) antitumour compounds: their bioinorganic chemistry. *Coord. Chem. Rev.* **232**, 49–67 (2002)
8. Barnes, K.R., Kutikov, A., Lippard, S.J.: Synthesis, characterization, and cytotoxicity of a series of estrogen-tethered platinum(IV) complexes. *Chem. Biol.* **11**, 557–564 (2004)
9. Giandomenico, C.M., Abrams, M.J., Murrer, B.A., Vollano, J.F., Rheinheimer, M.I., Wyer, S. B., Bossard, G.E., Higgins, J.D.: Carboxylation of kinetically inert platinum(IV) hydroxy complexes. An entree into orally active platinum(IV) antitumor agents. *Inorg. Chem.* **34**, 1015–1021 (1995)
10. Galanski, M., Keppler, B.K.: Carboxylation of dihydroxoplatinum(IV) complexes via a new synthetic pathway. *Inorg. Chem.* **35**, 1709–1711 (1996)
11. Galanski, M., Keppler, B.K.: Carboxylation of dihydroxoplatinum(IV) complexes with acyl chlorides. Crystal structures of the trans-R, R- and trans-S, S-isomer of (OC-6-33)-bis(1-adamantanecarboxylato)-(cyclohexane-1,2-diamine)dichloroplatinum(IV). *Inorg. Chim. Acta* **265**, 271–274 (1997)
12. Lee, E.J., Jun, M.-J., Lee, S.S., Sohn, Y.S.: Synthesis, structure, and properties of isopropylidene malonato platinum(IV) complexes. *Polyhedron* **16**, 2421–2428 (1997)
13. Ali, M.S., Ali Khan, S.R., Ojima, H., Guzman, I.Y., Whitmire, K.H., Siddik, Z.H., Khokhar, A.R.: Model platinum nucleobase and nucleoside complexes and antitumor activity: X-ray crystal structure of [PtIV(trans-1R,2R-diaminocyclohexane)trans-(acetate)2(9-ethylguanine)Cl]NO₃ · H₂O. *J. Inorg. Biochem.* **99**, 795–804 (2005)
14. Hambley, T.W., Battle, A.R., Deacon, G.B., Lawrenz, E.T., Fallon, G.D., Gatehouse, B.M., Webster, L.K., Rainone, S.: Modifying the properties of platinum(IV) complexes in order to increase biological effectiveness. *J. Inorg. Biochem.* **77**, 3–12 (1999)
15. Ang, W.H., Khalaila, I., Allardyce, C.S., Juillerat-Jeanneret, L., Dyson, P.J.: Rational design of platinum(IV) compounds to overcome glutathione-S-transferase mediated drug resistance. *J. Am. Chem. Soc.* **127**, 1382–1383 (2005)
16. Reithofer, M.R., Valiahi, S.M., Galanski, M., Jakupec, M.A., Arion, V.B., Keppler, B.K.: Novel endothallic-containing platinum(IV) complexes: Synthesis, characterization, and cytotoxic activity. *Chem. Biodivers.* **5**, 2160–2170 (2008)
17. Dhar, S., Lippard, S.J.: Mitaplatin, a potent fusion of cisplatin and the orphan drug dichloroacetate. *Proc. Natl. Acad. Sci. U. S. A.* **106**, 22199–22204 (2009)
18. Ang, W.H., Pilet, S., Scopelliti, R., Bussy, F., Juillerat-Jeanneret, L., Dyson, P.J.: Synthesis and characterization of platinum(IV) anticancer drugs with functionalized aromatic

- carboxylate ligands: Influence of the ligands on drug efficacies and uptake. *J. Med. Chem.* **48**, 8060–8069 (2005)
19. Perez, J.M., Camazón, M., Alvarez-Valdes, A., Quiroga, A.G., Kelland, L.R., Alonso, C., Navarro-Ranninger, M.C.: Synthesis, characterization and DNA modification induced by a novel Pt(IV)-bis(monoglutarate) complex which induces apoptosis in glioma cells. *Chem.-Biol. Interact.* **117**, 99–115 (1999)
 20. Reithofer, M., Galanski, M., Roller, A., Keppler, B.K.: An entry to novel platinum complexes: Carboxylation of dihydroxoplatinum(IV) complexes with succinic anhydride and subsequent derivatization. *Eur. J. Inorg. Chem.* **2006**, 2612–2617 (2006)
 21. Reithofer, M.R., Valiahdi, S.M., Jakupec, M.A., Arion, V.B., Egger, A., Galanski, M., Keppler, B.K.: Novel di- and tetracarboxylatoplatinum(IV) complexes. Synthesis, characterization, cytotoxic activity, and DNA platination. *J. Med. Chem.* **50**, 6692–6699 (2007)
 22. Dhar, S., Daniel, W.L., Giljohann, D.A., Mirkin, C.A., Lippard, S.J.: Polyvalent oligonucleotide gold nanoparticle conjugates as delivery vehicles for platinum(IV) warheads. *J. Am. Chem. Soc.* **131**, 14652–14653 (2009)
 23. Dhar, S., Liu, Z., Thomale, J., Dai, H., Lippard, S.J.: Targeted single-wall carbon nanotube-mediated Pt(IV) prodrug delivery using folate as a homing device. *J. Am. Chem. Soc.* **130**, 11467–11476 (2008)
 24. Mukhopadhyay, S., Barnes, C.M., Haskel, A., Short, S.M., Barnes, K.R., Lippard, S.J.: Conjugated platinum(IV) peptide complexes for targeting angiogenic tumor vasculature. *Bioconjugate Chem.* **19**, 39–49 (2007)
 25. Feazell, R.P., Nakayama-Ratchford, N., Dai, H., Lippard, S.J.: Soluble single-walled carbon nanotubes as longboat delivery systems for platinum(IV) anticancer drug design. *J. Am. Chem. Soc.* **129**, 8438–8439 (2007)
 26. Tiefenbrunn, T.K., Dawson, P.E.: Chemoselective ligation techniques: Modern applications of time-honored chemistry. *J. Pept. Sci.* **94**, 95–106 (2010)
 27. Hermanson, G.T.: *Bioconjugate Techniques*, 2nd edn, p. 1202. Academic Press, New York (2008)
 28. Dirksen, A., Dawson, P.E.: Rapid oxime and hydrazone ligations with aromatic aldehydes for biomolecular labeling. *Bioconjugate Chem.* **19**, 2543–2548 (2008)
 29. Prescher, J.A., Bertozzi, C.R.: Chemistry in living systems. *Nat. Chem. Biol.* **1**, 13–21 (2005)
 30. Lim, L.H.K., Pervaiz, S.: Annexin 1: the new face of an old molecule. *FASEB J* **21**, 968–975 (2007)
 31. Silistino-Souza, R., Rodrigues-Lisoni, F.C., Cury, P.M., Maniglia, J.V., Raposo, L.S., Tajara, E.H., Christian, H.C., Oliani, S.M.: Annexin 1: Differential expression in tumor and mast cells in human larynx cancer. *Int. J. Cancer* **120**, 2582–2589 (2007)
 32. Dirksen, A., Hackeng, T.M., Dawson, P.E.: Nucleophilic catalysis of oxime ligation. *Angew. Chem. Int. Ed.* **45**, 7581–7584 (2006)
 33. O’Ferrall, R.A.M., O’Brien, D.: Rate and equilibrium constants for hydrolysis and isomerization of (E)- and (Z)-p-methoxybenzaldehyde oximes. *J. Phys. Org. Chem.* **17**, 631–640 (2004)
 34. Lustig, E.: A nuclear magnetic resonance study of syn-anti isomerism in ketooximes. *J. Phys. Chem.* **65**, 491–495 (1961)
 35. Blanden, A.R., Mukherjee, K., Dilek, O., Loew, M., Bane, S.L.: 4-aminophenylalanine as a biocompatible nucleophilic catalyst for hydrazone ligations at low temperature and neutral pH. *Bioconjugate Chem.* **22**, 1954–1961 (2011)
 36. Masui, M., Ohmori, H.: Studies on Girard hydrazones. Part III. Further kinetic studies on the hydrolysis of Girard hydrazones. *J. Chem. Soc. B* 762–771 (1967)
 37. Dirksen, A., Dirksen, S., Hackeng, T.M., Dawson, P.E.: Nucleophilic catalysis of hydrazone formation and transimination: implications for dynamic covalent chemistry. *J. Am. Chem. Soc.* **128**, 15602–15603 (2006)
 38. Carr, J., Tingle, M., McKeage, M.: Rapid biotransformation of satraplatin by human red blood cells in vitro. *Cancer Chemother. Pharmacol.* **50**, 9–15 (2002)

39. Carr, J., Tingle, M., McKeage, M.: Satraplatin activation by haemoglobin, cytochrome C and liver microsomes in vitro. *Cancer Chemother. Pharmacol.* **57**, 483–490 (2006)
40. Gibson, D.: The mechanism of action of platinum anticancer agents-what do we really know about it? *Dalton Trans.* **48**, 10681–10689 (2009)
41. Aryal, S., Hu, C.-M.J., Zhang, L.: Polymer–cisplatin conjugate nanoparticles for acid-responsive drug delivery. *ACS Nano* **4**, 251–258 (2009)
42. Kalia, J., Raines, R.T.: Hydrolytic stability of hydrazones and oximes. *Angew. Chem. Int. Ed.* **47**, 7523–7526 (2008)
43. Kuroda, R., Ismail, I.M., Sadler, P.J.: X-ray and NMR studies of trans-dihydroxo-platinum (IV) antitumor complexes. *J. Inorg. Biochem.* **22**, 103–117 (1984)
44. Dhara, S.C.: A rapid method for the synthesis of cis-[Pt(NH₃)₂Cl₂]. *Indian J. Chem.* **8**, 193–194 (1970)
45. Fulmer, G.R., Miller, A.J.M., Sherden, N.H., Gottlieb, H.E., Nudelman, A., Stoltz, B.M., Bercaw, J.E., Goldberg, K.I.: NMR chemical shifts of trace impurities: Common laboratory solvents, organics, and gases in deuterated solvents relevant to the organometallic chemist. *Organometallics* **29**, 2176–2179 (2010)
46. Sadowski, J., Gasteiger, J., Klebe, G.: Comparison of automatic three-dimensional model builders using 639 X-ray structures. *J. Chem. Inf. Model.* **34**, 1000–1008 (1994)

Chapter 3

Probing the Platinum(IV) Prodrug Hypothesis. Are Platinum(IV) Complexes Really Prodrugs of Cisplatin?



3.1 Introduction

Amongst the metallopharmaceuticals in development, platinum(IV) complexes are unique because they are native prodrugs of clinically-relevant platinum(II) pharmacophores such as *cisplatin* and *oxaliplatin* (Fig. 3.1). These platinum(II) drugs are some of the most effective anticancer agents in clinical use and the first line treatment for many malignancies today (Fig. 3.1) [1–3]. The general consensus is that these platinum(IV) prodrug complexes are themselves pharmacologically inactive and must undergo reductive elimination by endogenous reductants to release the active square-planar platinum(II) core with concomitant dissociation of the axial ligands (Fig. 3.2) [1–3]. As such, the axial ligands confers unique possibilities of tuning the pharmacokinetic parameters such as lipophilicity and solubility as well as the attaching any targeting groups or synergistic co-drugs

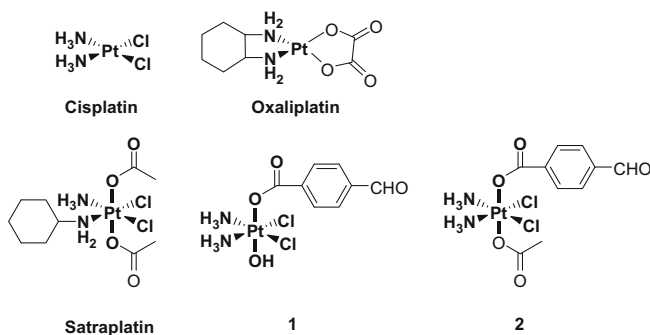


Fig. 3.1 Top: *cisplatin* and *oxaliplatin* are two platinum(II) agents in clinical use today. Bottom: Satraplatin is a promising platinum(IV) anticancer prodrug under clinical trials. Complexes **1** and **2** are newly synthesized asymmetrical platinum(IV) complexes bearing a benzaldehyde moiety for facile imine ligation to any therapeutically-relevant substrate

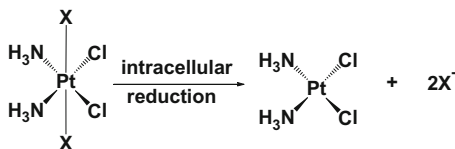


Fig. 3.2 The platinum(IV) prodrug hypothesis: reductive elimination of platinum(IV) prodrugs occurs with the release the active platinum(II) core as well as both axial carboxylate ligands

without altering the cellular mechanism of action of the innate platinum(II) pharmacophore [1–3].

The key impetus driving this study is the uncertainty whether asymmetrical aryl platinum(IV) complexes bearing a cisplatin-type scaffold (*cis,cis*-diam(m)inedichlorido equatorial ligands), which we are developing several applications for, are indeed prodrugs of cisplatin [4]. Based on the literature, there have been mixed evidence for and against the hypothesis that cisplatin-type platinum(IV) complexes are prodrugs of cisplatin. The strongest support for prodrug hypothesis appeared to be extrapolated from extensive *in vitro* and *in vivo* studies from *satraplatin* [5, 6] and *iproplatin* [7] which bear the *cis*-am(m)ine(cyclohexylamine) and *cis*-diisopropylamine core respectively (Fig. 3.1). These studies showed that that the expected platinum(II) congener was indeed the predominant product of reduction via HPLC. However to date, the same has never been shown from a cisplatin-type platinum(IV) scaffold. Indeed, subtle variation of the equatorial ligands, such as equatorial replacement of 1,2-DACH (diaminocyclohexane) with a 1,4-DACH ligand can have a profound and unexpected influence on the reduction behaviour of platinum(IV) complexes [8]. It was also observed that *trans*-analog of satraplatin bearing *trans*-dichloro ligands favored an inner-sphere reduction mechanism, resulting in retention of the diacetate ligands and loss of the chloride ligands [9].

Another study suggested that reduction of certain classes of *cis*-platinum(IV) complexes including satraplatin may actually proceed via multiple pathways leading to the loss of any combination of axial carboxylate and equatorial chloride ligands [10, 11]. Consequently, 4 different reduction products were formed instead of the expected sole product.

Validation of the platinum(IV) prodrug hypothesis is important because it is the underlying working assumption behind much effort which has been directed towards the design of platinum(IV)-conjugates in recent years [3]. Very diverse examples of platinum(IV)-conjugates have been reported including conjugation to targeting peptides, [12, 13] synergistic co-drugs, [14–16] as well as to macromolecular delivery vehicles [17–20]. Invalidation of this central hypothesis would bear negative implications against this burgeoning field. For instance, we reported a method of hydrophobic entrapment to encase strongly hydrophobic platinum(IV) complexes bearing axial aryl carboxylates within multiwalled carbon nanotubes via hydrophobic-hydrophobic interactions [20]. The premise was that hydrophilic *cis*-platin would be released as a result of drastic hydrophobic reversal upon reduction. Such a strategy hinged upon the release of the axial benzoyl ligands rather than the chloride ligands. In addition, asymmetric acylation of platinum(IV) complexes has gained substantial interest recently given its potential to significantly expand the current paradigm [4, 21, 22]. However, the reduction of such *mono*- and *bis*-functionalised asymmetrical platinum(IV) complexes, particularly aryl complexes **1** and **2** which represents useful scaffolds for facile imine ligation to therapeutically relevant biomolecules, [23] have scarcely been studied.

Thus far, the formation of cisplatin has mostly been demonstrated indirectly through the ability of the reduction product to form 1,2-GG-Pt adducts with DNA which was detected either by HPLC, [20] electrophoresis gel mobility [24] or antibody staining [15]. The drawback of detection by DNA-binding is that any platinum(II) product bearing diam(m)ine ligand would also bind to DNA in the same way as cisplatin. ^{195}Pt -NMR have also been used to demonstrate the formation of cisplatin from platinum(IV) complexes but the insensitivity of this method makes it difficult to detect the formation of any other plausible by-products [25]. One way of detecting cisplatin directly is by hydrophilic interaction liquid chromatography (HILIC) which is an useful approach to separate and quantify hydrophilic cisplatin both *ex-vitro* and *ex vivo*, [26, 27] but has not yet been applied to study the reduction of platinum(IV) complexes. In this study, we employed a combination of HILIC and RPLC (reversed-phase liquid chromatography) to probe the reduction of model platinum(IV) complexes **1** and **2** as well as satraplatin by ascorbic acid in order to establish whether they are true prodrugs of their platinum(II) congeners. Our results demonstrate that asymmetric aryl platinum(IV) complexes are indeed prodrugs of cisplatin upon reduction and that it is the predominant reduction product. In addition, we also observed that reduction rate of complex **1** and **2** contradicted established trends because reduction of complex **1** (bearing an axial OH) was unexpectedly faster compared to complex **2** (bearing an axial OAc).

3.2 Results and Discussion

Experimental design considerations. The prevailing hypothesis holds that platinum(IV) complexes are prodrugs which are activated via reduction elimination of the axial ligands to yield the pharmacologically active square-planar platinum(II) centre. In order to probe this hypothesis, we followed the reduction of platinum(IV) complexes by employing both conventional RPLC (silica-C18) and ZIC-HILIC since the two techniques exhibit orthogonal retention. Cisplatin, which has little to no retention on RPLC, is well separated on HILIC. Since RPLC and HILIC have opposite retention for analytes, the use of these two orthogonal separation techniques allows screening for possible reduction products across a breadth of polarities. This strategy ensured that all possible reduction products, which may otherwise co-elute using a single technique, were well-resolved.

Since our goal was to study the direct and immediate reduction product(s) of platinum(IV) without interference from subsequent ligand exchange reactions of the labile platinum(II) products, we chose a relatively simple reducing environment. Ascorbic acid in an aqueous phosphate buffered system was used as a model of an outer-sphere reductant [2], over more realistic *ex vivo* reducing conditions such as blood or whole cell extracts. The intracellular half-life of cisplatin has been estimated to be only about 75–120 min due to rapid aquation followed by displacement of the labile chloride ligands by numerous high molecular weight cytoplasmic nucleophiles [28, 29]. The multitude of products formed would obscure study of the direct reduction product(s). Other outer-sphere reducing agents such as cytochrome *c* and haemoglobin have been strongly implicated as biologically significant reducing agents for satraplatin [5, 30]. As these are macromolecular reducing agents where the electron is transferred through space from the reducing center to the acceptor, the immediate reduction outcome should be the same, regardless of outer-sphere reductants. Reduction experiments were done in the presence of 137 mM NaCl in order to suppress aquation of the platinum(II) reduction product. In the absence of chloride ions, we and others have observed very rapid aquation of cisplatin (Fig. S3.3) [31].

Reduction outcome and conversion yield. Reduction of **1** is expected to yield cisplatin alongside concomitant dissociation of the axial 4-carboxylbenzaldehyde ligand. The starting reactants, **1** and ascorbic acid, as well as the expected reduction products could be efficiently separated within 20 min via HILIC chromatography using a 70% ACN/aq. NH₄OAc (20 mM, pH 6.4) isocratic eluent system. The identity of all peaks was ascertained by LC-MS and by comparison of retention time against authentic standards obtained commercially. In particular, the retention time (12.3 min) and LC-ESIMS (*m/z* 318, Pt(Cl₂)(NH₃)₂ + NH₄⁺ adduct) of cisplatin coincide with an earlier published report by Nygren et al. using nearly identical separation condition [26]. On RPLC, only unreacted complex **1** and 4-carboxylbenzaldehyde could be observed but not cisplatin.

HPLC monitoring indicated that the reduction outcome was indeed consistent with the reduction hypothesis. At the start of the reaction, 3 peaks corresponding to

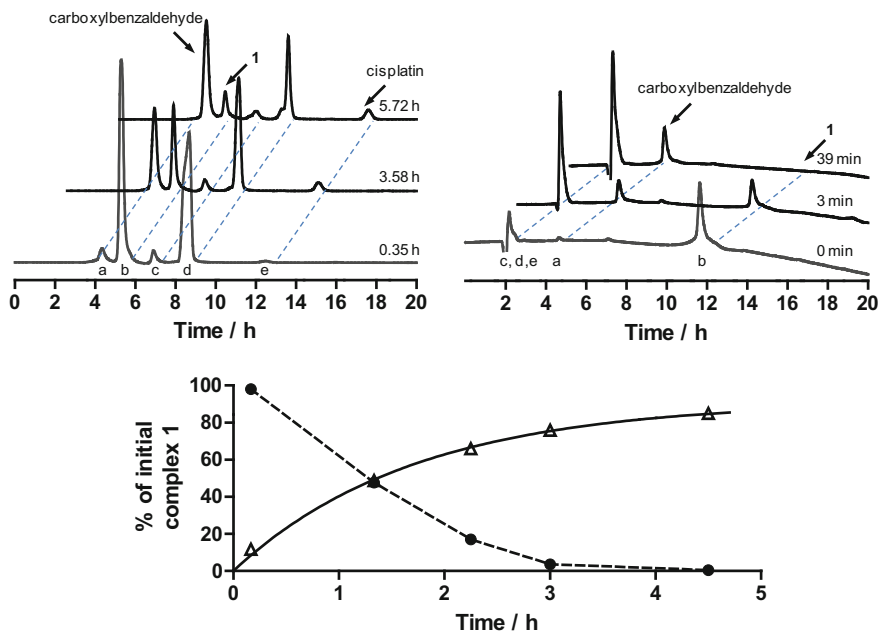


Fig. 3.3 Top left and top right: HILIC (230 nm) and RPLC (214 nm) chromatograms respectively of the reduction of **1** by ascorbic acid. Legend: **a** 4-carboxylbenzaldehyde, **b** **1**, **c** dehydroascorbic acid, **d** ascorbic acid, **e** cisplatin. Bottom: Release profile of cisplatin over time. Legend: ● **1**, ▲ cisplatin. Note that figures show representative experiments conducted at different times using different initial concentrations of **1**

unreacted **1** (5.1 min), dehydroascorbic acid (6.6 min) and ascorbic acid (8.6 min) were observed via HILIC (Fig. 3.3). Observable amounts of dehydroascorbic acid were already initially present in commercially obtained ascorbic acid due to air-oxidation. With time, **1** decreased in tandem with the appearance of 2 new emergent peaks corresponding to the axial release of 4-carboxylbenzaldehyde (4.2 min) and cisplatin (12.3 min). Complex **1** was stable in PBS and in the absence of ascorbic acid, no reduction was observed. Oddly, the peak attributable to dehydroascorbic acid did not increase visibly. This may be due to the low molar absorptivity of dehydroascorbic acid or also because the former is rapidly hydrolyzed to weakly UV-absorbing diketogulonic acid under physiological pH [32]. On RPLC, the release of cisplatin was not observed because it co-eluted with ascorbic acid at void retention. Nonetheless, it was clear that a decrease in **1** (11.6 min) was in tandem with a release of 4-carboxylbenzaldehyde (5.0 min). More significantly, the RPLC chromatogram supports the hypothesis that reduction of **1** occurred primarily via axial dissociation since no other platinum(II) by-products were observed. Plausible side-products retaining the benzaldehyde axial ligand would be fairly hydrophobic, UV-absorbing and therefore visible. One such reduction product, *cis*-Pt(NH₃)₂(Cl)(carboxylbenzaldehyde), was separately

synthesized and isolated via semi-preparative HPLC (see SI). This platinum(II) complex, which has a retention time of 10.7 min, was not observed in the reduction mixture.

At the crux of the issue, we wanted to establish if cisplatin was indeed the predominant reduction product of **1** and not simply a minor side-product. The conversion yield of complex **1** to cisplatin was calculated to be $89.5 \pm 2.0\%$ (SE) based on peak area against a calibration curve under HILIC (Fig. S3.5). Like **1**, complex **2** which has an OAc axial ligand instead of OH, was reduced to form cisplatin and 4-carboxylbenzaldehyde with a conversion yield of $92.6 \pm 10.1\%$ (SE) (Fig. S3.4). These results showed convincingly that the class of highly potent asymmetrical platinum(IV) aryl complexes under development are indeed true prodrugs of cisplatin. However, since the measured yields were $<100\%$, we cannot discount the possibility of other side-products which may be weakly UV-absorbing and therefore undetectable by the UV-vis detector on the HPLC. In this regard, hyphenation of HILIC to ICP-MS may be revealing. We also observed the formation of small peaks at 15.6 and 20.1 min upon prolonged standing of the reduction mixture. These were likely due to aquation of cisplatin rather than a direct result of reduction because they were also observed when a solution of cisplatin alone was left standing for 12 h. The latter peak at 20.1 min could be identified via LC-MS as the mono-aquated species $[\text{Pt}(\text{NH}_3)_2(\text{Cl})(\text{MeCN})]^+$ (m/z 305.9) with the aqua-ligand substituted by the HPLC eluent.

We studied the reduction of satraplatin to its postulated reduction product, JM118 *cis*-Pt(NH₃)(cyclohexylamine)Cl₂, using both RPLC and HILIC to validate our protocol. Unlike cisplatin, JM118 is hydrophobic and could be observed on RPLC (15.6 min). In keeping with **1** and **2**, the peak area attributable to satraplatin decreased over time and was accompanied by an increase in JM118 (Fig. 3.4). The reduction was quantitative and no other major by-products could be observed on both RPLC and HILIC, an observation consistent with the platinum(IV) reduction hypothesis. The conversion yield to JM118 which was calculated independently on both RPLC and HILIC were $83.2 \pm 0.8\%$ (SE) and $86.2 \pm 3.4\%$ (SE) respectively, demonstrating that JM118 was indeed the predominant reduction product of satraplatin.

Comparison of reduction rate. To date, it is generally agreed upon that the reduction potentials and reduction rates of platinum(IV) complexes are positively correlated [2, 33, 34]. For complexes bearing the same equatorial ligands, the trend of reduction rate and reduction potential could be predicted primarily based on the axial ligands as follows, OH < carboxylates < Cl, with hydroxido being reduced the slowest. In contrast, we observed a very pronounced and unexpected difference in the reduction rate of **1** (bearing an axial benzaldehyde and OH ligand) versus **2** (bearing an axial benzaldehyde and OAc ligand) (Fig. 3.5). In order to accurately compare the reduction rate of all three platinum(IV) complexes, we monitored the decline of the parent platinum(IV) peak by RPLC in ascorbic acid using a higher buffering capacity phosphate buffer (200 μM of complex dissolved in pH 7.4 200 mM phosphate buffer + 137 mM NaCl). This higher capacity buffer was necessary to maintain a constant pH since reduction rate by ascorbic acid is very

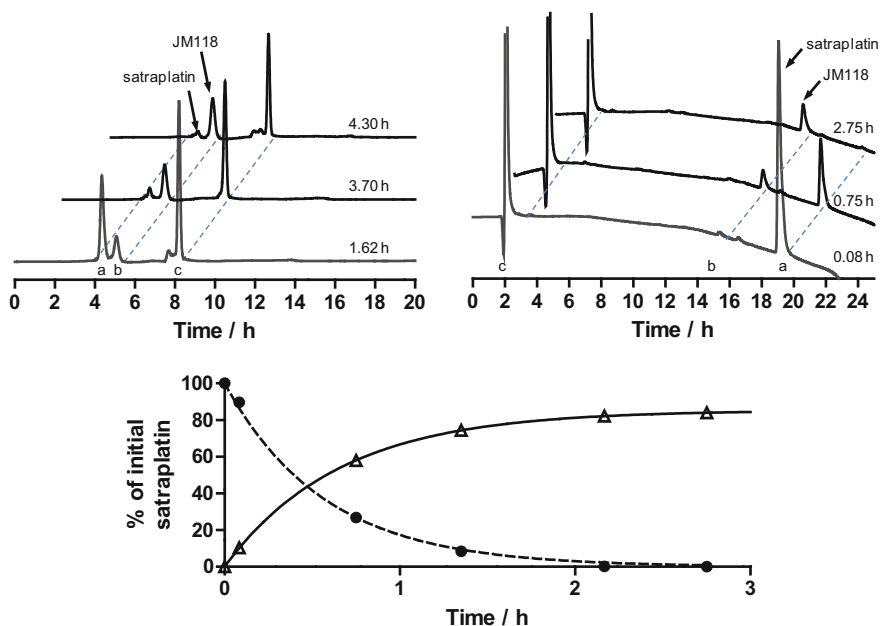
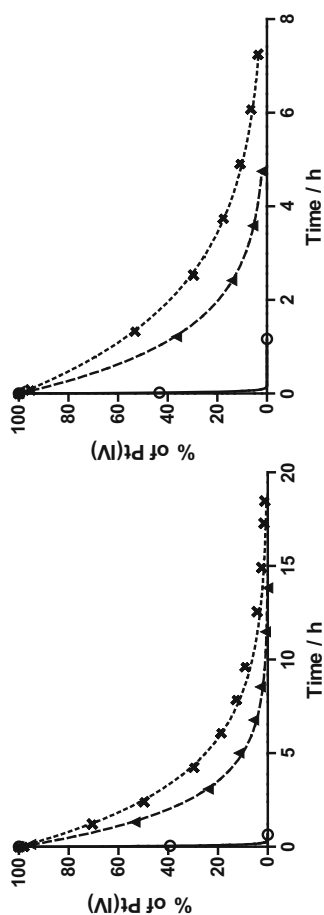


Fig. 3.4 Top left and top right: HILIC (214 nm) and RPLC (214 nm) chromatograms respectively of the reduction of satraplatin by ascorbic acid. Legend: **a** satraplatin, **b** JM118, **c** ascorbic acid. Bottom: Release profile of JM118 over time. Legend: • satraplatin, Δ JM118. Note that figures show representative experiments conducted at different times using different initial concentrations of satraplatin

pH-sensitive [35]. The experimentally determined half-lives of **1** and **2** in 2 mM ascorbic acid were significantly different at ca. 2 min and 2.50 h, respectively (Table 3.1). In 4 mM ascorbic acid, the half-lives of both complexes decreased to ca. 1 min and 1.48 h, respectively. Intriguingly, the simple acetylation of the axial OH ligand from **1** to **2** resulted in a vast improvement in terms of reduction resistance by a factor of 67–89 folds as well as aqueous kinetic solubility in PBS by tenfolds (Table S3.1). This vindicated the utility of the asymmetrical approach in the design of platinum(IV) anticancer prodrugs recently advocated by our group and others [4, 21, 22, 36].

The reduction rates we obtained were consistent with work reported by Gibson and Hambley studying platinum(IV) prodrug complexes bearing an oxaliplatin template, Pt(dach)(oxalate). It was observed that *cis,cis,trans*-Pt(dach)(oxalate)(OH)(OAc) was reduced faster than *cis,cis,trans*-Pt(dach)(oxalate)(OAc)₂ by ascorbic acid despite having a more negative reduction potential [37]. It was postulated that in the absence of a bridging chloride ligand (as typical of a cisplatin-type scaffold), hydroxido groups were much better bridging ligands to facilitate electron transfer compared to acetyl carboxylates. Our results extend their experimental findings from an oxaliplatin-type scaffold bearing [PtN₂O₂]-motif to



	$t_{1/2}$ (hr)		Pseudo 1 st order rate constant (hr ⁻¹)		2 nd order rate constant (mM ⁻¹ hr ⁻¹)	
	2 mM ascorbic acid	4 mM ascorbic acid	2 mM ascorbic acid	4 mM ascorbic acid	2 mM ascorbic acid	4 mM ascorbic acid
1	0.037	0.017	18.66 ± 0.00019	41.74 ± 0	9.88 ± 0.55	0.128 ± 0.011
2	2.502	1.482	0.2771 ± 0.0046	0.4677 ± 0.0051	0.216 ± 0.012	0.012 ± 0.002
satraplatin	1.517	0.851	0.4569 ± 0.0082	0.8142 ± 0.028		

Fig. 3.5 Rate of reduction of 180 μ M of **1**, **2** and satraplatin dissolved in 200 mM phosphate buffer + 137 mM NaCl in the presence of 2 mM ascorbic acid (left) or 4 mM ascorbic acid (right). Curve was fitted using graphpad prism 5

Table 3.1 Conversion yields of **1** and **2** to cisplatin as well as satraplatin to JM118. Values are reported as mean with standard error

Conversion Yield (%)	1 ^a (axial OH)	2 ^a (axial OAc)	Satraplatin ^b
HILIC	89.5 ± 2.0%	92.6 ± 10.1%	86.2 ± 3.4%
RPLC	–	–	83.2 ± 0.8%

^aReduction in PBS (10 mM phosphate, 137 mM NaCl and 2.7 mM KCl)^bReduction in 200 mM phosphate and 137 mM NaCl

cisplatin-type scaffolds bearing [PtN₂Cl₂]. Our results suggest that a bridging hydroxido ligand promotes reduction, with or without the presence of a bridging chloride ligand. To the best of our knowledge, this is the first reported study done on the relative reduction rate of asymmetrical platinum(IV) complexes bearing a cisplatin-type scaffold. Our results when taken together with Gibson and Hambley's reports highlights the importance of critically re-examining some of the commonly accepted assumptions guiding the platinum(IV) prodrug development since trends applicable to symmetrical platinum(IV) complexes may not apply within the newly emergent asymmetrical platinum(IV) complexes.

3.3 Conclusion

Despite the large body of work pursuing the use of platinum(IV) complexes as prodrugs of cisplatin, there has yet been a conclusive study demonstrating that these complexes would yield cisplatin upon reduction and not merely any DNA-reactive platinum(II) species. Our results showed unambiguously that asymmetrical platinum(IV) aryl carboxylates bearing the cisplatin-type template are indeed such prodrugs and they chemically reduce to form predominantly cisplatin. We further observed that reduction of asymmetric *mono*-carboxylate **1**, bearing an axial OH, was unexpectedly faster than asymmetric *bis*-carboxylate **2**, bearing an axial OAc, illustrating important differences between symmetrical and asymmetric platinum (IV) prodrug complexes.

3.4 Experimental

Chemicals and reagents. Satraplatin and JM118 were purchased from Merlin Standard Chemical (Singapore). Cisplatin and *Cis,cis,trans*-diamminedichlorodihydroxoplatinum(IV) were synthesized and purified as per literature procedures [38, 39]. Succinimidyl 4-formylbenzoate was synthesized as reported by Philips et al. [40]. All other chemicals and reagents were purchased from commercial vendors and used without further purification.

Instrumentation. ¹H NMR was recorded on a Bruker Avance 300 MHz. Chemical shifts are reported in parts per million relative to residual solvent peaks.

Electrospray ionization mass spectra (ESI-MS) were obtained on a Thermo Finnigan LCQ ESI-MS system. Elemental analysis was carried out on a Perkin-Elmer PE 2400 elemental analyzer by CMMAC (National University of Singapore). Platinum concentrations of stock solutions were measured externally by CMMAC (National University of Singapore) on an Optima ICP-OES (Perkin-Elmer). HPLC was performed on either an Agilent 1200 series DAD or a Shimadzu Prominence system. LC-MS was conducted on a Bruker AmaZonX ion-trap coupled to a Dionex Ultimate 3000 RSLC system. HILIC was performed using a SeQuant ZIC-HILIC column (150 × 2.1 mm i.d., 5 μm, 200 Å) at a 0.1 mL/min flow rate with 214, 230 and 305 nm UV detection. RPLC was performed using a Shimpack VP-ODS column (150 × 4.60 mm i.d., 5 μm, 120 Å) at 1.0 mL/min flow rate with 214, 230 and 305 nm UV detection.

Synthesis of *cis,cis,trans*-diamminedichloro(hydroxido)(4-formylbenzoate) platinum(IV) (1). *Cis,cis,trans*-diamminedichlorodihydroxoplatinum(IV) (300 mg, 0.898 mmol) was suspended in dry DMSO (120 mL). NHS-activated-ester, succinimidyl 4-formylbenzoate (300 mg, 1.347 mmol) was then added slowly to the suspension. The reaction mixture was stirred vigorously at r.t. for 72 h and subsequently filtered through Celite to remove unreacted *cis,cis,trans*-diamminedichlorodihydroxoplatinum(IV) and metallic platinum. The filtrate was reduced in volume to about 0.5–1 mL in a lyophilizer before being precipitated by addition of DCM (60 mL) and diethyl ether (20 mL). It was essential to prevent the filtrate from being lyophilized completely. The crude product was then washed sequentially by sonication with DCM (3 × 10 mL), water (3 × 5 mL) and acetone (3 × 5 mL) to yield the desired product as a white-colour precipitate. At each rinsing step, the washing was continued until the rinsing solvent turned from pale yellow to colourless. Yield: 180 mg (43%) ¹H NMR (DMSO-*d*₆, 300.13 Hz): δ 10.07 (s, 1H, CHO), 8.05 (d, 2H, Ar-H, ³J_{HH} = 8.04 Hz), 7.95 (d, 2H, Ar-H, ³J_{HH} = 8.04 Hz), 6.05 (m, 6H, NH₃, ¹J_{HN} = 52.4 Hz, ²J_{HPt} = 52.1 Hz); ESI-MS (-): m/z 464.9 [M-H]⁻; Anal. Calcd, C₈H₁₂Cl₂N₂O₄Pt (466.18): C, 20.61; H, 2.59; N, 6.01. Found: C, 20.88; H, 2.58; N, 5.75. Purity (HPLC): 97% at 254 nm.

Synthesis of *cis,cis,trans*-diamminedichloro(acetato)(4-formylbenzoate) platinum(IV) (2). Acetic anhydride (8 μL, 0.0848 mmol) was added to a solution of **1** (20 mg, 0.0429 mmol) dissolved in dry DMF (1 mL) and stirred vigorously for 48 h. The solution was evaporated to oil and precipitated with diethyl ether (5 mL). The precipitate was washed with DCM (5 mL). The crude product was then dissolved in acetone (10 mL) and filtered to remove insoluble unreacted complex **1**. This process of evaporation, precipitation with ether, washing with DCM, reconstitution in acetone and filtration was then repeated again. The crude product was then redissolved in THF (10 mL) and filtered. Likewise, the process was repeated. After drying, the crude product was washed with minimal cold water (0.5 mL) and the desired water-soluble product was isolated from insoluble impurities by extracting with water (3 × 15 mL). The combined water portions were pooled and evaporated to yield an off-white powder. Yield: 11 mg (50%) ¹H NMR (DMSO-*d*₆, 300.13 Hz): δ 10.08 (s, 1H, CHO), 8.05 (d, 2H, Ar-H, ³J_{HH} = 8.04 Hz), 7.96 (d, 2H, Ar-H, ³J_{HH} = 8.04 Hz),

6.65 (br m, 6H, NH₃), 1.95 (s, 3H, CH₃); ESI-MS (-): m/z 506.8 [M-H]⁻; Purity (HPLC): 97% at 254 nm.

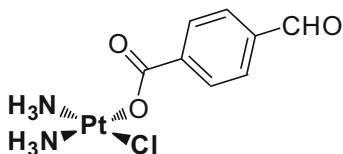
Monitoring reduction outcome of platinum(IV) complexes via HILIC. Stock solutions (ca. 1 mM) of **1**, **2** and satraplatin were prepared in phosphate buffer. Complexes **1** and **2** were dissolved in PBS pH 7.4 (containing 10 mM phosphate, 137 mM NaCl and 2.7 mM KCl) while satraplatin was dissolved in a higher capacity pH 7.4 phosphate buffer (200 mM phosphate buffer, 137 mM NaCl). The reductant, ascorbic acid, was then added to a 2 mL portion of the stock solutions to give 2–4 mM in the reduction mixture. The aqueous reaction mixture was monitored at periodic intervals as follows: 120 µL of reaction mixture was aliquoted and diluted with an equivolume of MeCN to form a 50% aqueous/MeCN injection mixture which was analyzed via HILIC (10 µL injection). An isocratic 70% MeCN/aq. NH₄OAc (20 mM, pH 6.4) elution condition was employed. We observed that sonication of the injection mixture prior to injection helped to level the solvent baseline at 214 nm. Freshly prepared stock solutions containing both parent complexes and their reduction products (cisplatin and JM118) at varying concentrations were injected in-between runs to establish a calibration curve by peak area. Concentrations of stock solutions were adjusted to [Pt] determined by ICP-OES. Complexes **1** and **2** were monitored at 214, 230 and 305 nm while satraplatin was monitored at 214 and 230 nm only. Initial concentration of platinum(IV) complexes were determined from the master stock solutions before addition of ascorbic acid using both the calibration curve and ICP-OES determination. The reduction yield (cisplatin and JM118) was determined at the point in time when the respective peak area plateau out. The identity of all the starting materials and reduction products were established by comparing the retention time against authentic standards as well as by LC-MS. Experiment was repeated in at least duplicates.

Monitoring reduction outcome of platinum(IV) complexes via RPLC. Reduction monitoring on RPLC was carried out in a similar manner as HILIC with appropriate modifications. Briefly, a reduction mixture contained approx. 500 µM platinum(IV) complex with 4 mM ascorbic acid in phosphate buffer was prepared. At periodic intervals, the aqueous reduction mixture was injected directly and monitored via RPLC (20 µL injection) using a gradient elution of 5–15% B over 8 min followed by 15–50% B for a further 10 min and finally 80% B from 20 min onwards where solvent A is aq. NH₄OAc buffer (10 mM, pH 7) and solvent B is MeCN. Reduction yield of satraplatin was determined using an established calibration curve by peak area. It was not possible to quantify the reduction yield of complexes **1** and **2** as polar cisplatin has void retention time via silica-C18.

Comparing reduction rate of platinum(IV) complexes. Stock solutions of **1**, **2** and satraplatin (200 µM dissolved in pH 7.4 200 mM phosphate buffer + 137 mM NaCl) were prepared from master stock solutions of known concentrations calibrated by ICP-OES. For each of the three platinum(IV) complexes, 900 µL of complex was added to 100 µL of ascorbic acid (40 mM in pH 7.4 200 mM phosphate buffer + 137 mM NaCl). For all 3 complexes, the final concentration of the reaction mixture was 180 µM complex and 4 mM ascorbic acid at pH 7.4. The decline of the parent peak area was then monitored at periodic intervals by RPLC

using the same gradient elution as described earlier. Initial peak area was determined by adding 900 μL of complex to 100 μL of buffer alone. The experiment was repeated at 2 mM final ascorbic acid concentration.

Supplementary Information



Synthesis of *cis*-diamminechloro(4-formylbenzoate) platinum(II). $\text{Pt}(\text{NH}_3)_2(\text{Cl})_2$ (50 mg, 0.167 mmol) and AgNO_3 (26.89 mg, 0.158 mmol) was stirred vigorously in H_2O (1 mL), heated at 40 $^\circ\text{C}$ for 2 h. The reaction suspension was filtered using a syringe filter to give a clear filtrate. Sodium formylbenzoate (31.55 mg, 0.183 mmol) was added to the filtrate and the reaction mixture was heated at 40 $^\circ\text{C}$ for 5 h. The resulting yellowish-white ppt was washed with H_2O (3×1 mL). At this stage, the pale-green crude product contained a mixture of *bis*-acylated *cis*-diamminebis(4-formylbenzoate) platinum(II) and the desired *mono*-acylated *cis*-diamminechloro(4-formylbenzoate) platinum(II). This was then dissolved in 70% MeCN/ H_2O and purified by semi-preparative HPLC Figs. S3.1, S3.2.

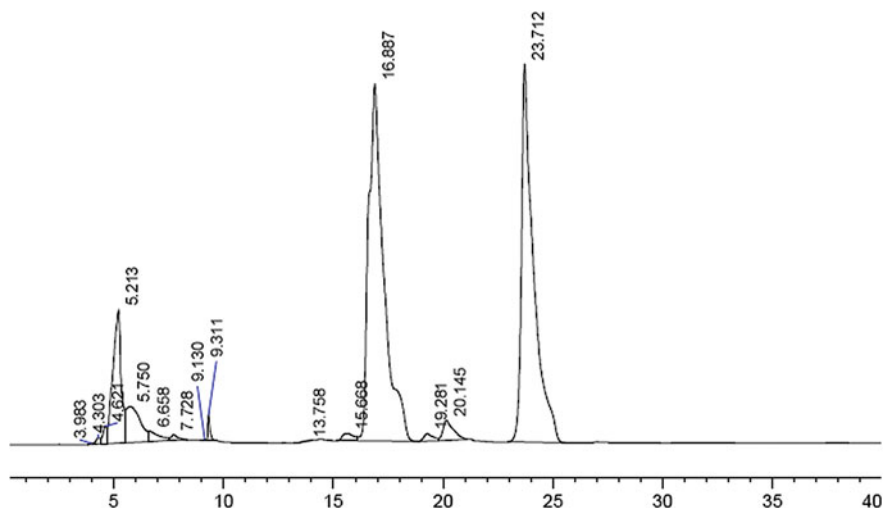


Fig. S3.1 Semi-preparative trace of the crude $\text{Pt}(\text{II})(\text{NH}_3)_2(\text{Cl})(\text{carboxylbenzaldehyde})$. The desired product is at 16.9 min

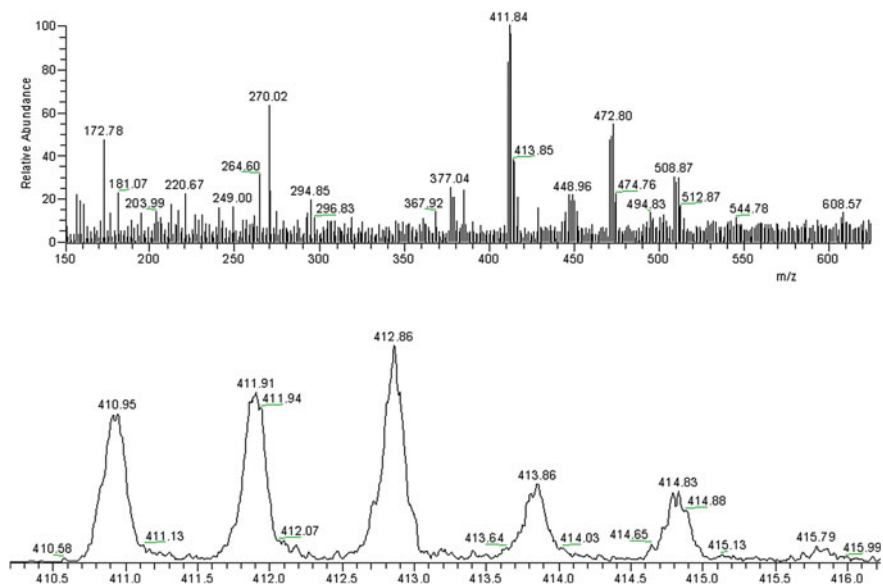


Fig. S3.2 ESI-MS of the isolated Pt(II)(NH₃)₂(Cl)(carboxylbenzaldehyde). m/z 411.8 [M-H]⁻

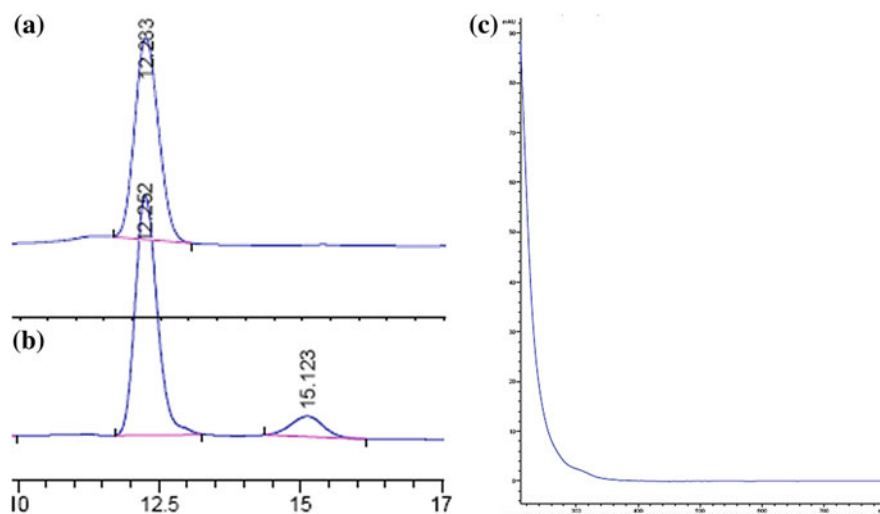


Fig. S3.3 Aquation of cisplatin to form an unidentified product. HILIC chromatograms of **a** cisplatin in PBS (containing 139 mM Cl⁻) after leaving to stand and **b** cisplatin in 50 mM phosphate buffer pH 7 (without Cl⁻) after 1 h, **c** the DAD-UV-vis spectrum of the peak at 15.6 min showed an absence of any chromophores, excluding the possibility that it was a reduction product containing a carboxylbenzaldehyde moiety since the latter has a characteristic absorbance at 258 nm

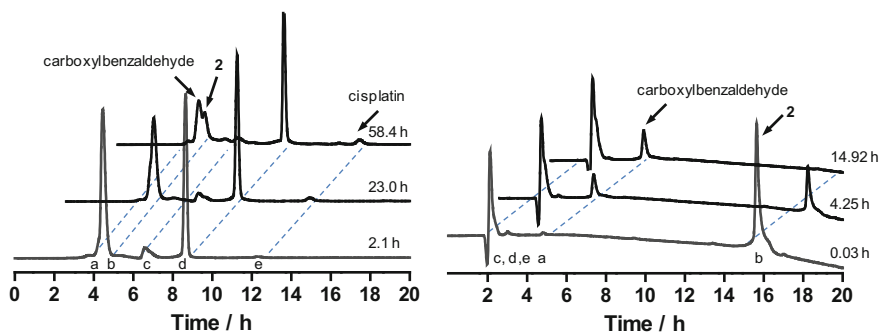


Fig. S3.4 Left and right: HILIC (230 nm) and RPLC (214 nm) chromatograms respectively of the reduction of **2** by 2–4 mM ascorbic acid. Legend: **a** 4-carboxylbenzaldehyde, **b** **2**, **c** dehydroascorbic acid, **d** ascorbic acid, **e** cisplatin

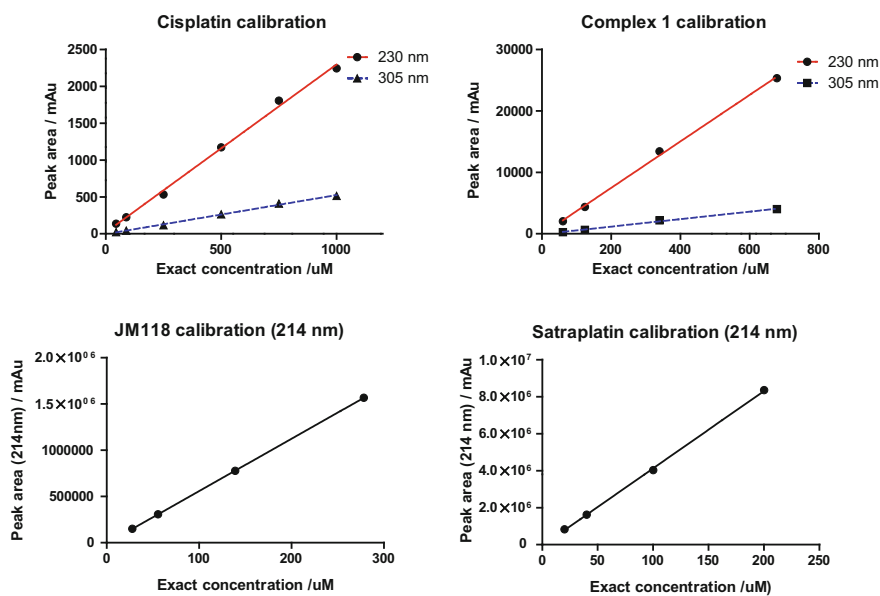


Fig. S3.5 Representative calibration curves. A fresh calibration curve was plotted per experiment. Top row: Calibration curves for cisplatin and **1** respectively at 230 and 305 nm. Bottom row: Calibration curve for JM118 and satraplatin respectively at 214 nm

Measurement of maximum aqueous kinetic solubility in PBS. Solid samples of **1**, **2** and satraplatin were continuously added to PBS (pH 7.4) with sonication for about 20 min until the point of turbidity. The suspension was then syringe-filtered to obtain the corresponding saturated solution. Maximum solubility was then determined by ICP-OES. Experiment was repeated in duplicates (Table S3.1).

Table S3.1 Maximum solubility of **1** and **2** and satraplatin in PBS (pH 7.4). Values are reported as mean with standard error

	1 (axial OH)	2 (axial OAc)	Satraplatin
Solubility/ μM	299.3 \pm 31.45	2928.7 \pm 134.2	581.1 \pm 31.1

References

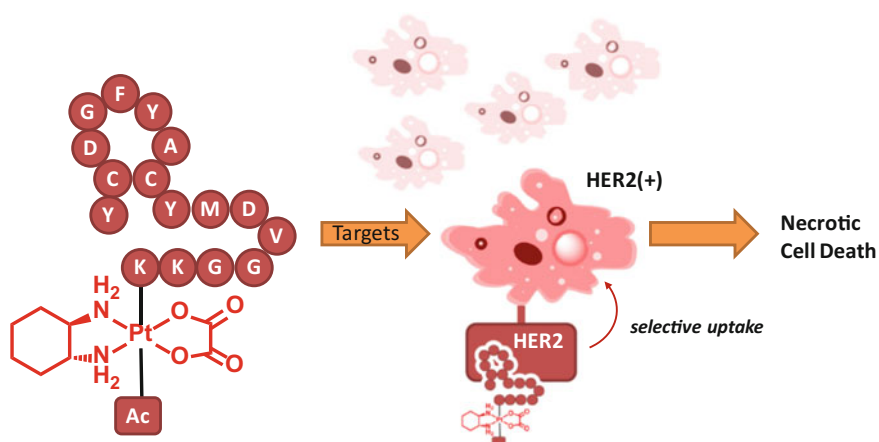
- Hall, M.D., Mellor, H.R., Callaghan, R., Hambley, T.W.: Basis for design and development of platinum(IV) anticancer complexes. *J. Med. Chem.* **50**, 3403–3411 (2007)
- Hall, M.D., Hambley, T.W.: Platinum(IV) antitumour compounds: their bioinorganic chemistry. *Coord. Chem. Rev.* **232**, 49–67 (2002)
- Chin, C.F., Wong, D.Y.Q., Jothibasur, R., Ang, W.H.: Anticancer platinum (IV) prodrugs with novel modes of activity. *Curr. Top. Med. Chem.* **11**, 2602–2612 (2011)
- Chin, C.F., Tian, Q., Setyawati, M.I., Fang, W., Tan, E.S.Q., Leong, D.T., Ang, W.H.: Tuning the activity of platinum(IV) anticancer complexes through asymmetric acylation. *J. Med. Chem.* **55**, 7571–7582 (2012)
- Carr, J., Tingle, M., McKeage, M.: Satraplatin activation by haemoglobin, cytochrome C and liver microsomes in vitro. *Cancer Chemother. Pharmacol.* **57**, 483–490 (2006)
- Raynaud, F.I., Mistry, P., Donaghue, A., Poon, G.K., Kelland, L.R., Barnard, C.F.J., Murrer, B.A., Harrap, K.R.: Biotransformation of the platinum drug JM216 following oral administration to cancer patients. *Cancer Chemother. Pharmacol.* **38**, 155–162 (1996)
- Pendyala, L., Cowens, J.W., Chheda, G.B., Dutta, S.P., Creaven, P.J.: Identification of cis-dichloro-bis-isopropylamine platinum(II) as a major metabolite of iproplatin in humans. *Cancer Res.* **48**, 3533–3536 (1988)
- Petruzzella, E., Margiotta, N., Ravera, M., Natile, G.: NMR Investigation of the spontaneous thermal- and/or photoinduced reduction of trans dihydroxido Pt(IV) derivatives. *Inorg. Chem.* **52**, 2393–2403 (2013)
- Sinisi, M., Intini, F.P., Natile, G.: Dependence of the reduction products of platinum(IV) prodrugs upon the configuration of the substrate, bulk of the carrier ligands, and nature of the reducing agent. *Inorg. Chem.* **51**, 9694–9704 (2012)
- Nemirovski, A., Vinograd, I., Takroui, K., Mijovilovich, A., Rompel, A., Gibson, D.: New reduction pathways for ctc-[PtCl₂(CH₃CO₂)₂(NH₃)(Am)] anticancer prodrugs. *Chem. Commun.* **46**, 1842–1844 (2010)
- Wexselblatt, E., Gibson, D.: What do we know about the reduction of Pt(IV) pro-drugs? *J. Inorg. Biochem.* **117**, 220–229 (2012)
- Mukhopadhyay, S., Barnés, C.M., Haskell, A., Short, S.M., Barnes, K.R., Lippard, S.J.: Conjugated platinum(IV)—peptide complexes for targeting angiogenic tumor vasculature. *Bioconjugate Chem.* **19**, 39–49 (2007)
- Gaviglio, L., Gross, A., Metzler-Nolte, N., Ravera, M.: Synthesis and in vitro cytotoxicity of cis, cis, trans-diamminedichloridodisuccinatoplatinum(IV)-peptide bioconjugates. *Metallomics* **4**, 260–266 (2012)
- Yang, J., Sun, X., Mao, W., Sui, M., Tang, J., Shen, Y.: Conjugate of Pt(IV)—histone deacetylase inhibitor as a prodrug for cancer chemotherapy. *Mol. Pharm.* **9**, 2793–2800 (2012)
- Dhar, S., Lippard, S.J.: Mitaplatin, a potent fusion of cisplatin and the orphan drug dichloroacetate. *Proc. Natl. Acad. Sci. U, S. A.* (2009)
- Aryal, S., Hu, C.M.J., Fu, V., Zhang, L.: Nanoparticle drug delivery enhances the cytotoxicity of hydrophobic-hydrophilic drug conjugates. *J. Mater. Chem.* **22**, 994–999 (2012)
- Dhar, S., Liu, Z., Thomale, J., Dai, H., Lippard, S.J.: Targeted single-wall carbon nanotube-mediated Pt(IV) prodrug delivery using folate as a homing device. *J. Am. Chem. Soc.* **130**, 11467–11476 (2008)

18. Duong, H.T.T., Huynh, V.T., de Souza, P., Stenzel, M.H.: Core-cross-linked micelles synthesized by clicking bifunctional Pt(IV) anticancer drugs to isocyanates. *Biomacromol* **11**, 2290–2299 (2010)
19. Graf, N., Bielenberg, D.R., Kolishetti, N., Muus, C., Banyard, J., Farokhzad, O.C., Lippard, S.J.: $\alpha_v\beta_3$ integrin-targeted PLGA-PEG nanoparticles for enhanced anti-tumor efficacy of a Pt (IV) prodrug. *ACS Nano* **6**, 4530–4539 (2012)
20. Li, J., Yap, S.Q., Chin, C.F., Tian, Q., Yoong, S.L., Pastorin, G., Ang, W.H.: Platinum(IV) prodrugs entrapped within multiwalled carbon nanotubes: selective release by chemical reduction and hydrophobicity reversal. *Chem. Sci.* **3**, 2083–2087 (2012)
21. Pichler, V., Valiahd, S.M., Jakupec, M.A., Arion, V.B., Galanski, M., Keppler, B.K.: Mono-carboxylated diaminedichloridoplatinum (IV) complexes—selective synthesis, characterization, and cytotoxicity. *Dalton Trans.* **40**, 8187–8192 (2011)
22. Zhang, J.Z., Bonnitcha, P., Wexselblatt, E., Klein, A.V., Najajreh, Y., Gibson, D., Hambley, T.W.: Facile preparation of mono-, di- and mixed-carboxylato platinum(IV) complexes for versatile anticancer prodrug design. *Chem. Eur. J.* **19**, 1672–1676 (2013)
23. Wong, D.Y.Q., Lau, J.Y., Ang, W.H.: Harnessing chemoselective imine ligation for tethering bioactive molecules to platinum(IV) prodrugs. *Dalton Trans.* **41**, 6104–6111 (2012)
24. Shi, Y., Liu, S.-A., Kerwood, D.J., Goodisman, J., Dabrowiak, J.C.: Pt(IV) complexes as prodrugs for cisplatin. *J. Inorg. Biochem.* **107**, 6–14 (2012)
25. Blatter, E.E., Vollano, J.F., Krishnan, B.S., Dabrowiak, J.C.: Interaction of the antitumor agents cis, cis, trans-Pt(IV)(NH₃)₂Cl₂(OH)₂ and cis, cis, trans-Pt(IV)[(CH₃)₂CHNH₂]₂Cl₂(OH)₂ and their reduction products with PM2 DNA. *Biochemistry* **23**, 4817–4820 (1984)
26. Nygren, Y., Hemstrom, P., Astot, C., Naredi, P., Bjorn, E.: Hydrophilic interaction liquid chromatography (HILIC) coupled to inductively coupled plasma mass spectrometry (ICPMS) utilizing a mobile phase with a low-volatile organic modifier for the determination of cisplatin, and its monohydrolyzed metabolite. *J. Anal. At. Spectrom.* **23**, 948–954 (2008)
27. Falta, T., Koellensperger, G., Sandler, A., Buchberger, W., Mader, R.M., Hann, S.: Quantification of cisplatin, carboplatin and oxaliplatin in spiked human plasma samples by ICP-SFMS and hydrophilic interaction liquid chromatography (HILIC) combined with ICP-MS detection. *J. Anal. At. Spectrom.* **24**, 1336–1342 (2009)
28. Kasherman, Y., Sturup, S., Gibson, D.: Is glutathione the major cellular target of cisplatin? a study of the interactions of cisplatin with cancer cell extracts. *J. Med. Chem.* **52**, 4319–4328 (2009)
29. Hermann, G., Heffeter, P., Falta, T., Berger, W., Hann, S., Koellensperger, G.: In vitro studies on cisplatin focusing on kinetic aspects of intracellular chemistry by LC-ICP-MS. *Metallomics* **5**, 636–647 (2013)
30. Carr, J., Tingle, M., McKeage, M.: Rapid biotransformation of satraplatin by human red blood cells in vitro. *Cancer Chemother. Pharmacol.* **50**, 9–15 (2002)
31. Hann, S., Koellensperger, G., Stefanka, Z., Stingeder, G., Furrhacker, M., Buchberger, W., Mader, R.M.: Application of HPLC-ICP-MS to speciation of cisplatin and its degradation products in water containing different chloride concentrations and in human urine. *J. Anal. At. Spectrom.* **18**, 1391–1395 (2003)
32. Deutsch, J.C.: Dehydroascorbic acid. *J. Chromatogr. A* **881**, 299–307 (2000)
33. Ellis, L., Er, H., Hambley, T.: The influence of the axial ligands of a series of platinum(IV) anti-cancer complexes on their reduction to platinum(II) and reaction with DNA. *Aust. J. Chem.* **48**, 793–806 (1995)
34. Choi, S., Filotto, C., Bisanzo, M., Delaney, S., Lagasee, D., Whitworth, J.L., Jusko, A., Li, C., Wood, N.A., Willingham, J., Schwenker, A., Spaulding, K.: Reduction and anticancer activity of platinum(IV) complexes. *Inorg. Chem.* **37**, 2500–2504 (1998)
35. Lemma, K., Sargeson, A.M., Elding, L.I.: Kinetics and mechanism for reduction of oral anticancer platinum(IV) dicarboxylate compounds by L-ascorbate ions. *J. Chem. Soc. Dalton Trans.* **7**, 1167–1172 (2000)

36. Pichler, V., Heffeter, P., Valiahd, S.M., Kowol, C.R., Egger, A., Berger, W., Jakupec, M.A., Galanski, M., Keppler, B.K.: Unsymmetric mono- and dinuclear platinum(IV) complexes featuring an ethylene glycol moiety: synthesis, characterization, and biological activity. *J. Med. Chem.* **55**, 11052–11061 (2012)
37. Zhang, J.Z., Wexselblatt, E., Hambley, T.W., Gibson, D.: Pt(IV) analogs of oxaliplatin that do not follow the expected correlation between electrochemical reduction potential and rate of reduction by ascorbate. *Chem. Commun.* **48**, 847–849 (2012)
38. Dhara, S.C.: A rapid method for the synthesis of cis-[Pt(NH₃)₂Cl₂]. *Indian J. Chem.* **8**, 193–194 (1970)
39. Kuroda, R., Ismail, I.M., Sadler, P.J.: X-ray and NMR studies of trans-dihydroxo-platinum (IV) antitumor complexes. *J. Inorg. Biochem.* **22**, 103–117 (1984)
40. Phillips, J.A., Morgan, E.L., Dong, Y., Cole, G.T., McMahan, C., Hung, C.-Y., Sanderson, S. D.: Single-step conjugation of bioactive peptides to proteins via a self-contained succinimidyl bis-arylhydrazone. *Bioconjug. Chem.* **20**, 1950–1957 (2009)

Chapter 4

Induction of Targeted Necrosis with HER2-Targeted Platinum(IV) Anticancer Prodrugs



Reproduced with permission from the Royal Society of Chemistry.

4.1 Introduction

Precision medicine in the form of molecularly-targeted therapies are now the frontline in the treatment of cancer, buoyed by tangible improvements in treatment tolerability and outcomes [1]. Nonetheless, drug resistance against targeted therapies almost inevitably arises eventually after several treatment cycles. In some cases, this failure is attributable to a defect in the apoptosis machinery at a cellular level [2, 3]. Pro-survival adaptations such as a mutated p53 or upregulation of the anti-apoptotic Bcl-2 signal bestows resistance against apoptotic cell death.

Attempts to restore apoptotic-sensitivity to molecular-targeted therapies using yet another molecular-targeted approach is perhaps condemned by the highly variable genetic diversity even within the same tumour mass. Molecularly-targeted intervention may suppress a particular cancer clone but often inadvertently exerts selective pressure for expansion of resistant clones instead [4]. On the other hand, necrotic cell death, which has recently been recognized as a regulated modality of cell death, may potentially be exploited as a means of bypassing defects in apoptosis machinery [5–7].

The human epidermal growth factor receptor 2 (HER2) is a well-known and validated oncogene, critical in the development and progression of certain cancers [8]. It is highly amplified on the cell surface of around 20–30% of breast [8] and 20% of gastric cancers [9] with correspondingly poorer prognosis. The clinically approved monoclonal antibody, trastuzumab, accentuates Her2-mediated pro-growth signalling by obstructing HER2 dimerization [10]. In this work, we have chosen to employ smaller rationally designed peptidomimetics of trastuzumab. These short exocyclic peptides named AHNP (anti-HER2/neu peptide) share the same CDR-H3 recognition sequence of the parental full length antibody and bind HER2 with high affinity [11, 12].

Here in this work, we have used chemoselective oxime ligation to attach the AHNP targeting peptide to platinum(IV) prodrug scaffolds [13, 14] of both cisplatin (CDDP) and oxaliplatin (OXP) (Fig. 4.1a) [15]. We report that the platinum(IV)-AHNP conjugates exhibited an unexpectedly curious biphasic killing behaviour. The first phase entails rapid killing via targeted necrosis possibly due to overwhelming platinum influx followed by a phenomenon of delayed cell death of the remaining surviving population. In line with our original goals, the platinum(IV)-AHNP conjugates were also selective towards HER2-overexpressing cancers without killing basal HER2-expressing cells. This work supports the idea of “targeted necrosis” as a viable strategy of circumventing apoptosis resistance while avoiding undesirable non-specificity associated with conventional necrosis-inducing agents [6].

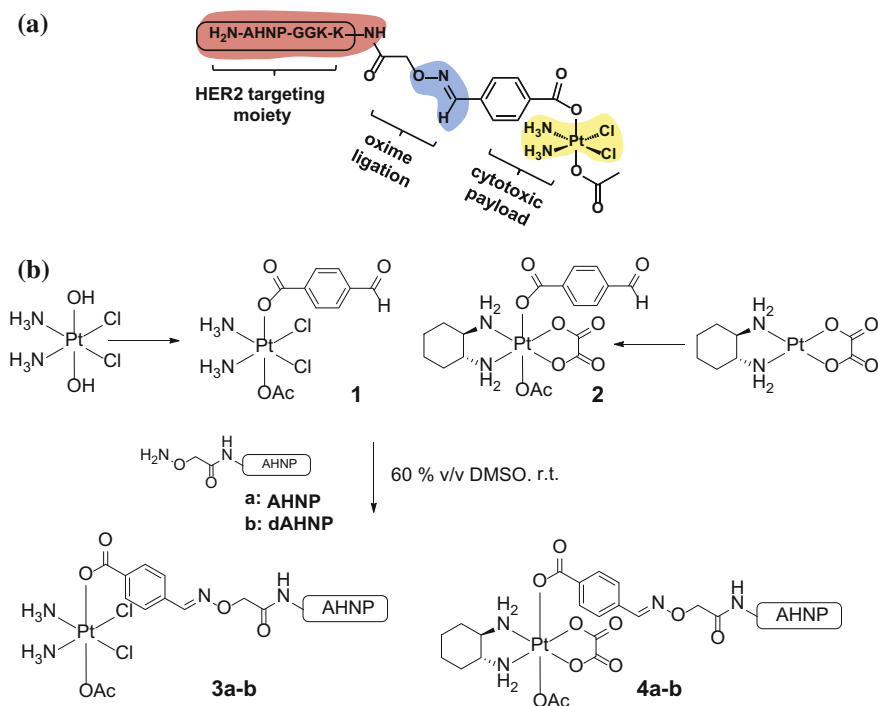


Fig. 4.1 Synthesis of HER2-targeted platinum(IV)-AHNP conjugate consisting of an AHNP motif tethered to a cytotoxic platinum pharmacophore. The AHNP motif was separated with a small tripeptide spacer (GGK) and functionalized with an aminoxy(acetate) linker at the terminal lysine residue. Peptide sequence: H₂N-YC*[†]DGFYAC*[†]YMDVGGKK(aminooxy)-CONH₂ (*—Linked disulfide bridge)

4.2 Results and Discussion

Synthesis of HER2-targeted platinum(IV)-AHNP conjugates. We believed that a platinum(IV) scaffold bearing the HER2-targeting AHNP peptide could selectively deliver CDDP or OXP to HER2-amplified cancers but not normal cells. The synthesis of CDDP-based platinum(IV) scaffold **1** has been reported [16]. Briefly, oxoplatin was reacted at one end with the *N*-hydroxylsuccinimide-ester of 4-formylbenzoic and capped at the other end with acetic anhydride (Fig. 4.1b and Scheme S4.1) [16]. The corresponding OXP-derived scaffold **2** was synthesized by acetylation of the synthetically accessible *trans*-OXP-(OH)(OAc) precursor [17] with the acid chloride of 4-formylbenzoic acid. It is worth noting that methanol should be thoroughly excluded in these reactions as the aldehyde functional group readily forms acetals in the presence of alcohols. Finally, the desired platinum(IV)-AHNP constructs, **3a** and **4a**, were created using the oxime ligation strategy previously reported by us [15, 16]. We also prepared the inactive controls, platinum

(IV)-dAHNP **3b** and **4b**, bearing a non-binding analog of AHNP. In general, these platinum(IV)-peptide conjugates were formed by treating a slight stoichiometric excess of the (aminoxy)acetylated peptide with **1** or **2**. The reactions finished quite cleanly within 2 h and were purified by semi-preparative HPLC with moderate yields between 19 and 51%. Characterization of the conjugates was carried out using ESI-MS and their purities were ascertained by analytical HPLC (SI).

Rapid and overwhelming platinum uptake with platinum(IV)-AHNP conjugates. We first ascertained if the HER2-targeting motif on platinum(IV)-AHNP improved cellular uptake of the cytotoxic platinum payload. Measurement of whole cell and nuclear uptake was quantified after nitric acid digestion by inductively-coupled plasma mass spectrometry. We observed superior uptake of **3a** and **4a** in the HER2-amplified NCI-N87 gastric cancer cell-line after a short 4 h treatment pulse. The unmodified CDDP and OXP exhibited similar whole cell uptake of 170.2 ± 3.5 and 170.1 ± 6.4 pmol per 10^6 cells respectively. Consistent with our hypothesis, the targeted CDDP-AHNP (**3a**) and OXP-AHNP (**4a**) conjugates presented dramatically higher whole-cell uptakes of 4246 ± 450 and 1598 ± 138 pmol per 10^6 cells respectively which was ca. 25-fold and 9-fold greater than their parental drug ($p < 0.01$). Nuclear uptake of **3a** and **4a** was 3-fold and 12-fold higher compared to CDDP and OXP respectively ($p < 0.05$). In contrast, the untargeted platinum(IV) precursors, **1** and **2**, as well as control platinum (IV)-dAHNP conjugates, **3b** and **4b**, were not as readily taken into NCI-N87. Since control peptide dAHNP differed minimally from AHNP, mainly by substitution of L to D-isomer amino acids, and is expected to have similar polarity, the superior uptake of **3a** and **4a** suggest selective uptake mediated by HER2 receptors rather than by passive diffusion. In agreement, both **3a** and **4a** were cytotoxic while the control conjugates **3b** and **4b** were effectively non-cytotoxic ($IC_{50} > 100 \mu\text{M}$) based on MTT metabolic activity assays after 72 h exposure (Fig. S4.2). We reasoned that the massive and rapid uptake of the targeted platinum agents relative to their parental drugs within a short time frame could explain for the conjugates' unique killing profile.

In line with our hypothesis of selective targeting, we further evaluated if **3a** and **4a** could selectively kill HER2 positive cells while sparing cells with basal HER2 levels. We utilized a co-culture model comprising NCI-N87, with high HER2 expression, and A2780 ovarian carcinoma, with significantly lower but still detectable levels of HER2 [18]. A co-culture of NCI-N87 (unstained) and A2780 (pre-stained with CellTrackerTM Green as a tracer) was drug-treated for 24 h before staining with propidium iodide (PI) to determine cell viability by flow cytometry analysis. A ratio of 4:1 NCI-N87 (48 h doubling time) to A2780 (13 h doubling time) was seeded 24 h prior to drug treatment so that both cell lines were at approximately equal proportions at the point of treatment as estimated by flow cytometry analysis. The platinum-sensitive A2780 ovarian cancer cell-line was chosen rather than healthy primary cultures as a more challenging co-culture model because both CDDP and OXP already feature modestly favourable therapeutic index, killing cancer cells over normal healthy cells in most cases. The results indicate that **3a** and **4a** not only demonstrated superior killing of NCI-N87 but were

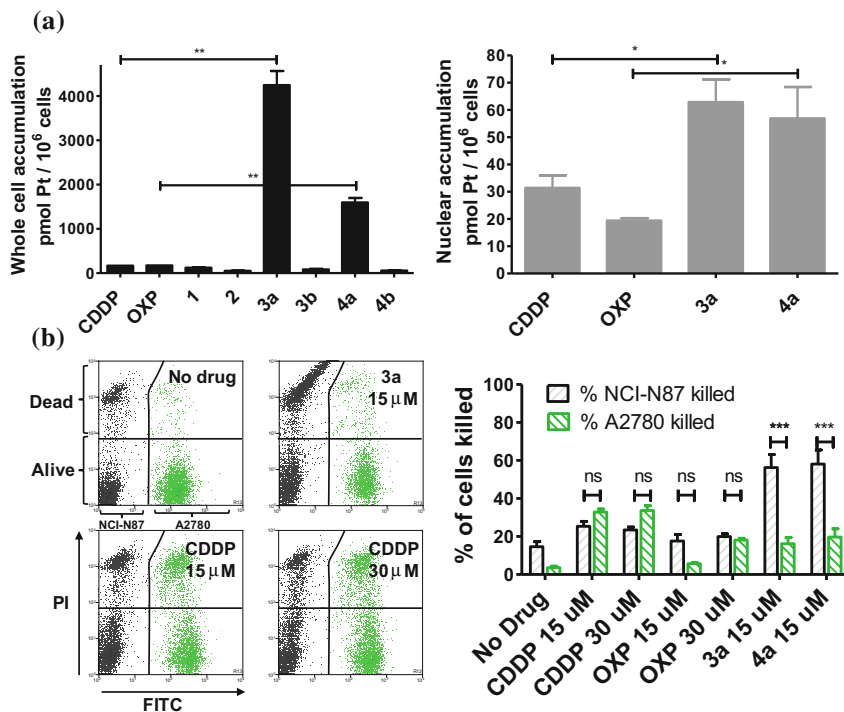


Fig. 4.2 **a** Platinum(IV)-AHNP conjugates are much more efficiently taken up into cells. Whole cell (left) and nuclear (right) uptake after drug treatment (20 μ M) for 4 h in NCI-N87 as measured by ICP-MS. Statistical analysis by unpaired Student's *t* test. **b** Platinum(IV)-AHNP conjugates selectively kill HER2 over-expressing NCI-N87 over the normal HER2 expressing A2780. A co-culture of NCI-N87 and A2780 (pre-stained with CellTracker™ Green) was drug-treated for 24 h before viability staining with PI. Statistical analysis by two-way ANOVA and Bonferroni post-tests. Means \pm s.e.m. (* p < 0.05, ** p < 0.01, *** p < 0.001)

more selective compared to the untargeted CDDP and OXP (p < 0.001) (Fig. 4.2b). CDDP and OXP treatment of the co-culture did not discriminate between NCI-N87 and A2780. In contrast, the trend was sharply reversed with **3a** and **4a** which killed a significantly higher percentage of NCI-N87 relative to A2780 (p < 0.001).

Distinctly different cell-killing profile of platinum(IV)-AHNP conjugates via targeted necrosis. Clinical platinum(II) agents namely CDDP, carboplatin and OXP induce tumor cell death through DNA-damage mediated apoptosis [3, 19]. We therefore employed the Annexin V apoptosis assay in order to evaluate the mode of cell death induced by platinum(IV)-AHNP conjugates **3a** and **4a**. Cells were exposed to the platinum agents for 24 h before staining with Annexin V-EGFP and PI (Table S4.1). Annexin V binds to surface-exposed phosphatidylserine residues, which migrates from the inner plasma membrane leaflet towards the outer leaflet during apoptosis [20, 21]. To facilitate comparison, the complexes were tested at equi-concentrations (15 μ M), close to the clinically relevant peak plasma CDDP

concentration of $13.03 \pm 4.70 \mu\text{M}$ after a standard intravenous dosage ($100 \text{ mg}/\text{m}^2$) [17]. As expected, both CDDP and OXP-treated NCI-N87 cells displayed appreciable apoptotic cell populations in early (Annexin V+/PI-) and late-stage apoptosis (Annexin V+/PI+) which increased in a dose-dependent manner (Fig. 4.3a, b (left)). In stark contrast, both **3a** and **4a**-treated NCI-N87 shown predominately cell death via primary necrosis (Annexin V-/PI+), indicating that the plasma membrane has been compromised without phosphatidylserine exposure (Fig. 4.3a, b (left)).

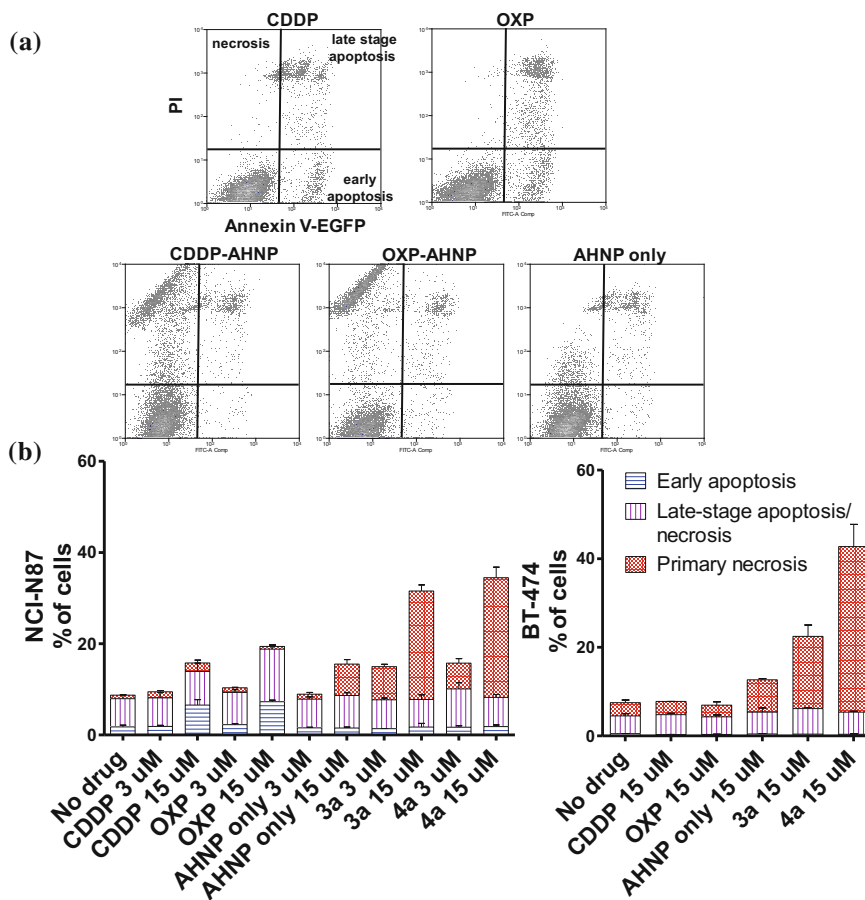


Fig. 4.3 Apoptosis was evaluated by AnnexinV/PI staining of drug-treated cells after 24 h. **a** Scatter plot of treated NCI-N87 cells (15 μM drug). **b** Barchart of apoptosis-sensitive NCI-N87 (left) and apoptosis-resistant BT-474 (right) after 24 h exposure. Each bar depicts % of cells at either early-stage apoptosis, late-stage apoptosis or necrosis. Tabulated data in Table S4.1

In agreement, the morphology of OXP-treated NCI-N87 cells displayed characteristic features of apoptotic cell death (cell rounding and shrinkage, blebbing of plasma membrane, condensation and fragmentation of DNA) (Fig. 4.4a) [22]. On the other hand, **4a**-treated NCI-N87 did not show the same defining morphology and instead presented irregular nuclear fragmentation (both karyolysis and karyorrhexis) as well as the appearance of dead de-nucleated cell-debris, still attached to

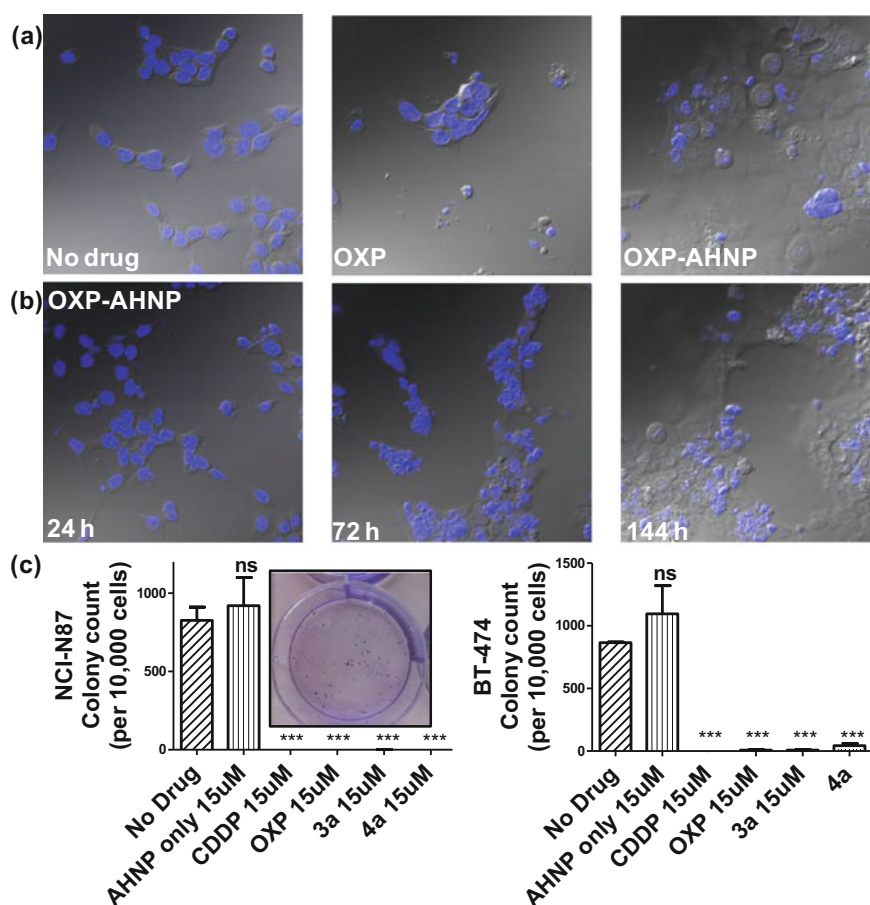


Fig. 4.4 **a** Representative overlaid microscopy images of control and treated NCI-N87 (15 μ M drug for 24 h and allowed to recover in fresh media for a week). Differences in nuclear morphology were visualized by Hoechst 3342 staining. Untreated cells were shown at day 1 while drug-treated cells were shown at day 6. **b** 4a-treated NCI-N87 undergoes short-term proliferation 24 h after drug treatment but display increasing severe nuclear fragmentation over 7 d (left to right). **c** Clonogenic assay of NCI-N87 (left) and BT-474 (right) to assess the long-term proliferation ability of single cells drug-treated for 24 h and allowed to recover in fresh complete media. Representative image of AHNP-treated NCI-N87 colonies shown in the inset. Statistical analysis by unpaired Student's *t* test against non-treated control. Means \pm s.e.m. (***) $p < 0.001$)

the substrate, bearing the same polygonal morphology as healthy cells. The exposure of phosphatidylserine is an early event in the apoptotic process which precedes many other characteristic features such as cell-shrinkage and nuclear condensation [20, 21]. Although platinum(IV)-AHNP conjugates displayed higher nuclear platinum levels than their platinum(II) congeners (Fig. 4.1a), therefore more DNA platination, only minimal apoptosis was observed in the former. This suggests that the platinum(IV)-AHNP conjugates induced very rapid membrane permeabilization before the apoptotic cascade of events could be initiated by DNA-damage recognition proteins.

As reactive oxygen species (ROS) is a well-known stimulus of necrosis, we further investigated if the observed necrosis was ROS-mediated. Cellular ROS on NCI-N87 was measured using 2',7'-dichlorofluorescein diacetate (DCFDA), a redox sensitive probe, 1 and 4 h after drug-treatment (Fig. S4.1). After 4 h, **3a** and **4a** gave a 1.7-fold and 1.3-fold signal increase respectively over non-treated control cells. In comparison, the AHNP peptide alone led a signal increase of 1.6-fold. Since the AHNP peptide was by itself a modest effector of ROS with associated necrotic cell death (Fig. 4.3b), a non-passive role of the targeting peptide in cell-killing cannot be dismissed. Nonetheless, ROS levels of **3a** and **4a**-treated cells was not correlated with its cell-killing ability and it is thus probable that ROS was not the sole factor in inducing necrotic cell death here.

The loss of a functional p53 is a well-established biomarker for platinum-associated apoptotic resistance both in vitro and in vivo which arises due to consequent failure in enacting the apoptotic cell death machinery in spite of DNA damage [3, 19]. In particular, BT-474 breast ductal carcinoma is resistant to apoptosis on the basis of its temperature-sensitive p53 status that is defective at 37 °C [23]. In keeping with NCI-N87, BT-474 cells exhibit high HER2 expression levels [24]. Platinum(IV)-AHNP conjugates were more potent in both apoptosis-sensitive NCI-N87 and apoptosis-resistant BT-474 cells compared to their parental drug following 24 h exposure (Fig. 4.3b). AHNP peptide alone displayed only modest cell-killing. In NCI-N87, about 31.6 and 34.5% of cells were non-viable (Annexin V+ or PI+) following 15 µM drug exposure of **3a** and **4a** compared to 15.8 and 18.8% with CDDP and OXP treatment, respectively. Against p53-dysfunctional BT-474 cells, no signs of early apoptosis (Annexin V+/PI-) were observed regardless of drug-treatment. Both CDDP and OXP-treated cells fared no better than untreated control cells (Fig. 4.3b). In contrast, platinum(IV) conjugates **3a** and **4a** surpassed their parental drugs at 22.5 and 47.2%, respectively, through induction of necrosis. Taken together, these results suggest that **3a** and **4a** can overcome apoptotic resistance through HER-2 targeted necrosis.

Surviving tumour cell population exhibit delayed cell death and suppression of long-term proliferation. We observed a curious biphasic killing mechanism on NCI-N87 cells by platinum(IV)-AHNP conjugates which was hinted at by visual monitoring of drug-treated cells under conventional microscopy (Figs. 4.4b and S4.3). The first phase comprised a rapid killing of between 30 and 35% of cells via necrosis (as ascertained by Annexin V), continued proliferation of the surviving population followed by an extended and gradual phase of delayed cell death

(Fig. S4.3). This sharp discernible two-phase rate of killing was not apparent with the free parental drugs. The surviving population of platinum(IV)-AHNP treated cells were still viable and retained limited proliferation capacity in the short term (but not long term). The surviving population of **3a** and **4a**-treated NCI-N87 cells were significantly more metabolically active compared to CDDP and OXP-treated cells after an intermediate 3-day period (Fig. S4.2). The MTT assay, which measures oxidoreductase activity, was used to assess metabolic activity of treated cells relative to non-treated cells after 72 h. **3a** and **4a**-treated cells (15 μ M) displayed higher metabolic activities of $48.2 \pm 2.3\%$ and $49.0 \pm 2.1\%$ compared to $25.0 \pm 4.3\%$ and $21.0 \pm 4.3\%$ with CDDP and OXP, respectively. This result suggested that there were more viable cells following treatment of **3a** and **4a** as compared to parental CDDP and OXP despite the more rapid induction of necrotic cell death by the conjugates. Yet the MTT assay cannot distinguish between cell-killing and the inhibition of cell proliferation (cytostasis) since both these factors could contribute to the measured metabolic activities.

One of the hallmarks of cancer is the capacity for indefinite growth and replication [25]. In order to track the long-term proliferation ability of the surviving cell population, we employed a combination of confocal microscopy and clonogenic assay to monitor the fate of treated cells (15 μ M for 24 h) which were subsequently allowed to recover in fresh media for a span of time. Under microscopy monitoring, **4a**-treated NCI-N87 cells undergo modest cellular expansion but displayed increasingly severe nuclear fragmentation 1–6 d after treatment (Fig. 4.4b). The nuclear morphology at 24 h (when **4a** was aspirated) was still relatively intact, indicating that subsequent nuclear deformation was independent of the acute necrotic phase. We hypothesized that the abnormal nuclear morphology observed with concomitant delayed cell death was due to mitotic catastrophe, a consequence of aberrant mitosis [5, 26]. **4a**-treated cells displayed micro-nucleation, multiple nuclei as well as enlarged irregular nuclei which are morphological features suggestive of mitotic catastrophe (Fig. 4.4a–b) [5, 26]. **4a**-treated cells gave rise to abnormal progeny suggesting that the mitotic defect, presumably due to a combination of DNA damage and impairment to the mitotic machinery, was durable even after the compound was removed. By day 6, all **4a**-treated cells were either dead (de-nucleated) or exhibited severely abnormal nuclear morphology implying that continued long-term proliferation was unviable. On the contrary, the few surviving cell population in OXP-treated NCI-N87 displayed a healthy-looking nuclear morphology which may suggest a capacity for re-growth if allowed to recover further (Fig. 4.4a). The cell cycle analysis of **4a**-treated NCI-N87 over 72 h indicated a transient G_0/G_1 arrest which occurred between the 27th to 49th hour followed by progression into the S phase and abrogation of the G_2/M mitotic checkpoint between the 49th to 72th h (Fig. S4.4). This mitotic entry of the cell despite cellular damage, and without an apoptotic response, is consistent with a hypothesis of genomic instability and mitotic catastrophe. On the other hand, OXP-treated cells indicated a markedly different DNA content profile, implying a different mechanistic action (Fig. S4.4). There was a slight accumulation into the early S phase (but not late S phase), paralleled by a sharp increase in the sub- G_0

phase (DNA laddering) which implied that cellular apoptosis was induced shortly after initiation of DNA synthesis.

Although the surviving population of **4a**-treated cells were more metabolically-active compared to OXP-treated cells and in fact exhibited transient cellular expansion, the progressively distorted nuclear morphology of **4a**-treated cells and its progeny suggested that long-term cellular division was unlikely. Thus, a clonogenic assay was performed in order to substantiate this hypothesis. The clonogenic assay measures the ability of single cells to divide through at least six generations (forming colonies ≥ 50 cells). In both NCI-N87 and BT-474, pre-treating the cells for 24 h was sufficient to induce a near complete abolishment of colony forming units with CDDP, OXP and the platinum(IV)-AHNP conjugates ($p < 0.001$) but not with free AHNP (Figs. 4.4c and S4.5). In NCI-N87, any significant differences between the free parental drug and conjugates **3a** and **4a** were not observed because both cell cycle arrest and cell death precluded colony formation. Furthermore, although the concentration tested of both CDDP and OXP were ineffective in triggering apoptosis in the resistant BT-474 cell-line, it was still sufficient to inhibit long-term proliferation. In contrast, free AHNP peptide was effective in directly killing both cell-lines (Fig. 4.3b) but was unable to halt long-term proliferation (Fig. 4.4c), indicating that these events are not necessarily correlated.

Taken together, our results indicate that the platinum(IV)-AHNP conjugates were mechanistically very different from their platinum(II) counterparts, and of comparable potency but with greater selectivity.

4.3 Conclusion

Unlike molecular targeted therapy, non-specific alkylating agents like CDDP and OXP may have multiple modes of action arising from different biological targets including DNA [27, 28]. A broader spectrum of action could be therapeutically favorable because it potentially circumvents multi-factorial apoptosis-resistance signaling pathways. We investigated two potent HER2-targeted platinum(IV)-AHNP agents based on the clinically-used platinum(II) drugs CDDP and OXP. Despite being prodrugs, conjugation of a HER2-targeting peptide drastically altered the mode of cell death, presumably via massive and rapid platinum influx. These conjugates exhibited a unique biphasic mode of action and selectively killed highly HER2-expressing cells under co-culture conditions, even against phenotypes that are resistant to apoptosis. Our work highlights targeted necrosis as a viable alternative cell death modality that can be harnessed to overcome defective apoptosis hampering many conventional chemo- and targeted anticancer agents.

4.4 Materials and Methods

General reagents. Unless otherwise stated, all starting reagents are commercially available. Cisplatin [4], *cis,cis,trans*-diamminedichloro(hydroxido)(4-formylbenzoate)platinum(IV) **1** [16], oxaliplatin [29], and *trans*-acetato[(1*R*,2*R*)-cyclohexane-1,2-diamine-*N,N'*](ethanedioato-*O,O'*)hydroxido-platinum(IV) [17] were synthesized as reported previously.

Peptides. The HER2/neu binding peptide (AHNP) and control non-binding peptide (dAHNP) were custom-synthesized by ChinaPeptides (Shanghai) and modified with an (aminoxy)acetic acid linker at the ϵ -amino group of the lysine residue as specified. The peptides AHNP and dAHNP has the following sequence: NH₂-Tyr-Cys-Asp-Gly-Phe-Tyr-Ala-Cys-Tyr-Met-Asp-Val-Gly-Gly-Lys-Lys(aminoxy)CONH₂ and *D*-Phe-Cys-Asp-Gly-Phe-Tyr-Ala-Cys-*D*-Tyr-Met-Asp-Val-Gly-Gly-Lys-Lys(aminoxy)-CONH₂ respectively.

Instrumentation. ¹H NMR was recorded on a Bruker Avance 300 or 400 MHz. Chemical shifts are reported in parts per million relative to residual solvent peaks [30]. Electrospray ionization mass spectra (ESI-MS) were obtained on a Thermo Finnigan LCQ ESI-MS system. Elemental analysis was carried out on a Perkin-Elmer PE 2400 elemental analyzer by CMMAC (National University of Singapore). Platinum concentrations of stock solutions were measured externally by CMMAC (National University of Singapore) on an Optima ICP-OES (Perkin-Elmer). In some cases, platinum concentrations were also measured on an Agilent 7500 Series ICP-MS. Analytical UV-vis absorbance was measured on a Shimadzu UV-1800 UV-vis spectrophotometer. Analytical reversed phase HPLC (RPLC) was conducted on a Shimadzu Prominence or an Agilent 1200 series DAD using Shimpack VP-ODS column (5 μ m, 120 Å, 150 \times 4.60 mm, 1.0 mL min⁻¹ flow). Semi-preparative HPLC was performed on a Shimadzu Prominence using YMC-Pack Pro C18 column (5 μ m, 120 Å, 250 \times 10 mm, 2.0 mL min⁻¹ flow).

Synthesis of *trans*-acetato[(1*R*,2*R*)-cyclohexane-1,2-diamine](ethanedioato-*O,O'*)(4-formylbenzoate)platinum(IV) (2**).** 4-formyl-benzoyl chloride (111.8 mg, 0.663 mmol) dissolved in dry acetone (2 mL) was added dropwise to a suspension of *trans*-acetato[(1*R*,2*R*)-cyclohexane-1,2-diamine-*N,N'*](ethanedioato-*O,O'*)hydroxido-platinum(IV) (105.1 mg, 0.222 mmol) and pyridine (680 μ L, 8.44 mmol) in dry acetone (15 mL). The reaction mixture was stirred vigorously and refluxed overnight to give a pale yellow suspension. The solvent was evaporated *in vacuo* and the precipitate was dissolved in minimal MeCN and precipitated with chilled 1:1 DCM/diethyl ether. The crude mixture was left at 4 °C for 1 h to promote further precipitation. The crude precipitate was then triturated with DCM, redissolved in acetonitrile and purified by flash silica gel chromatography (1:1 DCM/MeCN and 0.01% AcOH; R_f = 0.4) to yield a yellow powder. Yield: 14.2 mg (10.6%) ¹H NMR (DMSO-*d*₆, 300.13 Hz): δ 10.08 (s, 1H), 8.4 (br m, 4H), 8.05 (d, 2H), 7.97 (d, 2H), 2.66 (br m, 2H), 2.16 (m, 2H), 1.99 (s, 3H), 1.52 (m, 4H), 1.11 (m, 2H); ESI-MS (–ve): *m/z* 604.0 [M–H][–]; C₁₈H₂₂N₂O₉platinum.2H₂O (641.5 g/mol)

calc: C 33.70, H 4.09, N 4.37; found C 33.36, H 3.91, N 4.38. Purity (HPLC): 1 peak at 254 and 280 nm.

General procedure for synthesis of platinum(IV)-peptide conjugates. In general, the platinum(IV)-peptide conjugates (**3a-b** and **4a-b**) were prepared by treating the desired (aminoxy)acetylated peptide with slight stoichiometric deficit of **1** or **2** in 60% v/v DMSO. All reagents were pre-dissolved in DMSO to form stock solutions. Concentrations of the free peptide was determined by UV at 280 nm either in 50 mM pH 7 phosphate buffer or 1% aq. ammonia [31]. Reaction was generally completed within 2–4 h as determined by analytical HPLC. The desired products were subsequently isolated by semi-preparative HPLC using a gradient elution of 10–30% solvent B for the first 25 min followed by 30% B for another 17 min. Purity of the conjugates was assessed on an analytical column assessed using a gradient elution of 8–30% B for the first 10 min, 30% B for another 8 min and finally 30–80% B for 7 min. Solvent A is aq. NH₄OAc buffer (10 mM, pH 7) and solvent B is MeCN.

Cisplatin(IV)-AHNP conjugate (3a). Complex **1** (50.5 uL of a 60.19 mM stock solution, 3.04 μmol) was added to aminoxy-functionalized AHNP peptide (150 μL of a 23.76 mM stock solution, 3.56 μmol) in 1.4 mL 60% v/v DMSO. The reaction mixture was agitated for 2 h before purification by semi-preparative HPLC. Yield: ca. 1.5 mg (21%); ESI-MS (-): m/z 1188.6 [M-2H]²⁻; Purity (HPLC): 98% at 280 nm.

Cisplatin(IV)-dAHNP conjugate (3b). Synthesis of **3b** was similar to **3a**. Yield: ca. 43%; ESI-MS (-): m/z 1180.9 [M-2H]²⁻; Purity (HPLC): 97% at 280 nm.

Oxaliplatin(IV)-AHNP conjugate (4a). Synthesis of **4a** was similar to **3a** but using **2** as the platinum(IV) scaffold instead. Yield: ca. 19%; ESI-MS (-): m/z: 1237.1 [M-2H]²⁻; Purity (HPLC): 94% at 280 nm.

Oxaliplatin(IV)-dAHNP conjugate (4b). Synthesis of **4b** was similar to **4a**. Yield: ca. 51%. ESI-MS (-): m/z 1229.6 [M-2H]²⁻; Purity (HPLC): 96% at 280 nm.

Cell culture. The HER2/neu over-expressing human gastric cancer cell-line NCI-N87 and breast cancer cell-line BT474 were obtained from ATCC. The A2780 human ovarian cancer cell line was obtained from EACC. All cell-lines were cultured in complete RPMI 1640 medium containing 10% fetal bovine serum (FBS) and maintained in a humidified of 5% CO₂ at 37 °C.

Annexin-V apoptosis assay (24 h). Apoptosis induced by drug treatment was assessed by double staining drug-treated cells with Annexin V-EGFP (abcam) and PI. Briefly, 2 × 10⁵ cells were seeded per well in 12-well plates in complete media (1 mL) and allowed to adhere overnight. The test compounds were then diluted in complete medium and added to the cells at the concentrations indicated for 24 h. The old drug-containing media was then collected and the cells were harvested by trypsinization and subsequently combined with the old media to deactivate trypsin. 2 × 10⁵ cells per well were counted, pelleted and resuspended in 500 μL of Annexin-V binding buffer (10 mM HEPES/NaOH (pH 7.4), 140 mM NaCl and 2.5 mM CaCl₂) containing 1 x Annexin V-EGFP protein and PI (1 μg/mL).

Samples were kept in the dark and analysed immediately on a flow cytometer (BD LSRFortessa). Quantitative analysis was performed using Summit software.

MTT assay for evaluating intermediate-term cellular metabolic activity (72 h). The indicated cell-lines were harvested from culture flasks by trypsinization and seeded at a density of 4.0×10^3 cells/well in 100 μ L aliquots into flat-bottomed 96-well tissue-culture plates. Cells were allowed to adhere in drug-free complete media with 10% FBS for 24 h, followed by the addition of dilutions of drug in 100 μ L/well complete media and further incubated for 72 h. At the end of exposure, medium was replaced by 100 μ L/well MTT solution (0.5 mg/mL in PBS). After incubation for 4 h, MTT was aspirated and substituted with 100 μ L/well DMSO. UV-vis absorbance was measured at 570 nm using a microplate reader (Biotek). Experiments were performed in sextuplicates for each drug concentration and carried out independently in triplicates. Metabolic activity was evaluated with the reference to the absolute IC₅₀ value. IC₅₀ values were calculated from concentration-response curves (cell viability against log of drug concentration) obtained in repeated experiments and adjusted to the actual concentration of platinum administered as measured by ICP-OES.

Clonogenic assay for evaluating long term reproductive viability (11–15 d). The cells were harvested by trypsinization into a single-cell suspension and subsequently the indicated number of cells, in complete media (2 mL), was seeded per well into a 6-well plate. Cells were allowed to adhere for 4 h, followed by addition of drug diluted to the indicated concentrations in complete media for 24 h. After 24 h, the cells were refreshed with fresh media (4 mL) and the cells was incubated for an additional 11 (BT-474) or 15 d (NCI-N87) to allow the single cells to recover and form colonies. The cells was then rinsed carefully with PBS (2 \times 3 mL), fixed with 3:1 v/v MeOH: AcOH for 5 min, stained with crystal violet (0.5% w/v ddH₂O) for an additional 15 min before rinsing thoroughly with water. Colonies containing greater than 50 cells were counted.

Drug targeting assay via co-culture of NCI-N87 and A2780. A2780 and NCI-N87 were cultured separately in T75 tissue culture flasks. A2780 was stained with CellTracker™ Green (2 μ M) (Molecular Probes) in RPMI for 30 min. The media was aspirated and the cells were subsequently incubated with complete RPMI for a further 30 min. Both cell-lines were harvested by trypsinization and subsequently A2780 (2.5×10^4 cells/well) was co-cultured with unstained NCI-N87 (1×10^5 cells/well) in a 12-well plate. The cells were rested overnight before drug-treatment for 24 h. After 24 h, the old cell culture media (containing detached cells) was kept to deactivate the trypsin downstream. Trypsin-EDTA (300 μ L) added to the adherent cells for 5 min and the harvested cells were transferred to the old culture media to deactivate (mostly A2780). Fresh trypsin-EDTA (300 μ L) was added for a further 10 min and pooled together with the old culture media to deactivate (mostly NCI-N87). The combined cell fraction was washed with PBS (1 \times 500 μ L) and finally resuspended in PI (1 μ g/mL) before analysis on a flow cytometer (BD LSRFortessa).

Intracellular platinum accumulation. For whole platinum accumulation, NCI-N87 (4×10^5 cells/sample) was drug treated for 4 h at 37 °C. After 4 h, the drug-containing media was aspirated and the cells were washed with PBS ($2 \times 500 \mu\text{L}$). The cells was then centrifuged down and the cell pellet was digested by heating with 65% ultrapure HNO_3 (300 μL) at 90 °C overnight. The acid was boiled off and the cellular residue was re-dissolved by sonicating in 2% HNO_3 (500 μL) for analysis by ICP-MS. Nuclear platinum accumulation was carried out as reported previously [32]. All values were reported as pmol per 10^6 cells.

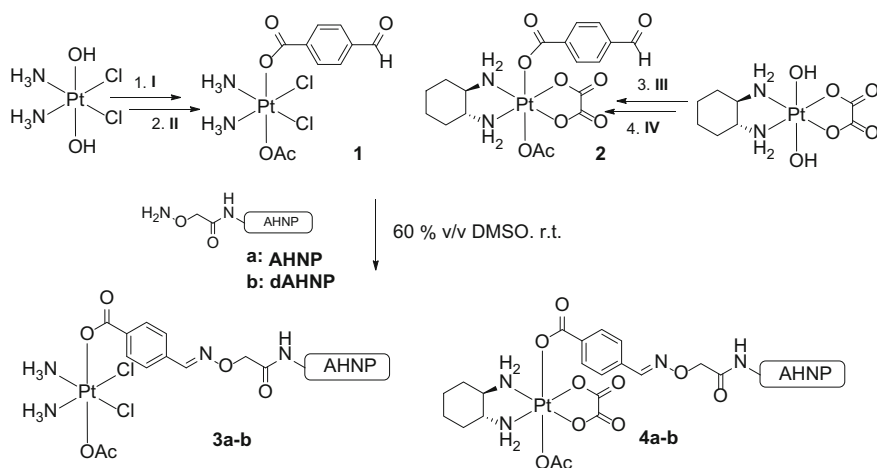
Measurement of intracellular ROS. 2×10^5 cells was seeded in clear-bottom black 96 well plate and allowed to adhere overnight. After 24 h, the cells was washed with HBSS (1 \times 100 μL) and prestained with 2',7'-dichlorodihydro-fluorescein diacetate (H_2DCFDA) (15 μM in 100 μL HBSS) for 45 min at 37 °C. After washing with HBSS (1 \times 100 μL), the cells were drug treated for the indicated duration. Drug were diluted in supplemented HBSS (containing 10% FBS). At the indicated time and without washing, the fluorescence signal on the plate bottom (Ex: 485 nm/Em: 535 nm) was read using a microplate reader (Biotek), taking into account background fluorescence.

Cell cycle analysis. 2×10^5 cells were seeded per well in 12-well plates in complete media (1 mL) and allowed to adhere overnight. The test compounds were then diluted in complete medium and added to the cells at the concentrations indicated. At various time intervals, the culture media (containing detached cells) was removed and kept to deactivate trypsin downstream. The adherent cells was washed with trypsin-EDTA (500 μL) and fresh trypsin-EDTA (500 μL) was added to harvest the cells and the detached cells was then pooled together with the old culture media. The combined cell fraction was washed with chilled PBS (1 \times 500 μL), followed by dropwise addition of chilled 70% v/v EtOH/water (500 μL) with constant mixing. After 1 h at 4 °C, the fixed cells were washed with PBS (1 \times 500 μL) and finally resuspended in RNase (MpBio, 500 μL of a 100 $\mu\text{g}/\text{mL}$ in PBS) and PI (50 $\mu\text{g}/\text{mL}$ in PBS) for 1 h at r.t before analysis in a flow cytometer (BD LSRFortessa).

Visualisation of cellular morphology via fluorescence microscopy. 1×10^5 cells were seeded per well in 24-well plates in complete media (500 μL) on poly-L-lysine coated coverslips and allowed to adhere overnight. The cells were drug treated in complete media at the indicated concentrations for 24 h. After 24 h, the drug-containing media was replaced with fresh com. RPMI (1 mL). At various time intervals, the 90% of the old media was aspirated, leaving just sufficient to cover the cells and fixed with an equiv.-volume of 3:1 v/v MeOH/AcOH for 5 min. The fixative was carefully aspirated and fresh fixative (300 μL per well) was added for another 10 min before washing with PBS (1 \times 500 μL). Finally, the cells was stained with Hoescht 3342 (2 $\mu\text{g}/\text{mL}$ in PBS) for about 15 min at r.t and the coverslips was mounted onto slides for analysis on a confocal microscopy (FV1000, Olympus).

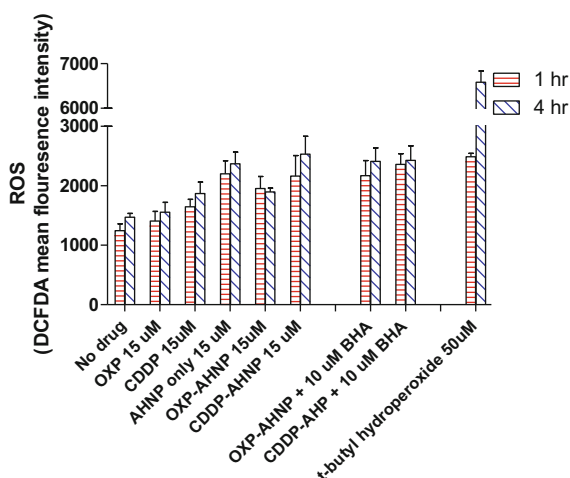
Supplementary Information

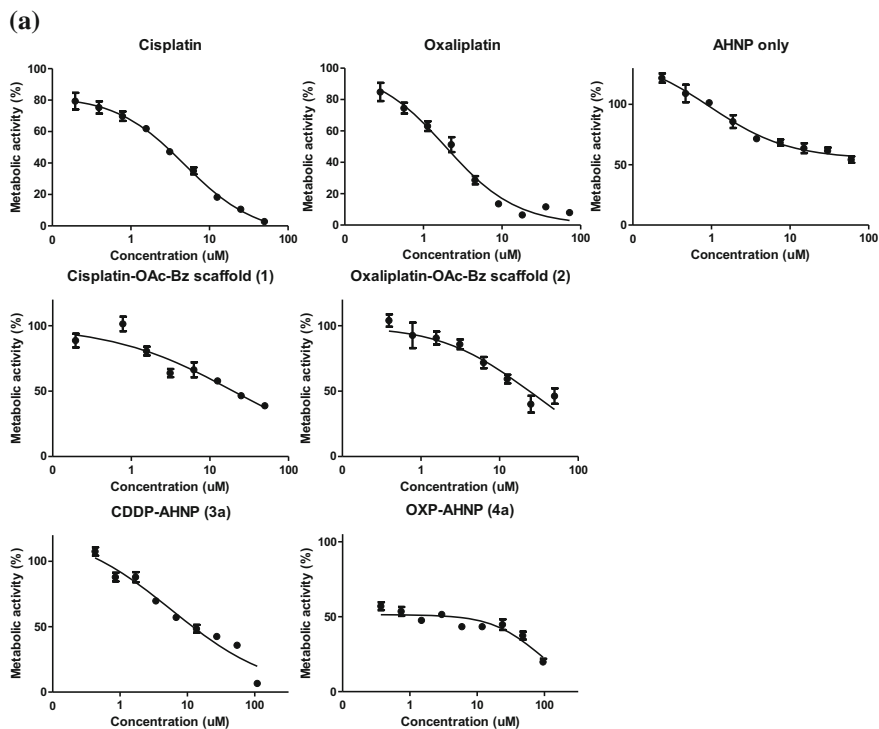
Supplementary Scheme



Scheme S4.1 Synthesis of platinum(IV)-AHNP conjugates. Reaction conditions: (I) succinimidyl 4-formylbenzoate, in DMSO, r.t. (II) acetic anhydride in DMF, r.t. (III) H₂O₂ in acetic acid, r.t. (IV) 4-formyl-benzoyl chloride in acetone, pyridine, reflux. AHNP: H₂N-YC**D*GFYAC*YMDVGGKK(aminooxy)-CONH₂; dAHNP: fC**D*GFYAC*yMDVGGKK(aminooxy)-CONH₂ (*—Linked disulfide bridge)

Fig. S4.1 Measurements of cellular ROS on NCI-N87 after drug-treatment using 2',7'-dichlorofluorescein diacetate (DCFDA) which measures general oxidative stress. In some cases, cells were co-treated with butylated hydroxyanisole (BHA), an antioxidant. t-butyl hydroperoxide-treated cells was included as a positive control





(b)

Compound	AHP only	CDDP	1	3a	3b
IC₅₀ (µM)	> 60	2.9 ± 0.3	23.1 ± 2.9	15.5 ± 2.4	> 100
Compound	OXP	2	4a	4b	
IC₅₀ (µM)	2.8 ± 0.6	21.8 ± 2.6	4.1 - 14.1	> 100	

Fig. S4.2 Intermediate-term potency of the drug conjugates as determined by MTT measurements of cellular metabolic activity after 72 h drug treatment against the NCI-N87 gastric cancer cell line. **a** Representative dosage-response curves. **b** Table of absolute IC₅₀ (µM). Platinum concentrations were calibrated by ICP-OES

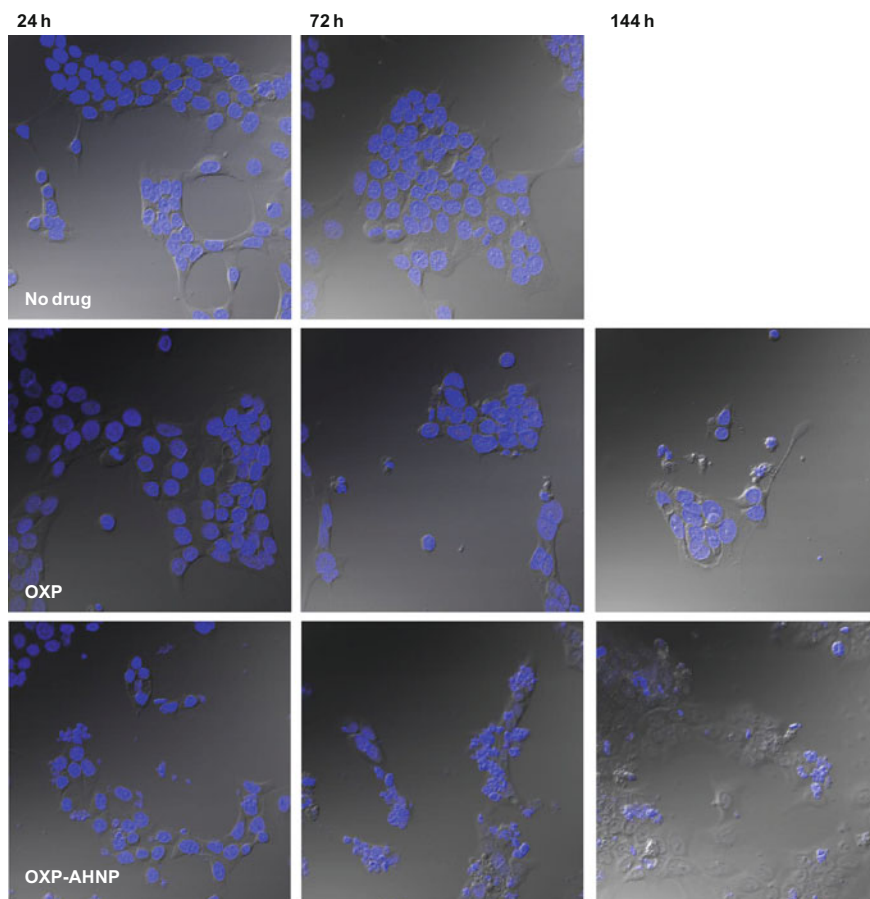


Fig. S4.3 Visual fluorescence microscopy monitoring of drug-treated NCI-N87 over time. NCI-N87 was drug-treated (15 μ M for 24 h and then allowed to recover in fresh media). Nuclear morphology were visualized by Hoechst 3342 staining. There were substantial floating dead cells in drug-treated cells in the initial 24 h drug-treatment period (not shown here). When allowed to recover after 24 h drug-treatment, **4a**-treated cells undergoes a transient phase of cell-proliferation, as evidenced by a decrease in empty space at 144 h. The cells exhibited increasingly abnormal nuclear morphology over time, implying that continued long-term proliferation was unviable

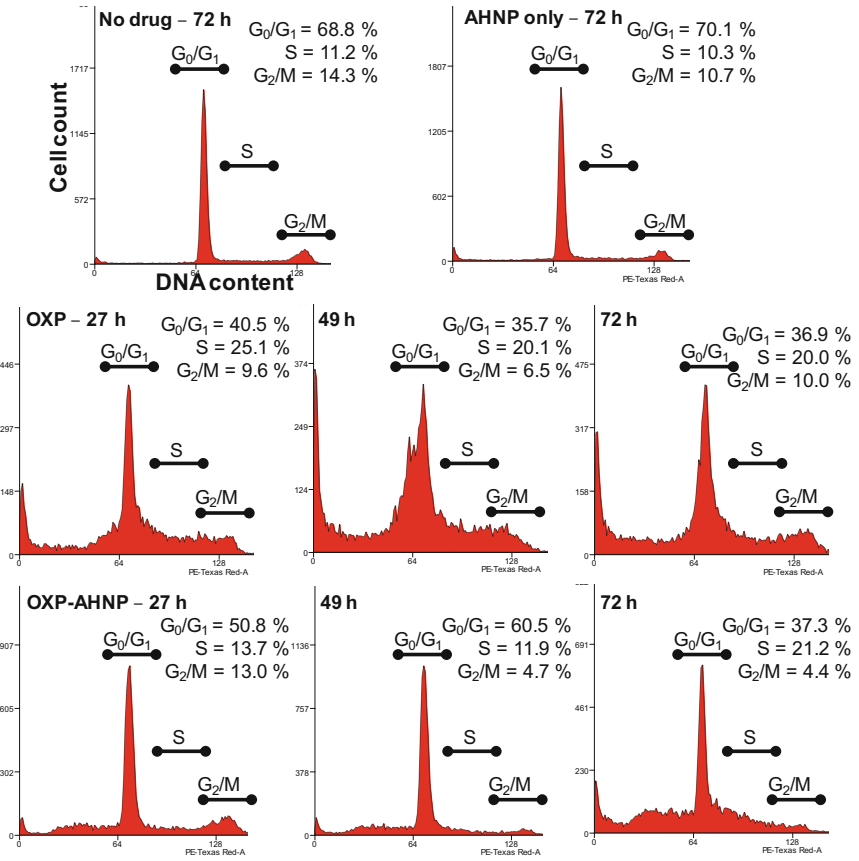
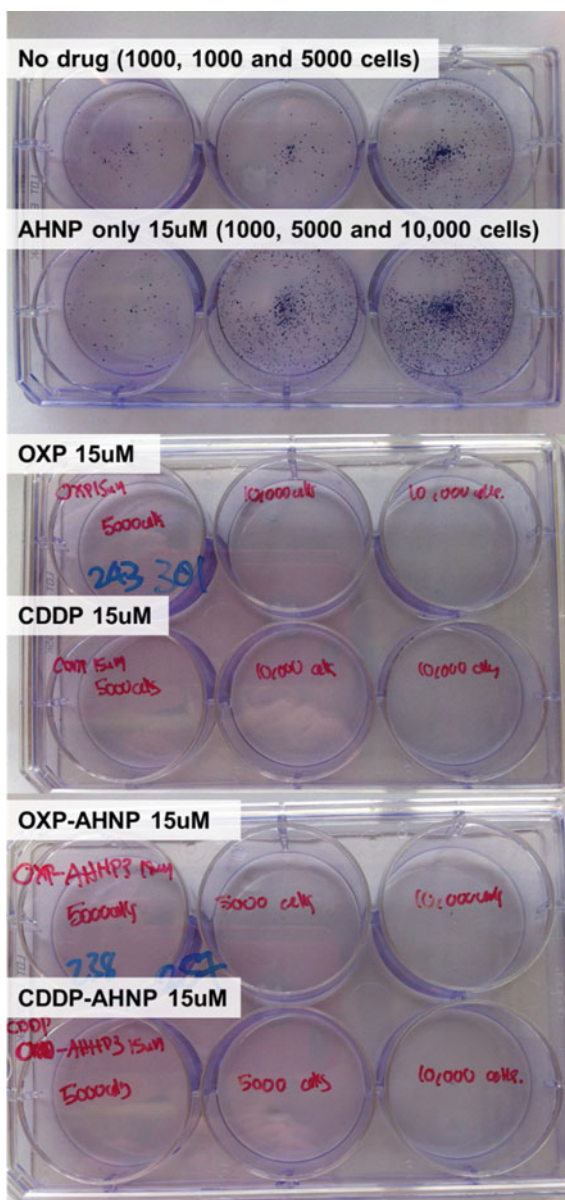


Fig. S4.4 Cell-cycle distribution of drug-treated NCI-N87 cells over time. Drug-treated cells were permeabilized with 70% v/v ethanol and stained with propidium iodide to determine DNA content

Fig. S4.5 Representative photos of clonogenic assay on NCI-N87 to assess the long-term proliferation ability of drug-treated cells. Single cells were seeded in a 6-well plate, drug-treated for 24 h and allowed to recover in fresh complete media for a further 15 d before counting the number of colonies formed. The number of single cells seeded per well is written on the plates



Supplementary Table

Table S4.1 Tabulated data of apoptosis as evaluated by AnnexinV/PI staining of drug-treated NCI-N87 or BT-474 cells after 24 h. Each cell depicts mean % of cells at either early apoptosis, late apoptosis or necrosis

	% of cell in various stage of cell death (mean values)					
	NCI-N87			BT-474		
	ANXV +/PI-	ANXV +/PI+	ANXV -/PI+	ANXV +/PI-	ANXV +/PI+	ANXV -/PI+
No drug	1.8	6.2	0.8	0.5	4.0	3.0
CDDP3 (μM)	1.9	6.3	1.3	–	–	–
CDDP15 (μM)	6.6	7.4	1.9	0.3	4.5	3.0
OXP3 (μM)	2.3	7.1	1.0	–	–	–
OXP 15 (μM)	7.3	11.5	0.6	0.3	4.0	2.6
AHNP only 3 (μM)	1.6	6.3	1.1	–	–	–
AHNP only 15 (μM)	1.5	7.2	6.9	0.5	4.9	7.3
3a 3 (μM)	1.4	6.4	7.3	–	–	–
3a15 (μM)	1.8	6.0	23.8	0.4	5.8	16.3
4a 3 (μM)	1.7	8.4	5.7	–	–	–
4a 15 (μM)	1.8	6.4	26.2	0.4	5.0	37.4

Characterisation of Compounds

See Figs. [S4.6a, b, c](#), [4.7a, b](#), [S4.8a, b](#), [S4.9a, b](#), [S4.10a, b](#).

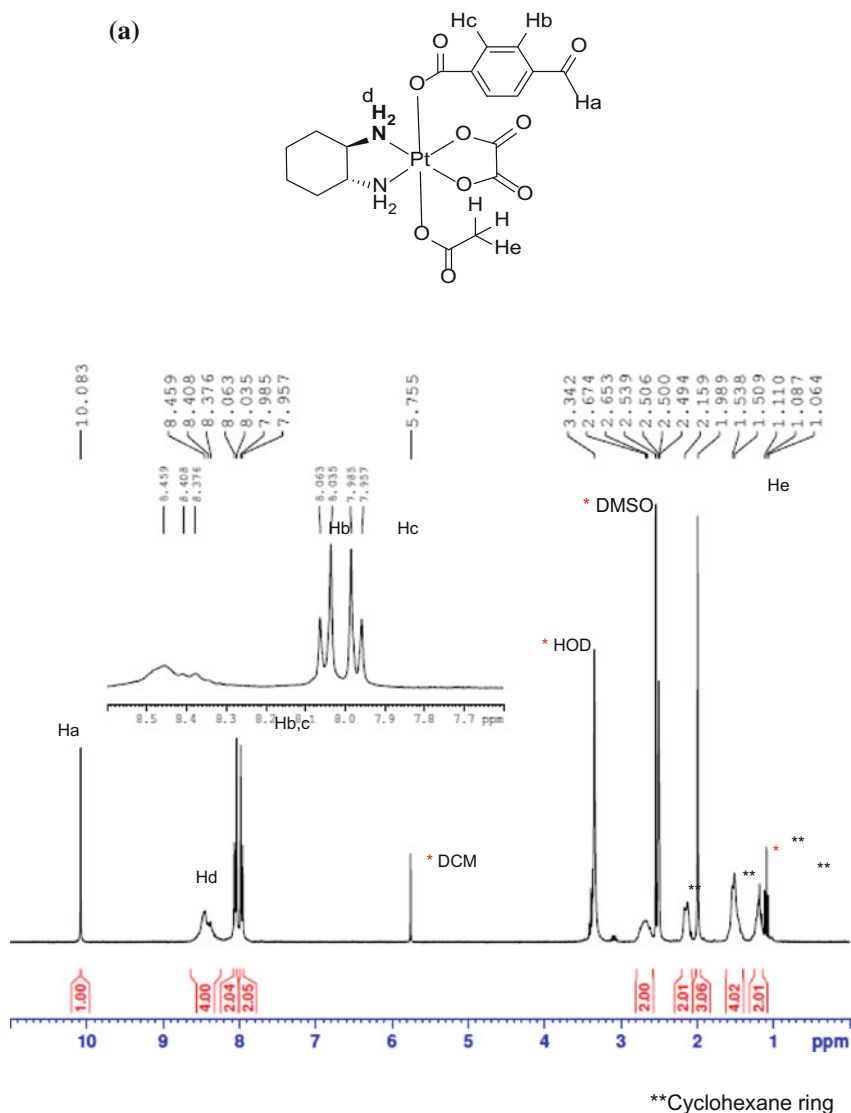


Fig. S4.6 **a** ^1H NMR of oxaliplatin(IV)-benzaldehyde scaffold **2** in DMSO-d_6 . **b** ESI-MS ($-$) characterisation of **2**: Fullscan, zoom scan (isotopic pattern) and MS/MS (top to bottom). m/z : Calculated 604.5 $[\text{M-H}]^-$, found 604.0. **c** RP-HPLC purity assessment of **2** dissolved in MeCN-H₂O using Shimpack VP-ODS column (150×5.60 mm i.d.). Elution condition: 8–30% solvent B for 10 min, 30% solvent B for 8 min and finally 30–80% solvent B for 7 min

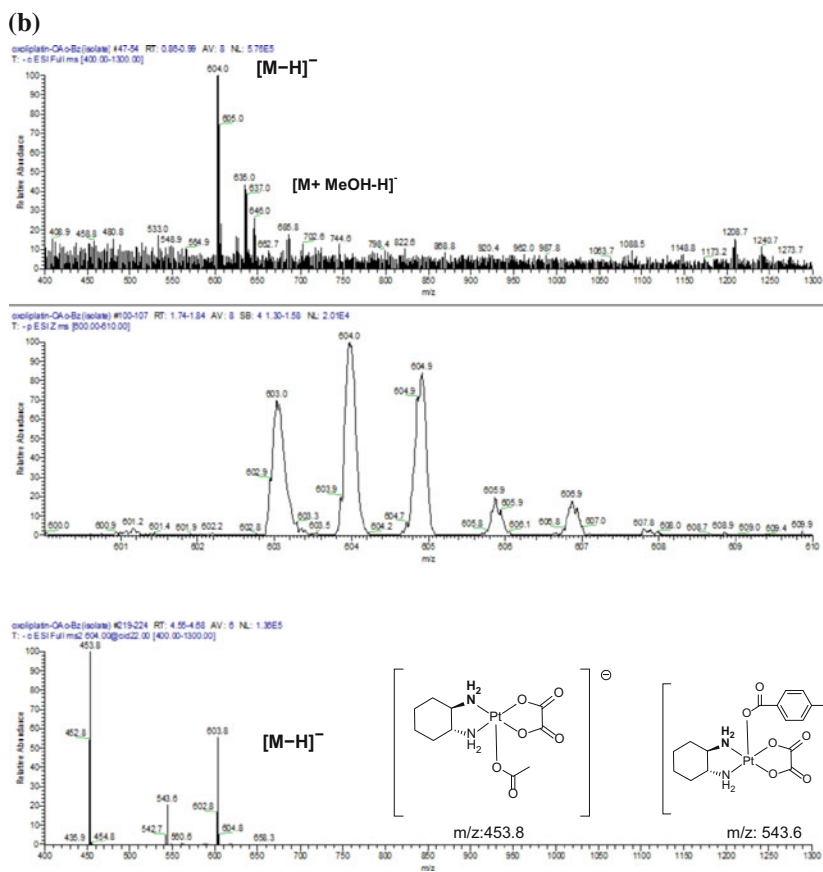


Fig. S4.6 (continued)

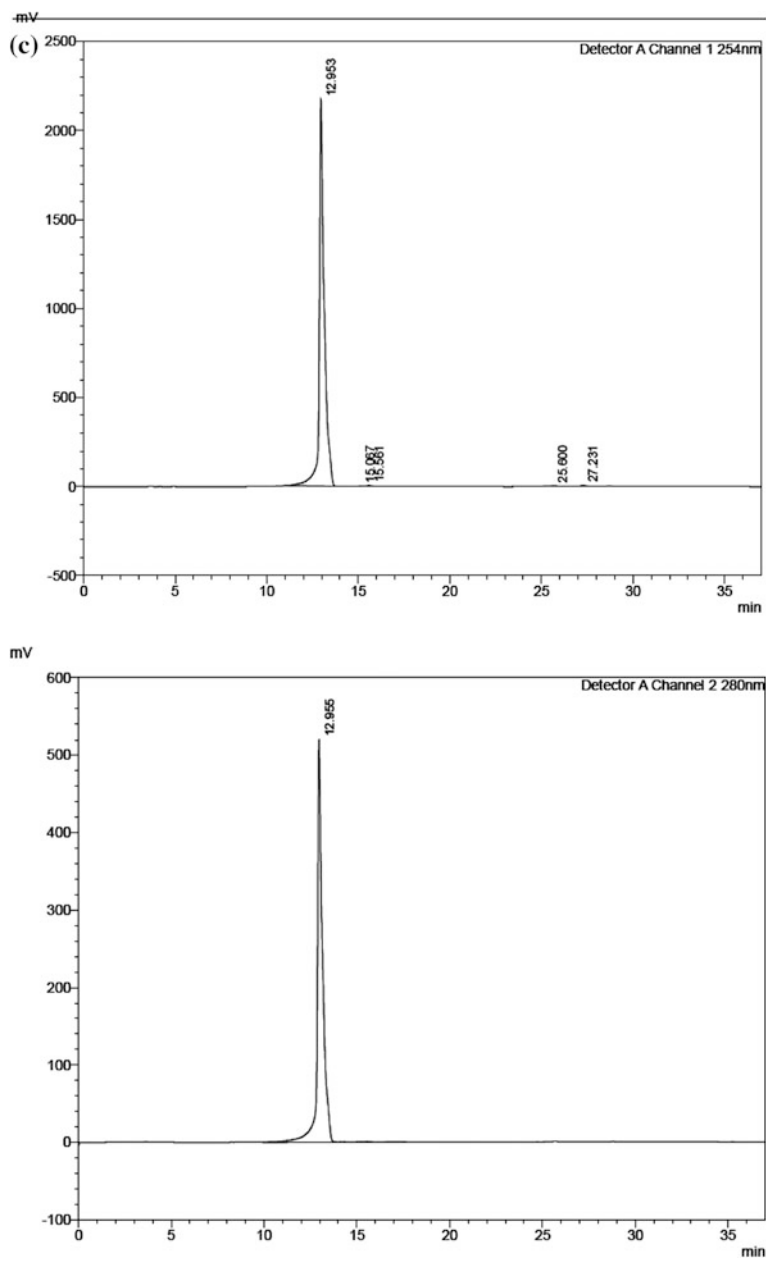


Fig. S4.6 (continued)

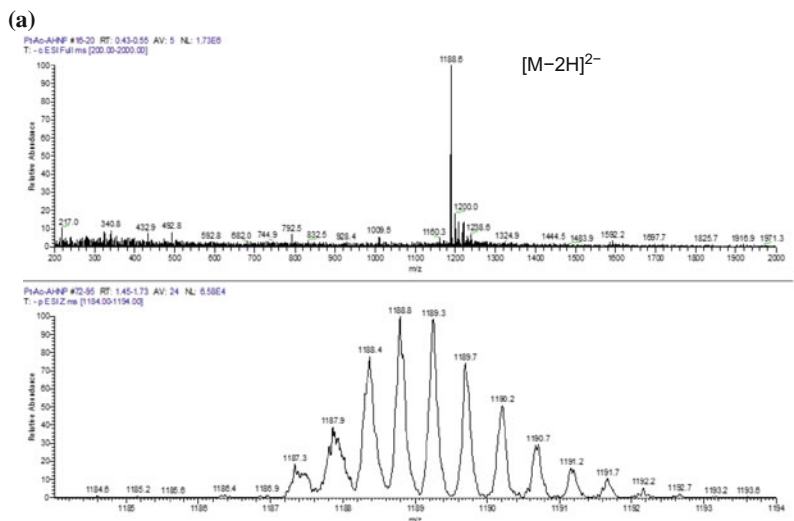


Fig. S4.7 a ESI-MS ($-$) characterisation of cisplatin(IV)-AHNP conjugate **3a**: Fullscan and zoom scan (isotopic pattern) m/z : calculated 1189.1 $[M-2H]^{2-}$, found 1188.6. **b** HPLC chromatogram of cisplatin(IV)-AHNP conjugate **3a**. The purity of the compound was assessed using Shimpack VP-ODS column (150×5.60 mm i.d.). Elution Condition: 8–30% solvent B for 10 min, 30% solvent B for 8 min and finally 30–80% solvent B for 7 min

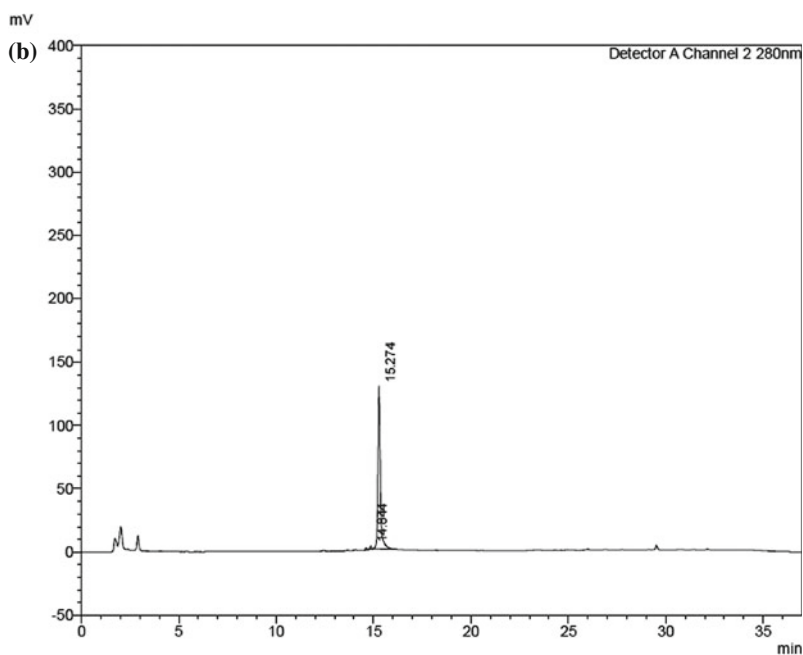


Fig. S4.7 (continued)

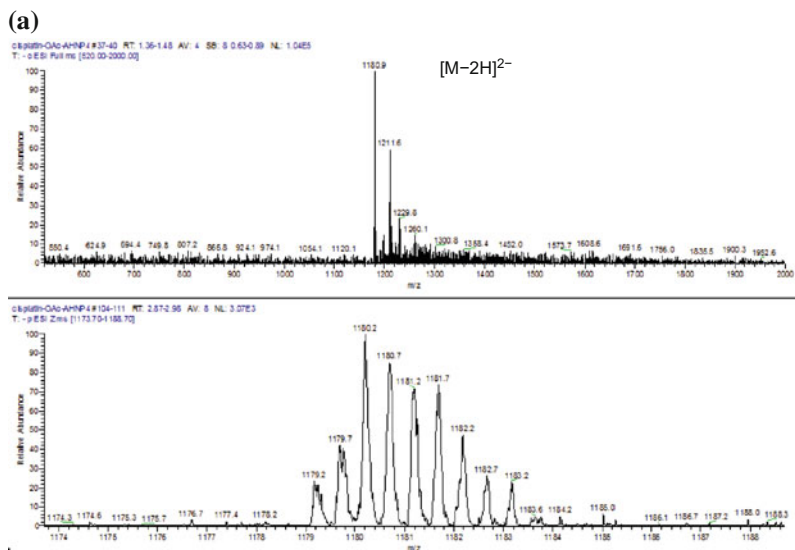


Fig. S4.8 a ESI-MS (-) characterisation of cisplatin(IV)-dAHP conjugate **3b**: Fullscan and zoom scan (isotopic pattern) m/z: calculated 1181.1 $[M-2H]^{2-}$, found 1180.9. **b** HPLC chromatogram of cisplatin(IV)-dAHP conjugate **3b**. The purity of the compound was assessed using Shimpack VP-ODS column (150 × 5.60 mm i.d). Elution Condition: 8–30% solvent B for 10 min, 30% solvent B for 8 min and finally 30–80% solvent B for 7 min

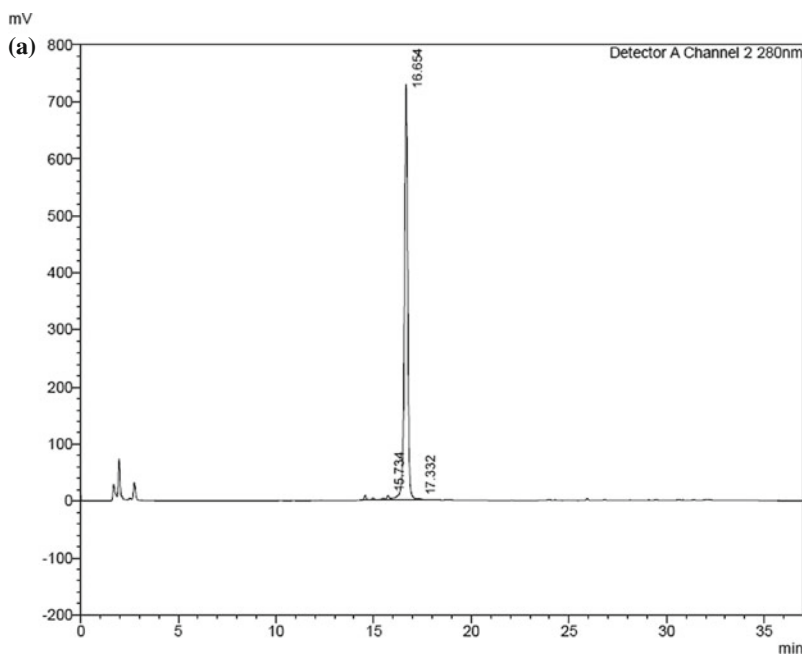


Fig. S4.8 (continued)

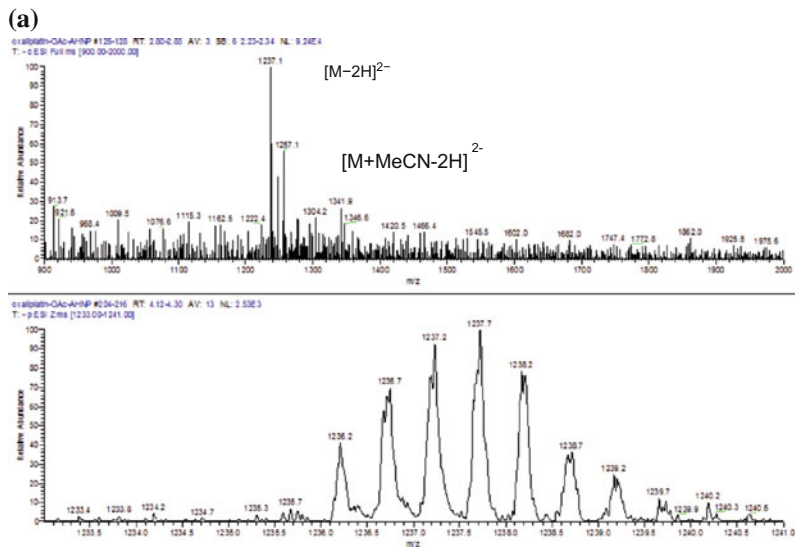


Fig. S4.9 a ESI-MS ($-$) characterisation of oxaliplatin(IV)-AHNP conjugate **4a**: Fullscan and zoom scan (isotopic pattern) m/z : calculated 1237.8 $[M-2H]^{2-}$, found 1237.1. **b** HPLC chromatogram of oxaliplatin(IV)-AHNP conjugate **4a**. The purity of the compound was assessed using Shimpack VP-ODS column (150×5.60 mm i.d). Elution Condition: 8–30% solvent B for 10 min, 30% solvent B for 8 min and finally 30–80% solvent B for 7 min

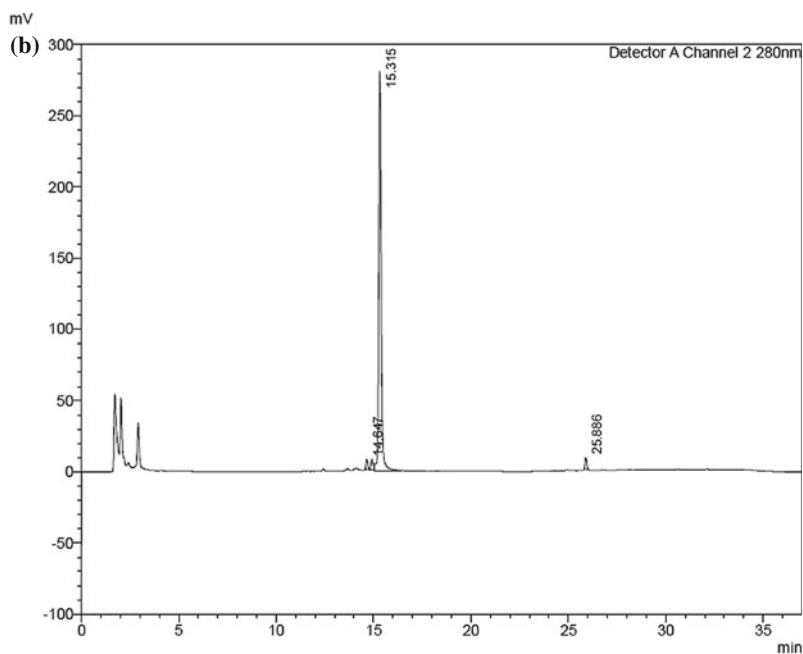


Fig. S4.9 (continued)

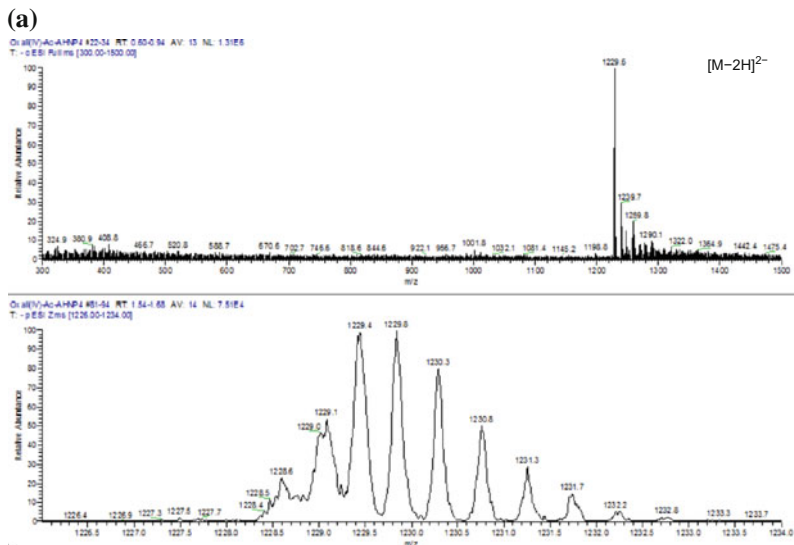


Fig. S4.10 a ESI-MS (-) characterisation of oxaliplatin(IV)-dAHP2 conjugate **4b**: Fullscan and zoom scan (isotopic pattern) m/z : calculated 1229.8 $[M-2H]^{2-}$, found 1229.6. **b** HPLC chromatogram of oxaliplatin(IV)-dAHP2 conjugate **4b**. The purity of the compound was assessed using Shimpack VP-ODS column (150 × 5.60 mm i.d). Elution Condition: 8–30% solvent B for 10 min, 30% solvent B for 8 min and finally 30–80% solvent B for 7 min

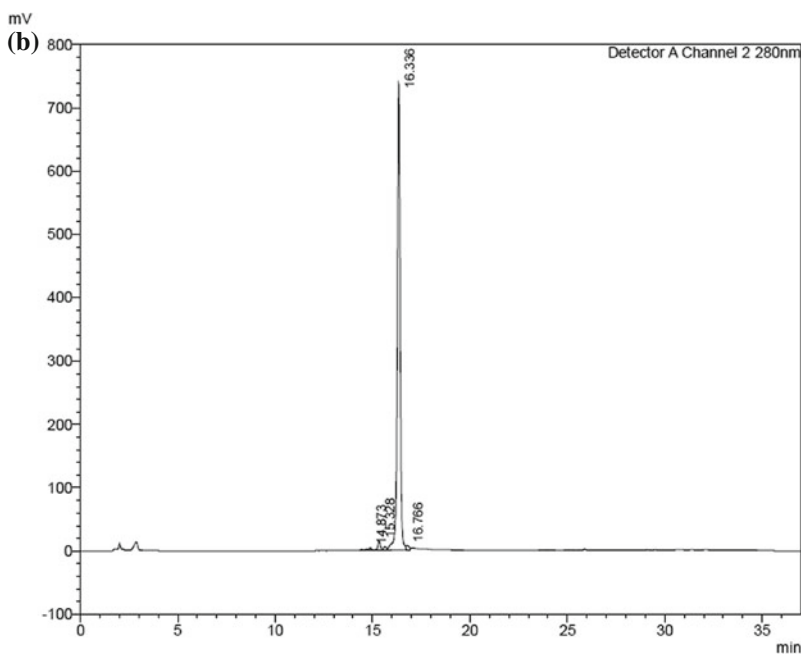


Fig. S4.10 (continued)

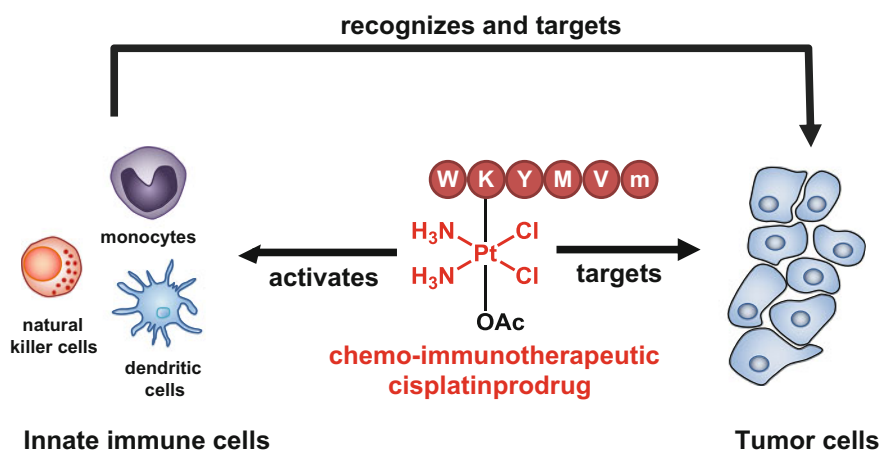
References

1. Teicher, B.A.: Molecular cancer therapeutics: will the promise be fulfilled? *Mol. Cancer Ther.*, 7–40 (2005)
2. Shah, M.A., Schwartz, G.K.: Cell cycle-mediated drug resistance: an emerging concept in cancer therapy. *Clin. Cancer Res.* **7**, 2168–2181 (2001)
3. Siddik, Z.H.: Cisplatin: mode of cytotoxic action and molecular basis of resistance. *Oncogene* **22**, 7265–7279 (2003)
4. Gerlinger, M., Rowan, A.J., Horswell, S., Larkin, J., Endesfelder, D., Gronroos, E., Martinez, P., Matthews, N., Stewart, A., Tarpey, P., Varela, I., Phillimore, B., Begum, S., McDonald, N. Q., Butler, A., Jones, D., Raine, K., Latimer, C., Santos, C.R., Nohadani, M., Eklund, A.C., Spencer-Dene, B., Clark, G., Pickering, L., Stamp, G., Gore, M., Szallasi, Z., Downward, J., Futreal, P.A., Swanton, C.: Intratumor heterogeneity and branched evolution revealed by multiregion sequencing. *N. Engl. J. Med.* **366**, 883–892 (2012)
5. Galluzzi, L., Vitale, I., Vacchelli, E., Kroemer, G.: Cell death signaling and anticancer therapy. *Front. Oncol.* **1** (2011)
6. Dinnen, R.D., Drew, L., Petrylak, D.P., Mao, Y., Cassai, N., Szmulewicz, J., Brandt-Rauf, P., Fine, R.L.: Activation of targeted Necrosis by a p53 Peptide: a novel death pathway that circumvents apoptotic resistance. *J. Biol. Chem.* **282**, 26675–26686 (2007)
7. Hu, X., Xuan, Y.: Bypassing cancer drug resistance by activating multiple death pathways—a proposal from the study of circumventing cancer drug resistance by induction of necroptosis. *Cancer Lett.* **259**, 127–137 (2008)
8. Rubin, I., Yarden, Y.: The basic biology of HER2. *Ann. Oncol.* **12**, S3–S8 (2001)
9. Jorgensen, J.T., Hersom, M.: HER2 as a prognostic marker in gastric cancer—a systematic analysis of data from the literature. *J. Cancer* **3**, 137–144 (2012)
10. Claret, F.X., Vu, T.T.: Trastuzumab: updated mechanisms of action and resistance in breast cancer. *Front. Oncol.* **2** (2012)
11. Park, B.-W., Zhang, H.-T., Wu, C., Berezov, A., Zhang, X., Dua, R., Wang, Q., Kao, G., O'Rourke, D.M., Greene, M.I., Murali, R.: Rationally designed anti-HER2/neu peptide mimetic disables P185HER2/neu tyrosine kinases in vitro and in vivo. *Nat. Biotech.* **18**, 194–198 (2000)
12. Berezov, A., Zhang, H.-T., Greene, M.I., Murali, R.: Disabling erbB receptors with rationally designed exocyclic mimetics of antibodies: structure–function analysis†. *J. Med. Chem.* **44**, 2565–2574 (2001)
13. Chin, C.F., Wong, D.Y.Q., Jothibasu, R., Ang, W.H.: Anticancer platinum (IV) prodrugs with novel modes of activity. *Curr. Top. Med. Chem.* **11**, 2602–2612 (2011)
14. Zhang, J.Z., Wexselblatt, E., Hambley, T.W., Gibson, D.: Pt (IV) analogs of oxaliplatin that do not follow the expected correlation between electrochemical reduction potential and rate of reduction by ascorbate. *Chem. Commun.* **48**, 847–849 (2012)
15. Wong, D.Y.Q., Lau, J.Y., Ang, W.H.: Harnessing chemoselective imine ligation for tethering bioactive molecules to platinum(IV) prodrugs. *Dalton Trans.* **41**, 6104–6111 (2012)
16. Wong, D.Y.Q., Yeo, C.H.F., Ang, W.H.: Immuno-chemotherapeutic platinum(IV) prodrugs of cisplatin as multimodal anticancer agents. *Angew. Chem. Int. Ed.* **53**, 6752–6756 (2014)
17. Zhang, J.Z., Bonnitcha, P., Wexselblatt, E., Klein, A.V., Najajreh, Y., Gibson, D., Hambley, T.W.: Facile preparation of mono-, di- and mixed-carboxylato platinum(IV) complexes for versatile anticancer prodrug design. *Chem. Eur. J.* **19**, 1672–1676 (2013)
18. Wilken, J., Webster, K., Mahle, N.: Trastuzumab sensitizes ovarian cancer cells to EGFR-targeted therapeutics. *J. Ovarian Res.* **3**, 7 (2010)
19. Boulikas, T., Vougiouka, M.: Cisplatin and platinum drugs at the molecular level (review). *Oncol. Rep.* **10**, 1663–1682 (2003)
20. Martin, S.J., Reutelingsperger, C.P., McGahon, A.J., Rader, J.A., van Schie, R.C., LaFace, D. M., Green, D.R.: Early redistribution of plasma membrane phosphatidylserine is a general

- feature of apoptosis regardless of the initiating stimulus: inhibition by overexpression of Bcl-2 and Abl. *J. Exp. Med.* **182**, 1545–1556 (1995)
21. Denecker, G., Doms, H., Van Loo, G., Vercammen, D., Grooten, J., Fiers, W., Declercq, W., Vandenabeele, P.: Phosphatidyl serine exposure during apoptosis precedes release of cytochrome c and decrease in mitochondrial transmembrane potential. *FEBS Lett.* **465**, 47–52 (2000)
 22. Ziegler, U., Groscurth, P.: Morphological features of cell death. *News Physiol. Sci.* **19**, 124–128 (2004)
 23. Smardová, J., Pavlová, S., Svitáková, M., Grochová, D., Ravčuková, B.: Analysis of p53 status in human cell lines using a functional assay in yeast: Detection of new non-sense p53 mutation in codon 124. *Oncol. Rep.* **14**, 901–907 (2005)
 24. Lewis Phillips, G.D., Li, G., Dugger, D.L., Crocker, L.M., Parsons, K.L., Mai, E., Blättler, W. A., Lambert, J.M., Chari, R.V.J., Lutz, R.J., Wong, W.L.T., Jacobson, F.S., Koeppen, H., Schwall, R.H., Kenkare-Mitra, S.R., Spencer, S.D., Sliwkowski, M.X.: Targeting HER2-positive breast cancer with trastuzumab-DM1, an antibody-cytotoxic drug conjugate. *Cancer Res.* **68**, 9280–9290 (2008)
 25. Hanahan, D., Weinberg, R.: Hallmarks of cancer: the next generation. *Cell* **144**, 646–674 (2011)
 26. Maskey, D., Yousefi, S., Schmid, I., Zlobec, I., Perren, A., Friis, R., Simon, H.-U.: ATG5 is induced by DNA-damaging agents and promotes mitotic catastrophe independent of autophagy. *Nat. Commun.* **4** (2013)
 27. Fuentès, M.A., Alonso, C., Perez, J.M.: Biochemical modulation of cisplatin mechanisms of action: enhancement of antitumor activity and circumvention of drug resistance. *Chem. Rev.* **103**, 645–662 (2003)
 28. Wang, D., Lippard, S.J.: Cellular processing of platinum anticancer drugs. *Nat. Rev. Drug Discov.* **4**, 307–320 (2005)
 29. Burgos, A., Ellames, G.J.: Synthesis of [3H2]-(R, R)-1,2-diaminocyclohexaneoxalatoplatinum (II), [3H2]-Oxaliplatin. *J. Labelled Compd. Radiopharm.* **41**, 443–449 (1998)
 30. Fulmer, G.R., Miller, A.J.M., Sherden, N.H., Gottlieb, H.E., Nudelman, A., Stoltz, B.M., Bercaw, J.E., Goldberg, K.I.: NMR chemical shifts of trace impurities: common laboratory solvents, organics, and gases in deuterated solvents relevant to the organometallic chemist. *Organometallics* **29**, 2176–2179 (2010)
 31. Gill, S.C., von Hippel, P.H.: Calculation of protein extinction coefficients from amino acid sequence data. *Anal. Biochem.* **182**, 319–326 (1989)
 32. Park, G.Y., Wilson, J.J., Song, Y., Lippard, S.J.: Phenanthriplatin, a monofunctional DNA-binding platinum anticancer drug candidate with unusual potency and cellular activity profile. *Proc. Natl. Acad. Sci.* **109**, 11987–11992 (2012)

Chapter 5

Immuno-Chemotherapeutic Platinum(IV) Prodrugs of Cisplatin as Multimodal Anticancer Agents



5.1 Introduction

For the longest time, the contribution of the immune system in chemotherapy has been disregarded as cytotoxic drugs are generally believed to be immunosuppressive [1–5]. Consequently, evaluation of new chemotherapeutic agents involved screening of drug candidates upon xenografted tumors in immunodeficient mice which neglects any possible immune contribution. However, a substantial body of recent work has challenged this assumption. There is now a growing consensus that a number of chemotherapeutics do stimulate the innate and/or the adaptive immune

This article is reproduced with permission from Wiley

system and that at least part of the observed clinical therapeutic efficacy of these agents actually hinges on its off-target immunostimulating mechanisms [1–5]. Despite this, there has been surprisingly little development in the rational design of chemotherapeutic agents with the aim of combining both direct cytotoxicity and immunostimulation. Indeed, a multi-pronged immune-chemotherapeutic approach would not only shrink tumours but more importantly, reactivate dormant immune response against malignancies, therefore conveying long-term immunity and preventing cancer relapse.

Platinum(II) drugs such as cisplatin, carboplatin and oxaliplatin are some of the most effective and widely adopted anti-cancer agents in clinical use today [6–8]. They form the first line of treatment for many malignancies including testicular, ovarian, bladder and non-small cell lung cancer [9, 10]. Although formation of covalent platinum-DNA adducts is generally accepted as the principal mode of action [11], classical platinum agents like cisplatin have also been known to exert off-target effects on the immune system and are potent immunomodulators of both the innate and adaptive immune system [12]. Platinum agents can indirectly promote immune-mediated killing of cancer cells through its action on cancer cells by (1) triggering an immunogenic mode of tumor cell death via exposure of specific “eat-me” signals [13], (2) increasing tumour-cell susceptibility for T-cell killing [14, 15], and (3) by down-regulating immunosuppressive PD-L2 in a STAT6-dependent manner on tumour cells leading to enhanced recognition by T-cells [16]. In addition, platinum agents can also directly engage immune effector functions by (1) stimulating both monocyte and natural killer (NK) cell mediated cytotoxicity [17–21], (2) promoting antigen-presenting capacity of dendritic cells [22, 23], and (3) by reversing immunosuppressive tumour microenvironments by downregulating PD-L2 on dendritic cells [16] and by selective depletion of inhibitory myeloid-derived suppressor cells (MDSC) and T_{reg} cells [24]. As far back as 1970s, the immunostimulating potential of cisplatin had already been recognised by Rosenberg, who discovered the antineoplastic properties of cisplatin [25]. Since then, there has been more compelling empirical evidence corroborating the immunomodulating capacity of platinum-based therapy with favourable chemotherapy outcomes [13, 24, 26]. Nonetheless, the immune-mediating activity of platinum-based agents has been neglected in the development of new therapeutics which has focused primarily on the principle of targeting DNA within tumour cells.

In this work, we designed a novel immune-chemotherapeutic agent by tethering a dual-purpose peptide sequence, which behaves as both a FPR1/2-targeting moiety and an immune adjuvant, to a platinum(IV) prodrug scaffold using a chemoselective imine ligation strategy (Fig. 5.1) [27]. Platinum(IV) complexes are native prodrugs which are themselves pharmacologically inactive and must undergo reductive elimination by endogenous reductants to release cisplatin with concomitant dissociation of the axial ligands [6–8]. Formyl peptide receptors (FPRs), a family of GPCRs which includes FPR1 and FPR2 (formally designated as FPR and FPR1 respectively), are selectively overexpressed in certain tumors such as breast cancers [28], ovarian cancers [29] and glioblastomas [30, 31] and has been implicated with a more invasive and malignant phenotype owing to its role in

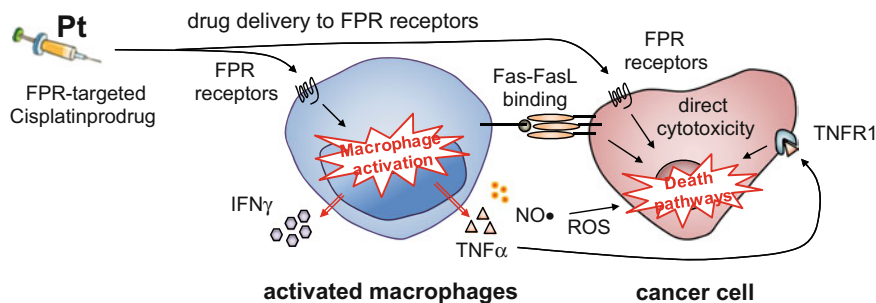


Fig. 5.1 Putative multimodal immuno-chemotherapeutic action

mediating metastasis [30, 31]. At the same time, FPR1/2-binding ligands like WKYMVm and fMLF are also potent immunostimulators, activating innate effectors such as monocytes, dendritic cells and natural killer (NK) cells, leading to increased cytolytic activity, phagocytosis, chemotaxis, cytokine production and superoxide generation [32–34]. FPR1/2 ligands can thus act as both a targeting moiety to deliver cisplatin to FPR1/2 overexpressing cancer cells and immune cells [35, 36] via rapid receptor-mediated internalization [37] as well as a potent immune adjuvant to provoke an immune anticancer response [38]. Our work is the first attempt of a rationally-designed platinum-based anticancer agent combining chemotherapy with immunotherapy to achieve therapeutic synergy. Herein, we report a proof-of-concept to demonstrate the feasibility of this approach which may encourage future systematic evaluation of immuno-chemotherapeutic agents.

5.2 Results and Discussion

Design and synthesis of FPR1/2-targeted platinum(IV)-peptide conjugates. In this two-pronged approach, we postulated that a cisplatin prodrug scaffold tethered to a FPR1/2 targeting peptide could simultaneously exert direct cytotoxicity against metastatic cancers overexpressing FPR1/2 receptors as well as to activate both FPR1/2 expressing monocytes and NK cells with the platinum(IV)-peptide adjuvant. From a design standpoint, the platinum(IV) scaffold was essential to preserve the immunomodulating cisplatin pharmacophore while accommodating the additional peptide group. Otherwise, direct conjugation of the peptide to cisplatin at either the ammine or chloride ligand positions would inadvertently alter its core structure. The asymmetrical mono-functionalised platinum(IV) scaffold **1** was synthesized via a new *N*-hydroxysuccinimide(NHS)-ester activated carboxylic acid route which gave the mono-carboxylated product preferentially over the di-carboxylated product. Presumably, the NHS-activated acid was insufficiently reactive to react with the second hydroxido group which is less nucleophilic than the first [39]. This method is similar to a technique using carbodiimide coupling

reagents reported by Zhang et al. [39] but with the added advantage of using an easily isolatable activated NHS-ester instead of in situ formation of the activated acid. Scaffold **2** was synthesized by subsequent acetylation of **1** using acetic anhydride (Fig. 5.2).

The platinum(IV)-peptide conjugate was synthesized via an chemoselective oxime ligation strategy we previously reported [27], which exploited the facile and stable bond formed between an aromatic aldehyde group with an aminoxy-functionalised peptide. Four different peptide agonists of FPR1/2 were conjugated to the platinum(IV) scaffold. Annexin1 2-12 (ANXA1 2-12), Annexin1 2-26 (ANXA1 2-26), WKYMVm and formyl-MLFK (Fig. 5.3). The ANXA1 2-12 and 2-26 sequences were reported to have a moderate binding affinity to both FPR1 and FPR2 (μM range) [40, 41]. WKYMVm has high binding affinity to both FPR1 and FPR2 (nm range) while fMLFK preferentially binds to FPR1 (nm range) over FPR2 (μM range) [34, 41]. FPR1/2 agonists activate phagocytes through a G-protein mediated pathway, leading to increased chemotaxis, phagocytosis and cytokine production [32–34].

Treatment of a slight excess of the platinum(IV) scaffold **1** and **2** with the desired aminoxy-functionalised peptide in DMSO/aq. buffer (pH 5.5 or 7.5) yielded the platinum(IV)-peptide drug conjugates, **3a–d** and **4**, quantitatively which were subsequently isolated by semi-preparative HPLC and characterised by ESI-MS (mass spectral analysis). The products were stable in aqueous solution for over one week as ascertained by HPLC. Characterisation of all compounds are given in Fig S5.2 to 21.

FPR-targeted platinum(IV)-peptide prodrugs are selectively cytotoxic against FPR1/2 overexpressing tumor cells. The effects of the FPR-targeting platinum(IV)-peptide drug conjugates, **3a–d** and **4**, on in vitro proliferation against three FPR1/2 overexpressing tumor cell-lines were assessed via MTT assay which

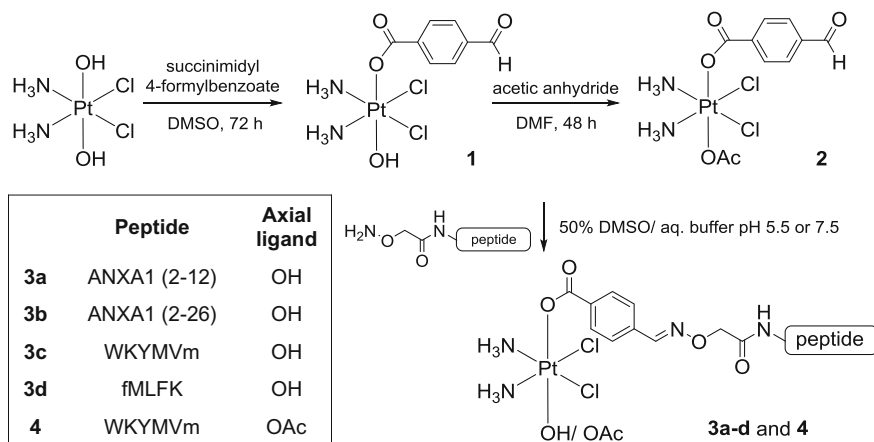


Fig. 5.2 Synthesis of *cis,cis,trans*-diamminedichlorohydroxy(4-formylbenzoate) platinum(IV) (**1**), *cis,cis,trans*-diamminedichloro(acetato)(4-formylbenzoate) platinum(IV) (**2**) and subsequent oxime ligation with various peptides

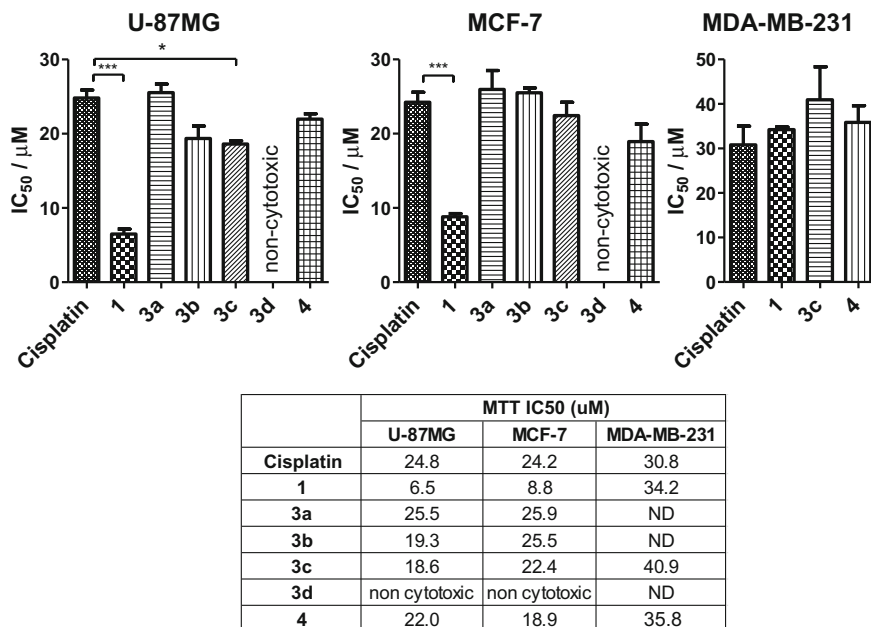


Fig. 5.3 Cytotoxicity IC_{50} of FPR1/2-targeted platinum(IV)-peptide prodrugs against FPR1/2 overexpressing cell-lines. The cell-viability of drug-treated cells was measured after 72 h incubation to plot a dose-response curve and determine the absolute IC_{50} . Drug concentrations were calibrated to platinum measurements via ICP-OES. Means \pm s.e.m. (* $p < 0.05$, *** $p < 0.0001$; Student's t test)

measures cell viability (Fig. 5.3). U-87MG is a highly malignant human glioblastoma cancer whose invasive behaviour has been linked to FPR1 overexpression [30, 31]. The two human breast cancer lines, MCF-7 and MDA-MB-231, overexpress both FPR1 and FPR2 receptors [28]. The cell viability of treated cells were measured after 72 h incubation and the dose-response curve obtained was used to determine the absolute IC_{50} , defined as the drug concentration required to inhibit cell viability by 50%. Cisplatin and **1** were included for comparison. For accuracy, drug concentrations were calibrated to platinum concentrations measured by inductively coupled plasma optical emission spectrometry (ICP-OES).

In general, all drug conjugates, with the exception of **3d** (fMLFK conjugate), exhibited a comparable, if not slightly better, dose-dependent response compared to cisplatin across all three cell-lines tested. The IC_{50} values followed a general trend: **1** \ll **3c** (WKYMVm) $<$ cisplatin \approx **3b** (ANXA1 2-26) \approx **3a** (ANXA1 2-12) \ll **3d** (fMLFK). Against U-87MG and MCF-7, **1** was the most cytotoxic followed by **3c** which was marginally more efficacious than cisplatin, **3b** and **3a**. Complex **3d** was effectively non-cytotoxic ($IC_{50} > 100 \mu\text{M}$). Against MDA-MB-231, **1**, cisplatin and **3c** all bear similar IC_{50} . Since the WKYMVm conjugate **3c** was the most potent of the peptide series, we further evaluated the cytotoxicity of related WKYMVm

conjugate **4**. The IC_{50} values of **3c** and **4** were similar across all 3 cell-lines, indicating that the differences in reduction rate between the parent scaffolds did not affect observed cytotoxicity *in vitro*. The precursor scaffold **1** was the most potent against MCF-7 and U-87MG but comparable to cisplatin on the p53-mutant MDA-MB-231. The cytotoxicity of **1** was mostly likely attributable to non-specific uptake by passive diffusion rather than by active targeting. In contrast to MCF-7 and U-87MG, increased accumulation of platinum was not likely to improve cytotoxicity on the cisplatin-resistant MDA-MB-231 due to its impaired p53 status [42]. We postulate that the unexpectedly poor cytotoxicity of the short fMLFK conjugate **3d** was most likely due to the loss of binding affinity due to close proximity to the platinum scaffold.

The specificity of uptake of the platinum(IV)-WKYMVm conjugate **4** was further investigated by pre-treating U-87MG cells with increasing concentrations of free competitive WKYMVm peptide in order to pre-saturate the FPR1/2 receptors. Thereafter, the cells were exposed to **4** for 4 h, before being harvested for platinum uptake studies using ICP-MS. Pre-treatment with 1-, 2- and 5-fold excess of the free WKYMVm peptide led to a corresponding decrease in mean platinum accumulation of **4** in the treated cells to approximately 76, 64 and 35%, respectively (Fig. S5.1). The reduction of platinum uptake by FPR1/2 ligands was attributable to competitive binding and consistent with studies conducted with other FPR1/2 targeted agents [36, 43]. Some non-specific binding may account for the fact that complete inhibition of uptake was not observed regardless of stoichiometric excess of free WKYMVm [36]. The uptake inhibition by free WKYMVm was consistent with a model of selective drug uptake mediated by FPR1/2 receptors.

To date, only a handful of targeted platinum(IV)-peptide drug conjugates have been reported [44–47]. Although these targeted prodrugs demonstrated improved selectivity, their cytotoxicity does not exceed the parental drug, perhaps possibly due to sequestration of active cisplatin away into lysosomal organelles. In general, most platinum(IV) prodrugs which achieved greater potency than its platinum(II) congener do so by virtue of increased drug uptake via passive diffusion due to increased lipophilicity complexes rather than by active targeting [48–50]. The potential of FPR1/2-targeting peptides as vectors for selective drug delivery to immune cells has been already been borne out with several examples in literature such as the delivery of anti-HIV and anti-inflammatory agents to macrophages [51–53]. In particular, internalisation of the peptide drug conjugates was found to be rapid and specific [53]. Here, we show that FPR1/2-targeted drug conjugates can be used for cancer therapy as well. We have demonstrated that **3c** and **4** had comparable, if not slightly better cytotoxicity, compared to cisplatin which suggest active-targeting since platinum (IV) complexes tend to be less potent than their platinum(II) congener. This is reinforced by the observation that **3d** (fMLFK) was effectively non-cytotoxic implying that the targeting sequence plays a crucial role. Finally, drug uptake was FPR1/2-mediated could be inhibited by free competitive agonists in a dose-dependent manner. Complexes **3c** and **4** were selected for further studies due to their favourable cytotoxicity profile. While the *in vitro* cytotoxicity of both complexes

were similar, **4** which has a slower reduction rate, may be a better candidate due to its increased stability against a premature extracellular reducing environment.

Platinum(IV)-WKYMVm drug conjugates activates PBMCs towards a tumoricidal stage. The cell-mediated cytotoxicity of drug-activated peripheral blood mononuclear cells (PBMCs) against various tumour cell-lines was evaluated by adapting a MTT-based assay described by Loosdrecht et al. [54]. Briefly, PBMCs were pre-treated with 10 μ M each of the compounds for 24 h, washed, and co-cultured with pre-seeded tumor cells at a 10:1 ratio for a further 72 h. MTT was used to determine the percentage of residual viable tumor cells post-incubation. Both tumor cells and PBMCs alone were plated as control groups.

The cell-mediated cytotoxicity of PBMCs incubated in suspension for 24 h with drugs were significantly enhanced against MCF-7 and MDA-MB-231 but not against U-87MG (Fig. 5.4). In the absence of drugs, PBMCs incubated in medium

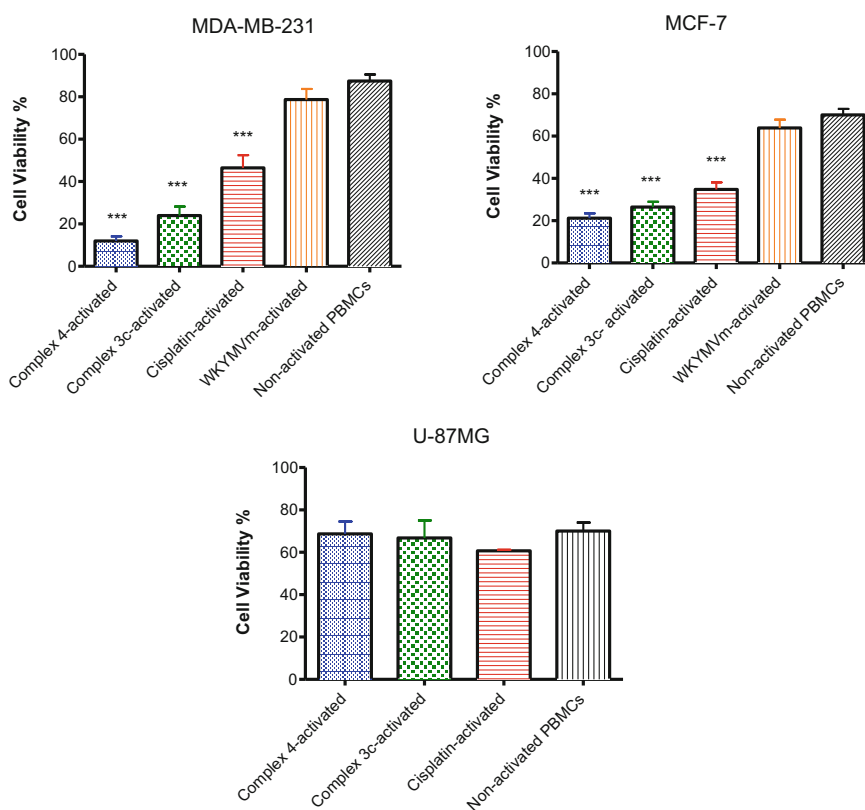


Fig. 5.4 Summary of drug induced cell-mediated cytotoxicity. Average cell viability (%) of U-87MG, MCF-7 and MDA-MB-231 when co-incubated with drug-treated PBMCs after 72 h. Means \pm s.e.m. (***) $p < 0.0001$; Student's t test compared against non-activated PBMCs)

alone exerted a basal cytotoxicity with a mean cell-viability of 70.0, 87.5 and 70.1% against MCF-7, MDA-MB-231 and U-87MG respectively with reference to tumour cells cultured in the absence of PBMCs. Encouragingly, the FPR-targeted platinum(IV)-WKYMVm conjugates, **3c** and **4**, were more potent than the positive control cisplatin (Fig. 5.4). It is unclear why complex **4** was slightly more potent than **3c** but we postulate that this could be due to the slower rate of reduction of **4** in RPMI (containing strongly reducing glutathione), shielding complex **4** from getting reduced prematurely in the extracellular milieu before drug uptake can occur. Free WKYMVm peptide alone did not exert significant cell-mediated cytotoxicity despite reportedly being a potent activator of monocytes and NK cells [32–34]. The levels of the extracellular proinflammatory cytokines, tumour necrosis factor α (TNF- α) and interferon γ (IFN- γ), were also measured to assess monocyte and NK cell activation (Fig. 5.5). Drug treatment of PBMCs with **4**, dramatically enhanced secretion of both TNF- α and IFN- γ compared to non-treated PBMCs ($p < 0.0001$) and the positive control cisplatin ($p < 0.0001$). While cisplatin treatment alone significantly increased both TNF- α and IFN- γ secretion compared to non-treated PBMCs ($p < 0.01$ and $p < 0.0001$ respectively), the levels of the cytokines secreted were much lower as compared to PBMCs treated with the FPR1/2-targeted complex **4**, consistent with the results of the cell-mediated cytotoxicity assay.

Cisplatin is a potent activator of monocytes [17, 55] and NK cells [19, 21, 55] both in vitro and in vivo. Tumoricidal activity due to cisplatin activation is believed to be due to a combination of two closely intertwined mechanisms due to (1) secretion of the proinflammatory messenger cytokines TNF- α , IFN- γ and interleukin1 (IL-1) [56], which dramatically potentiates the cytolytic capacity of monocytes and NK cells, and (2) triggering of a contact-dependent cell death by a torrent of reactive oxygen species (ROS), nitric oxide (NO), Fas-FasL, TNF-TNFR1 and TRAIL mediated cell death.

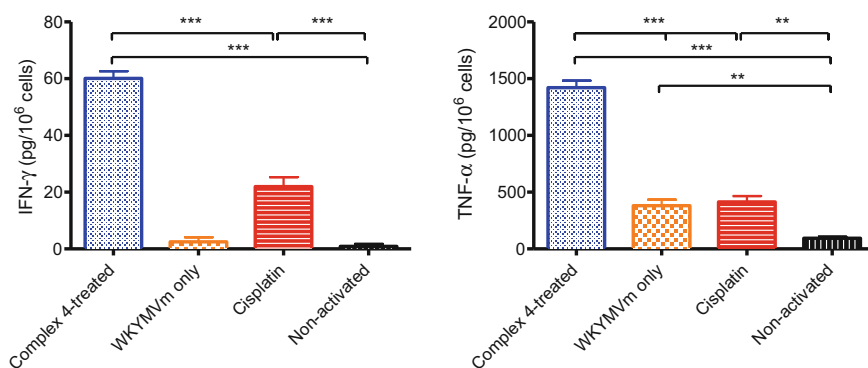


Fig. 5.5 Secretion of the extracellular cytokines, IFN- γ and TNF- α , after treatment of the complex **4**, free WKYMVm peptide and cisplatin for 24 h, as determined by sandwich ELISA of the cellular supernatant. Means \pm s.e.m. (** $p < 0.01$, *** $p < 0.0001$; Student's t test)

Briefly, cisplatin-exposed macrophages lead to a significant enhancement of iNOS-mediated cell death [20, 57]. This may be a direct result of cisplatin-treatment in a cytokine-independent pathway [57] or indirectly through a cytokine-dependent pathway mediated by TNF- α and IFN- γ secretion [20]. Contact-mediated apoptosis of tumor cells, expressing the membrane-bound death receptors Fas, TNFR and/or TRAIL-receptor, may also occur due to a cytokine-dependent monocyte membrane-bound exposure of the corresponding apoptosis inducing ligands (FasL, TNF- α and TRAIL) after cisplatin treatment [58, 59].

In this work, the platinum(IV)-WKYMVm conjugate, **4**, was identified as a potent activator of innate immune effectors. Complex **4** was more effective than **3c**, cisplatin and the free WKYMVm peptide in triggering cell-mediated cytotoxicity of MDA-MB-231 and MCF-7 but not U-87MG. This trend was corroborated by the extracellular secretion of TNF- α and IFN- γ of drug-treated PBMCs. These pro-inflammatory cytokines are key mediators of the innate immune system, are themselves cytotoxic and can also induce several possible pathways of contact-mediated killing of tumor cells downstream as described earlier. It is unknown why treated PBMCs were ineffective against U-87MG but this immune evasion may be due to dysregulation of contact-mediated apoptosis pathways. Intriguingly, we observed a disconnect on the susceptibility of the various cell-lines to immune-mediated cytotoxicity and direct cytotoxicity. MCF-7 was vulnerable to both mechanisms of cell death while U-87MG was vulnerable to DNA-damage induced cell death only. The p53 mutant, MDA-MB-231, was resistant to DNA-damage triggered cell death but was the most susceptible to immune-mediated cytotoxicity. This observation supports the utility of a multi-pronged immuno-chemotherapy approach in the treatment of drug-resistant tumors.

5.3 Conclusion

Over the last decade, there has been substantial evidence supporting the pivotal role of the immune system inducing tumour regression following conventional chemotherapy. Even though platinum-based agents dominate conventional chemotherapy and are included in around 50% of all chemotherapies combinations [60], there has been little interest neither in deciphering the molecular mechanism of platinum-mediated immunomodulation nor the design of combined immuno-chemotherapeutic platinum drugs. We have demonstrated here the feasibility of a rationally-designed immuno-chemotherapeutic platinum-based agent in achieving selective cancer cell-targeting as well as eliciting an immune-response. This approach complements conventional chemotherapy with the aim of destroying micro-metastasis. We believe that this work could spur for the development of clinically-useful immuno-chemotherapeutic platinum-based agents with improved therapeutic outcomes.

5.4 Methods

General reagents. Cisplatin and *cis,cis,trans*-diamminedichlorodihydroxoplatinum (IV) were synthesized and purified as per literature procedures [61, 62]. Succinimidyl 4-formylbenzoate was synthesized as reported by Philips et al. [63]. All other chemicals and reagents were purchased from commercial vendors.

Peptides. All peptides were modified with the (aminooxy)acetic acid linker at either the N terminal or to a lysine residue as specified. The four (aminooxy)acetylated peptides ANXA1 (2-12) *aminooxy-Ala-Met-Val-Ser-Glu-Phe-Leu-Lys-Gln-Ala-Trp*, ANXA1 (2-26) *aminooxy-Ala-Met-Val-Ser-Glu-Phe-Leu-Lys-Gln-Ala-Trp-Phe-Ile-Glu-Asn-Glu-Glu-Gln-Glu-Tyr-Val-Gln-Thr-Val-Lys*, WKYVMV *Trp-Lys(aminooxy)-Tyr-Met-Val-D-Met-NH₂* and fMLFK *formyl-Met-Leu-Phe-Lys(aminooxy)-COOH* were custom-synthesized by ChinaPeptides (Shanghai).

Instrumentation. ¹H NMR was recorded on a Bruker Avance 300 MHz or 400 MHz. Chemical shifts are reported in parts per million relative to residual solvent peaks [64]. Electrospray ionization mass spectra (ESI-MS) were obtained on a Thermo Finnigan LCQ ESI-MS system. Elemental analysis was carried out on a Perkin-Elmer PE 2400 elemental analyzer by CMMAC (National University of Singapore). Platinum concentrations of stock solutions were measured externally by CMMAC (National University of Singapore) on an Optima ICP-OES (Perkin-Elmer). In some cases, platinum concentrations were also measured on an Agilent 7500 Series ICP-MS. Analytical UV-vis absorbance was measured on a Shimadzu UV-1800 UV-vis spectrophotometer. Analytical reversed phase HPLC (RPLC) was conducted on a Shimadzu Prominence or an Agilent 1200 series DAD using Shimpack VP-ODS column (5 μm, 120 Å, 150 × 4.60 mm, 1.0 mL min⁻¹ flow). Semi-preparative HPLC was performed on a Shimadzu Prominence using YMC-Pack Pro C18 column (5 μm, 120 Å, 250 × 10 mm, 2.0 mL min⁻¹ flow). Analytical hydrophilic interaction liquid chromatography (HILIC) was performed using a SeQuant ZIC-HILIC column (150 × 2.1 mm i.d., 5 μm, 200 Å) at a 0.1 mL/min flow rate with 214, 230 and 305 nm UV detection. LC-MS was conducted on a Bruker AmaZonX ion-trap coupled to a Dionex Ultimate 3000 RSLC system.

Synthesis of *cis,cis,trans*-diamminedichloro(hydroxido)(4-formylbenzoate)platinum(IV) (1). *cis,cis,trans*-diamminedichlorodihydroxoplatinum(IV) (300 mg, 0.898 mmol) was suspended in dry DMSO (120 mL). NHS-activated-ester, succinimidyl 4-formylbenzoate (300 mg, 1.347 mmol) was then added slowly to the suspension. The reaction mixture was stirred vigorously at r.t. for 72 h and subsequently filtered through Celite to remove unreacted *cis,cis,trans*-diamminedichlorodihydroxoplatinum(IV) and metallic platinum. The filtrate was reduced in volume to about 0.5–1 mL in a lyophilizer before being precipitated by addition of DCM (60 mL) and diethyl ether (20 mL). It was essential to prevent the filtrate from being lyophilized completely. The crude product was then washed sequentially by sonication with DCM (3 × 10 mL), water (3 × 5 mL) and acetone (3 × 5 mL) to yield the desired product as a white-colour precipitate. At each

rinsing step, the washing was continued until the rinsing solvent turned from pale yellow to colourless. Yield: 180 mg (43%) ^1H NMR (DMSO- d_6 , 300.13 Hz): δ 10.07 (s, 1H, CHO), 8.05 (d, 2H, Ar-H, $^3J_{\text{HH}} = 8.04$ Hz), 7.95 (d, 2H, Ar-H, $^3J_{\text{HH}} = 8.04$ Hz), 6.05 (m, 6H, NH_3 , $^1J_{\text{HN}} = 52.4$ Hz, $^2J_{\text{HPt}} = 52.1$ Hz); ESI-MS (-): m/z 464.9 $[\text{M-H}]^-$; Anal. Calcd, $\text{C}_8\text{H}_{12}\text{Cl}_2\text{N}_2\text{O}_4\text{Pt}$ (466.18): C, 20.61; H, 2.59; N, 6.01. Found: C, 20.88; H, 2.58; N, 5.75. Purity (HPLC): 97% at 254 nm.

Synthesis of *cis,cis,trans*-diamminedichloro(acetato)(4-formylbenzoate)platinum(IV) (2). Acetic anhydride (8 μL , 84.8 μmol) was added to a solution of **1** (20 mg, 42.9 μmol) dissolved in dry DMF (1 mL) and stirred vigorously for 48 h. The solution was evaporated to oil and precipitated with diethyl ether (5 mL). The precipitate was washed with DCM (5 mL). The crude product was then dissolved in acetone (10 mL) and filtered to remove insoluble unreacted **1**. This process of evaporation, precipitation with ether, washing with DCM, reconstitution in acetone and filtration was then repeated again. The crude product was then redissolved in THF (10 mL) and filtered. Likewise, the process was repeated. After drying, the crude product was washed with minimal cold water (0.5 mL) and the desired water-soluble product was isolated from insoluble impurities by extracting with water (3×15 mL). The combined water portions were pooled and evaporated to yield an off-white powder. Yield: 11 mg (50%) ^1H NMR (DMSO- d_6 , 300.13 Hz): δ 10.08 (s, 1H, CHO), 8.05 (d, 2H, Ar-H, $^3J_{\text{HH}} = 8.04$ Hz), 7.96 (d, 2H, Ar-H, $^3J_{\text{HH}} = 8.04$ Hz), 6.65 (br m, 6H, NH_3), 1.95 (s, 3H, CH_3); ESI-MS (-): m/z 506.8 $[\text{M-H}]^-$; Purity (HPLC): 97% at 254 nm.

General procedure for synthesis of platinum(IV)-peptide conjugates. In general, the platinum(IV)-peptide conjugates (**3a-d** and **4**) were prepared by treating the desired (aminoxy)acetylated peptide with 2x stoichiometric excess of **1** or **2** in an aq. buffered solution containing 50% v/v DMSO. All reagents were pre-dissolved in DMSO to form stock solutions. Concentrations of the free peptides were measured by UV at 280 nm in 50 mM pH 7 phosphate buffer [65]. Reaction progress was followed by analytical HPLC over 24 h using a gradient elution of 5–30% B in the first 15 min followed by 30–80% B for 10 min. The desired products were subsequently isolated by semi-preparative HPLC. Purity of the conjugates was assessed using a gradient elution of 20–80% B over 20 min. Unless otherwise stated, solvent A is aq. NH_4OAc buffer (10 mM, pH 7) and solvent B is MeCN. See Supplementary Information for detailed synthesis procedure, characterization and semi-preparative separation conditions of **3a-d** and **4**.

Cell lines and cell culture. Human glioblastoma (GBM) cell line U-87MG and adenocarcinoma cell lines MCF-7 and MDA-MB-231 were obtained from ATCC. All cells were grown in high glucose Dulbecco's modified Eagle medium (DMEM) containing 10% fetal bovine serum (FBS) and maintained in a 5% CO_2 incubator at 37 $^\circ\text{C}$.

Cell viability assay of platinum(IV)-peptide conjugates on FPR1/2 over-expressing tumors. The indicated cell-lines were harvested from culture flasks by trypsinization and seeded at a density of 6.0×10^3 cells/well in 100 μL aliquots into flat-bottomed 96-well tissue-culture plates. Cells were allowed to adhere in drug-free complete DMEM with 10% FBS for 24 h, followed by the addition of

dilutions of drug in 100 μL /well complete media and further incubated for 72 h. At the end of exposure, medium was replaced by 100 μL /well MTT solution (0.5 mg/mL in PBS). After incubation for 4 h, MTT was aspirated and substituted with 100 μL /well DMSO. UV-vis absorbance was measured at 570 nm using a microplate reader (Biotek). Experiments were performed in sextuplicates for each drug concentration and carried out independently in triplicates. Cytotoxicity was evaluated with the reference to the absolute IC_{50} value. IC_{50} values were calculated from concentration-response curves (cell viability against log of drug concentration) obtained in repeated experiments and adjusted to the actual concentration of Pt administered as measured by ICP-OES.

Cellular platinum accumulation of complex 4 in the presence of free competitive WKYMVm. U-87MG was seeded in 35 mm tissue-culture petridishes in DMEM supplemented with 2% FBS (5×10^5 cells in 2 mL media) and incubated for 24 h. To inhibit uptake of complex 4, the tumor cells were pre-treated with increasing concentrations of free WKYMVm or DMSO vehicle control and incubated for a further 1 h. The media was aspirated and the cells were subsequently treated with complex 4 (10 μM in 1 mL DMEM) and incubated for a further 8 h. The cells were then washed carefully with PBS and harvested by scraping into microtubes. The cells were centrifuged and washed again twice with PBS to remove residual drug. The number of U-87MG in each microtube was counted accurately followed by acid digestion (by heating in 300 μL 65% ultrapure nitric acid at 90 $^\circ\text{C}$ overnight, boiling to dryness and re-dissolving the residue in 500 μL 2% nitric acid) for platinum quantification by ICP-MS. The measured platinum levels were adjusted to pmol Pt/ 10^6 cells for comparison.

Cytotoxicity of drug-activated human peripheral blood mononuclear cells (PBMCs) against tumor cell-lines. Prior to activation, frozen PBMCs (AllCells LLC, USA) were thawed and washed twice with complete RPMI to remove freezing medium. 4.1×10^6 PBMCs were incubated in 5 mL of complete RPMI for 24 h at 37 $^\circ\text{C}$. Suspension cultures of PBMCs were drug activated by incubating 4.8×10^5 PBMCs with either 10 μM of cisplatin, 3c or 4 each respectively in an Eppendorf tube in 1 mL of complete RPMI for 24 h with gentle shaking periodically at 37 $^\circ\text{C}$. After activation, PBMCs were washed twice with complete DMEM to remove residual drug and resuspended in 1.2 mL of complete DMEM. PBMCs were then co-cultured with the indicated tumor cells (pre-seeded 24 h beforehand at a density of 4.0×10^3 cells/well in 100 μL aliquots into flat-bottomed 96-well tissue-culture plates) at an 10:1 effector to target ratio and incubated for 72 h. At the end of exposure, medium was replaced by 100 μL /well MTT solution (0.5 mg/mL in PBS). After incubation for 4 h, MTT was aspirated and substituted with 100 μL /well DMSO. UV-vis absorbance was measured at 570 nm using a microplate reader (Biotek). Experiments were performed in triplicates for each drug-activated PBMCs and carried out independently for three times. Cell viability was calculated from the absorbance value of the tumor cells cultured with drug-activated PBMCs and non-activated PBMCs (A), the absorbance value of PBMCs only (B), the absorbance value of DMSO only (C), and the absorbance value of the tumor cells only (D) as follows;

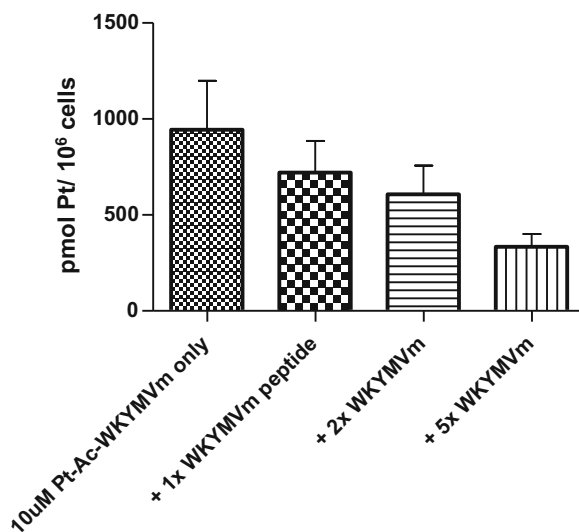
$$\frac{(A - C) - (B - C)}{D - C} \times 100\%.$$

Measurements of TNF α and IFN γ via ELISA. The amount of the cytokines, TNF- α and IFN- γ , secreted by drug-treated PBMCS after 24 h into the complete RPMI supernatant was measured using the commercially available human TNF- α and IFN- γ sandwich ELISA screening kits (Pierce) as per the manufacturer's protocol. Calibration standards provided by the kits were reconstituted and diluted in complete RPMI. Readings were adjusted to pg/10⁶ cells for comparison.

Supplementary Information

Supplementary Figures

Fig. S5.1 Platinum uptake studies of platinum(IV)-WKYMVM conjugate **4** in FPR1/2-expressing U-87MG cells after 4 h of incubation following pre-incubation with increasing concentrations of free competitive WKYMVM. ICP-MS readings were adjusted to pmol Pt per 10⁶ cells



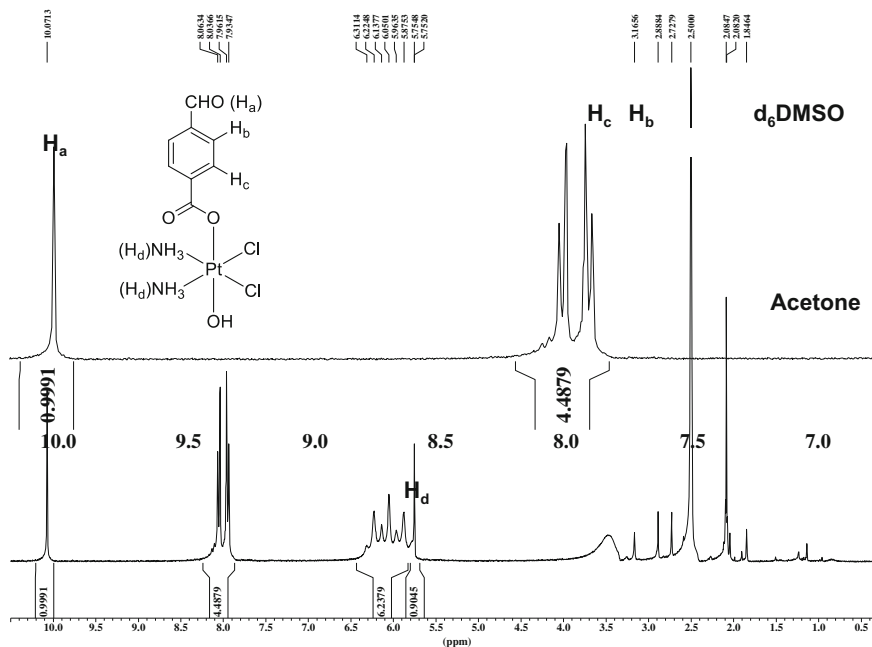


Fig. S5.2 ^1H NMR spectra of complex **1** in DMSO-d_6 with water suppression

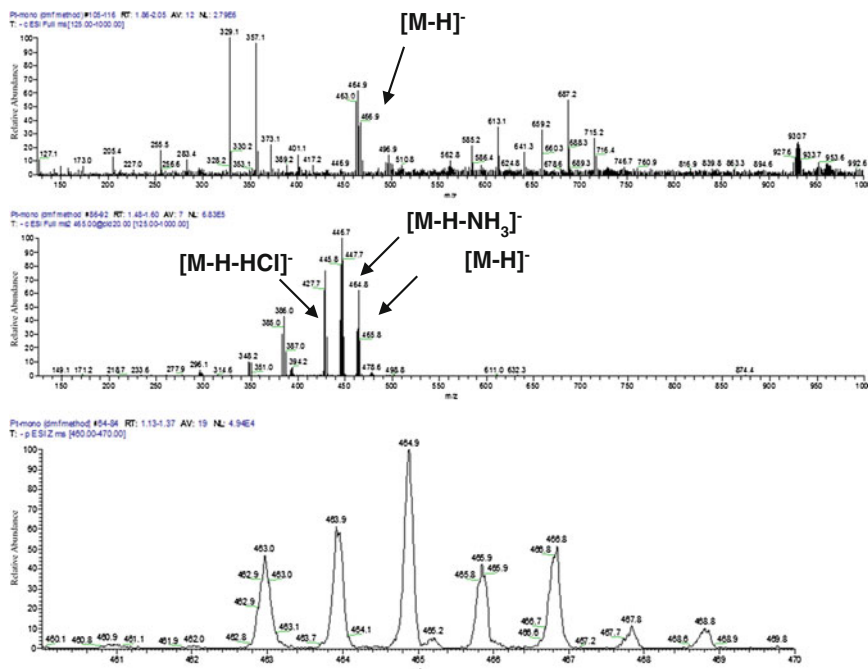


Fig. S5.3 ESI-MS (Methanol, $-ve$ mode) characterization of complex **1**: Fullscan, MS/MS and zoomscan (top to bottom): m/z : found: 464.9 $[\text{M-H}]^-$, calculated: 466.1

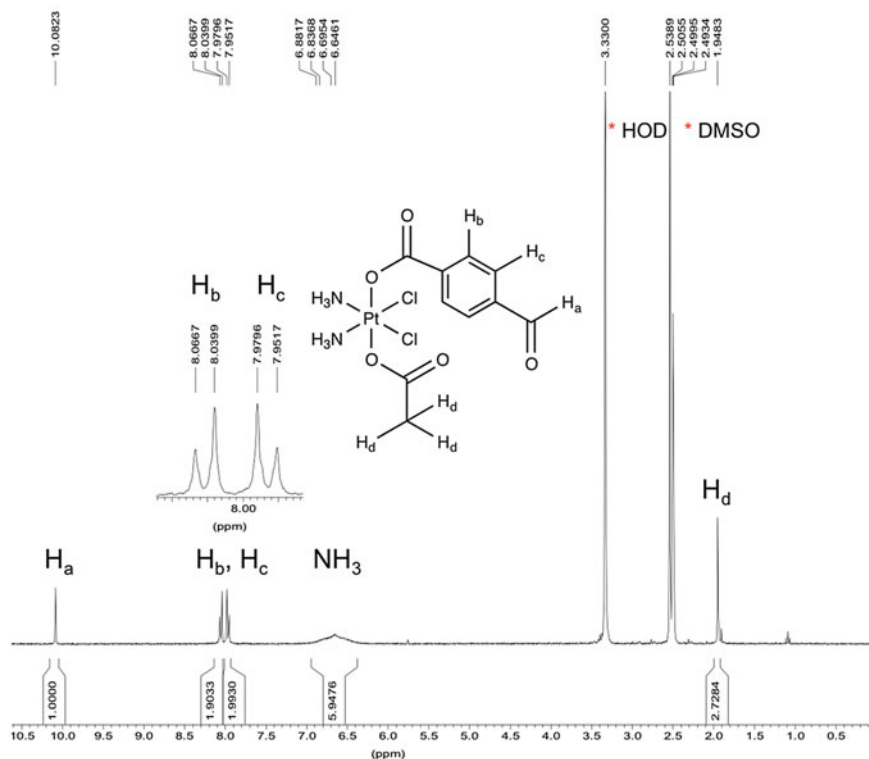


Fig. S5.4 ^1H NMR spectra of complex **2** in DMSO-d_6

Supplementary Methods

General procedure for synthesis of platinum(IV)-peptide conjugates. In general, the platinum(IV)-peptide conjugates (**3a–d** and **4**) were prepared by treating the desired (aminoxy)acetylated peptide with $2 \times$ stoichiometric excess of **1** or **2** in an aq. buffered solution containing 50% v/v DMSO. All reagents were pre-dissolved in DMSO to form stock solutions for addition. Concentrations of the free peptides were measured by UV at 280 nm in 50 mM pH 7 phosphate buffer. Reaction progress was followed by analytical HPLC over 24 h using a gradient elution of 5–30% B in the first 15 min followed by 30–80% B for 10 min. The desired products were subsequently isolated by semi-preparative HPLC. Purity of the conjugates was assessed using a gradient elution of 20–80% B over 20 min. Unless otherwise stated, solvent A is aq. NH_4OAc buffer (10 mM, pH 7) and solvent B is MeCN.

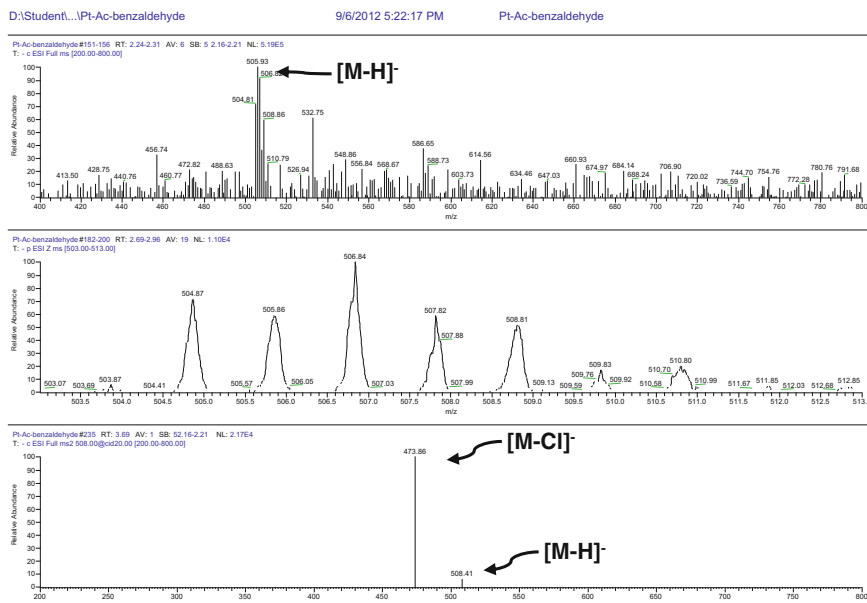


Fig. S5.5 ESI-MS (Methanol, $-ve$ mode) characterization of complex **2**: Fullscan, zoomscan and MS/MS (top to bottom): m/z : found: 506.82 $[M-H]^-$, calculated: 508.2

Platinum(IV)-peptide conjugate of 1 and ANXA1(2-12) (3a). Complex **1** (50 μ L of a 75.1 mM stock solution) was added to aminoxy-functionalized ANXA1 (2–12) peptide (50 μ L of a 35 mM stock solution) in 1 mL 50% DMSO–NaOAc (50 mM, pH 5.5) and stirred overnight. The mono-conjugated product was subsequently purified by semi-preparative HPLC using a gradient elution system of 8–45% B for 30 min followed by 90% B for the next 10 min; ESI-MS (+): m/z 915.6 $[M+2H]^{2+}$ 1831.3 $[M+H]^+$; Purity (HPLC): 99% at 254 nm.

Platinum(IV)-peptide conjugate of 1 and ANXA1(2-26) (3b). Synthesis is similar to **3a** but in 1 mL DMSO– KH_2PO_4 (50 mM, pH 7.5). The mono-conjugated product was subsequently purified by semi-preparative HPLC using a gradient elution system of 8–45% B for 38 min, 45–80% B for 2 min followed by 90% B for the next 10 min where solvent A is aq. NH_4OAc buffer (20 mM, pH 7); ESI-MS (+): m/z 1784.2 $[M+2H]^{2+}$; Purity (HPLC): 95% at 254 nm.

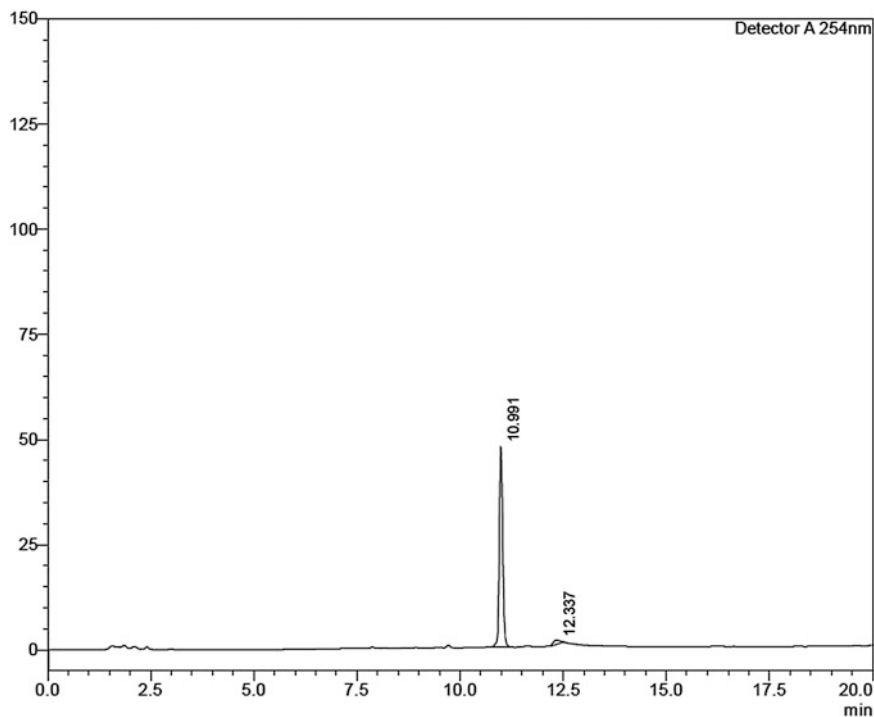


Fig. S5.6 RP-HPLC assessment of purity of Pt–Ac-benzaldehyde **2** dissolved in MeCN–H₂O. Elution conditions for both spectra (A) and (B): 20–80% gradient elution system with aq. NH₄OAc buffer (10 mM, pH 7) (solvent A) and MeCN (solvent B) over 20 min at 1.0 mL/min. Column used is: Shimpack VP-ODS column (150 × 4.60 mm i.d)

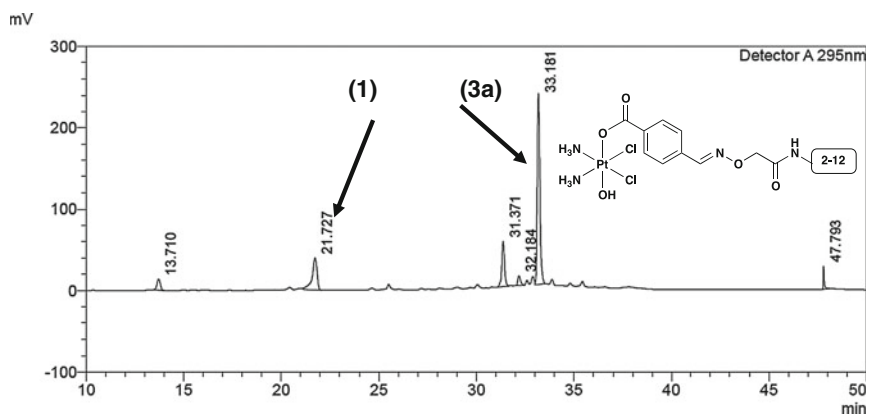


Fig. S5.7 HPLC spectra of crude reaction mixture of Pt(IV)-OH-aminooxy-2-12 (**3a**) at 295 nm. Elution conditions: 8–45% B for 30 min followed by 90% B for the next 10 min. NH₄OAc buffer (10 mM, pH 7) (solvent A) and MeCN (solvent B) at 2.0 mL/min

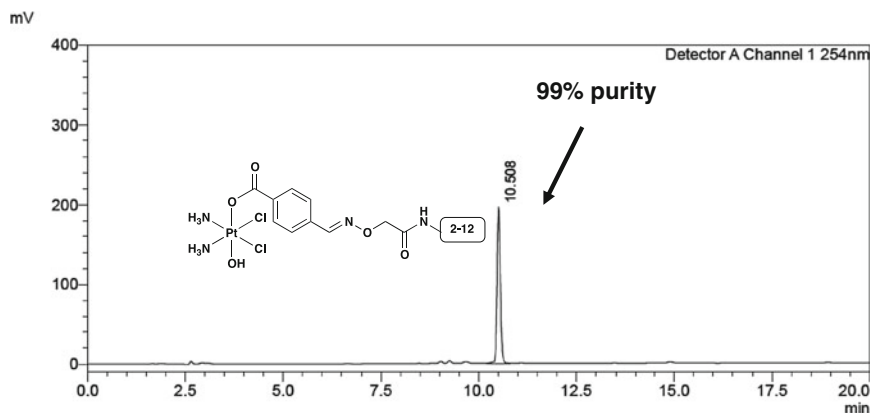


Fig. S5.8 RP-HPLC assessment of purity of Pt(IV)-OH-aminooxy-2-12 (**3a**) dissolved in MeCN–H₂O. Elution conditions: 20–80% gradient elution system with aq. NH₄OAc buffer (10 mM, pH 7) (solvent A) and MeCN (solvent B) over 20 min at 1.0 mL/min. Column used is: Shimpack VP-ODS column (150 × 4.60 mm i.d.)

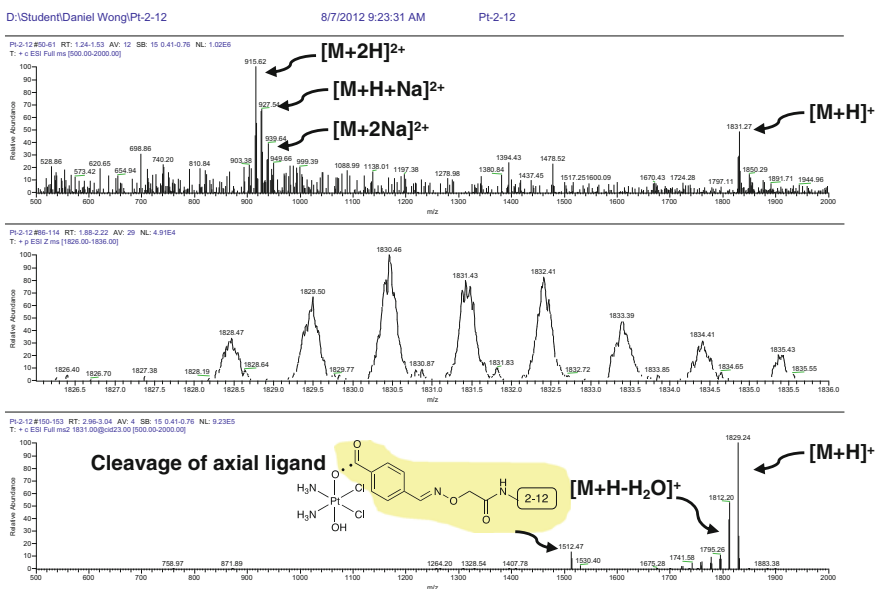


Fig. S5.9 ESI-MS (Methanol, +ve) characterization of conjugate **3a**: fullscan, zoomscan and MS/MS (top to bottom): m/z: found: 915.6 [M+2H]²⁺ and 1831.3 [M+H]⁺; calculated: 1830.7

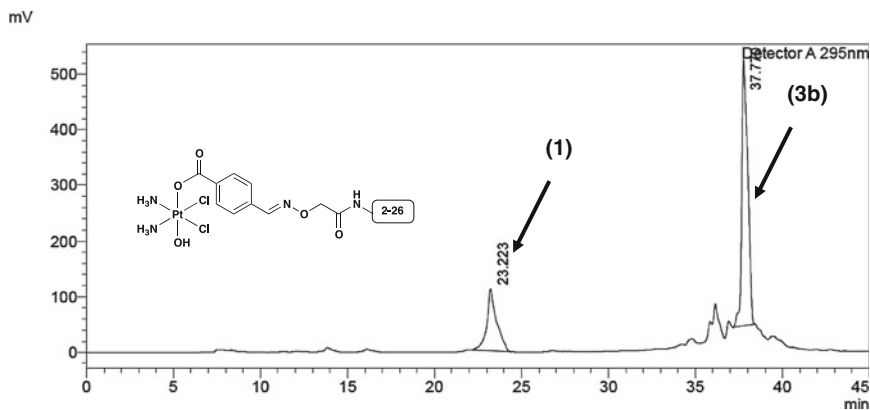


Fig. S5.10 HPLC spectra of crude reaction mixture of Pt(IV)-OH-aminooxy-2-26 (**3b**) at 295 nm. Elution conditions: 8–45% B for 38 min, 45–80% B for 2 min followed by 90% B for the next 10 min. NH_4OAc buffer (20 mM, pH 7) (solvent A) and MeCN (solvent B) at 2.0 mL/min

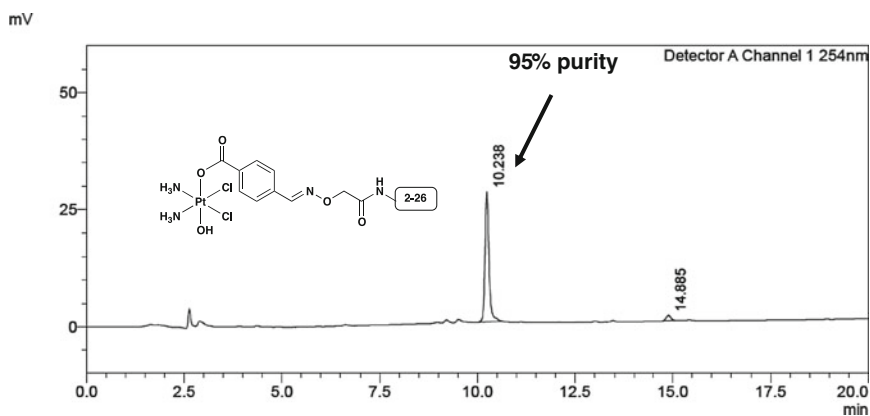
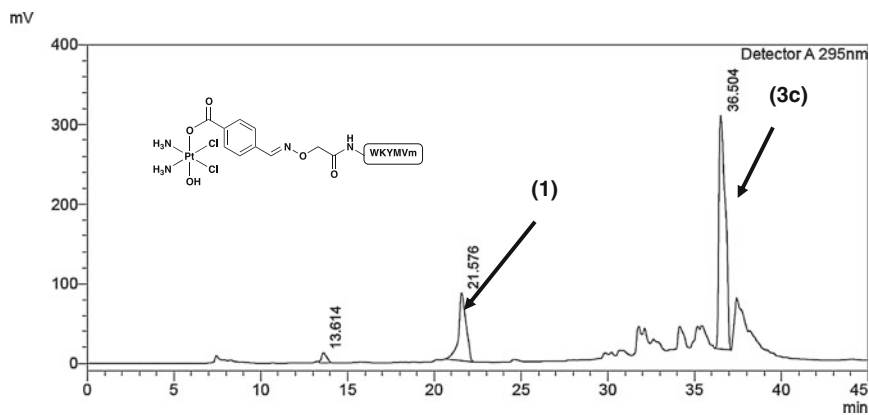
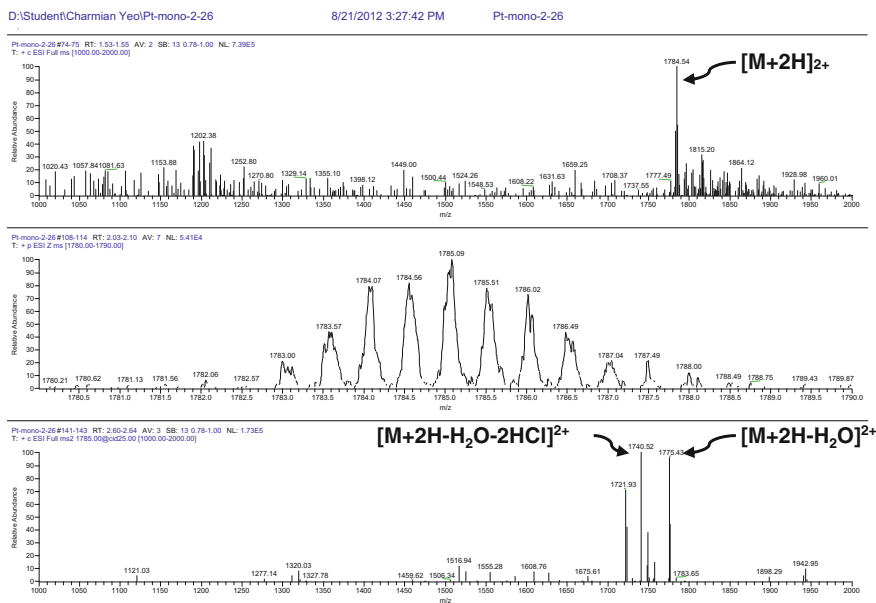


Fig. S5.11 RP-HPLC assessment of purity of Pt(IV)-OH-aminooxy-2-26 (**3b**) dissolved in MeCN– H_2O . Elution conditions: 20–80% gradient elution system with aq. NH_4OAc buffer (10 mM, pH 7) (solvent A) and MeCN (solvent B) over 20 min at 1.0 mL/min. Column used is: Shimpack VP-ODS column (150 × 4.60 mm i.d)



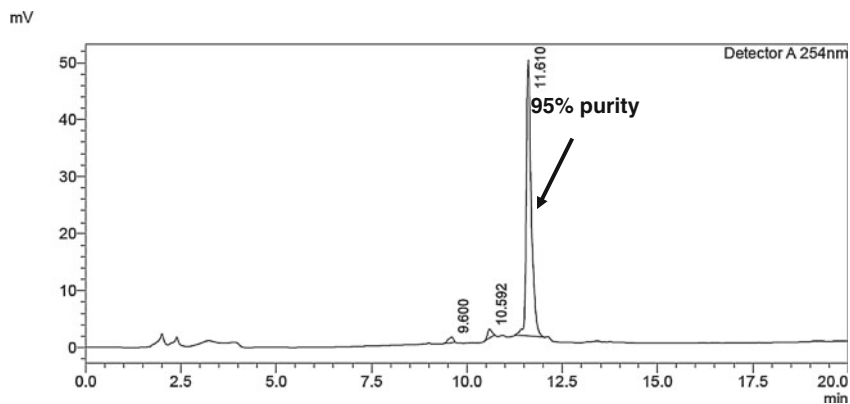


Fig. S5.14 RP-HPLC assessment of purity of Pt(IV)-OH-aminoxy-WKYMVm (**3c**) dissolved in MeCN–H₂O. Elution conditions: 20–80% gradient elution system with aq. NH₄OAc buffer (10 mM, pH 7) (solvent A) and MeCN (solvent B) over 20 min at 1.0 mL/min. Column used is: Shimpack VP-ODS column (150 × 4.60 mm i.d)

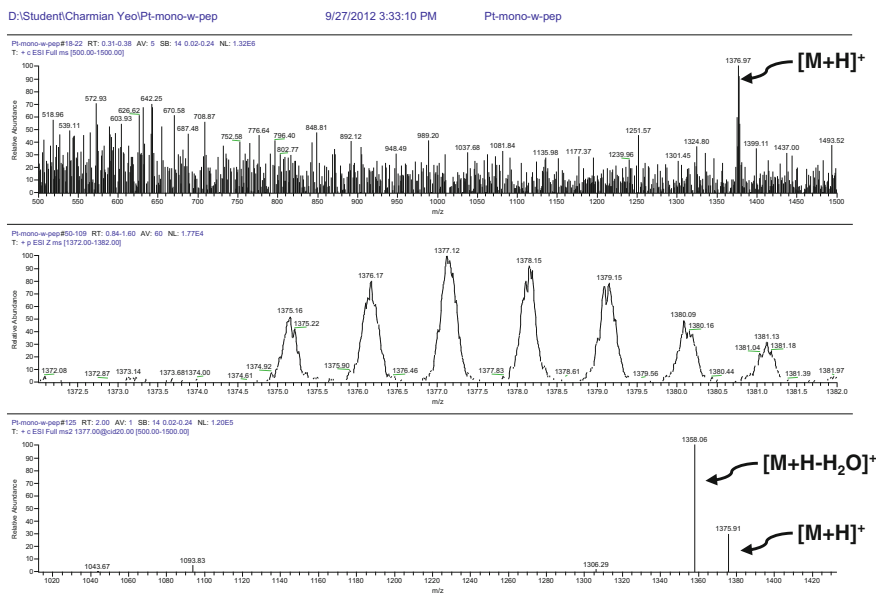


Fig. S5.15 ESI-MS (Methanol, +ve) characterization of conjugate **3c**: fullscan, zoomscan and MS/MS (top to bottom): m/z: found: 1376.9 $[M+H]^+$; calculated: 1375.4

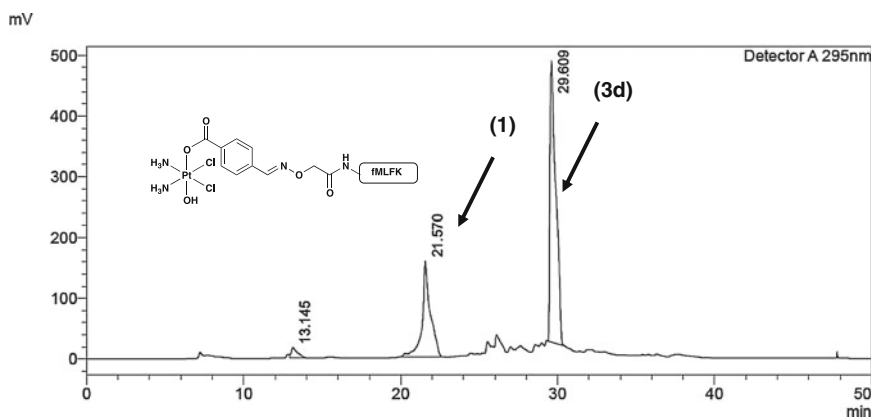


Fig. S5.16 HPLC spectra of crude reaction mixture of Pt(IV)-OH-aminoxy-fMLFK (**3d**) at 295 nm. Elution conditions: 8–45% B for 30 min followed by 90% B for the next 10 min. NH_4OAc buffer (10 mM, pH 7) (solvent A) and MeCN (solvent B) at 2.0 mL/min

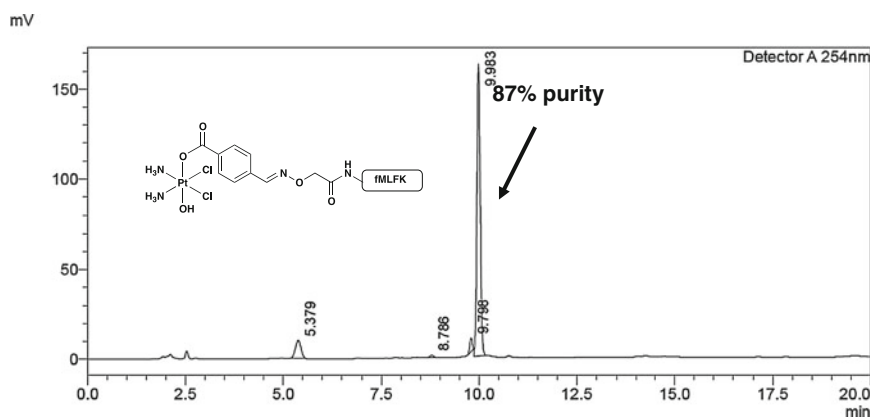


Fig. S5.17 RP-HPLC assessment of purity of Pt(IV)-OH-aminoxy-fMLFK (**3d**) dissolved in MeCN– H_2O . Elution conditions: 20–80% gradient elution system with aq. NH_4OAc buffer (10 mM, pH 7) (solvent A) and MeCN (solvent B) over 20 min at 1.0 mL/min. Column used is: Shimpack VP-ODS column (150 × 4.60 mm i.d)

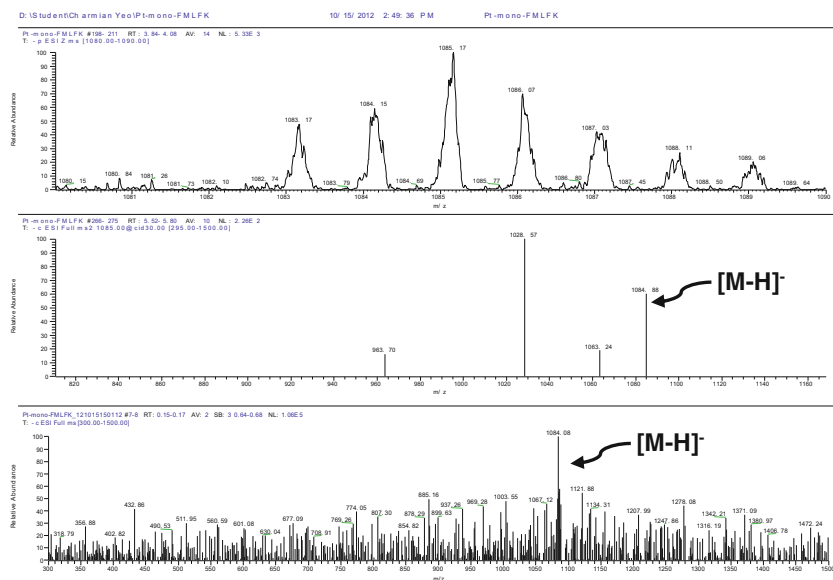


Fig. S5.18 ESI-MS (Methanol, $-ve$) characterization of conjugate **3d**: zoomscan, MS/MS and fullscan (top to bottom); m/z: found: 1084.1 $[M-H]^-$; calculated: 1085.3

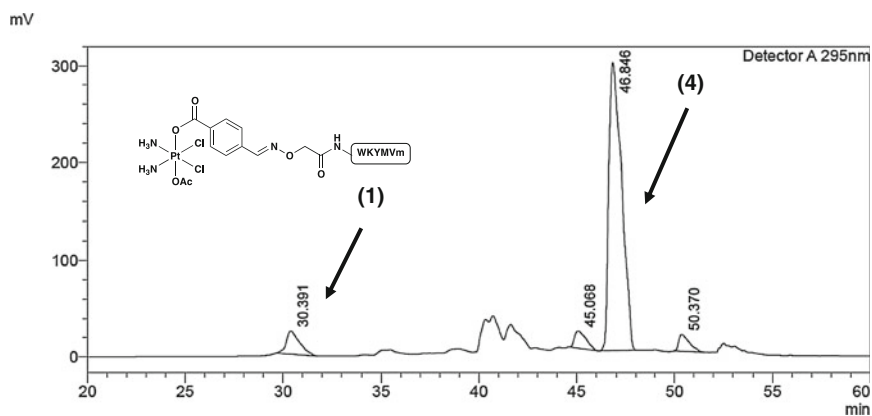


Fig. S5.19 HPLC spectra of crude reaction mixture of Pt(IV)-Ac-aminoxy-WKYMVm (**4**) at 295 nm. Elution conditions: 8–50% B for 45 min followed by 90% B for the next 15 min. NH_4OAc buffer (10 mM, pH 7) (solvent A) and MeCN (solvent B) at 2.0 mL/min

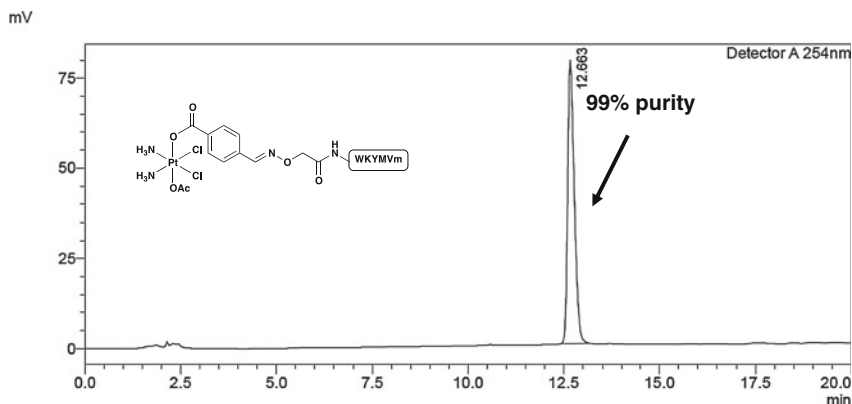


Fig. S5.20 RP-HPLC assessment of purity of Pt(IV)-Ac-aminoxy-WKYMVm (**4**) dissolved in MeCN–H₂O. Elution conditions: 20–80% gradient elution system with aq. NH₄OAc buffer (10 mM, pH 7) (solvent A) and MeCN (solvent B) over 20 min at 1.0 mL/min. Column used is: Shimpack VP-ODS column (150 × 4.60 mm i.d)

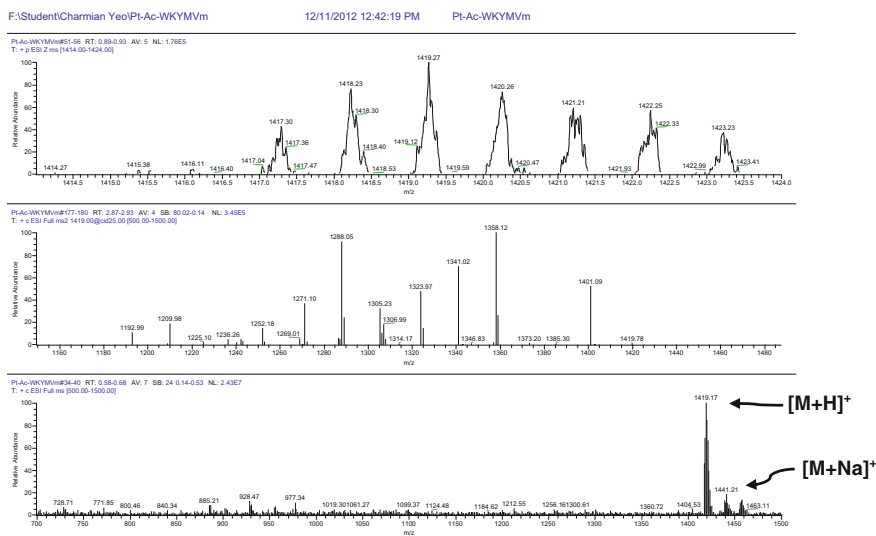


Fig. S5.21 ESI-MS (Methanol, +ve) characterization of conjugate **4**: zoomscan, MS/MS and fullscan (top to bottom); m/z: found: 1419.1 [M–H][–]; calculated: 1419.4

Platinum(IV)-peptide conjugate of 1 and WKYMVm (3c). Synthesis was as **3a**. The mono-conjugated product was subsequently purified by semi-preparative HPLC using a gradient elution system of 8–50% B in the first 45 min followed by 90% B for 15 min. ESI-MS (+): m/z 1376.9 [M+H]⁺; Purity (HPLC): 95% at 254 nm.

Platinum(IV)-peptide conjugate of 1 and fMLFK (3d). Synthesis was as **3a**. The mono-conjugated product was subsequently purified by semi-preparative HPLC using a gradient elution system of 8–45% B for 30 min followed by 90% for the next 10 min; ESI-MS (–): m/z 1084.1 $[M-H]^-$; Purity (HPLC): 87% at 254 nm.

Platinum(IV)-peptide conjugate of 2 and WKYVMv (4). Synthesis was similar to **3c** but with complex **2**. ESI-MS (+): m/z 1419.1 $[M+H]^+$; Purity (HPLC): 99% at 254 nm.

References

1. Lake, R.A., Robinson, B.W.S.: Immunotherapy and chemotherapy—a practical partnership. *Nat. Rev. Cancer* **5**, 397–405 (2005)
2. Zitvogel, L., Apetoh, L., Ghiringhelli, F., Kroemer, G.: Immunological aspects of cancer chemotherapy. *Nat. Rev. Immunol.* **8**, 59–73 (2008)
3. Lesterhuis, W.J., Haanen, J.B.A.G., Punt, C.J.A.: Cancer immunotherapy—revisited. *Nat. Rev. Drug Discov.* **10**, 591–600 (2011)
4. Galluzzi, L., Senovilla, L., Zitvogel, L., Kroemer, G.: The secret ally: immunostimulation by anticancer drugs. *Nat. Rev. Drug Discov.* **11**, 215–233 (2012)
5. Krysko, D.V., Garg, A.D., Kaczmarek, A., Krysko, O., Agostinis, P., Vandenabeele, P.: Immunogenic cell death and DAMPs in cancer therapy. *Nat. Rev. Cancer* **12**, 860–875 (2012)
6. Hall, M.D., Mellor, H.R., Callaghan, R., Hambley, T.W.: Basis for design and development of Platinum(IV) anticancer complexes. *J. Med. Chem.* **50**, 3403–3411 (2007)
7. Hall, M.D., Hambley, T.W.: Platinum(IV) antitumour compounds: their bioinorganic chemistry. *Coord. Chem. Rev.* **232**, 49–67 (2002)
8. Chin, C.F., Wong, D.Y.Q., Jothibasu, R., Ang, W.H.: Anticancer Platinum(IV) prodrugs with novel modes of activity. *Curr. Top. Med. Chem.* **11**, 2602–2612 (2011)
9. Kelland, L.: The resurgence of platinum-based cancer chemotherapy. *Nat. Rev. Cancer* **7**, 573–584 (2007)
10. Abu-Surrah, A.S., Kettunen, M.: Platinum group antitumor chemistry: design and development of new anticancer drugs complementary to cisplatin. *Curr. Med. Chem.* **13**, 1337–1357 (2006)
11. Wang, D., Lippard, S.J.: Cellular processing of platinum anticancer drugs. *Nat. Rev. Drug Discov.* **4**, 307–320 (2005)
12. Reed, E.: Cisplatin, carboplatin, and oxaliplatin. In: Chabner, B.A., Longo, D.L. (eds.) *Cancer chemotherapy and biotherapy: principles and practice*, 5th edn, pp. 333–341. Lippincott Williams & Wilkins, Philadelphia (2011)
13. Tesniere, A., Schlemmer, F., Boige, V., Kepp, O., Martins, I., Ghiringhelli, F., Aymeric, L., Michaud, M., Apetoh, L., Barault, L., Mendiboure, J., Pignon, J.P., Jooste, V., van Endert, P., Ducreux, M., Zitvogel, L., Piard, F., Kroemer, G.: Immunogenic death of colon cancer cells treated with oxaliplatin. *Oncogene* **29**, 482–491 (2009)
14. Merritt, R.E., Mahtabifard, A., Yamada, R.E., Crystal, R.G., Korst, R.J.: Cisplatin augments cytotoxic T-lymphocyte-mediated antitumor immunity in poorly immunogenic murine lung cancer. *J. Thorac. Cardiovasc. Surg.* **126**, 1609–1617 (2003)
15. Ramakrishnan, R., Assudani, D., Nagaraj, S., Hunter, T., Cho, H.-I., Antonia, S., Altioek, S., Celis, E., Gabrilovich, D.I.: Chemotherapy enhances tumor cell susceptibility to CTL-mediated killing during cancer immunotherapy in mice. *J. Clin. Invest.* **120**, 1111–1124 (2010)
16. Lesterhuis, W.J., Punt, C.J.A., Hato, S.V., Eleveld-Trancikova, D., Jansen, B.J.H., Nierkens, S., Schreiber, G., de Boer, A., Van Herpen, C.M.L., Kaanders, J.H., van Krieken, J.H.J.M., Adema, G.J., Figdor, C.G., de Vries, I.J.M.: Platinum-based drugs disrupt STAT6-mediated

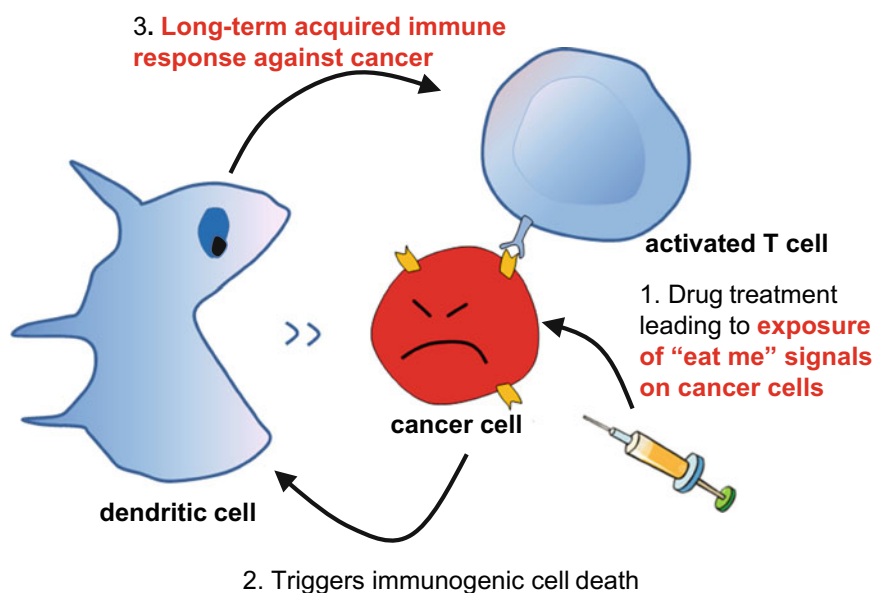
- suppression of immune responses against cancer in humans and mice. *J. Clin. Investig.* **121**, 3100–3108 (2011)
17. Kleinerman, E.S., Zwelling, L.A., Muchmore, A.V.: Enhancement of naturally occurring human spontaneous monocyte-mediated cytotoxicity by *cis*-Diamminedichloroplatinum(II). *Cancer Res.* **40**, 3099–3102 (1980)
 18. Kleinerman, E., Howser, D., Young, R., Bull, J., Zwelling, L., Barlock, A., Decker, J., Muchmore, A.: Defective monocyte killing in patients with malignancies and restoration of function during chemotherapy. *Lancet* **316**, 1102–1105 (1980)
 19. Lichtenstein, A.K., Pende, D.: Enhancement of natural killer cytotoxicity by *cis*-Diamminedichloroplatinum(II) in vivo and in vitro. *Cancer Res.* **46**, 639–644 (1986)
 20. Son, K., Kim, Y.-M.: In vivo cisplatin-exposed macrophages increase immunostimulant-induced nitric oxide synthesis for tumor cell killing. *Cancer Res.* **55**, 5524–5527 (1995)
 21. Okamoto, M., Kasetani, H., Kaji, R., Goda, H., Ohe, G., Yoshida, H., Sato, M., Kasatani, H.: *cis*-Diamminedichloroplatinum and 5-fluorouracil are potent inducers of the cytokines and natural killer cell activity in vivo and in vitro. *Cancer Immunol. Immunother.* **47**, 233–241 (1998)
 22. Singh, R.A.K., Sodhi, A.: Antigen presentation by cisplatin-activated macrophages: role of soluble factor(s) and second messengers. *Immunol. Cell Biol.* **76**, 513–519 (1998)
 23. Hu, J., Kinn, J., Zirakzadeh, A.A., Sherif, A., Norstedt, G., Wikström, A.C., Winqvist, O.: The effects of chemotherapeutic drugs on human monocyte-derived dendritic cell differentiation and antigen presentation. *Clin. Exp. Immunol.* **172**, 490–499 (2013)
 24. Chang, C.-L., Hsu, Y.-T., Wu, C.-C., Lai, Y.-Z., Wang, C., Yang, Y.-C., Wu, T.-C., Hung, C.-F.: Dose-dense chemotherapy improves mechanisms of antitumor immune response. *Cancer Res.* **73**, 119–127 (2013)
 25. Rosenberg, B.: Possible mechanisms for the antitumor activity of platinum coordination complexes. *Cancer Chemother. Rep.* **59**, 589–598 (1975)
 26. Taniguchi, K., Nishiura, H., Yamamoto, T.: Requirement of the acquired immune system in successful cancer chemotherapy with *cis*-Diamminedichloroplatinum(II) in a syngeneic mouse tumor transplantation model. *J. Immunother.* **34**, 480–489 (2011)
 27. Wong, D.Y.Q., Lau, J.Y., Ang, W.H.: Harnessing chemoselective imine ligation for tethering bioactive molecules to platinum(IV) prodrugs. *Dalton Trans.* **41**, 6104–6111 (2012)
 28. Khau, T., Langenbach, S.Y., Schuliga, M., Harris, T., Johnstone, C.N., Anderson, R.L., Stewart, A.G.: Annexin-1 signals mitogen-stimulated breast tumor cell proliferation by activation of the formyl peptide receptors (FPRs) 1 and 2. *FASEB J* **25**, 483–496 (2011)
 29. Coffelt, S.B., Tomchuck, S.L., Zvezdaryk, K.J., Danka, E.S., Scandurro, A.B.: Leucine Leucine-37 uses formyl peptide receptor-like 1 to activate signal transduction pathways, stimulate oncogenic gene expression, and enhance the invasiveness of ovarian cancer cells. *Mol. Cancer Res.* **7**, 907–915 (2009)
 30. Huang, J., Chen, K., Chen, J., Gong, W., Dunlop, N.M., Howard, O.M.Z., Gao, Y., Bian, X. W., Wang, J.M.: The G-protein-coupled formylpeptide receptor FPR confers a more invasive phenotype on human glioblastoma cells. *Br. J. Cancer* **102**, 1052–1060 (2010)
 31. Zhou, Y., Bian, X., Le, Y., Gong, W., Hu, J., Zhang, X., Wang, L., Iribarren, P., Salcedo, R., Howard, O.M.Z., Farrar, W., Wang, J.M.: Formylpeptide receptor FPR and the rapid growth of malignant human gliomas. *J. Natl. Cancer Inst.* **97**, 823–835 (2005)
 32. Kim, S.D., Lee, H.Y., Shim, J.W., Kim, H.J., Baek, S.-H., Zabel, B.A., Bae, Y.-S.: A WKYMVm-containing combination elicits potent anti-tumor activity in heterotopic cancer animal model. *PLoS ONE* **7**, e30522 (2012)
 33. Kim, S.D., Kim, J.M., Jo, S.H., Lee, H.Y., Lee, S.Y., Shim, J.W., Seo, S.-K., Yun, J., Bae, Y.-S.: Functional expression of formyl peptide receptor family in human NK cells. *J. Immunol.* **183**, 5511–5517 (2009)
 34. Le, Y., Yang, Y., Cui, Y., Yazawa, H., Gong, W., Qiu, C., Wang, J.M.: Receptors for chemotactic formyl peptides as pharmacological targets. *Int. Immunopharmacol.* **2**, 1–13 (2002)

35. Tsubery, H., Yaakov, H., Cohen, S., Giterman, T., Matityahou, A., Fridkin, M., Ofek, I.: Neopeptide antibiotics that function as opsonins and membrane-permeabilizing agents for gram-negative bacteria. *Antimicrob. Agents Chemother.* **49**, 3122–3128 (2005)
36. Wan, L., Zhang, X., Pooyan, S., Palombo, M.S., Leibowitz, M.J., Stein, S., Sinko, P.J.: Optimizing size and copy number For PEG-fMLF (*N*-Formyl-methionyl-leucyl-phenylalanine) nanocarrier uptake by macrophages. *Bioconjug. Chem.* **19**, 28–38 (2007)
37. Niedel, J.E., Kahane, I., Cuatrecasas, P.: Receptor-mediated internalization of fluorescent chemotactic peptide by human neutrophils. *Science* **205**, 1412–1414 (1979)
38. Lee, C.G., Choi, S.Y., Park, S.-H., Park, K.S., Ryu, S.H., Sung, Y.C.: The synthetic peptide Trp-Lys-Tyr-Met-Val-d-Met as a novel adjuvant for DNA vaccine. *Vaccine* **23**, 4703–4710 (2005)
39. Zhang, J.Z., Bonnitich, P., Wesselblatt, E., Klein, A.V., Najajreh, Y., Gibson, D., Hambley, T.W.: Facile preparation of mono-, di- and mixed-Carboxylato Platinum(IV) complexes for versatile anticancer prodrug design. *Chem. Eur. J.* **19**, 1672–1676 (2013)
40. Perretti, M.: The annexin 1 receptor(s): is the plot unravelling? *Trends Pharmacol. Sci.* **24**, 574–579 (2003)
41. Le, Y., Murphy, P.M., Wang, J.M.: Formyl-peptide receptors revisited. *Trends Immunol.* **23**, 541–548 (2002)
42. Alborzinia, H., Can, S., Holenya, P., Scholl, C., Lederer, E., Kitanovic, I., Wöfl, S.: Real-time monitoring of cisplatin-induced cell death. *PLoS ONE* **6**, e19714 (2011)
43. Pooyan, S., Qiu, B., Chan, M.M., Fong, D., Sinko, P.J., Leibowitz, M.J., Stein, S.: Conjugates bearing multiple formyl-methionyl peptides display enhanced binding to but not activation of phagocytic cells. *Bioconjug. Chem.* **13**, 216–223 (2002)
44. Graf, N., Mokhtari, T.E., Papayannopoulos, I.A., Lippard, S.J.: Platinum(IV)-chlorotoxin (CTX) conjugates for targeting cancer cells. *J. Inorg. Biochem.* **110**, 58–63 (2012)
45. Mukhopadhyay, S., Barnés, C.M., Haskel, A., Short, S.M., Barnes, K.R., Lippard, S.J.: Conjugated Platinum(IV)–Peptide complexes for targeting angiogenic tumor vasculature. *Bioconjug. Chem.* **19**, 39–49 (2007)
46. Gaviglio, L., Gross, A., Metzler-Nolte, N., Ravera, M.: Synthesis and in vitro cytotoxicity of *cis,cis,trans*-diamminedichloridodisuccinatoplatinum(IV)-peptide bioconjugates. *Metallomics* **4**, 260–266 (2012)
47. Abramkin, S., Valiahdi, S.M., Jakupec, M.A., Galanski, M., Metzler-Nolte, N., Keppler, B. K.: Solid-phase synthesis of oxaliplatin-TAT peptide bioconjugates. *Dalton Trans.* **41**, 3001–3005 (2012)
48. Chin, C.F., Tian, Q., Setyawati, M.I., Fang, W., Tan, E.S.Q., Leong, D.T., Ang, W.H.: Tuning the activity of Platinum(IV) anticancer complexes through asymmetric acylation. *J. Med. Chem.* **55**, 7571–7582 (2012)
49. Ang, W.H., Pilet, S., Scopelliti, R., Bussy, F., Juillerat-Jeanneret, L., Dyson, P.J.: Synthesis and characterization of Platinum(IV) anticancer drugs with functionalized aromatic carboxylate ligands: influence of the ligands on drug efficacies and uptake. *J. Med. Chem.* **48**, 8060–8069 (2005)
50. Varbanov, H., Valiahdi, S.M., Legin, A.A., Jakupec, M.A., Roller, A., Galanski, M., Keppler, B.K.: Synthesis and characterization of novel bis(carboxylato)dichloridobis(ethylamine)platinum(IV) complexes with higher cytotoxicity than cisplatin. *Eur. J. Med. Chem.* **46**, 5456–5464 (2011)
51. Gunaseelan, S., Gunaseelan, K., Deshmukh, M., Zhang, X., Sinko, P.J.: Surface modifications of nanocarriers for effective intracellular delivery of anti-HIV drugs. *Adv. Drug Deliv. Rev.* **62**, 518–531 (2010)
52. Qin, Y., Li, Z.-W., Yang, Y., Yu, C.-M., Gu, D.-D., Deng, H., Zhang, T., Wang, X., Wang, A.-P., Luo, W.-Z.: Liposomes formulated with fMLP-modified cholesterol for enhancing drug concentration at inflammatory sites. *J. Drug Target.* **22**, 165–174 (2014)
53. Banerjee, G., Medda, S., Basu, M.K.: A novel peptide-grafted liposomal delivery system targeted to macrophages. *Antimicrob. Agents Chemother.* **42**, 348–351 (1998)

54. van de Loosdrecht, A.A., Nennie, E., Ossenkoppele, G.J., Beelen, R.H.J., Langenhuijsen, M. M.A.C.: Cell mediated cytotoxicity against U 937 cells by human monocytes and macrophages in a modified colorimetric MTT assay: a methodological study. *J. Immunol. Methods* **141**, 15–22 (1991)
55. Sodhi, A., Pai, K., Singh, R.K., Singh, S.M.: Activation of human NK cells and monocytes with cisplatin in vitro. *Int. J. Immunopharmacol.* **12**, 893–898 (1990)
56. Sodhi, A., Pai, K.: Increased production of interleukin-1 and tumor necrosis factor by human monocytes treated in vitro with cisplatin or other biological response modifiers. *Immunol. Lett.* **34**, 183–188 (1992)
57. Sodhi, A., Chauhan, P.: Interaction between cisplatin treated murine peritoneal macrophages and L929 cells: involvement of adhesion molecules, cytoskeletons, upregulation of Ca²⁺ and nitric oxide dependent cytotoxicity. *Mol. Immunol.* **44**, 2265–2276 (2007)
58. Griffith, T.S., Wiley, S.R., Kubin, M.Z., Sedger, L.M., Maliszewski, C.R., Fanger, N.A.: Monocyte-mediated tumoricidal activity via the tumor necrosis factor–related cytokine. TRAIL. *J. Exp. Med.* **189**, 1343–1354 (1999)
59. Chauhan, P., Sodhi, A., Tarang, S.: Cisplatin-treated murine peritoneal macrophages induce apoptosis in L929 cells: role of Fas-Fas ligand and tumor necrosis factor–tumor necrosis factor receptor 1. *Anticancer Drugs* **18**, 187–196 (2007)
60. Galanski, M., Jakupec, M.A., Keppler, B.K.: Update of the preclinical situation of anticancer platinum complexes: novel design strategies and innovative analytical approaches. *Curr. Med. Chem.* **12**, 2075–2094 (2005)
61. Dhara, S.C.: A rapid method for the synthesis of cis-[Pt(NH₃)₂Cl₂]. *Indian J. Chem.* **8**, 193–194 (1970)
62. Kuroda, R., Ismail, I.M., Sadler, P.J.: X-ray and NMR studies of trans-dihydroxo-platinum (IV) antitumor complexes. *J. Inorg. Biochem.* **22**, 103–117 (1984)
63. Phillips, J.A., Morgan, E.L., Dong, Y., Cole, G.T., McMahan, C., Hung, C.-Y., Sanderson, S. D.: Single-step conjugation of bioactive peptides to proteins via a self-contained succinimidyl *Bis*-Arylhdyrazone. *Bioconjug. Chem.* **20**, 1950–1957 (2009)
64. Fulmer, G.R., Miller, A.J.M., Sherden, N.H., Gottlieb, H.E., Nudelman, A., Stoltz, B.M., Bercaw, J.E., Goldberg, K.I.: NMR chemical shifts of trace impurities: common laboratory solvents, organics, and gases in deuterated solvents relevant to the organometallic chemist. *Organometallics* **29**, 2176–2179 (2010)
65. Gill, S.C., von Hippel, P.H.: Calculation of protein extinction coefficients from amino acid sequence data. *Anal. Biochem.* **182**, 319–326 (1989)

Chapter 6

Induction of Immunogenic Cell Death by Chemotherapeutic Platinum Complexes



6.1 Introduction

There is growing evidence that conventional chemotherapeutics can modulate the immune system and trigger an immune response which sustains a long term durable therapeutic outcome [1, 2]. It has been proposed that the therapeutic efficacy of certain agents (e.g. anthracyclines, taxanes and gemcitabine) depends, at least partially, on such off-target immune effects [1, 3]. Accordingly, higher densities of

tumor-infiltrating lymphocytes following chemotherapy has been correlated with significantly better survival outcomes in colorectal and breast cancers [4, 5]. One of several ways in which chemotherapeutics engage a tumor-specific immune response is by triggering immunogenic cell death (ICD) whereby the dying cancer cells initiate a robust immune response, acting as a de facto anticancer vaccine [6, 7]. Thus, immunocompetent (but not immunodeficient) mice vaccinated with dying cancer cells pre-treated with ICD inducers (e.g. anthracyclines, shikonin and hypericin-PDT) are protected against subsequent challenges with live cancer cells [8]. Retrospective analysis of multiple cancers suggest that human patients treated with chemotherapy together with digoxin, an ICD-promoting agent, had improved overall survival, especially when the chemotherapy cocktail does not already contain an ICD inducer [9].

The ICD-inducing capacity of anticancer drugs has been tied with their capacity to elicit endoplasmic reticulum (ER) stress and associated reactive oxygen species (ROS) (Fig. 6.1) [6, 7, 10]. It is believed that cancer cells dying in response to ROS-mediated ER stress emit a combination of three distinct spatiotemporally-defined “danger” signals, which are recognized by the immune system and required for ICD [9]. These signals, which are now established as the biochemical hallmarks of ICD, are: (i) translocation of ER-resident calreticulin (CRT) to the cell surface during early apoptosis (ii) active secretion of ATP and (iii) extracellular secretion of nuclear high-mobility group box 1 protein (HMGB1) at late-stage apoptosis. Cell-surface CRT, the dominant pro-phagocytotic “eat me” signal [11], promotes the engulfment of cancer cells by professional macrophages such as dendritic cells (DCs) for tumour antigen presentation [8]. Secreted ATP acts as a “find me” signal as well as stimulating purinergic P2RX7 receptors on DCs, triggering production of IL-1 β , a pro-inflammatory cytokine which is required for IFN- γ production by

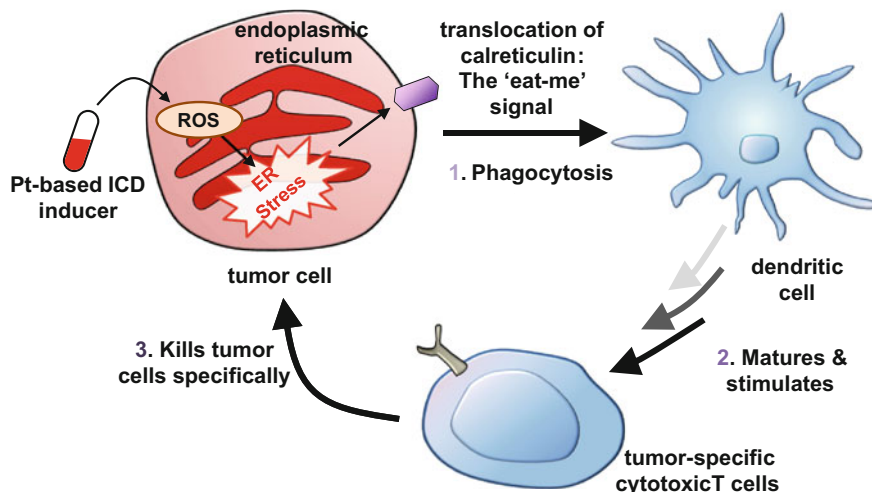


Fig. 6.1 Schematic of drug-induced immunogenic cell death (ICD)

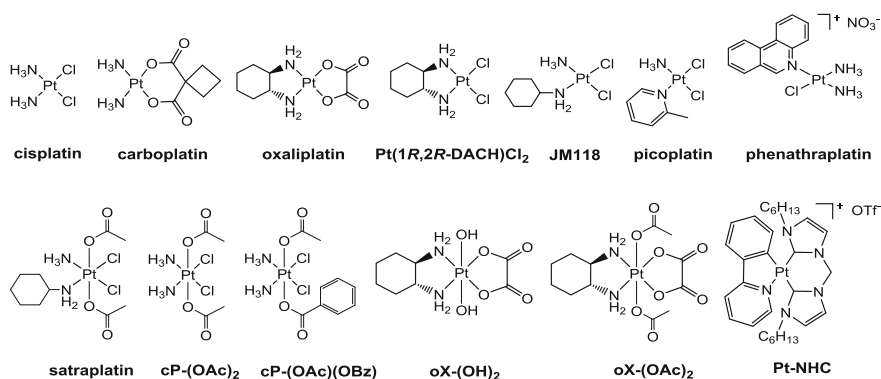


Fig. 6.2 Structures of platinum agents used in this study

tumour-specific cytotoxic T cells [6, 7, 10]. Finally, HMGB1 binds to toll-like receptor 4 (TLR4) on DCs, triggering a myeloid differentiation primary response gene 88 (MYD88)-dependent signalling cascade, which promotes antigen processing and presentation to T cells [6, 7, 10]. Thus, a dysfunctional P2RX7 or TLR4 has been correlated with negative therapeutic outcomes in both mice and human studies with ICD-inducing chemotherapeutics such as doxorubicin, highlighting the immune component as an essential contribution to the efficacy of these agents [6, 7, 10].

Although a mainstay of chemotherapy, there has not been a systematic attempt to screen both existing and upcoming Pt agents for ICD. It has been reported that oxaliplatin but not cisplatin, could induce ICD [12]. We evaluated a library of Pt agents (Fig. 6.2) containing compounds which are either clinically-relevant or of upcoming interest, as well as structurally-related analogues. The library includes cisplatin, oxaliplatin and carboplatin, all of which are in clinical use [13]. Pt(1R,2R-DACH)Cl₂ is a structural analogue of oxaliplatin. Picoplatin, satraplatin and phenanthriplatin are examples of novel Pt compounds either in clinical trials or pre-clinical development while JM118 is the active Pt^{II} species of satraplatin [14–16] Pt-NHC is a unique cyclometalated complex which selectively localizes in the ER and induces ER stress [17]. The remaining complexes are Pt^{IV} prodrugs of cisplatin and oxaliplatin.

6.2 Results and Discussion

Identification of ICD inducers from an in vitro phagocytosis assay. Since a critical step for ICD is the engulfment of dying cancer cells by professional macrophages [8], we first applied an in vitro phagocytosis assay [18] to identify possible ICD inducers. Briefly, murine CT-26 tumour cells (pre-stained with CellTracker Orange) were treated briefly (4 h) before co-incubation (2 h) with

murine J774 macrophages (pre-stained with CellTracker Green). Double-stained macrophages indicated phagocytosis (Fig. 6.3b). With the exception of Pt-NHC, which was both very cytotoxic and fluorescent above 10 μM , all other Pt agents were screened at 50 μM . Pt-NHC (5 μM) sharply increased tumour cell phagocytosis over non-treated controls ($38.2 \pm 3.5\%$ vs. $12.8 \pm 0.2\%$, $p < 0.0001$) followed distantly by phenantriaplatin ($20.1 \pm 3.6\%$), cisplatin ($20.0 \pm 1.0\%$ at 100 μM only), satraplatin ($18.8 \pm 0.9\%$) and picoplatin ($17.6 \pm 2.8\%$) (Fig. 6.3a). In contrast, none of the clinically-used Pt drugs nor their related analogues promoted phagocytosis at 50 μM . Our results diverged from a recent work which found oxaliplatin could induce ICD as we observed neither increased phagocytosis nor ER-ROS (Fig. S6.1) [12]. Nonetheless, there was a certain concentration dependence observed with cisplatin (50 and 100 μM) and Pt-NHC (1 and 5 μM), which correlated well with qualitative measurements of ER ROS (Fig. S6.1). The addition of 2 axial acetato ligands to JM118 elevated phagocytosis in satraplatin, which could reflect differences in subcellular localisation or accumulation. Phagocytosis was corroborated by fluorescence microscopy which shows cytosolic mixing of the green and red dyes at the area of contact between CT-26 and J774 (Fig. 6.3a).

We determined that the observed phagocytosis was indeed mediated by cell-surface exposure of CRT. Although other recognition ligands had been identified [19], ecto-CRT was shown to be the dominant “eat-me” signal and key mediator of immunogenicity in cancer cells [11, 20]. CRT, normally located in the ER, would be translocated to the outer surface of the plasma membrane in response to ER-stress [7]. This was then recognized by low-density lipoprotein-related protein (LRP) receptors on macrophages. Coating the cell surface with recombinant murine CRT to CT-26 without drug or treated with 50 μM cisplatin, resulted in a significant increase in tumor cell phagocytosis over basal levels (Fig. 6.3c). On the other hand, blocking the CRT-LRP interactions via a CRT blocking peptide abolished phagocytosis of Pt-NHC-treated CT-26 (Fig. 6.3c). Hence, these results underscored the requirement of ecto-CRT on tumor cells for inducing phagocytosis in our screening methodology.

Pt-NHC elicits biochemical hallmarks of ICD. We proceeded to evaluate the capacity of Pt-NHC to elicit the distinct biochemical hallmarks of ICD, namely CRT exposure, ATP secretion and extracellular HMGB1 release. Surface immunostaining under non cell-permeabilising conditions indicated that CRT exposure with Pt-NHC (5 μM) was a rapid process, detectable as soon as 1 h after drug-exposure (Fig. 6.4a, b). Furthermore, surface-CRT was detected on treated-cells with intact membrane integrity and also before phosphatidylserine exposure, implying that the translocation occurred at an early stage of apoptosis (Fig. 6.4b). Under identical conditions, no immuno-detectable CRT was observed on the surface of non-treated cells. Confocal microscopy analysis of both Pt-NHC (5 μM) and cisplatin (100 μM) treated cells revealed that ecto-CRT was distributed in uneven clusters, which was consistent with prior observations of other ICD-inducers (Fig. 6.4a) [12, 20, 21]. It was proposed that the uneven distribution reflected the segregation of CRT away from CD47 (the “don’t-eat-me” signal) and

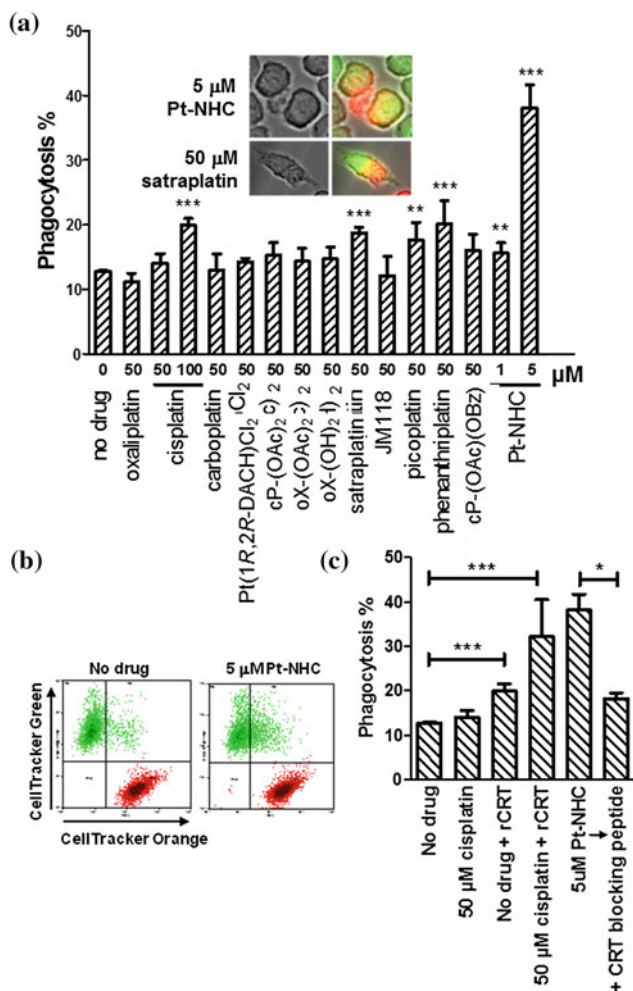


Fig. 6.3 Phagocytosis screening: **a** orange-stained CT-26 cells were drug-treated (4 h) before co-incubating (2 h) with green-stained J774 macrophages and analysed by flow cytometry. The phagocytosis % was calculated from the no. of double-stained macrophages over total no. of macrophages. Inset: Fluorescence microscopy of J774 macrophages (green) engulfing CT-26 (red) as evident by mixing of the dyes. **b** Representative flow cytometry scatter plots showing increased phagocytosis (top right quadrant) with Pt-NHC over control. **c** Coating CT-26 with rCRT enabled phagocytosis while co-incubation with a CRT blocking peptide abolished phagocytosis. Means \pm s.e.m. (* $p < 0.05$, ** $p < 0.01$, *** $p < 0.0001$; Student's t test)

thus promoting phagocytosis [20]. The release of both ATP and HMGB1 was also clearly evident with Pt-NHC treatment (5 μ M). ATP secretion into the supernatant after 24 h treatment was measured via a luciferase-based assay (Fig. 6.4c). The extracellular release of nuclear HMGB1 was detected as an absence of nuclear fluorescence after staining (with Triton-X permeabilisation) of treated cells (24 h)

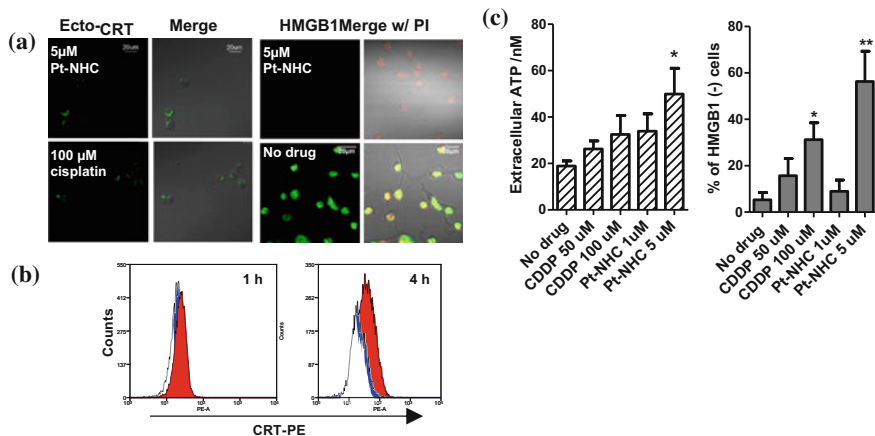


Fig. 6.4 **a** Left: rapid patch-like surface exposure of CRT observed by confocal microscopy after drug-treatment (1 h) of CT-26 followed by surface immuno-fluorescence staining with anti-CRT mAb. Right: HMGB1 release from the nuclei of CT-26 after 24 h drug-exposure (permeabilised and stained with both anti-HMGB1-Dy488 mAb and PI). **b** Pt-NHC enhanced ecto-CRT exposure in live cells (red shaded) compared to non-treated control (dotted line). CT26 cells were treated for 1 h (gated against PI-cells) and 4 h (gated against AnnexinV-cells) and surface-stained with an anti-CRT-PE mAb. **c** Left: extracellular release of ATP (left) and HMGB1 (right) of CT-26 after 24 h exposure. Means \pm s.e.m. (* p < 0.05, ** p < 0.01; Student's t test)

with an anti-HMGB1-Dy488 antibody and subsequent analysis by both confocal microscopy (Fig. 6.4a) and flow cytometry (Fig. 6.4c). In contrast, the presence of nuclear HMGB1 was clearly evident in non-drug treated controls. Thus, Pt-NHC fulfilled all three molecular hallmarks of ICD, a feature unique to all other validated ICD inducers such as UVC irradiation, anthracyclines and cardiac glycosides [6, 7, 9].

Pt-NHC triggers ROS-mediated ER stress. It is believed that ER stress, either in tandem with or in parallel to an over-generation of ROS, plays a prominent role in ICD. The ER stress response elicited by ICD-inducers would ignite a cascade of danger signalling pathways, including the activation of protein kinase-like ER kinase (PERK), which is mandatory for CRT exposure and possibly ATP secretion [6, 7, 10, 22]. Nonetheless, not all ER-stressors (e.g. tunicamycin) are ICD-inducers but the converse was a pre-requisite [10]. ICD-inducers have been classified into two categories: Type I inducers which triggers ER stress via off-target secondary mechanisms, and Type II inducers which selectively triggers focused ROS-mediated ER stress and shown to be more efficient in emitting danger signals [7, 21, 23]. Type II ICD inducers are believed to be superior to the more common Type I inducers, which only induce collateral ER stress [7, 24]. Till date, only a handful of Type II ICD-inducers had been identified (e.g. photodynamic therapy with hypericin, an ER-specific photosensitizer, and certain oncolytic viruses) [7]. Pt-NHC, which had minimal DNA-binding affinity, was previously reported to specifically localize in the ER and induced an ER stress response via PERK

activation [17]. In this context, we sought to demonstrate that the ER stress response was in fact ROS-mediated, qualifying Pt-NHC as a Type II ICD inducer. ROS production was tracked after short-term drug exposure (4 h) using 2',7'-dichlorodihydrofluorescein diacetate (H₂DCFDA) as a general ROS indicator [25], and ER being visualized by ER-Tracker Red, which bind to sulphonylurea receptors on ER. In MDA-MB-231, there was clear colocalisation of ROS with the ER (89.2% as determined by Costes method [26]) with Pt-NHC (1 μ M) (Fig. S6.1). At 5 μ M Pt-NHC, ER exhibited severe deformation and ROS was correspondingly more diffuse and less colocalised, possibly as a consequence of increased ER membrane permeability associated with ER-stress induced apoptosis [27]. In CT-26, ROS was only observed with 5 μ M Pt-NHC but not at 1 μ M. In keeping with MDA-MB-231, the observed ROS was relatively diffuse. The absence of ROS with Pt-NHC at a lower concentration (1 μ M) corresponded to significantly lower phagocytosis, ATP secretion and HMGB1 release, implying that ROS played a key role in Pt-NHC associated ICD. Likewise, phagocytosis was only observed with cisplatin at 100 μ M (where intense ROS was observed in a subpopulation of cells) but not at 50 μ M (a concentration where ROS was not observed). In general, all Pt compounds which promoted phagocytosis had measurable ROS production (Fig. S6.1). Phagocytosis induced by Pt-NHC was significantly reduced when tumour cells were co-incubated with trolox, an antioxidant which quenches ROS (Fig. 6.5). Thus, oxidative ER-stress triggered by Pt-NHC plays a crucial role in ICD.

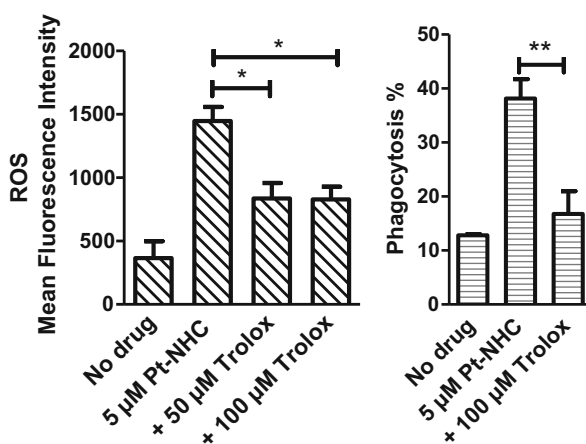


Fig. 6.5 The anti-oxidant, trolox, quenches cellular ROS and this in turn inhibits phagocytosis. CT-26 was first pre-treated with trolox (30 min) prior to drug exposure and later co-treated with trolox and Pt-NHC (4 h). **a** Trolox quenched Pt-NHC induced ROS as analysed by flow cytometry. **b** Co-incubation of Pt-NHC with trolox significantly inhibited tumour cell phagocytosis. Means \pm s.e.m. (* p < 0.05, ** p < 0.01; Student's t test)

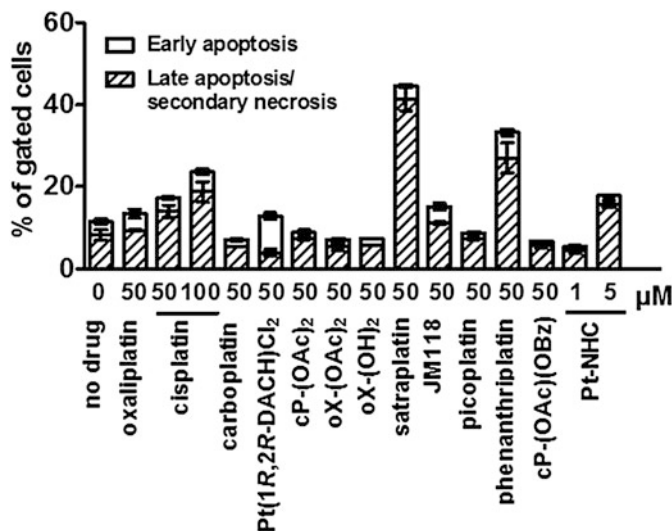


Fig. 6.6 Cytotoxicity of Pt agents via Annexin V apoptosis assay. CT-26 cells were treated for 24 h and stained with AnnexinV-eGFP and propidium iodide. Means \pm s.e.m.

Traditionally, new platinum agents were evaluated primarily by direct cytotoxicity against cancer cell lines. We observed no correlation between the propensity of Pt agents to trigger tumor cell phagocytosis and cytotoxicity (Fig. 6.6, evaluated by Annexin V assay) suggesting that ICD is independent of cytotoxicity. It was demonstrated that the therapeutic efficacy of anthracyclines (ICD-inducer) was negated in mice models when the host immune system was compromised [3, 28]. This observation suggested that, at least in some models of cancer, it was the immune-modulating capacity of chemotherapeutics, and not cytotoxicity, which was important. In keeping with this strategy, we recently reported platinum(IV)-peptide agents that directly activated macrophages as another pathway of eliciting an anticancer immune response [29].

6.3 Conclusion

Over the last decade, there has been substantial evidence supporting the pivotal role of the immune system in inducing tumour regression following conventional chemotherapy [1, 2]. It is probable that many highly promising immunogenic and/or immune-stimulating Pt candidates might have been neglected. This work, which represents one of the very first few attempts to exploit the immune-modulating properties of Pt agents, could pave the way for the development of combined Pt-based immuno-chemotherapeutics.

6.4 Methods

Preparation of platinum compounds. The platinum complexes cisplatin [30], Pt (1*R*,2*R*-DACH)Cl₂, [31] cP-(OAc)₂, [32] oX-(OH)₂, [33] oX-(OAc)₂, [33] cP-(OAc)(OBz), [32] picoplatin, [34] phenathraplatin¹⁴ and Pt-NHC¹⁷ were synthesized and characterized as previously reported in literature. Complexes oxaliplatin, carboplatin, satraplatin and JM118 were purchased from commercial vendors. Stock solutions of cisplatin, Pt(1*R*,2*R*-DACH)Cl₂, picoplatin, satraplatin and JM118 were dissolved in 0.9% NaCl. Complexes oxaliplatin, carboplatin, cP-(OAc)₂, oX-(OH)₂, oX-(OAc)₂ and phenathraplatin were dissolved in H₂O. Complexes cP-(OAc)(OBz) and Pt-NHC were dissolved in DMSO. Platinum concentrations of stock solutions were measured externally by CMMAC (National University of Singapore) on an Optima ICP-OES (Perkin-Elmer).

Cell lines and cell culture. The murine colon cancer cell-line CT-26 and murine macrophages J774A.1 were kind gifts of Dr Ian Cheong (Temasek Life Sciences Laboratory) and Dr. Gan Yunn Hwen (National University of Singapore) respectively. Human breast cancer cell-line MDA-MB-231 was obtained from ATCC. CT-26 cells were cultured in Roswell Park Memorial Institute (RPMI) 1640 medium. J774A.1 and MDA-MB-231 cells were cultured in Dulbecco's Modified Eagle Medium (DMEM). All media were supplemented with 10% heat-deactivated Fetal Bovine Serum (FBS) and the cells were maintained in a 5% CO₂ incubator at 37 °C.

Reagents and antibodies. CellTracker Orange CMTMR (5-(and-6)-(((4-Chloromethyl)Benzoyl)Amino)Tetramethylrhodamine), CellTracker Green CMFDA (5-Chloromethylfluorescein Diacetate), 2',7'-dichlorodihydrofluorescein diacetate (H₂DCFDA) and ER-Tracker Red were purchased from Life Technologies. Annexin V-Enhanced Green Fluorescent Protein (EGFP) Apoptosis Detection Kit (ab14153), Phycoerythrin-conjugated mouse monoclonal anti-calreticulin antibody (ab83220), rabbit polyclonal anti-calreticulin antibody (ab2907), Dy488-conjugated rabbit monoclonal anti-HMGB1 antibody (epr3506) and secondary FITC-conjugated anti-rabbit mouse monoclonal antibody (ab99700) were purchased from Abcam. Murine recombinant CRT was purchased from MyBioSource. CRT blocking peptide was bought from MBL International.

In vitro phagocytosis assay. J774 cells were seeded at 5×10^4 cells/well in a 24-well plate in heat deactivated complete DMEM for 48 h. On the same day, adherent CT-26 cells were seeded in heat deactivated complete RPMI in a T75 flask such that 80% confluency would be achieved 48 h later. 2 d later, CT-26 cells were labelled with 1 μ M Celltracker Orange (540 nm/566 nm), harvested by trypsin-EDTA and counted. Exactly 5×10^5 cells were transferred to each 1.5 mL Eppendorf microtube and treated with indicated drug for 4 h in an Eppendorf shaker at 37 °C. Simultaneously, J774 cells was labelled with 1 μ M Celltracker

Green (492 nm/516 nm). 4 h later, orange-labelled CT-26 cells were washed 3 times with heat deactivated complete DMEM while green-labelled J774 cells were washed twice with PBS. CT-26 was co-cultured with J774 at a 1:10 effector-target ratio for 2 h. 2 h later, cells were harvested with 1 mM cold EDTA followed by scraping. Cold Hanks' Balanced Salt solution (HBSS) buffer was added to the cells to deactivate EDTA activity before the cells were fixed with 4% formaldehyde for 15 min at r.t. Phagocytosis was assessed by a flow cytometer (BD LSRFortessa cell analyser) using Summit software. At least 10,000 macrophages were analysed for each sample. Phagocytosis % refers to the number of double positive macrophages over the total number of macrophages analyzed. In some experiments CT-26 were pre-treated with Trolox for 30 min before they were co-treated with indicated drug and Trolox for 4 h at 37 °C to quench cellular ROS. To restore ecto-CRT expression, CT-26 were treated with rCRT as previously described [8]. In other experiments, 8 µg/mL CRT blocking peptide was co-incubated with CT-26 and J774 to block ecto-CRT. In some experiments, J774 cells were plated on poly-L-lysine coated cover slips and 1×10^5 CT-26 cells were added to J774 at a 1:2 effector: target ratio. 2 h later, cells were washed once with PBS and fixed with 1% paraformaldehyde for 15 min. Cover-slips were washed gently in ultrapure H₂O before they were mounted onto slides and analysed with a fluorescence microscope. Fluorescent and brightfield images were taken separately and merged using ImageJ software.

Visualization of production of ROS in the ER by confocal microscopy. CT-26 cells were plated at 2×10^5 cells/well on poly-L-lysine coated cover slips in 12-well plates in heat deactivated complete RPMI. Cells were treated with drugs for 4 h before they were washed thrice with pre-warmed HBSS and incubated with 25 µM pre-warmed H₂DCFDA (488 nm/515 nm) for 15 min at 37 °C. 15 min later, H₂DCFDA was removed from the cells and 1 µM pre-warmed ER-Tracker Red (587 nm/615 nm) was added to the cells for 15 min. After the incubation time, cells were washed thrice with HBSS before the cover slips were washed with ultrapure water, mounted onto slides and analysed with confocal microscopy (FV1000, Olympus) immediately. Images were taken using 10× and 60× objective lens and processed using Olympus FLUOVIEW Viewer.

Measurement of cellular reactive oxygen species by flow cytometry. 2×10^5 CT-26 cells were pre-treated with Trolox for 30 min before they were co-treated with indicated drug and Trolox for 4 h at 37 °C. 4 h later, cells were washed twice with pre-warmed HBSS before they were incubated with 25 µM pre-warmed H₂DCFDA for 30 min at 37 °C. Cells were then washed once with HBSS before they were analysed immediately on a flow cytometer (BD LSRFortessa cell analyser). Quantitative analysis was performed using Summit software.

Visualization of cell surface CRT by confocal microscopy. 2×10^5 CT-26 cells were treated with drug for 1 h, washed with cold PBS twice before they were incubated with rabbit anti-CRT (diluted in cold 2% FBS in PBS) for 30 min on ice.

Cells were then washed with cold PBS twice, then incubated with a secondary FITC-conjugated anti-rabbit mouse monoclonal antibody (diluted in cold 2% FBS in PBS) for 30 min on ice. Cells were washed once with cold PBS, fixed with 4% paraformaldehyde for 15 min, then mounted onto slides. Cells were visualized with confocal microscopy (FV1000, Olympus) immediately. Images were taken using 60× objective lens and processed using Olympus FLUOVIEW Viewer.

Flow cytometric analysis of cell surface CRT. 2×10^5 CT-26 cells were treated with drug, washed twice with cold 2% FBS in PBS before they were incubated with PE-conjugated anti-CRT (diluted in cold 2% FBS in PBS) for 30 min. Cells were washed once with cold 2% FBS in PBS, pelleted, resuspended in PBS containing 1 $\mu\text{g}/\text{mL}$ 7-AAD and analysed immediately on a flow cytometer (BD LSRFortessa cell analyser). Quantitative analysis was performed using Summit software.

Visualization of HMGB1 by confocal microscopy. CT-26 cells were plated at 1×10^5 cells/well on poly-L-lysine coated cover slips in 12-well plates in heat deactivated complete RPMI. The next day, cells were drug-treated for 24 h and washed with PBS. The cells was then fixed with 4% paraformaldehyde for 10 min and permeabilised with 0.1% TritonX-100 for a further 10 min. The cells was then washed twice with supplemented PBS (w/10% FBS) and incubated with Dy488-conjugated rabbit anti-HMGB1 mab (prediluted 1:100 in supplemented PBS) for 30 min. Cells were then washed once with PBS, co-stained with propidium iodide (1 $\mu\text{g}/\text{mL}$) and mounted onto slides. Cells were visualized with confocal microscopy (FV1000, Olympus) immediately. Images were taken using 60× objective lens and processed using Olympus FLUOVIEW Viewer.

Flow cytometric analysis of HMGB1 release. 2×10^5 CT-26 cells were treated with drug for 24 h and washed twice with PBS. Cells were fixed, permeabilised and stained with Dy488-conjugated rabbit anti-HMGB1 mab as above and analyzed by flow cytometry.

ATP secretion assay. 4×10^3 CT-26 cells per well were seeded in 96-well plates in heat deactivated complete RPMI. The next day, cells were drug-treated for 24 h and the conditioned media was carefully extracted for extracellular ATP measurement by the luciferin-based ENLITEN ATP Assay Kit (Promega).

Quantification of apoptosis by flow cytometry. Apoptosis induced by drug treatment was assessed by double staining CT-26 cells with Annexin V-EGFP and propidium iodide. Briefly, 2×10^5 CT-26 cells were seeded per well in 12 well plates in heat deactivated complete RPMI and on the next day, the cells were treated with drugs. 24 h later, the cells were detached using trypsin-EDTA and exactly 2×10^5 cells per well were counted, pelleted and resuspended in 500 μL of annexin-V binding buffer (10 mM HEPES/NaOH (pH 7.4), 140 mM NaCl and 2.5 mM CaCl_2) containing 1 μL annexin V-EGFP protein and 1 $\mu\text{g}/\text{mL}$ PI. Samples were kept in the dark and analysed immediately on a flow cytometer (BD LSRFortessa cell analyser). Quantitative analysis was performed using Summit software.

Supplementary Information

Supplementary Figures

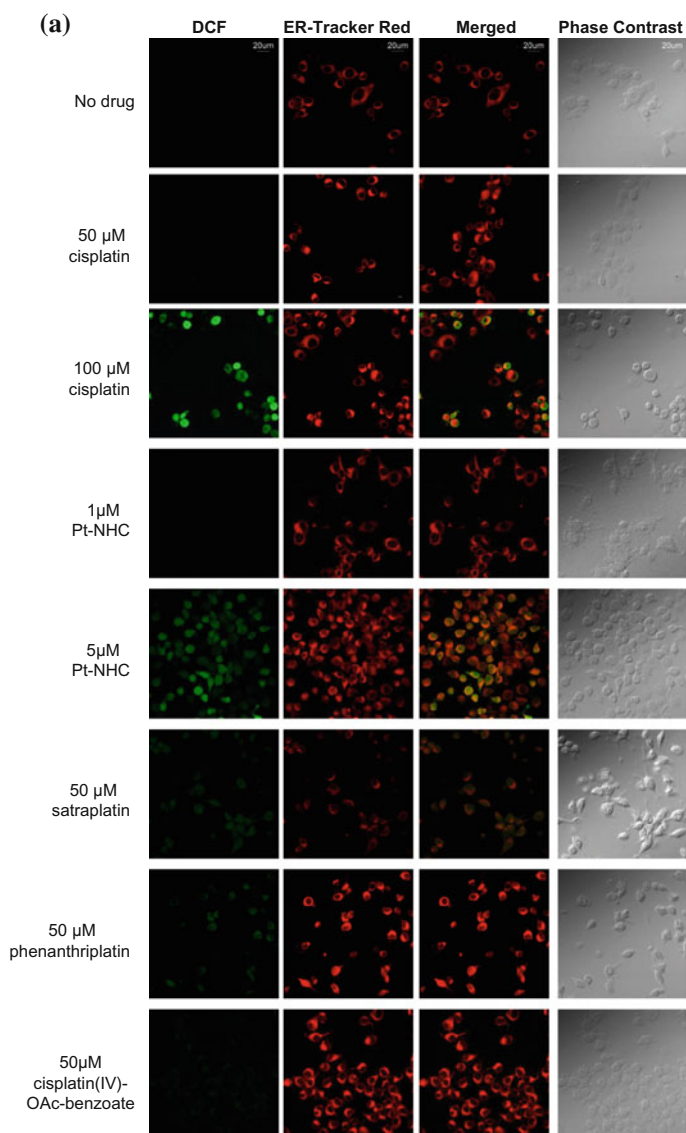


Fig. S6.1 Cells observed under confocal microscopy after drug treatment (4 h) and incubation with H₂DCFDA (ROS indicator, green) and ER-Tracker Red (red). **a** CT-26. **b** MDA-MB-231. **c** Colocalisation analysis after Pt-NHC treatment (1 μ M) on MDA-MB-231. White pixels indicate areas of colocalisation as determined by Costes method

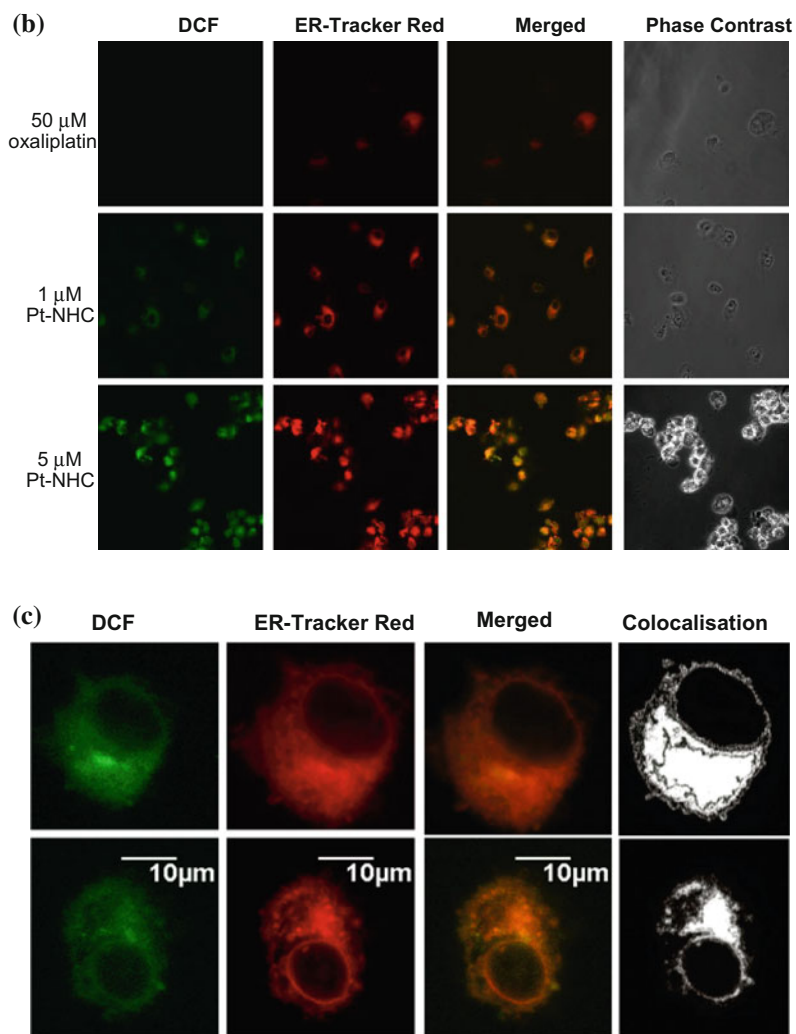


Fig. S6.1 (continued)

References

1. Galluzzi, L., Senovilla, L., Zitvogel, L., Kroemer, G.: The secret ally: immunostimulation by anticancer drugs. *Nat. Rev. Drug Discov.* **11**, 215–233 (2012)
2. Zitvogel, L., Galluzzi, L., Smyth, M.J., Kroemer, G.: Mechanism of action of conventional and targeted anticancer therapies: reinstating immunosurveillance. *Immunity* **39**, 74–88 (2013)
3. Mattarollo, S.R., Loi, S., Duret, H., Ma, Y., Zitvogel, L., Smyth, M.J.: Pivotal role of innate and adaptive immunity in anthracycline chemotherapy of established tumors. *Cancer Res.* **71**, 4809–4820 (2011)
4. Halama, N., Michel, S., Kloor, M., Zoernig, I., Benner, A., Spille, A., Pommerencke, T., von Knebel, D.M., Folprecht, G., Luber, B., Feyen, N., Martens, U.M., Beckhove, P., Gnjatic, S., Schirmacher, P., Herpel, E., Weitz, J., Grabe, N., Jaeger, D.: Localization and density of immune cells in the invasive margin of human colorectal cancer liver metastases are prognostic for response to chemotherapy. *Cancer Res.* **71**, 5670–5677 (2011)
5. Dieci, M.V., Criscitiello, C., Goubar, A., Viale, G., Conte, P., Guarneri, V., Ficarra, G., Mathieu, M.C., Delalogue, S., Curigliano, G., Andre, F.: Prognostic value of tumor-infiltrating lymphocytes on residual disease after primary chemotherapy for triple-negative breast cancer: a retrospective multicenter study. *Ann. Oncol.* **25**, 611–618 (2014)
6. Kroemer, G., Galluzzi, L., Kepp, O., Zitvogel, L.: Immunogenic cell death in cancer therapy. *Annu. Rev. Immunol.* **31**, 51–72 (2013)
7. Krysko, D.V., Garg, A.D., Kaczmarek, A., Krysko, O., Agostinis, P., Vandenabeele, P.: Immunogenic cell death and DAMPs in cancer therapy. *Nat. Rev. Cancer* **12**, 860–875 (2012)
8. Obeid, M., Tesniere, A., Ghiringhelli, F., Fimia, G.M., Apetoh, L., Perfettini, J.L., Castedo, M., Mignot, G., Panaretakis, T., Casares, N., Metivier, D., Larochette, N., van Endert, P., Ciccocanti, F., Pientini, M., Zitvogel, L., Kroemer, G.: Calreticulin exposure dictates the immunogenicity of cancer cell death. *Nat. Med.* **13**, 54–61 (2007)
9. Menger, L., Vacchelli, E., Adjemian, S., Martins, I., Ma, Y., Shen, S., Yamazaki, T., Sukkurwala, A. Q., Michaud, M., Mignot, G., Schlemmer, F., Sulpice, E., Locher, C., Gidrol, X., Ghiringhelli, F., Modjtahedi, N., Galluzzi, L., André, F., Zitvogel, L., Kepp, O., Kroemer, G.: Cardiac glycosides exert anticancer effects by inducing immunogenic cell death. *Sci. Transl. Med.* **4**, 143ra99 (2012)
10. Kepp, O., Menger, L., Vacchelli, E., Locher, C., Adjemian, S., Yamazaki, T., Martins, I., Sukkurwala, A.Q., Michaud, M., Senovilla, L., Galluzzi, L., Kroemer, G., Zitvogel, L.: Crosstalk between ER stress and immunogenic cell death. *Cytokine Growth Factor Rev.* **24**, 311–318 (2013)
11. Chao, M.P., Jaiswal, S., Weissman-Tsukamoto, R., Alizadeh, A.A., Gentles, A.J., Volkmer, J., Weiskopf, K., Willingham, S.B., Raveh, T., Park, C.Y., Majeti, R., Weissman, I.L.: Calreticulin is the dominant pro-phagocytic signal on multiple human cancers and is counterbalanced by CD47. *Sci. Transl. Med.* **2**, 63ra94 (2010)
12. Tesniere, A., Schlemmer, F., Boige, V., Kepp, O., Martins, I., Ghiringhelli, F., Aymeric, L., Michaud, M., Apetoh, L., Barault, L., Mendiboune, J., Pignon, J.P., Jooste, V., van Endert, P., Ducreux, M., Zitvogel, L., Piard, F., Kroemer, G.: Immunogenic death of colon cancer cells treated with oxaliplatin. *Oncogene* **29**, 482–491 (2009)
13. Shah, N., Dizon, D.S.: New-generation platinum agents for solid tumors. *Future Oncol.* **5**, 33–42 (2009)
14. Park, G.Y., Wilson, J.J., Song, Y., Lippard, S.J.: Phenanthriplatin, a monofunctional DNA-binding platinum anticancer drug candidate with unusual potency and cellular activity profile. *Proc. Natl. Acad. Sci. U. S. A.* **109**, 11987–11992 (2012)
15. Bhargava, A., Vaishampayan, U.N.: Satraplatin: leading the new generation of oral platinum agents. *Expert Opin. Investig. Drugs* **18**, 1787–1797 (2009)
16. Holford, J., Sharp, S.Y., Murrer, B.A., Abrams, M., Kelland, L.R.: In vitro circumvention of cisplatin resistance by the novel sterically hindered platinum complex AMD473. *Br. J. Cancer* **77**, 366–373 (1998)

17. Zou, T., Lok, C.N., Fung, Y.M., Che, C.M.: Luminescent organoplatinum(II) complexes containing bis(N-heterocyclic carbene) ligands selectively target the endoplasmic reticulum and induce potent photo-toxicity. *Chem. Commun.* **49**, 5423–5425 (2013)
18. Hoffmann, P.R., deCathelineau, A.M., Ogden, C.A., Leverrier, Y., Bratton, D.L., Daleke, D.L., Ridley, A.J., Fadok, V.A., Henson, P.M.: Phosphatidylserine (PS) induces PS receptor-mediated macropinocytosis and promotes clearance of apoptotic cells. *J. Cell Biol.* **155**, 649–659 (2001)
19. Savill, J., Dransfield, I., Gregory, C., Haslett, C.: A blast from the past: clearance of apoptotic cells regulates immune responses. *Nat. Rev. Immunol.* **2**, 965–975 (2002)
20. Gardai, S.J., McPhillips, K.A., Frasnich, S.C., Janssen, W.J., Starefeldt, A., Murphy-Ullrich, J.E., Bratton, D.L., Oldenborg, P.-A., Michalak, M., Henson, P.M.: Cell-Surface calreticulin initiates clearance of viable or apoptotic cells through trans-activation of LRP on the phagocyte. *Cell* **123**, 321–334 (2005)
21. Garg, A., Krysko, D., Vandenabeele, P., Agostinis, P.: Hypericin-based photodynamic therapy induces surface exposure of damage-associated molecular patterns like HSP70 and calreticulin. *Cancer Immunol. Immunother.* **61**, 215–221 (2012)
22. Garg, A.D., Krysko, D.V., Verfaillie, T., Kaczmarek, A., Ferreira, G.B., Marysael, T., Rubio, N., Firczuk, M., Mathieu, C., Roebroek, A.J.M., Annaert, W., Golab, J., de Witte, P., Vandenabeele, P., Agostinis, P.: A novel pathway combining calreticulin exposure and ATP secretion in immunogenic cancer cell death. *EMBO J.* **31**, 1062–1079 (2012)
23. Garg, A.D., Krysko, D.V., Vandenabeele, P., Agostinis, P.: The emergence of phox-ER stress induced immunogenic apoptosis. *OncoImmunology* **1**, 786–788 (2012)
24. Inoue, H., Tani, K.: Multimodal immunogenic cancer cell death as a consequence of anticancer cytotoxic treatments. *Cell Death Differ.* **21**, 39–49 (2014)
25. Hempel, S.L., Buettner, G.R., O'Malley, Y.Q., Wessels, D.A., Flaherty, D.M.: Dihydrofluorescein diacetate is superior for detecting intracellular oxidants: comparison with 2',7'-dichlorodihydrofluorescein diacetate, 5-(and 6)-carboxy-2',7'-dichlorodihydrofluorescein diacetate, and dihydrorhodamine 123. *Free Radic. Biol. Med.* **27**, 146–159 (1999)
26. Costes, S.V., Daelemans, D., Cho, E.H., Dobbin, Z., Pavlakis, G., Lockett, S.: Automatic and quantitative measurement of protein-protein colocalization in live cells. *Biophys. J.* **86**, 3993–4003 (2004)
27. Wang, X., Olberding, K.E., White, C., Li, C.: Bcl-2 proteins regulate ER membrane permeability to luminal proteins during ER stress-induced apoptosis. *Cell Death Differ.* **18**, 38–47 (2011)
28. Sukkurwala, A.Q., Adjemian, S., Senovilla, L., Michaud, M., Spaggiari, S., Vacchelli, E., Baracco, E.E., Galluzzi, L., Zitvogel, L., Kepp, O., Kroemer, G.: Screening of novel immunogenic cell death inducers within the NCI mechanistic diversity set. *OncolImmunology* **3**, e28473 (2014)
29. Wong, D.Y.Q., Yeo, C.H.F., Ang, W.H.: Immuno-chemotherapeutic platinum(IV) prodrugs of cisplatin as multimodal anticancer agents. *Angew. Chem. Int. Ed.* **53**, 6752–6756 (2014)
30. Dhara, S.C.: A rapid method for the synthesis of cis-[Pt(NH₃)₂Cl₂]. *Indian J. Chem.* **8**, 193–194 (1970)
31. Pepels, A., Rauter, H., Schnebeck, R.D., Wissmann, F.: Process for the preparation of 1,2-diaminocyclohexane-platinum(II) complexes. In Google Patents (2007)
32. Chin, C.F., Tian, Q., Setyawati, M.I., Fang, W., Tan, E.S., Leong, D.T., Ang, W.H.: Tuning the activity of platinum(IV) anticancer complexes through asymmetric acylation. *J. Med. Chem.* **55**, 7571–7582 (2012)
33. Zhang, J.Z., Bonnitcha, P., Wexselblatt, E., Klein, A.V., Najajreh, Y., Gibson, D., Hambley, T.W.: Facile preparation of mono-, di- and mixed-carboxylato platinum(IV) complexes for versatile anticancer prodrug design. *Chem. Eur. J.* **19**, 1672–1676 (2013)
34. Battle, A.R., Choi, R., Hibbs, D.E., Hambley, T.W.: Platinum(IV) analogues of AMD473 (cis-[PtCl₂(NH₃)(2-picolone)]): preparative, structural, and electrochemical studies. *Inorg. Chem.* **45**, 6317–6322 (2006)

Chapter 7

Concluding Remarks



*What we call the beginning is often the end.
And to make an end is to make a beginning.
The end is where we start from.*
—T. S. Elliot

7.1 Concluding Remarks

In this thesis, the author rationalised that new platinum complexes which cling to the existing paradigms of targeting DNA and evaluated primarily based on the criteria of cytotoxicity are unlikely to have actual therapeutic relevance because they are unlikely to offer distinct clinical advantages over existing platinum-based agents. Instead, the author has proposed and described several ideas which reconceptualises and reinvents conventional approaches towards platinum-based anticancer drug design. One such approach was through the development of targeted platinum(IV) agents which does not act via apoptosis, as is customary, but instead selectively overwhelms targeted cells via necrosis. This strategy which was termed “targeted necrosis”, is one way of outwitting the defective apoptosis pathways in many resistant cancers hampering many conventional chemotherapeutics. In addition, the author has initiated pioneering work to exploit and leverage upon the untapped immuno-modulating capacity of platinum-based agents. The author muses that many potentially promising immuno-stimulating platinum complexes synthesized in the past may have “fallen through the cracks” simply because this criterion was never considered previously. In this work, the author has demonstrated that it is possible to either via screening techniques or by careful rationale design to develop new platinum complexes which are even more (a) macrophage-activating or (b) immunogenic than current platinum agents in clinical use. This research has thus opened up a new subfield within platinum drug design which may warrant further exploration. In closing, the author hope that this dissertation may spur other researchers to relook platinum anticancer drug design and may one day, be the new beginning for the development of the next generation of platinum-based agents in clinical use.